CHARACTERISATION OF THREE BACTERIOPHAGES INFECTING SEROVARS OF *SALMONELLA ENTERICA*

DANN TURNER BSc. MSc.

A thesis submitted in partial fulfilment of the requirements of the University of the West of England, Bristol for the degree of Doctorate of Philosophy.

Department of Applied Sciences, University of the West of England, Bristol

October 2013

Author's Declaration

Abstract

A collection of three newly isolated *Salmonella* bacteriophages, vB_SenS-Ent1, vB_SenS-Ent2 and vB_SenS-Ent3 was established. These bacteriophages were characterised by electron microscopy, host range, sensitivity to restriction enzymes and profiles of structural proteins on SDS-PAGE gels. The complete genome sequences of each bacteriophage were established to greater than 30x coverage and bioinformatics analysis identified the functions of a number of coding sequences.

Since the last update of virus taxonomy by the ICTV a number of additional genome sequences for bacteriophages infecting the genus *Salmonella* have been reported in the literature. To date, all but one of the *Siphoviridae* comprising the *Salmonella* bacteriophages with fully sequenced genomes remain unclassified by the ICTV. Comparative genomic analysis reveals that a number of these phages form a coherent group within the *Siphoviridae* and supports the establishment of a new genus, the "*Setp3likeviruses*". The proposed genus includes 5 bacteriophages infecting *Salmonella*; SETP3, vB_SenS-Ent1, SE2, wksl3 and SS3e, and 5 infecting *Escherichia*; K1G, K1H, K1ind1, K1ind2 and K1ind3. This group share identical virion morphology, have terminally redundant, circularly permuted genomes ranging between 42-45 kb in size and are characterised by high nucleotide sequence similarity, shared homologous proteins and conservation of gene order.

Bioluminescent bacterial reporters, transformed to express the *luxCDABE* operon of *Photorhabdus luminescens*, were used to establish the activity of the vB_SenS-Ent bacteriophages in microtitre broth lysis assays, efficacy as biological control agents for the removal of *Salmonella* in contaminated foods and for spatial measurements of plaque expansion in agar overlays.

Acknowledgements

It would not have been possible to complete this doctoral thesis without the humour, friendship, and support of those around me. I am indebted to my supervisor, Dr. Darren Reynolds for his support and instruction throughout this project and for providing an open and positive environment in which to work. I would like to extend my thanks to the members of my project supervisory team, Professor Vyv Salisbury, Dr. Shona Nelson and Dr. Gareth Robinson for all their guidance, support and patience over the years of this project.

Many thanks are also due to Pablo Ledezma, Dr. Ben Taylor, David and Laura Corry, Dr. Robin Thorn and Dr. Natasha McGuire for their friendship, support in and outside of the laboratory and many a shared evening of beer and laughter! Special thanks go to my girlfriend Jenny, mostly for putting up with me but also for her unending support and encouragement.

I am most grateful to Professor Steve Abedon of Ohio State University for providing invaluable discussions about plaques and copies of published and unpublished work. Further thanks are due to Professor Hans Wolfgang Ackermann for his kind permission to reproduce figures and electron micrographs and also to Seth Bunton-Stashyshn, Professor Don Seto and Dr. Padmanabhan Mahadevan for their help and support in developing the CoreGenes3.5 batch submission tool.

I would like to acknowledge the financial, academic and technical support of the University of the West of England, Bristol and its staff. This studentship was funded by the Higher Education Funding Council for England.

My family is my bedrock, without whose love, support and encouragement I would have never made it this far. This thesis is dedicated to my parents, Guy and Mary, and siblings Matthew, Edward and Nicola Turner.

Table of Contents

List of Figures

List of Tables

Abbreviations

Abbreviation	Definition
aa	Amino acid(s).
ATCC	American Type Culture Collection, USA.
ATP	Adenosine 5'-triphosphate.
BIM	Bacteriophage insensitive mutant.
BLI	Bioluminescence imaging.
bp	Base pair(s).
CFRA	Campden Food Research Association.
cfu	Colony-forming units.
CCD	Charge-coupled device.
CDS	Coding sequence.
CMOS	Complementary metal oxide semiconductor.
CsCl	Cesium chloride.
dsDNA	Double-stranded DNA.
DSM	German Collection of Microorganisms and Cell Cultures.
EMCCD	Electron multiplying charge-coupled device.
EOP	Efficiency of plating.
FDA	Food and Drug Administration, USA.
FMN	Flavin mononucleotide.
g	Gravity.
Gm	Gentamycin.
iCCD	Intensified charge-coupled device.
ICTV	International committee on the Taxonomy of Viruses.
ID	Identity.
(k)bp	(Kilo)-base pairs.
(k)Da	(Kilo)-Daltons.
Km	Kanamycin.
LB	Luria Bertani Miller.
LDA	Lithoum dodecyl sulphate
LPS	Lipopolysaccharide.
MCP	Major capsid protein.
MOI	Multiplicity of infection.
MTP	Major tail protein.
MW	Molecular weight.
MWCO	Molecular weight cut-off value.
NADP	Nicotinamide adenine dinucleotide phosphate.
NCIMB	National Collection of Industrial Bacteria, UK.
NCTC	National Collection of Type Cultures, UK.
nt	Nucleotides.
ORF(s)	Open reading frame(s).
PBSA	Dulbecco's phosphate buffered saline.
PFGE	Pulsed field gel electrophoresis.
pfu	Plaque forming units.
RBP	Receptor binding protein.
RFLP	Restriction fragment length polymorphism.

RS	Ringer's solution.
RTE	Ready-to-eat.
SDS	Sodium dodecyl sulphate
SDS-PAGE	Sodium dodecyl sulphate polyacrylamide gel electrophoresis.
SM	Sodium-magnesium buffer.
SPI-1	*Salmonella* pathogenicity island 1.
SPI-2	*Salmonella* pathogenicity island 2.
TAE	Tris-Acetate EDTA buffer.
TE	Tris-Chloride EDTA buffer.
TEM	Transmission electron microscopy.
TMP	Tape measure protein.
tRNA	Transfer RNA.
TSP	Tailspike protein.
TTP	Tail tip protein
VLA	Veterinary Laboratories Agency, UK.

Chapter 1 Introduction

1.1 Overview

Members of the genus *Salmonella* continue to represent significant aetiological agents of disease in humans and animals. With the continued rise in antibiotic resistance it is imperative to identify and investigate alternative strategies for the development of novel antimicrobials for use as clinical therapeutics or for the control of bacterial pathogens in industry. The bacteriophages, obligate parasites of bacteria, represent one such potential source of antimicrobial agents.

The present study was carried out to further understand the biology of phages infecting the genus *Salmonella* and the potential of such phages to act as biological control agents. To achieve this, the specific aims of this thesis were five-fold:

1. To isolate, select and characterise bacteriophages specific for *Salmonella*.
2. To sequence and annotate the genomes of the isolated bacteriophages
3. To investigate the chosen phages for their ability to function as biological control agents
4. To investigate the use of bioluminescent bacterial reporters as a sensitive and non-destructive method to monitor bacteriophage-mediated lysis of *Salmonella*.
5. To employ bioluminescent imaging as a method to follow the expansion of plaques in overlay agar.

This thesis is composed of eight chapters. Chapter one provides a general introduction to the bacteriophages, the genus *Salmonella* and bacterial bioluminescence. Chapter two describes the methodologies employed to achieve the aims of this project. Chapter three details the isolation, microbiological characterisation, sequencing and annotation of three bacteriophages specific for *Salmonella*: vB_SenS-Ent1, vB_SenS-Ent2 and vB_SenS-Ent3. Chapter four summarises a comparative genomics study of 42 *Salmonella* bacteriophages whose complete genome sequences are available within the international nucleotide sequence database and a proposal for the formation of a novel genus within the family *Siphoviridae*. Chapter five describes the use of *Salmonella* serovars transformed to express a bioluminescent phenotype to monitor the effects of co-incubation of bacteria and bacteriophage in liquid media. Chapter six investigates the use of the vB_SenS-Ent bacteriophages as biological control agents for the reduction of *Salmonella* on a variety raw and ready to eat food matrices. Chapter seven describes the application of bioluminescence imaging to monitor the formation and expansion of plaques on host bacterial lawns in overlay agar plates. Lastly, chapter eight presents the main conclusions of the studies presented in this thesis and outlines recommendations for future work.

1.2 The Bacteriophages

The word virus stems from the Latin meaning 'poison' or 'venom'. Every domain of life is affected by the actions of viruses. The Bacteria are no exception to this rule, providing a nice analogy that the bacteria can catch colds too. Discovered independently by Frederick Twort (1915) and Felix D'Herelle (1917), the bacteriophages (phages) are obligate intracellular parasites of bacteria, that is, they are unable to reproduce without the presence of the intact molecular machinery constituting the host cell. Despite the independent reports and that Twort did not pursue his finding, it is d'Herelle who is accredited with the discovery of these viruses and who coined the name for viruses of bacteria: the bacteriophages. 'Phage' derives from the Greek 'phagos' literally translating as 'to eat', 'devour' or 'consume', hence bacteriophages are the 'eaters of bacteria'. It was suggested early on that the bacteriophages could be employed to prevent or treat bacterial infections. Many of the early phage therapy trials were reported to be successful and several preparations were marketed by companies such as Eli Lily and L'Oreal. However, the advent of antibiotics diverted interest in the United States and Western Europe away from the study of bacteriophages as therapeutic agents. Rather, research in the West focussed upon a few model phages and led to fundamental discoveries which formed the backbone of modern molecular biology. In contrast, the use of bacteriophages as therapeutic agents was continued in Eastern Europe and the former Soviet Union where several institutions were founded, including the Eliava Institute in Tbilisi, Georgia. Subsequently, with the current rise of antibiotic resistance possibly representing the advent of a new 'pre-antibiotic' era, the exploitation of bacteriophages as therapeutic and biological control agents is subject to renewed interest.

1.2.1 Morphology forms the basis for classification

Phage classification began in earnest with the definition of six morphotypes, based upon virion morphology and type of nucleic acid (Bradley, 1967). This system was revised by Ackermann and Eisenstark (1974) and has subsequently been reviewed and updated over time (Ackermann, 1987, Ackermann, 1996, Ackermann, 2001, Ackermann, 2007a, Ackermann and Prangishvili, 2012). The taxonomic classification of bacteriophages is coordinated by an international body, the International Committee for the Taxonomy of Viruses (ICTV). For bacterial viruses, in the ninth report on virus taxonomy the ICTV recognise one order, the *Caudovirales* comprising the tailed bacteriophages and seven other families (King *et al.,* 2011). Bacteriophages are classified into families on the basis of up to 70 criteria (Ackermann, 2009a) but most consideration is given to physical characteristics including virion shape (tailed, polyhedral, filamentous or pleomorphic), type and structure of nucleic acid and genomic information, if available. In a recent update Ackermann summarised the morphological descriptions of nearly 6,300 bacteriophages examined under the electron microscope (Ackermann and Prangishvili, 2012). Reports of bacteriophages in the literature overwhelmingly belong to the order *Caudovirales.* Polyhedral, filamentous and pleomorphic phages are reported, but represent a very low fraction of studied phages (Figure 1). These phages represent seven families, some of which

have very few members (Ackermann, 2007a). The tailed dsDNA phages, classified in the order *Caudovirales* are represented by three families (Figure 2), the *Siphoviridae* (non-contractile tails), *Myoviridiae* (contractile tails) and *Podoviridae* (very short tails). This literature review is limited exclusively to the *Caudovirales* as all the phages isolated during the course of this work belonged to this order (Chapter 3).

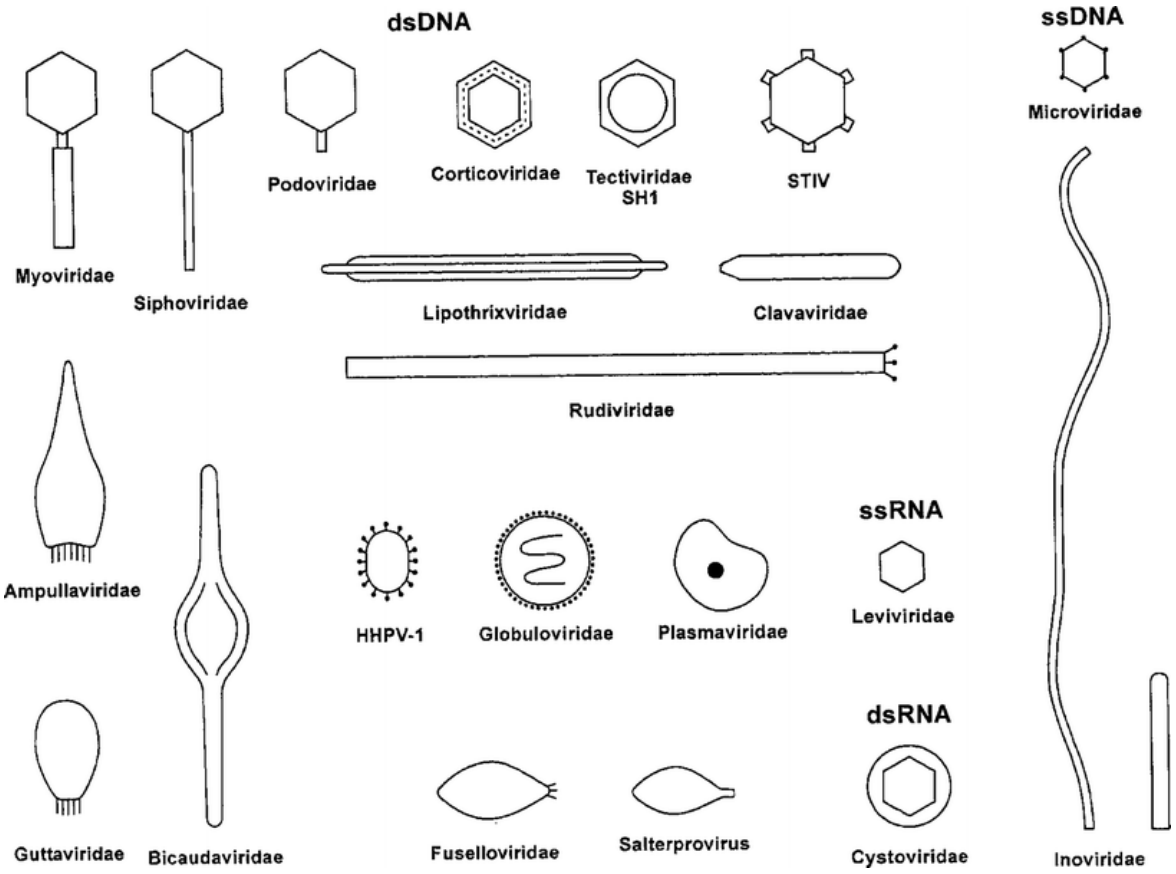

Figure 1. Schematic diagram of the different morphologies of prokaryotic viruses. Each morphotypes is labelled with Reproduced with permission from Ackermann and Prangishvili (2012).

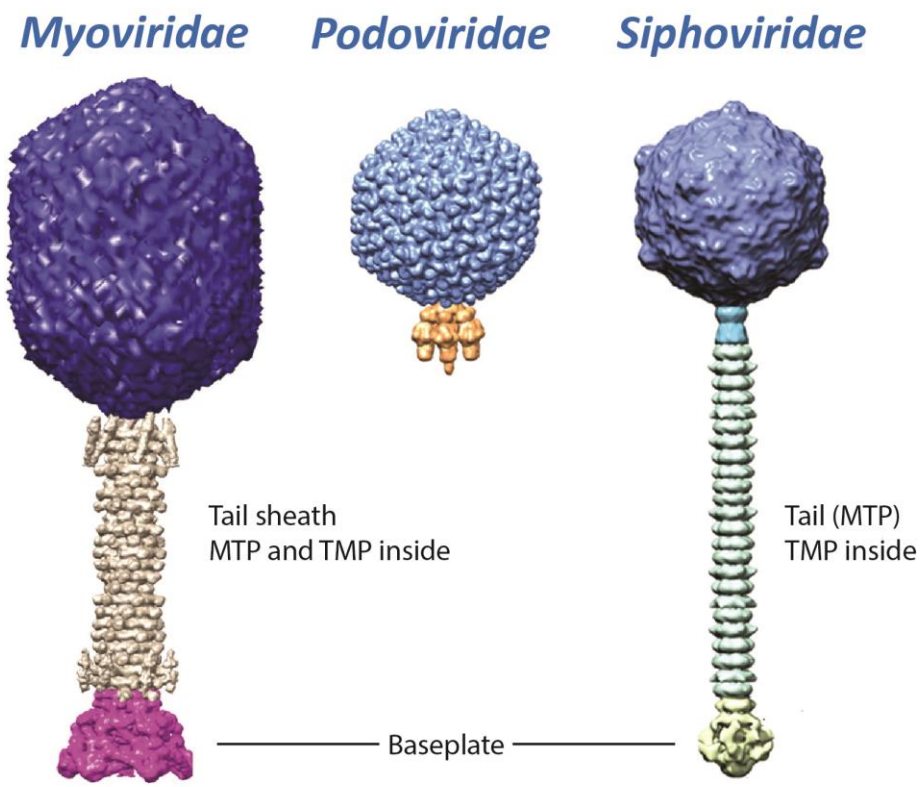

Figure 2. Representatives of the three families of the order *Caudovirales*, the tailed dsDNA bacteriophages. The capsid enclosing the virion nucleic acid is coloured purple for each family. The tail is composed of the major tail (MTP) and tapemeasure (TMP) proteins and extends from the capsid, which for *Myoviridae* is enclosed by the tail sheath. The tail terminates at the baseplate to which the apparatus (not shown) required for adsorption and infection of host cells is attached. Reproduced with permission from Veesler and Cambillau (2011).

The classification of bacteriophages is subject to continuous discussion and debate, particularly with the increasing volume of available genomic and proteomic data. New approaches to phage taxonomy are complicated as no single candidate gene analogous to the 16S rRNA gene used for the classification of bacteria exists in all phage families. Additionally comparative genomic studies have demonstrated that phage genomes are mosaic, that is, are subject to horizontal transfer events at relatively high frequency, further complicating approaches for classification. As such, there is no single criterion for the demarcation of bacteriophage species and genera. Instead a polypthetic approach is favoured, where clades are delineated by a set of properties, some of which may be absent among related members. A number of alternative taxonomic approaches have been proposed in the literature. These include classification based upon terminase amino acid sequence similarity (Casjens *et al.*, 2005), structural genes (Deveau *et al.,* 2006) and whole proteomes (Rohwer and Edwards, 2002). One promising approach is described by Lavigne *et al.,* (2008, 2009) where BLAST-based tools were used to delineate shared orthologous proteins between different phage genomes. Combining these data with literature reviews, the authors were able to classify 120 *Myoviridae* and 55 *Podoviridae*. While approaches to taxonomy are improving and under continued development, the system, or rather lack of one, for the naming of isolated bacteriophages follows no convention.

Recently a systematic method of nomenclature has been proposed (Kropinski *et al.,* 2009). This system allows the rapid identification of bacteriophage family, lifestyle and host genus for a specific phage isolate.

1.2.2 Bacteriophage lifecycles

The first stage in infection of a host cell is the primary adsorption event. Adsorption refers to reversible and irreversible binding events between a phage receptor binding protein and a bacterial cell surface structure such as LPS, one or more outer membrane proteins, fimbriae or flagella. Primary adsorption is mediated by phage protein structures including tailspikes and tail fibres while irreversible binding tends to be a function of secondary binding proteins localised at the baseplate. Irreversible adsorption results in the transfer of the virion genome to the host cell cytoplasm, a unidirectional process termed ejection or injection. Quite how the phage genome travels across the bacterial cell wall and inner membrane remains unclear, although a conformational change is likely transmitted along the tail in order to open the closed phage capsid upon irreversible binding. It is probable that the bacteriophages have evolved a number of different methods to facilitate this translocation event.

Bacteriophages possess several lifecycles; lytic (virulent), lysogenic (temperate), pseudolysogenic and chronic. The lytic cycle is where phages infect and rapidly replicate within a host bacteria. The lytic lifecycle results in the release of newly formed progeny virions and death of the host cell through lysis, mediated by phage-encoded proteins which enzymatically degrade the cell wall. Lytic infection results in clear plaques on the respective host bacterial lawns. The period encompassing phage adsorption to genome replication, production of progeny virions and lysis of the host cell is described as the latent period. The duration from adsorption to the time of formation of progeny virions, when intracellular virions can be detected by plaque assay after prematurely lysing the host cell, is described as the eclipse phase (Ellis and Delbrück, 1939).

Temperate phages are those which possess a lytic life cycle and a lysogenic life cycle. In the lysogenic life cycle, the infecting phage does not directly kill the host cell but instead either integrates into the host bacterial chromosome by transposition or site-specific recombination or resides as a plasmid within the host cell cytoplasm. In the integrated state, the phage DNA is termed a prophage and through gene expression can confer new or additional properties to the bacterial cell when expressed, a process termed lysogenic conversion (Brüssow *et al.,* 2004). The prophage can stably reside within the host cell for many generations until appropriate environmental or physiological conditions trigger the lytic lifecycle, a process termed induction. Genome sequencing has revealed that many bacteria contain viable or cryptic prophage sequences encoded within the chromosome (Canchaya *et al.,* 2003b, Casjens, 2003). A common feature of lysogeny is that the bacterial host subsequently becomes resistant to infection by related phages that share the same immunity group

profile or repressor specificity or by alteration of the cell surface epitope used for adsorption. Through various mutation events, the ability of a prophage to form functional virions upon activation of the lytic cycle may be lost whereby such prophages are termed cryptic prophages. Temperate phages tend to form cloudy plaques on bacterial lawns as the probability of infection leading to lysogeny is greater than for lytic infection.

A further state, pseudolysogeny, has been proposed and is defined as a non-replicative and non-productive state following a successful adsorption and genome transfer event (Ripp and Miller, 1997). Pseudolysogeny is thought to occur in the presence of adverse conditions which prevent either genome integration or replication, perhaps caused by host cell starvation. This strategy has the potential to enhance bacteriophage survival, as the phage genome is protected from environmental conditions by 'sheltering' within the host cell (Miller and Ripp, 2002). A final lifestyle, termed chronic infection, is observed for some archaeal viruses and filamentous phage. In this scenario, progeny virions are slowly and continuously shed or extruded from the cell surface rather than being released as a single burst event (Lopez and Webster, 1983).

An infection event which results in either integration or replication of the virion genome may be termed a successful infection. A productive infection is one which results in the assembly and release of progeny virions competent for subsequent infection of host bacteria. Infection does not always result in the death of the host cell and survival of the bacteriophage (Figure 3). Bacteria have evolved a number of resistance mechanisms including preventing uptake of the phage genome, superinfection immunity, clustered regularly inter-spaced palindromic repeats (CRISPR) and restriction modification systems (Labrie *et al.,* 2010).

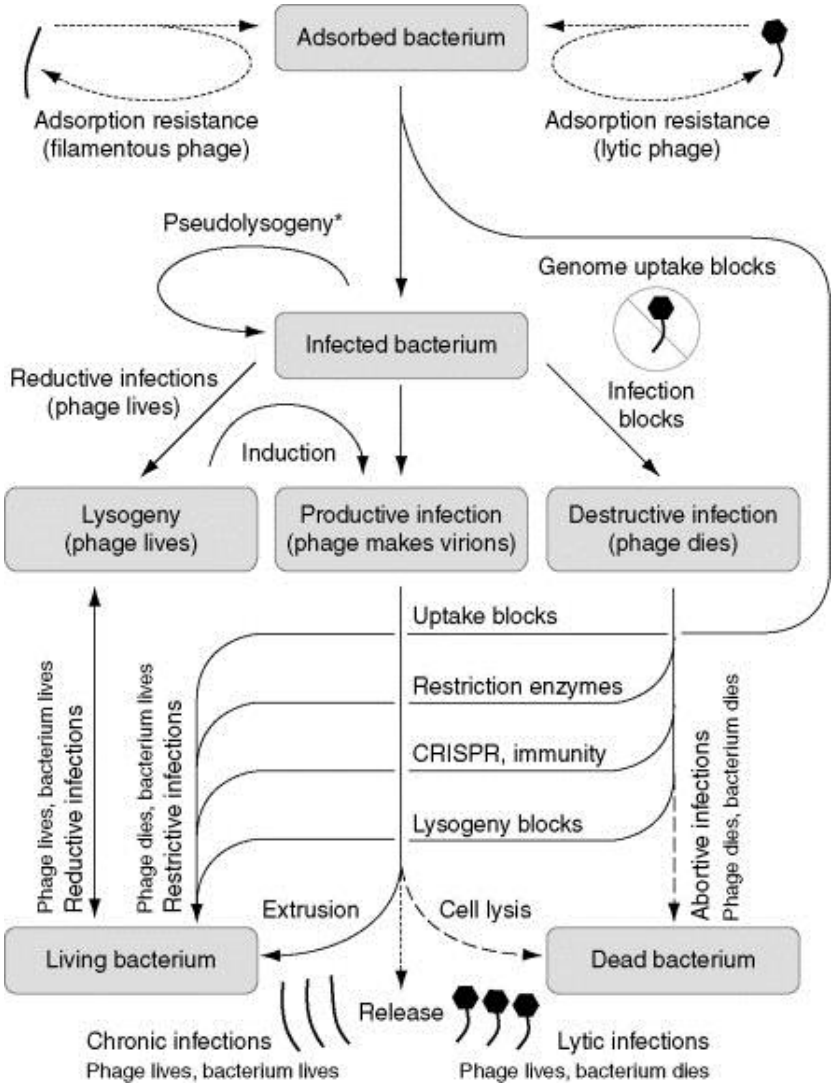

Figure 3. Schematic representation of the possible outcomes of infection of bacteria by filamentous and tailed bacteriophages. The diagram depicts the interactions between phage and host and the survival outcome for each. Adsorption to and release from bacterial cells are shown as short dashed lines. Infections leading to death of the bacterial cell are shown as long dashed lines. Reproduced with permission from Hyman and Abedon (2010).

1.2.3 Bacteriophage structure

A bacteriophage virion consists of a single or double stranded DNA or RNA encapsulated within either a protein or lipoprotein coat. For members of the *Caudovirales* the nucleic acid is exclusively double-stranded DNA and ranges in size from 22.2 kb for *Lactococcus* phage c2 to 497.5 kb for *Bacillus* phage G. Irrespective of the target host organism, the virion structure is designed to contain and protect the viral chromosome, facilitating its safe transfer to a host cell to allow subsequent replication. The binary symmetry, or head to tail structure, of the *Caudovirales* is unique in virology and phages of this order are also differentiated from animal viruses in that the delivery of their genetic material occurs by an ejection mechanism, rather than by an un-coating process, following adsorption to the host cell surface. Capsid and tail assembly occur by separate pathways involving the sequential addition of component subunits. The process of virion assembly and morphogenesis has been studied in extensive detail for P22, SPP1 and T4. More recently, the application of atomic

force microscopy (AFM) and 3D reconstruction from cryo-electron microscopy has yielded additional insights into the structure and location of these proteins *in situ* (Guerrero-Ferreira and Wright, 2013, Kuznetsov *et al.,* 2011, Parent *et al.,* 2012).

1.2.4 Capsid assembly

The head or capsid forms the protective container for the condensed bacteriophage chromosome and the formation of this closed shell for genome packaging requires the recruitment and organisation of multiple copies of protein subunits. Recent studies using 3D reconstructions from cryo-electron microscopy have shown that DNA resides within the mature capsid as a tightly wound spool (Cerritelli *et al.,* 2003, Parent *et al.,* 2012). It is estimated that the pressure within the capsid is as much as 20 atmospheres (Cordova *et al.,* 2003) and as such, the mature capsid lattice must be sufficiently robust to withstand the pressure of the condensed chromosome. In general, the size of the phage capsid is correlated to the size of the genome being packaged.

All members of the *Caudovirales* have capsids with icosahedral (20 sides/12 vertices) symmetry or prolate derivatives thereof, providing a characteristic appearance under the electron microscope. The icosahedral structure forms with known triangulation numbers T=4, 7, 13, 16 and 52, assembled from many copies of one or two major coat proteins (MCP). The triangulation number system was introduced by Caspar and Klug (1962) to describe the relationship between the number of pentameric and hexameric subunits giving rise to the quasi-symmetry of the capsid shell. Each corner of the icosahedron is generally made up of pentamers of the MCP, while the rest of each side is made up of hexamers of the same or a similar protein.

Three gene products are critical for capsid formation; the portal, scaffold and MCP. Several other factors, including accessory proteins, chaperones and proteases are also required. The first stage in capsid formation is the production of assembly intermediate, precursor structures called procapsids. The scaffold proteins co-assemble with the MCP subunits, forming a core inside the prohead. The scaffold is provided either by a separately encoded protein, as for P22 (Greene and King, 1994), or from a region of the major coat protein itself as for HK97 (Huang *et al.,* 2011).

The true T=7 symmetry of the capsid is broken locally at one of the five-fold vertices by the portal protein complex. The portal vertex is formed as a dodecameric ring of portal protein subunits and serves as the gateway through which DNA enters the pro-capsid during particle assembly, and exits during infection (Johnson and Chiu, 2007). The portal also forms part of the junction or neck connecting the capsid and tail. Like other phage structural proteins, the portal proteins from different bacteriophages vary widely in sequence and molecular mass. The terminase complex, made up of small and large subunits, associates with the portal vertex and facilitates DNA packaging. The mechanism initiating DNA packaging differs according to the replication strategy of the viral DNA.

With the start of DNA packaging the scaffold is removed signalling the start of maturation. Two mechanisms for removal of the scaffold have been identified. For phages T4, HK97 and λ scaffold proteins are proteolytically cleaved by a phage-encoded protease (Liu and Mushegian, 2004), while for P22 and ϕ29 the scaffold proteins exit the procapsid (Eppler *et al.,* 1991). With maturation the procapsid undergoes a structural transition, enlarging, becoming more angular and taking on the characteristic isometric shape.

Most characterised tailed dsDNA phages assemble the capsid structure from multiple copies of one MCP. The exceptionally well characterised myovirus T4 is an exception, encoding two capsid proteins: gp24, forming the pentameric vertex capsomers and gp23, forming hexameric capsomers (Olson *et al.,* 2001). The MCPs of the tailed phages show extreme amino acid sequence variation. Despite such disparate sequences, the 3D structure of MCPs examined at high resolution by X-ray crystallography exhibit the presence of HK97-like fold, named after the bacteriophage in which this structure was first described (Wikoff *et al.,* 2000). High resolution structures of MCPs have been resolved for phages T4 (Fokine *et al.,* 2005); ϕ29 (Morais *et al.,* 2005), ε15 (Jiang *et al.,* 2006), T7 (Agirrezabala *et al.,* 2007), λ (Lander *et al.,* 2008), BPP-1 (Dai *et al.,* 2010) and P22 (Jiang *et al.,* 2003) all of which possess the HK97-like fold. These data are indicative of a common, very ancient evolutionary ancestor; it has long been recognised that 3D structure tends to be more highly conserved over much greater timespans than either nucleotide or amino acid sequence (Rossmann *et al.,* 1974). Moreover, Baker *et al.,* (2005) demonstrated similarities between the HK97-like fold of MCPs of the *Caudovirales* with those of herpesviruses and suggested that the existence of related viruses infecting different domains of life might have arisen from a progenitor virus predating the separation of the different domains of life or one that arose from a later adaptation event.

Once the capsid is packaged with DNA, the terminase complex is substituted by neck proteins, variously described as connector, tail terminator or head completion proteins, which together with the portal form successive rings with the bottom ring being termed the gatekeeper complex (Orlova *et al.,* 2003). For bacteriophage SPP1 the gatekeeper has been demonstrated to prevent premature exit or leakage of DNA (Lhuillier *et al.,* 2009).

Some bacteriophages have been found to recruit additional accessory proteins to the capsid, termed head decoration or capsid stabilisation proteins. Studies of the Dec protein of bacteriophage L (Gilcrease *et al.,* 2005) found that this protein increased tolerance to EDTA of the closely related P22 virion. The authors suggested that a loss of divalent cations by the chelating activity of EDTA causes an increase in pressure upon the condensed chromosomal DNA resulting in capsid disruption or DNA ejection. Similarly, the *soc* gene product provides stabilisation to the T4 capsid when exposed to extremes of pH or temperature (Qin *et al.,* 2010).

1.2.5 The Bacteriophage tail

The tail functions to facilitate adsorption and attachment of the phage to the host cell surface and provide a conduit for genome ejection and it is this feature which distinguishes the three families of the *Caudovirales*. Analogous to genes encoding capsid assembly components, genes encoding elements for tail structure and assembly show great variation in sequence composition. However, the order of genes tends to be conserved, providing valuable information for the prediction of gene function. Genes tend to follow a 'body plan' of consecutive open reading frames beginning with the major tail protein (MTP) and ending with genes encoding the baseplate and adsorption apparatus (Veesler and Cambillau, 2011). Tail assembly occurs separately to the capsid and occurs by the addition of components in a strict sequential order (Aksyuk and Rossmann, 2011).

The architecture of the long, flexible siphovirus tail is relatively simple, reflected in the use of the Greek *siphon*, meaning tube. The tail is based upon three main components: the tape measure protein, the major tail protein and the tail terminator protein. In contrast, the *Myoviridae* (Greek *myos*, muscle) are characterised by a complex rigid tail apparatus. For this family of phages the tail tube is enclosed by an outer contractile sheath. This added layer of complexity is reflected by the number of genes encoding the tail structure and assembly components; at least 22 genes are involved in assembly of the T4 bacteriophage tail (Miller *et al.,* 2003). The *Podoviridae* (Greek *podos*, meaning foot) possess no real tail, rather the adsorption apparatus is connected directly to the neck region.

The tail tube is formed by the polymerisation of multiple copies of the MTP and there is evidence for structural conservation of this protein in both contractile and non-contractile tails (Pell *et al.,* 2009a). The length of the tail is determined by the tape measure protein (TMP), located inside the tail shaft. All long-tailed phages sequenced to date possess a large gene, usually greater than 2 kbp in length, encoding the TMP. This family of proteins is characterised by the presence of long hydrophobic α-helices and the relationship between tail length and TMP length has been shown by insertion and deletion studies to be precisely correlated, with an approximate length of 0.15 nm per amino acid residue for phage λ (Katsura, 1990, Katsura and Hendrix, 1984). However, the position and precise molecular mechanism governing tail length determination by these proteins has not been unequivocally determined. Binding of the tail terminator protein halts polymerisation of the tail tube, completing the tail assembly. The tail terminator also interacts with the capsid to facilitate joining of the head and tail (Pell *et al.,* 2009b, Zhao *et al.,* 2003). In addition to the MTP and TMP, tailed phages encode a number of tail assembly chaperones and completion proteins. One common feature of these scaffold proteins is the presence of translational frameshifts which are conserved across a diverse range of long tailed phages. In λ gpGT is formed by a -1 translational frameshift occurring at the C-terminal end of gpG. The frameshift occurs at a frequency of approximately 4 % which results

in a fixed abundance ratio between gpG and gpGT. These proteins are thought to form a spiral scaffold with dimensions similar to the internal diameter of the tail tube (Xu *et al.,* 2004). Notably, functional and sequence comparisons of the tail tube and head-tail connector proteins suggest that the tail proteins of *Myoviridae* and *Siphoviridae* arose from a single ancestral gene (Cardarelli *et al.,* 2010).

The apparatus facilitating host adsorption is located at the distal end of the phage tail. Binding to the host cell surface occurs as a result of interactions with one or more host receptors by one or more phage receptor binding proteins. The recognition event is highly specific and facilitates rapid and efficient attachment to the host cell. Bacteriophages are capable of binding to a wide range of cell surface structures including proteins, LPS and components of the cell wall and this ability is reflected by a stunning diversity of distal tail morphologies. Phage receptor binding proteins are generally either described as tail fibres or tail spikes. Tail fibres refer to long, thin, flexible structures composed of one or more proteins, which extend from the top of the tail tip assembly in siphoviruses and to the baseplate of myoviruses. Tailspikes, in contrast, tend to be much shorter and appear as globular or tear-shaped structures. Transmission and cryo-electron microscopy have amply illustrated the diversity of tail-tip/baseplate complexes among the bacteriophages. Despite low levels of sequence identity, many of the characterised tail fibres and tailspikes of the *Caudovirales* form homotrimers rich in β structure. The N-terminal domain is exclusively associated with attachment of the RBP to the phage tail, either directly or through interaction with an adaptor protein, while the C-terminal domain is responsible for receptor binding.

1.3 The *Salmonella*e

The *Salmonella*e remain significant aetiological agents of zoonotic and food-borne disease world-wide. Members of the genus are Gram-negative, facultatively anaerobic, non-sporulating bacilli that are the causative agents of typhoid fever, gastroenteritis and enteric fever in both humans and animals. With the exception of *S.* Gallinarum, serovars (serotypes) of *Salmonella* are motile, possessing peritrichous flagellae.

The first successful clinical definition of typhoid fever was undertaken in 1851 by Sir William Jenner who differentiated the disease from Typhus, a vector borne disease caused by transmission of *Rickettsia typhi* or *Rickettsia prowazekii* by ticks and lice. In 1880, Karl Joseph Eberth isolated a bacillus suspected of causing typhoid from spleen sections and mesenteric lymph nodes, and in 1884 Georg Gaffky confirmed Eberth's findings. The bacillus reported by Eberth and Gaffky was first identified as a separate genus by Dr Theobald Smith, a researcher investigating swine cholera under the auspices of the USDA Bureau of Animal Industry. Despite identifying the bacteria, Salmon, as Smith's administrator, took priority on the research paper and hence the new bacterium was named *Salmonella* (Salmon, 1884).

The nomenclature of *Salmonella* is complex and continues to be frequently revised. The differentiation of *Salmonella* isolates was initially performed using clinical evidence, serological and biochemical tests. Serological analysis of *Salmonella* dates back to the beginning of the 20th century with a study of antigenic components in motile and non-motile strains of *S.* Choleraesuis (Smith and Reagh, 1903). Phase variation of flagella was subsequently discovered in *S.* Typhimurium by Andrewes (1922). The first systematic serological analysis of *Salmonella* was initiated by White (1926) and continued and extended by Kauffmann (1961). Prior to the introduction of the Kauffmann-White scheme in 1946 by the World Health Organisation (W.H.O.) serovar names were allocated according to clinical manifestation, geographic location or source from which the serovar was first isolated. Subsequent DNA-DNA hybridisation analysis demonstrated that the *Salmonella* serovars form a single hybridisation group sharing between 70 % and 90 % DNA content, demonstrating that relatedness between different serovars existed at the species level (Crosa *et al.,* 1973). That is, rather than possessing many species, the genus is constituted of a single species comprised of many serovars, a hypothesis subsequently supported by rRNA studies (Chang *et al.,* 1997, Christensen *et al.,* 1998) and sequence evidence from housekeeping and invasion genes (Li *et al.,* 1995, Boyd *et al.,* 1997). Further analysis by multi-locus enzyme electrophoresis (MLEE) and DNA hybridisation provided evidence that *S. bongori* should be considered a distinct species (Le Minor L *et al.,* 1986).

Table 1. Differential biochemical characteristics of species and subspecies of *Salmonella*. Reproduced from Grimont and Weill (2007).

Species	**S. *enterica***						**S. *bongori***
Subspecies	*enterica* (I)	*salamae* (II)	*arizonae* (IIIa)	*diarizonae* (IIIb)	*houtenae* (IV)	*indica* (VI)	
Dulcitol	+	+	-	-	-	d	+
ONPG (2 h)	-	-	+	+	-	d	+
Malonate	-	+	+	+	-	-	-
Gelatinase	-	+	+	+	+	+	-
Sorbitol	+	+	+	+	+	-	+
Growth with KCN	-	-	-	-	+	-	+
L(+)-tartrate[(a)]	+	-	-	-	-	-	-
Galacturonate	-	+	-	+	+	+	+
γ-glutamyltransferase	+(*)	+	-	+	+	+	+
β-glucuronidase	d	d	-	+	-	d	-
Mucate	+	+	+	- (70 %)	-	+	+
Salicine	-	-	-	-	+	-	-
Lactose	-	-	- (75 %)	+ (75 %)	-	d	-
Lysed by phage O1	+	+	-	+	-	+	d
Usual habitat	Warm-blooded animals		Cold-blood animals and the environment				

(a) = *d*-tartrate. (*) = Typhimurium d, Dublin -. + = 90 % or more positive reactions. - = 90 % or more negative reactions. d = different reactions given by different serovars.

The current consensus is that the genus *Salmonella* consists of two species, *S. enterica* and *S. bongori*. *S. enterica* is divided into five subspecies based upon biochemical tests (Table 1) and serotyping is used for the differentiation of isolates beyond the subspecies level. Serovars are distinguished on the basis of the somatic (O) and flagellar (H1 and H2) antigens. A capsular polysaccharide, the Vi antigen, is also present on a limited number of serovars including Typhi and Dublin. The list of designated serovars and their antigenic formulae, now known as the Le Minor-Kauffmann White Scheme, is maintained by the WHO Collaborating Centre for Reference and Research on *Salmonella* at the Pasteur Institute in Paris (Grimont and Weill, 2007). The total number of reported serovars for all subspecies currently stands at 2,610 and continues to grow (Guibourdenche *et al.,* 2010). Serovars belonging to subspecies I have retained their common names, due to their familiarity with clinical practitioners, and are formally presented as *Salmonella enterica* subspecies *enterica* serovar Enteritidis. Those serovars belonging to subspecies other than *enterica* are designated by antigenic formulae; (i) subspecies numeral, (ii) O antigen followed by a colon, (iii) Phase 1 H antigen followed by a colon and (iv) Phase 2 H antigen (e.g. *S.* IIIa 50:g,z_{51}:-). In practice, many scientists, clinicians and physicians continue to use a simplified nomenclature omitting the subspecies epithet as the majority of infections in both humans and animals are caused by serovars belonging to subspecies *enterica*.

Two principle clinical syndromes are associated with infection by *Salmonella*; typhoid fever and gastroenteritis. Typhoid fever is a protracted systemic illness that results from infection with the

exclusively human pathogens, *S.* Typhi and *S.* Paratyphi. Typhoid is characterised by an array of clinical manifestations including fever, abdominal pain and transient diarrhoea. The pathological features of typhoid fever are mononuclear cell infiltration and hypertrophy of the reticulo-endothelial systems including the intestinal Peyer's patches, mesenteric lymph nodes, spleen and bone marrow arising from the intracellular invasion and dissemination of the bacillus. In the absence of treatment, mortality ranges between 10 and 15 % (Parry *et al.,* 2002). Non-typhoidal infections by *Salmonella* serovars other than Typhi and Paratyphi are generally self-limiting with clinical manifestations ranging from mild to severe gastroenteritis. Like many other infections by pathogenic bacteria, the susceptibility, severity and predisposition to serious complications upon infection by *Salmonella* are dependent upon a number of intrinsic host factors. Associated risk factors include age, immunosuppressive drugs, the presence underlying medical states (morbidities) and an altered endogenous bowel microflora resulting either from antibiotic therapy or from surgical procedures (Acheson and Hohmann, 2001). The incubation period varies depending upon these host factors, the causative serovar and size of the infectious dose ingested (Blaser and Newman, 1982). Patients typically present with headache, nausea, vomiting, fever, diarrhoea and abdominal cramps. In a small proportion of cases further complications arise including bacteraemia, gastrointestinal bleeding and focal infections (Acheson and Hohmann, 2001). The development bacteraemia, potentially leading to bacterial endarteritis and or endocarditis, is associated almost exclusively with the presence of underlying co-morbidities (Laupland *et al.,* 2010). Focal infections may occur at virtually any anatomical site, arising from dissemination by intra-cellular invasion or bacteraemia. Specifically, focal infections may lead to osteomyelitis, polyarticular reactive joint disease, splenic abscesses, CNS infection, meningitis and urinary tract infection (Acheson and Hohmann, 2001). Whilst most non-typhoidal *Salmonella* infections are transient and self-limiting, it has been demonstrated that the bacteria may be detected for a period after the cessation of symptoms. The median duration of faecal shedding is reported to be about one month in adults and over seven weeks in children under five years of age (Buchwald and Blaser, 1984).

Transmission of *Salmonella* to humans is primarily associated with the ingestion of a wide variety of contaminated foods but may also arise by contact with animals, contaminated water and infected individuals (Hanning *et al.,* 2009). Upon entry to the gastrointestinal tract, *Salmonella* preferentially invade microfold (M) cells overlying the lymphoid follicles of Peyer's patches facilitated by the *Salmonella* pathogenicity island 1 (SPI-1) encoded type 3 secretion system (Jones *et al.,* 1994, Wallis and Galyov, 2000). Type 3 secretion systems (T3SS) act as a molecular needle, facilitating the translocation of an array of effector proteins into the host cell cytosol. Dissemination away from the gastro-intestinal tract/mucosa occurs by uptake of the bacteria by CD18+ phagocytes and intestinal macrophages (Vazquez-Torres *et al.,* 1999). The ability of *Salmonella* bacteria to promote uptake by CD18+ phagocytes and subsequently survive within the phagosome is dependent on a second T3SS

encoded within *Salmonella* Pathogenicity Island-2 (Hensel *et al.,* 1998, Cirillo *et al.,* 1998). After uptake by $CD18^+$ phagocytes or macrophages, the acidic environment of the phagosome causes the induction of regulatory systems promoting intracellular survival including surface remodelling and induction of the SPI-2 T3SS. The SPI2 T3SS effectors are translocated across the phagosomal membrane and result in remodelling of the phagosome, cytoskeletal rearrangements, alterations to gene expression and mitigation of the oxidative burst. These protein allow *Salmonella* to survive within the host cell, where the phagosome is termed the *Salmonella*-containing vacuole (Haraga *et al.,* 2008). A further action of the SPI2 T3SS effectors is the inhibition of antigen presentation by dendritic cells to naïve $CD4^+$ T-cells. (Tobar *et al.,* 2006), thereby limiting the host innate (adaptive) immune response (van Diepen *et al.,* 2005). Systemic infection is characterised by dissemination and colonisation of *Salmonella* to the liver, spleen and lymph nodes. A further aspect of *Salmonella* pathogenesis is the establishment of an asymptomatic carrier state that serves as a reservoir of infection. Asymptomatic carriers of S. Typhi discontinuously shed the bacilli thereby facilitating the dissemination of this pathogen into the environment.

Serovars of *Salmonella* can be coarsely differentiated as host-adapted, host-restricted or promiscuous based upon their ability to colonise and cause disease in related and unrelated species (Uzzau *et al.,* 2000). Host-restricted serotypes typically cause systemic disease in a limited number of related species. Those serotypes frequently associated with a specific host and infrequently in unrelated hosts are termed host-adapted, whilst promiscuous serotypes are defined as those capable of causing disease in a wide range of unrelated host species. Over the past decade a number of *Salmonella* genomes have been sequenced and from subsequent comparisons, the underlying genetic and phenotypic characteristics contributing to host specificity and promiscuity are starting to be elucidated. Anjum *et al.,* (2005) summarise the genus *Salmonella* as comprising a composite gene pool, within which distinctive variants (serovars) have arisen, possessing different degrees of specialisation by the acquisition, loss or mutation of different genes.

Epidemiological data shows that the majority of non-typhoidal infections by *Salmonella* are limited to relatively few serovars, belonging predominantly to subspecies *enterica* and serogroups A, B, C_1, C_2, D and E (ECDC, 2010, Uzzau *et al.,* 2000). In the US, the annual economic burden associated with medical care and lost productivity due to Salmonellosis is estimated at several billion dollars (Voetsch *et al.,* 2004). In 2009 over 49,000 laboratory confirmed cases of *Salmonella* in humans were reported in the US while 109,885 confirmed cases were reported in the EU for the same period. The increased resistance of *Salmonella* isolates to antibiotics, particularly extended spectrum cephalosporins and fluoroquinolones, necessitates the identification and investigation of alternative strategies to conventional antimicrobial therapy (Velge *et al.,* 2005). The bacteriophages, either as whole virions or derivatives of their genes represent one such alternative path for controlling this pathogen.

1.4 Bacterial Bioluminescence

The ethereal qualities of bioluminescence has always attracted and intrigued human kind, evidenced by a wealth of historical records spanning some 3000 years (Lee, 2008, Newton, 1957). The light emitting enzymes responsible for bioluminescence, termed luciferases by the French physiologist Raphael Dubois, have been characterised in both eukaryotic and prokaryotic organisms. The term "luminescenz" was first coined by Elihard Wiedemann (Harvey, 1957) and literally, bioluminescence means “living light” comprising the Greek words bios for “living” and lumen for “light”. Luciferases from different phyla have evolved independently, made evident by markedly different tertiary and quaternary structures, substrate requirements, reaction kinetics and wavelength of emitted light. The single common requirement of all luciferase systems is oxygen (O_2), a characteristic first demonstrated in the 17th century by Robert Boyle (1672), long before the discovery of bacteria. Although many luminescent species exist in nature (Widder, 2010, Wilson and Hastings, 1998), luciferases from six sources have been widely studied (Table 2).

Table 2. Sources and characteristics of Luciferases in nature.

Source	Requirements	Peak Emission	Structure
Bacterial *Various*	Flavin mononucleotide Fatty acid aldehyde O_2	490 nm	Heterodimer, 77 kDa
Firefly *Photinus pyralis*	D-Luciferin ATP O_2	562 nm	Monomer, 62 kDa
Click Beetle *Pyrophorus plagiophthalamus*	D-luciferin ATP O_2	Green: 537 nm Red: 613 nm	Monomer, 62 kDa
Ostracod crustacean *Cypridinia noctiluca*	Cypridina luciferin	465 nm	Monomer, 62 kDa
Cocepod crustacean *Gaussia princeps*	Coelenterazine O_2	460 nm	Monomer, 35 kDa
Sea pansy *Renilla reniformis*	Coelenterazine O_2	480 nm	Monomer, 19 kDa

Of the different luciferases, the bacterial system is best understood both in terms of regulation and biochemistry. In bacteria, luciferase enzymes are FMN-linked alkanal monooxygenases [E.C. 1.14.14.3] and are found within eleven species comprising five genera; *Aliivibrio*, *Vibrio*, *Photobacterium*, *Shewanella* and *Photorhabdus* (Ulitzer, 2003). Light production is known only within the eubacteria, specifically the Gram-negative γ-proteobacteria. With the sole exception of the wound-colonising bacterium *Photorhabdus luminescens*, bioluminescent bacteria are exclusively marine in origin where they occupy a diverse range of ecological habitats and symbioses (Meighen, 1991). Various functions have been proposed to explain the symbioses of luminescent bacteria with marine organisms. These include illumination of the surrounding environment, avoidance of

predation (through flashing and counter-illumination), defence (using light as a decoy), communication and the attraction of prey, the latter exemplified by the *Photobacterium*-containing lure of the deep sea Angler fish (Haddock *et al.,* 2010). In many cases the bacteria colonise specialised light emitting organs, termed photophores. Many marine organisms possess photophores containing bioluminescent bacteria including members of Sepiolid and Lolliginid squid and various fish.

Bioluminescence caused by free-living bacteria in the sea can encompass vast areas given appropriately high concentrations of bacteria, a phenomenon termed milky seas. Recently, Miller *et al.,* (2005) corroborated reports from merchant ships off the east coast of Africa with satellite imagery, providing the first geographic identification of this phenomenon from space (Figure 4).

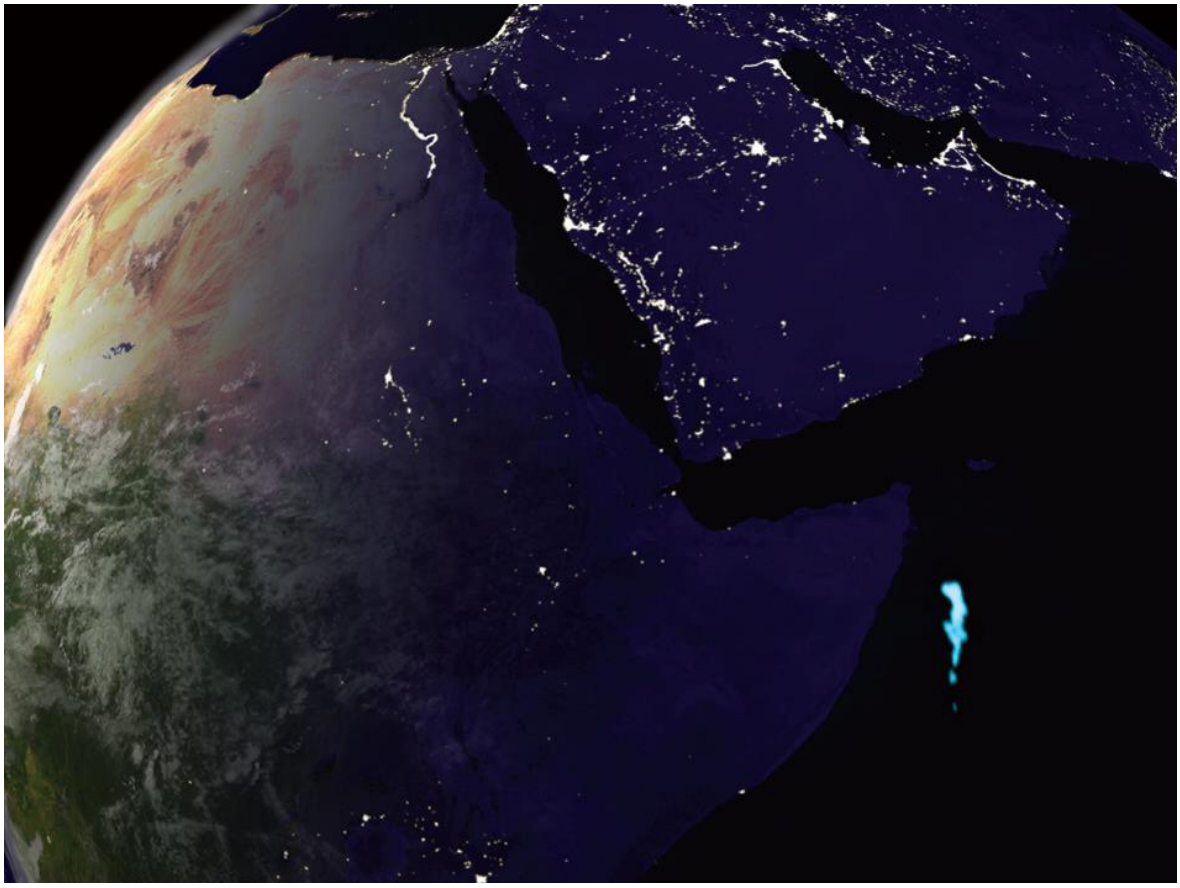

Figure 4. Enhanced satellite image of a bioluminescent milky sea projected onto the Blue Marble (NASA). Reproduced with permission from Haddock *et al.,* (2010).

Luminescence in bacteria is conferred by a contiguous sequence of DNA, the *luxCDABE* operon (Meighen, 1991) and the order of lux genes is conserved within all characterised bacterial systems. The most widely studied of these luciferases originate from the species *Vibrio harveyi, Aliivibrio fischeri* (previously *Vibrio fischeri*), *Photobacterium phosphereum, Photobacterium leiognathi* and *Photorhabdus luminescens*. The *luxAB* genes encode the two subunits; α (40.11 kDa) and β (36.35 kDa), which comprise the 76 kDa hetero-dimeric luciferase enzyme (Meighen. 1990). A fatty

acid reductase, the multi-enzyme complex responsible for biosynthesis and turnover of the fatty acid aldehyde substrate is encoded by three genes, *luxC*, *luxD* and *luxE*. These three genes code for a reductase, a transferase and a synthetase of molecular weights 54 kDa, 42 kDa and 32 kDa respectively (Boylan *et al.,* 1988). Nucleotide sequences of the *luxA* and *luxB* genes have been determined for *V. harveyi*, *A. fischeri* and *P. phosphorum*, *P. leigionathi* and *P. luminescens* (Cohn *et al.,* 1985, Johnston *et al.,* 1986, Miyamoto *et al.,* 1986, Johnston *et al.,* 1990, Xi *et al.,* 1991). Bioinformatics evidence suggests that the α and β subunits arose by gene duplication within a common ancestral species, as approximately 30 % nucleotide sequence homology exists between the two subunits independent of the bacterial source (Cohn *et al.*, 1985, Johnston *et al.*, 1986, Szittner and Meighen, 1990). The 3-D structure of *A. fischeri* luciferase has been determined at low (2.7 Å) and high (1.5 Å) resolution by x-ray crystallography (Fisher *et al.,* 1996). These data show that the α and β subunits are non-covalently bound and that each folds into a single domain $(\beta/\alpha)_8$ barrel conformation (Figure 5).

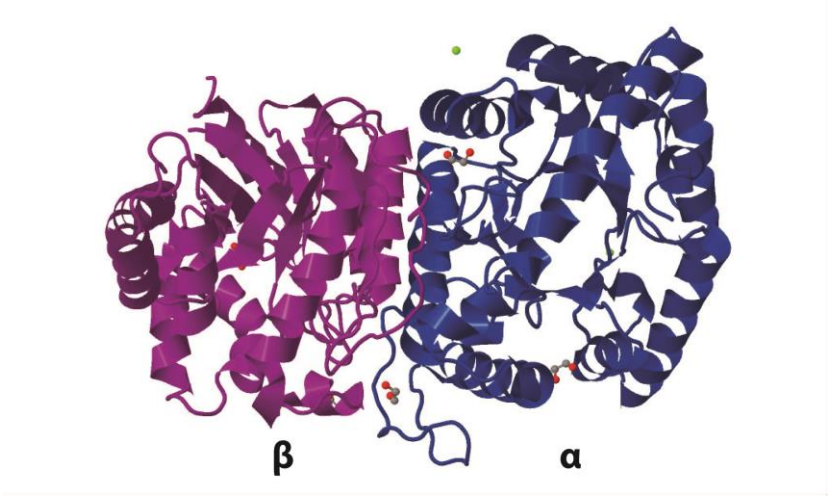

Figure 5. Ribbon cartoon of the quaternary structure of *Vibrio harveyii* bacterial luciferase. The alpha subunit is shown in blue and the beta subunit in purple. The image was rendered with Jmol Version 12.2.15 using Protein Databank Entry: 1LUC.

1.4.1 Biochemical characteristics of Bacterial Luciferases

Bacterial luciferase catalyses the oxidation of reduced flavin mononucleotide ($FMNH_2$) using molecular O_2 and a long chain aliphatic aldehyde, yielding FMN, carboxylic acid and a photon of blue-green light (Equation 1). The reaction is highly exergonic with the primary energy source for light supplied by conversion of aldehyde to fatty acid (60 kcal $Enstein^{-1}$).

Equation 1. Bacterial luciferase reaction.

$$FMNH_2 + RCHO + O_2 \rightarrow FMN + H_2O + RCOOH + h\nu\ (\lambda\ 490\ nm)$$

Two assays have been described for the quantification luciferase enzymatic activity which differ in the method of FMN reduction (Hastings *et al.,* 1978). Due to the rapid oxidation of flavin in these assays and slow decay of the EFO-A complex, the luciferase enzyme undergoes only a single turnover under these assay conditions, a feature which has allowed detailed investigation of the kinetics of these enzymes (Gibson and Hastings, 1962). The complex bioluminescence reaction (Figure 6) depends upon the sequential formation of enzyme-flavin intermediates (Hosseinkhani *et al.,* 2005). Firstly, luciferase (E) reversibly binds $FMNH_2$ via the alpha subunit to form the Enzyme-$FMNH_2$ (EF) complex. The enzyme-flavin complex then reacts rapidly with O_2 forming a C4a-peroxy-flavin (EFO) (intermediate II). The EFO complex may either decompose to yield oxidized FMN and H_2O_2 or interact with an aliphatic aldehyde (A), supplied by the LuxCDE fatty acid reductase complex, to form the tetrahenal intermediate (EFO-A). Decay of the EFO-A complex occurs by either dissociation of the aldehyde followed by dark pathway decomposition or upon completion of the reaction to yield blue-green light with an emission maximum at 490 nm, an aliphatic carboxylic acid and oxidised flavin. The dark- and light-side reactions possess distinct rate constants, termed kD and kL, respectively (Hastings and Balny, 1975).

A. Simplified *in vitro* kinetic model

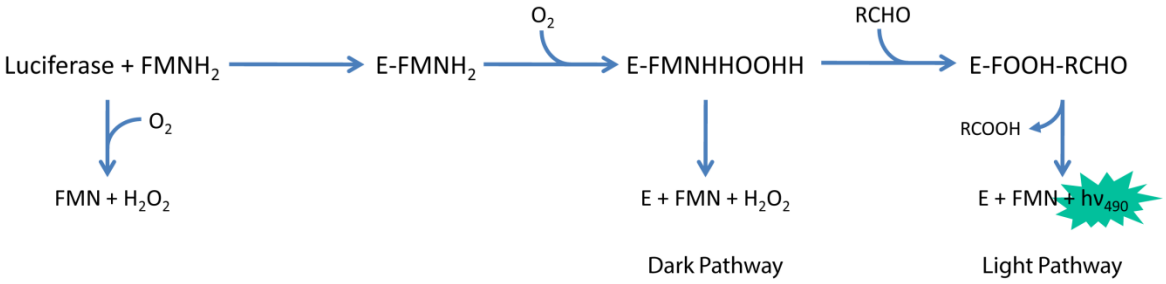

B. Simplified *in vivo* kinetic model

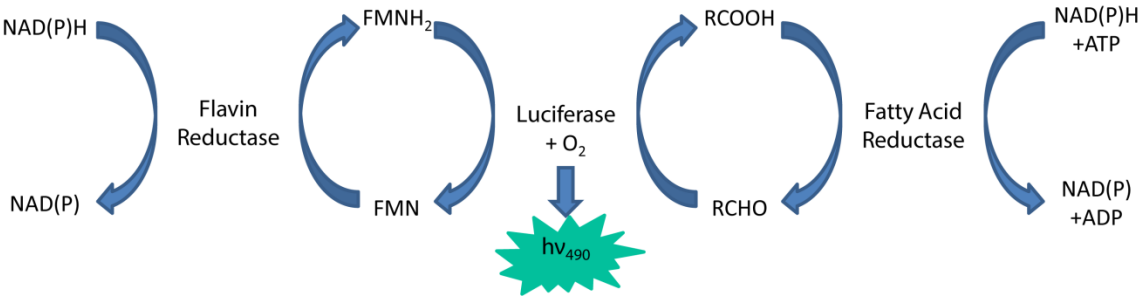

Figure 6. Simplified kinetic models of the bacterial luciferase reaction (A) *in vitro* and (B) *in vivo*. Blue arrows denote the conversion of substrate to product. Light emission is shown within the green star. Adapted from Campbell and Baldwin (2009).

The aldehyde substrate *in vivo* is proposed to be the 14-carbon tetradecanal, derived from Co-Acyl Enzyme A, based upon analysis of lipid extracts and specificity of the fatty acid reductase system

(Ulitzur and Hastings, 1979, Wall *et al.,* 1984). The net reaction involves reduction of fatty acid with the oxidation of NADPH and cleavage of ATP to AMP and PPi, catalysed by the *luxCDE* gene products. Biosynthesis of the long chain aldehyde is catalysed by the action of the *luxCDE* gene products. LuxC and LuxE are required for the reduction of myristic acid to myristic aldehyde while LuxD transports the fatty acid between the synthase and reductase complexes (Meighen, 1991).

The second substrate require for bioluminescence is Flavin mononucleotide (FMN). FMN belongs to the family of flavoproteins whose members all contain a nucleic acid derivative of riboflavin. Reduced FMN is provided by species specific oxidoreductases; Frp in *A. harveyi*, Frase-I in *V. fischeri* and Fre in *Escherichia coli* (Campbell and Baldwin, 2009). These enzymes show broad substrate specificity but little sequence homology despite their functional similarities. Flavin mononucleotide plays an important role in electron transport since it can accept and donate one or two electrons and is involved in initial electron transfer with bacterial complex I leading to the oxidation of NADH with reduction of coenzyme Q (Friedrich *et al.,* 1995). Two models are proposed for the mechanism of transfer of the flavin substrate from oxidoreductase to luciferase. The first proposes that a stable complex is formed between the oxidoreductase and luciferase (Lei and Tu, 1998). However, formation of a stable complex would necessitate the presence of specific recognition domains in the luciferase structure. The flavin oxidoreductase of *E. coli* shows little homology with that of *A. fischeri* yet luciferase activity is adequately expressed in transformed cells, apparently discounting the interaction model. A second model proposes that transfer of the flavin substrate occurs by free diffusion (Campbell and Baldwin, 2009).

1.4.2 Luciferases of bioluminescent bacteria

Luciferases encoded by different bacteria have been differentiated by turnover rate, thermostability and rates of decay over time from *in vitro* assays of the purified enzymes. Luciferases from the genus *Photobacterium* are characterised as possessing a rapid decay rate whereas those from *Vibrio* and *Photorhabdus* exhibit slow decay rates. The structural region responsible for this trait has been identified through the creation of chimeric luciferases. Chimeric luciferases were prepared by substituting regions of *luxA* in one bacterium with the same region from another. Substitution of a 67 amino acid sequence in the central region of LuxA from *P. luminescens* with the corresponding sequence from *P. phosphoruem* resulted in a chimera exhibiting a significantly greater decay rate than the wild-type enzyme (Valkova *et al.,* 1999). Hosseinkhani *et al.,* (2005) furthered these observations by demonstrating that substitution of the glutamic acid residue at position 175 of LuxA to glycine results in the conversion of the LuxAB of *P. luminescens* from a slow to rapid decay rate, suggesting that the Glu175 residue is involved in aldehyde binding and turnover of intermediates.

The terrestrial bacterium *Photorhabdus luminescens* luciferase possesses markedly greater thermostability than luciferases of marine bacteria. The luciferase from *V. harveyi* is rapidly

denatured at temperatures of 45°C whereas *P. luminescens* luciferase has a half-life of greater than 3 hours at this temperature (Szittner and Meighen, 1990). Thermal stability is conferred by the α subunit, as demonstrated by hybrid luciferases containing combinations of *luxA* and *luxB* genes from *V. harveyi* or *P. luminescens* (Li *et al.,* 1993). For temperature-critical applications where the required growth temperature is greater than 30°C, the *P. luminescens lux* cassette must be considered the bioluminescent system of choice for the transformation of bacterial reporters.

1.4.3 Bioluminescent bacterial reporters

Bacterial luciferases have been used extensively for the generation of biosensors, for studies of gene expression and transcriptional regulation. A bioluminescent phenotype may be conferred by the introduction of either the *luxAB* genes, or the entire *luxCDABE* operon using a suitable vector and transformation method. The *lux* genes may be integrated into the bacterial chromosome or encoded on plasmids. Expression may be controlled using a promoter allowing constitutive expression or linked to a specific promoter for expression under conditions of transcriptional activation. As such, use of the *lux* genes presents two complementary methods by which data may be obtained for bacterial metabolism, stress responses or gene expression.

Vectors encoding *luxAB* alone generate luminescent bacteria upon addition of a long chain aldehyde. Aldehyde is required because an appropriate fatty-acid reductase is not encoded by the vast majority of microorganisms (Meighen, 1991, Meighen and Dunlap, 1993). Luciferase activity occurs in the presence of aldehydes of greater than 8 carbons *in vitro* (Francisco *et al.,* 1993) and although quantum yields obtained with different aldehydes are similar, bacterial luciferases exhibit decreasing values of Km with increasing aldehyde chain length. Whilst the greatest luminescent response is achieved with tetradecanal *in vitro*, luciferases from different bacterial sources show different specificities to shorter-chain aldehydes. Blisset & Stewart (1989) demonstrated that, unlike tetradecanal, no appreciable diffusion barrier to shorter chain aldehydes such as decanal, dodecanal and nonanal, exists in either Gram positive or Gram negative bacteria.

In contrast, transformation using the entire *luxCDABE* operon generates luminescent bacteria without the need for exogenous addition of substrate, but requires that sufficient $FMNH_2$ is present within the bacterial cell for high activity. Pre-cursors for aldehyde biosynthesis catalysed by the LuxCDE fatty-acid reductase complex are present in most, if not all, bacterial species (Meighen, 1991). Use of the entire *lux* operon provides the additional advantage that a single sample population may be monitored continuously without interruption, whether expression of the operon is constitutive or inducible.

The majority of bioluminescent reporters have been generated using plasmid constructs and transposon mutagenesis, either for constitutive or promoter-linked expression. Under such

strategies, the bioluminescent phenotype is maintained by the expression of a selective marker, usually genes conferring resistance to an antibiotic. However, experimental design may dictate that addition of selective agents to maintain plasmid expression is undesirable. In such situations the risk exists that plasmid loss may occur. While transposon mutagenesis may avoid effects of varying gene dosage and plasmid loss, such an approach may also result in insertions that alter the subject's normal cellular physiology or phenotype. Sensitivity may also be reduced due to the presence of only a single copy of the reporter within the bacterial chromosome. The issue of gene inactivation may be addressed by site-directed insertion, but this approach requires careful identification and characterisation of appropriate target sites.

To date more than 30 different genera, both Gram positive and Gram negative, have been transformed to express the lux genes (Meighen, 1991). In contrast to Gram negative bacteria, the native *luxCDABE* operon of *A. fischeri*, *V. harveyi* and *P. luminescens* is poorly expressed in many Gram-positive bacteria. Early Gram-positive transformants exhibited weak light emission due to low levels of endogenous FMNH2 and fatty acid aldehyde production and transformation of this group was limited primarily due to differing genetics and gene transcription mechanisms. Several strategies have been used to approach this problem. Light emission was improved by rearrangement of gene order to *luxABCDE*, and by the addition of enhanced promoters upstream of *luxA*, *luxC* and *luxE* (Qazi *et al.*, 2001a, Beard *et al.*, 2002a). Work continues seeking to improve expression the *lux* genes in Gram positive bacteria. Recent developments include improved expression in *S. aureus* (Mesak *et al.,* 2009) and the development of a synthetic lux reporter where modifications, based upon codon usage in *Streptomyces coelicolor*, have allowed expression high GC content bacteria (Craney *et al.,* 2007). In addition, Andreu *et al.,* (2010) have reported the first successful expression of the entire *lux* operon in *Mycobacterium tuberculosis*.

1.4.4 Applications of bioluminescent bacterial reporters

Bacterial luciferase reporters have developed into versatile tools which have been exploited by a wealth of different applications. Applications of bacterial luciferases include reporter gene assays, efficacy of antimicrobials (antibiotics and biocides), detection of compounds in environmental samples and as traps to identify DNA fragments with promoter activity in clone libraries (Waidmann *et al.,* 2011).

Three strategies have been developed using bacterial luciferases for determining susceptibility to antibiotics; the lysis test, the induced test and the phage-coupled test (Ulitzur, 1986). The lysis test ascertains the relative decrease in bioluminescence of a culture exposed to an antibiotic compared to one grown in the absence of the antibiotic (Ulitzur, 1986). Using either dark or inducer-requiring mutants the activity antibiotics inhibiting protein synthesis, for example aminoglycosides or macrolides, may be quantified. In the presence of antibiotics inhibiting protein synthesis, *de novo*

production of luciferase is retarded when compared to control cultures grown in the absence of antibiotic (Ulitzur and Weiser, 1981). In the phage-coupled antibiotic assay the addition of an antibiotic inhibiting protein synthesis, DNA or RNA replication prevents completion of the bacteriophage lytic cycle hence 'rescuing' the bioluminescent cell. In the absence of such antibiotics the cells lyse and levels of bioluminescence fall (Ulitzur, 1986). Continuous measurement of growing cultures of constitutively bioluminescent bacteria exposed to an antimicrobial agent has been used to determine pharmacodynamics of antibiotics *in vitro* (Alloush *et al.*, 2003, Beard *et al.*, 2002b, Salisbury *et al.*, 1999). This approach allows the determination of killing or inhibition kinetics as well as recovery of bacterial populations exposed to sub-lethal concentrations of antibiotics. In a similar manner, highly bioluminescent bacterial reporters have also been employed to determine the efficacy of biocide-killing in liquids and on environmental or organic surfaces (Robinson *et al.,* 2011, Walker *et al.,* 1992, Jones *et al.,* 2002).

Using the bacterial lux operon in conjunction with a regulatory gene or promoter responsible for the induction of enzymes involved in the degradation of a specific substance has been shown to allow detection of a wide range of compounds within the environment. Examples include mercury, lead, cadmium and napthalene (Tauriainen *et al.,* 1998, Selifonova *et al.,* 1993, Heitzer *et al.,* 1994). Similarly, fusions with promoters involved in DNA repair such as *uvrA, recA* and *alkA* have been used to detect the presence of genotoxic agents in the environment (van der Lelie *et al.,* 1997, Ulitzur and Barak, 1988, Biran *et al.,* 2010). Commercial assays utilising bioluminescent reporters to determine biological oxygen demand (BOD) and assimilable organic carbon (AOC) are available (CheckLight, Israel).

Bacterial pathogens require the expression of multiple genes within their host to establish a successful infection. Gene products contributing towards the survival within and establishment of a disease state are termed virulence factors or virulence-associated genes. Fusions of the bacterial luciferase genes with promoters regulating virulence factors have been used to monitor the induction and expression of virulence factors by bacterial pathogens in batch culture or in co-culture with mammalian tissues (Pfeifer *et al.*, 1999, Park *et al.*, 1992, Qazi *et al.*, 2001b, Riedel *et al.*, 2009).

The examples presented here are but a small representation of the myriad of applications and studies that have used bacterial luciferases as a reporter system. The vast number of reports within the literature is a testament to the versatility and utility of this system.

1.4.5 Bioluminescence imaging

Traditionally, applications employing bioluminescent bacterial reporters have been performed within tube or microplate format luminometers or scintillation counters. More recently the availability of intensified charge-coupled device (iCCD) and electron multiplying (EMCCD) imaging technologies,

initially pioneered for astronomical studies, has provided the ability to study the spatial and temporal distribution of light emission within experimental models, a process termed bioluminescence imaging (BLI). The visual dimension of image analysis allows localisation and analysis of specific spatial regions of interest within the applied experimental model.

The instrumentation required for BLI is comprised of four essential components, a sensitive imaging detector coupled to a macro lens contained within a light tight imaging chamber and a software facility for imaging and device control. Optional components may include an illumination source for bright-field imaging or for the excitation of fluorophores, a computer controlled object stage and temperature control.

The sensitivity and spatial resolution of bioluminescence imaging systems is largely dependent upon four elements. The imaging sensor represents the first element. Three technologies are widely used for scientific imaging: iCCD, EMCCD and complementary metal-oxide semiconductor (CMOS) sensors. Relevant sensor characteristics include quantum efficiency, number of pixels and pixel dimensions. A second critical element comprises the noise characteristics of the system. Within BLI systems noise comprises dark current noise, shot noise and readout noise. Read out noise is defined as the noise generated during charge-voltage conversion at the CCD amplifier while dark current noise arises due to the thermal generation of electron-hole pairs in the photodiode. Thermal noise is reduced to negligible levels by cooling of the sensor, usually to below -80^{o}C. Shot noise comprises the variation of photons reaching the detector, either from the source of the bioluminescent signal, or the presence of extraneous background light. A final consideration is the spectral characteristics of the matrix or tissue to be examined, including but not limited to, the degree of associated reflectance, absorbance and scattering.

The study and validation of BLI applied to *in vivo* models of bacterial infection was first demonstrated by Contag and co-workers (1995) using strains of *Salmonella* Typhimurium transformed to express the *lux* operon. They and others have subsequently extended this approach to include studies of infection by bioluminescent Gram positive and Gram negative bacterial reporters within a multitude of animal infection models. The imaging of bioluminescent bacteria *in vivo* requires more rigorous validation as the light source is located at depth within the matrix or tissue. Under such conditions emitted photons are subject to the effects of absorption and scattering, both of which are a function of the matrix or tissue under investigation. In tissues shorter wavelengths show greater absorption by tissues than wavelengths >600 nm, primarily due to the presence of haemoglobin which exhibits strong absorbance at blue-green wavelengths. At wavelengths greater than 600 nm scattering becomes the predominant effect (Zhao *et al.,* 2005). The peak spectral emission of bacterial luciferases, at 490 nm, falls within the absorbance region of haemoglobin which results in reduced sensitivity in comparison to firefly or colentrazine luciferase reporter systems. However, this

reduction in sensitivity is offset as bacterial reporters expressing the lux operon have no requirement for the exogenous addition of substrate.

In the relatively short period of time since its introduction, BLI has become an invaluable technique for the steady state imaging of bioluminescent bacterial reporters in a wide variety of experimental models (Table 3). The ability to locate, track and visualise bacteria in real time is of enormous value and bioluminescent imaging presents a number of significant advantages when compared to traditional in vivo models of bacterial infection. Firstly, infection may be monitored longitudinally and in the presence of intact and functional organ systems. Secondly, the measurement of light emission may be performed using a single animal rather than from individuals within a cohort, leading to the generation of statistically improved data sets (Rocchetta *et al.*, 2001). Moreover, there is a reduced requirement for animal sacrifice and tissue harvesting for *ex vivo* analyses which in itself represents a time-consuming process and potentially limits large scale investigations. For applications of BLI involving animal models, bioluminescent bacterial reporters may be used to monitor the dissemination and localisation of bacteria in tissues and organs, expression of virulence factors and the efficacy and pharmacodynamics of antimicrobial agents *in vivo*. Away from animal models, BLI has been used to ascertain the survival and recovery of bacterial pathogens on food, biocide efficacy and the formation and development of biofilms.

Table 3. Selected microbiological applications of bioluminescence imaging. Adapted and updated from Close *et al.,* (2010b).

Organism	Application	References
Escherichia coli	Detection in foods and water	(Siragusa *et al.*, 1999) (Ripp *et al.,* 2008)
	Colonisation and survival on foods	(Siragusa *et al.*, 1999) (Warriner *et al.,* 2001)
	Colonisation in mice	(Foucault *et al.,* 2010)
	Cutaneous wound infections and antimicrobial therapy	(Jawhara and Mordon, 2004) (Hamblin *et al.*, 2002) (Rocchetta *et al.*, 2001)
Salmonella	Food safety	(Karsi *et al.,* 2008)
	Colonisation and dissemination	(Contag *et al.,* 1995)
	Intracellular invasion	(Piwnica-Worms *et al.,* 2008)
	Age related susceptibility	(Burns-Guydish *et al.,* 2005)
	Role of nitric oxide in cancer cell killing	(Barak *et al.,* 2010)
	Vaccines & neonates	(Burns-Guydish *et al.,* 2007)
	Thermal inactivation and recovery on foods	(Lewis *et al.,* 2006b)
Pseudomonas	Wound infection model and antimicrobial therapy	(Thorn *et al.,* 2007) (Hamblin *et al.,* 2003)
	Parallel plate biofilm formation	(Mittelman *et al.,* 1992)
Streptococcus pneumoniae	Lung infection and antimicrobial therapy	(Francis *et al.,* 2001)
	Dissemination	(Kadurugamuwa *et al.,* 2005)
	Antimicrobial therapy	(Beard *et al.*, 2002b)
Staphylococcus aureus	Colonisation and dissemination *in vivo*	(Francis *et al.,* 2000)
	Biomaterial/implant associated infections	(Engelsman *et al.,* 2009)
	Catheter infection and antimicrobial therapy	(Kadurugamuwa *et al.,* 2003)
	Intracellular replication	(Qazi *et al.,* 2004)
	Antimicrobial therapy *in vivo*	(Xiong *et al.,* 2005) (Mortin *et al.,* 2007)
	Antimicrobial treatment of foreign body and wound infection	(Kuklin *et al.,* 2003)
	Antimicrobial therapy of vascular grafts	(Lorenz *et al.,* 2011)
	Hla expression	(Steinhuber *et al.,* 2008)
	Photodynamic therapy of burn wounds	(Lambrechts *et al.,* 2005)
Listeria monocytogenes	Dissemination, virulence factor expression	(Bron *et al.,* 2006)
	Colonisation and replication within murine gall bladder	(Hardy *et al.,* 2004) (Hardy *et al.,* 2006)
	Persistence within the bone marrow	(Hardy *et al.,* 2009)
	Improved reporter construct	(Riedel *et al.,* 2007)
Acinetobacter baumanni	Photodynamic therapy of burns	(Dai *et al.,* 2009)
Bacillus anthracis	Spore germination *in vivo*	(Sanz *et al.*, 2008a)
Yersinia enterolitica	Colonisation and dissemination *in vivo*	(Trček *et al.,* 2010) (Gonzalez *et al.,* 2012)
Citrobacter rodentium	Colonisation and dissemination *in vivo*	(Wiles *et al.,* 2004)
Mycobacterium spp	Optimisation of reporter constructs.	(Andreu *et al.,* 2010) (Heuts *et al.,* 2009)

To date very few studies have investigated the effects of co-incubating bioluminescent bacterial reporters and bacteriophages in either liquid or solid environmental matrices. Since bioluminescence is intrinsically linked to bacterial metabolism and thus viability, these reporters present themselves as a powerful tool to monitor the effects of bacteriophage-mediated lysis of bacterial populations. By

using bioluminescence imaging these interactions may also be able to be resolved spatially as well as temporally.

Chapter 2 Materials and Methods

2.1 Bacterial strains and plasmids

Bacterial strains (Table 4) were obtained from the culture collections: the National Collection of Type Cultures, UK (NCTC); the American Type Culture Collection, USA (ATCC); the National Collection of Industrial, Food and Marine Bacteria, UK (NCIMB); the Veterinary Laboratories Agency, UK (VLA) and Campden BRI (CBRI). Stock bacterial cultures were stored at -80^{o}C (Protect Cryovials, ProLab, UK). Working cultures were maintained on Luria Bertani (LB) or Tryptone soya (TSA) agar plates. For cultures transformed with plasmids, solid and liquid media were supplemented with either 10 μg ml^{-1} kanamycin (Km) or 10 μg ml^{-1} gentamicin (Gm) in order to maintain plasmid selection. *Escherichia coli* DH5α (NCTC 10418) was used as a host for the propagation of all plasmids. A complete listing of the plasmids used within this study is provided (Table 5).

Table 4. Bacterial strains used in this study.

No.	Isolate	Accession Number	Source
	***Salmonella enterica* serovar Enteritidis**		
1	*S.* Enteritidis	VLA S07533-07	-
2	*S.* Enteritidis PT 13	VLA S04967-07	Swine
3	*S.* Enteritidis PT1	CBRI 1937	Chicken
4	*S.* Enteritidis PT4	VLA S07544-07	Clinical isolate
5	*S.* Enteritidis	CBRI 1869	Chicken
6	*S.* Enteritidis	CBRI 1870	Chicken
7	*S.* Enteritidis	CBRI 1951	Egg
8	*S.* Enteritidis	CBRI 1944	Chicken
	***S. enterica* serovar Typhimurium**		
9	*S.* Typhimurium	VLA S07519-07	Environmental isolate
10	*S.* Typhimurium	VLA S07540-07	Animal tissue
11	*S.* Typhimurium	VLA S07541-07	-
12	*S.* Typhimurium DT104b	VLA S01523-08	Canine faeces
13	*S.* Typhimurium	CBRI 1960	Chicken
14	*S.* Typhimurium	CBRI 1962	Chicken
15	*S.* Typhimurium	CBRI 1005	Raw egg
16	*S.* Typhimurium	CBRI 1006	Sausage
17	*S.* Typhimurium	CBRI 1007	Chicken
	Other Serovars		
18	*S.* Agona	NCTC 11377	Cattle, Ghana
19	*S.* Brandenberg	VLA S07530-07	-
20	*S.* Braenderup	VLA S02130-08	-
21	*S.* Braenderup	VLA S07531-07	-
22	*S.* Concord	NCTC 6588	Avian
23	*S.* Crossness	NCTC 11059	Sewage
24	*S.* Derby	HPA	
25	*S.* Dublin	VLA S07539-07	-
26	*S. enterica* 4, 12: e, h: -	VLA S07521-07	Swine
27	*S. enterica* 6, 8: -: e, n, x	VLA S07523-07	-
28	*S. enterica* O-Rough: z10: -	VLA S07520-07	Unknown
29	*S. enterica* O-Rough: e, h: e, n, x, z15	VLA S07538-07	-
30	*S. arizonae* 6: 13, 14	NCTC 7308	spray-dried egg powder
31	*S.* Hadar	CBRI 1973	Turkey
32	*S.* Heidelberg	VLA S07546-07	-
33	*S.* Heidelberg	VLA S07529-07	-
34	*S.* Infantis	CBRI 1037	Prawns
35	*S.* Inverness	NCTC 6591	Human faeces
36	*S.* Jerusalem	NCTC 8146	-
37	*S.* Mbandaka	VLA S07524-07	-
38	*S.* Molade	VLA S07526-07	-
39	*S.* Montevideo	CBRI 1030	Animal feed
40	*S.* Napoli	NCTC 6853	Human
41	*S.* Newport	BRI 1938	Chicken
42	*S.* Orion var. 15+	VLA S07525-07	-
43	*S.* Panama	CBRI 1045	Mussels
44	*S.* Poona	NCTC 4840	Infant enteritis
45	*S.* Seftenberg	VLA S07528-07	-
46	*S.* Tennessee	NCTC 6388	-
47	*S.* Typhisuis	NCTC 347	-
48	*S.* Utrecht	NCTC 10077	-
49	*S.* Virchow	CBRI 1012	Chicken
50	*S.* Virchow	CBRI 1010	Chicken
	Other Gram-negative bacteria		
1	*Escherichia coli* Nissle 1917	Ardeypharm GmbH	Human faeces
2	*E. coli*	NCTC 10418	-
3	*E. coli* O157:H7 tox$^-$	NCTC 12900	-
4	*Pseudomonas aeruginosa* PAO1	ATCC 15692	Infected wound
5	*P. aeruginosa*	NCTC 13359	-
6	*Citrobacter freundii*	NCTC 6266	-
7	*Klebsiella aerogenes*	NCTC 9660	-

Table 5. Plasmids used in this study.

Plasmid	Description	Selective Marker	Reference
pGLITE	pBBR1MCS-2 derivative containing the *luxCDABE* operon of *Photorhabdus luminescens*	Kanamycin resistance cassette	(Parveen *et al.,* 2001)
pMCS5-LITE	pBBR1MCS-5 derivative containing the *luxCDABE* operon of *Photorhabdus luminescens*	Gentamicin resistance cassette	(Lewis *et al.,* 2006a)

2.2 Enumeration of bacteria

Plate counts of bacteria were performed using either the spread plate method or by use of a spiral plating system (WASP, Don Whitley Scientific, UK). Bacterial counts in cfu ml^{-1} were calculated according to ISO 4833: standard methods for the enumeration of bacteria (Anonymous, 2003), where ∑c is the sum of all colonies, *d* is the dilution factor corresponding to the first dilution retained and n_1 and n_2 the number of plates retained at the first and second dilutions, respectively:

$$\text{cfu ml}^{-1} = \frac{\sum c}{(n_1 + 0.1n_2) \cdot d}$$

For counts comprising a single dilution, colony counts were calculated as the arithmetic mean of colonies from triplicate plates.

2.3 Determination of bacteriophage titres

Phage concentrations were determined using soft agar overlay assays. Briefly, 10 µl of a log-fold dilution of bacteriophage was added to 150 µl of host cells and allowed to adsorb for 5 minutes prior to addition of 4 ml of molten (45°C) soft LB agar (0.6 % w/v bacteriological agar) supplemented with 10 mmol l^{-1} $MgSO_4$ and 1 mmol l^{-1} $CaCl_2$. Soft agar mixtures were poured onto the surface of a 90 mm LB agar plate to create an overlay, and allowed to solidify at room temperature for 10 minutes before overnight incubation at 37°C. After incubation plates were examined for plaques and where possible, the counts of triplicate plates over two consecutive dilutions were recorded. Plaque counts in pfu ml^{-1} were calculated according to ISO 4833 standard methods for the enumeration of bacteria (Anonymous, 2003), where ∑c is the sum of all plaques, *d* is the dilution factor corresponding to the first dilution retained and n_1 and n_2 the number of plates retained at the first and second dilutions, respectively:

$$\text{pfu ml}^{-1} = \frac{\sum c}{(n_1 + 0.1n_2) \cdot d}$$

For counts comprising a single dilution, phage titres were calculated as the arithmetic mean of plaques from triplicate plates.

2.4 Isolation of bacteriophages

Bacteriophages were isolated by incubation of filtered (0.2 µm pore size) swine lagoon effluent, diluted 10-fold in LB broth supplemented with 10 mmol l^{-1} $MgSO_4$ and 1 mmol l^{-1} $CaCl_2$, at 37°C for 18 hours in the presence of either *Salmonella* Enteritidis (VLA S07544-07), *Salmonella* Typhimurium DT104 (VLA S07519-07) or *Salmonella* Dublin (VLA S07539-07). After incubation, suspensions were clarified by filtration (0.2 µm pore size), serially diluted and 10 µl aliquots plated on overlay agar plates of LB agar (1.0 % w/v agarose) and LB overlay agar (0.6 % w/v agarose). Mid-exponential phase cultures of *Salmonella* serovars were used as host strains. After incubation, plates were examined for the presence of plaques. Individual plaques were numbered, excised and suspended in SM buffer for 24 hours at 4°C in order to elute bacteriophages from the lysate in the overlay agar. Each excised plaque was subjected to a further 3 rounds of purification by plating on double agar overlay plates until a single plaque morphology was observed. Phages isolated from plaques were named according to the recommendations of Kropinski et al. (2009). In this system of nomenclature the phage isolate name is preceded by the prefix vB or vA denoting bacterial and archaeal viruses, respectively. The prefix is linked by an underscore to the host abbreviation system based upon genus and species used for restriction enzymes, followed by S, M or P denoting the isolate as a member of the *Siphoviridae*, *Myoviridae* or *Podoviridae*, respectively. For example, under this system myoviruses isolated from *Salmonella enterica* are named as vB_SenM. A final mnemonic comprised a three letter abbreviation of the host serovar from which the phage isolate was obtained, e.g. Enteritidis or Dublin, and a numeral allocated at the plaque identification stage. Bacteriophage T4 was obtained from the ATCC (ATCC 11303-B4) and Felix O1a and O1b were the kind gift of Dr Pradip Patel.

2.5 Purification of bacteriophages

Standard methods were used to obtain high titre stocks of bacteriophages. Plaque suspensions were titrated and used to inoculate 1 litre of early exponential phase cultures (OD_{540} 0.1) at an approximate multiplicity of infection (MOI) of 0.1. Growth and lysis of bacterial cultures was monitored by hourly measurements of absorbance at 540 nm. Chloroform (1 % v/v) was added to each flask to terminate enrichment and prevent further microbial growth. Lysates were then treated with 1 µg/ml DNase I and RNase A (Sigma Aldrich, UK) prior to removal of bacterial debris by centrifugation at 11,000 x *g* for 10 minutes at 4°C. The supernatant was filtered (0.2 µm pore size) and bacteriophage particles precipitated by addition of NaCl to a concentration of 1 mol l^{-1} and 10 % w/v polyethylene glycol (PEG) prior to two-step cesium chloride (CsCl) density-gradient centrifugation (Sambrook, 2001). Briefly, PEG-precipitated bacteriophage particles were recovered by centrifugation at 11,000 x *g* for 10 minutes at 4°C. The supernatant was discarded and pellets re-suspended in 8 ml of sodium magnesium buffer (SM; 100 mM Tris-Cl, 8 mM $MgSO_4$, 100 mM NaCl, pH 7.5) for every 500 ml of clarified lysate. Re-suspended pellets were mixed with an equal volume of chloroform and centrifuged at 3000 x *g* for 15 minutes at 4°C and the aqueous phase retained.

Treatment with chloroform was repeated until no PEG could be observed at the interface between the organic and aqueous phases. Solid CsCl was added to samples to a final concentration of 0.5 g ml^{-1} to yield a density of ρ = 1.15. Samples were carefully layered on top of CsCl step gradients consisting of equal volumes of CsCl at densities of ρ = 1.45, ρ = 1.50 and ρ = 1.7 in SM buffer. Step gradients were spun using a SW40 rotor and ultracentrifuge (Beckman Coulter, UK, Optima LX-P) at 87,000 x *g* for 2 hours at 4°C. Bands containing bacteriophage particles were recovered using a 21 gauge syringe, layered on top of an ultracentrifuge tube containing CsCl at a density of ρ = 1.50 and then centrifuged at 160,000 x *g* for a further 24 hours at 4°C. Bands containing bacteriophage particles were recovered and CsCl removed by diafiltration (MWCO 100 kDa) against two 500-fold volume changes of SM buffer. The resulting pure suspensions of bacteriophages were adjusted to 10 ml with SM buffer, titrated using double agar overlay plates and stored at 4°C.

2.6 Morphological examination of bacteriophages by transmission electron microscopy

Transmission electron microscopy (TEM) of bacteriophages was performed using the method described by Ackermann (2009b). Purified bacteriophages were concentrated by centrifugation (Beckman Coulter, Optima LX-P ultracentrifuge, 70Ti Rotor) at 25,000 x *g* for 60 minutes and re-suspended in 0.1 M ammonium acetate (pH 7.0). One drop of bacteriophage suspension was spotted on to a formvar carbon-coated 400-mesh TEM grid (TAAB Laboratory Equipments, UK) and stained by transferring grids to a 1 % (w/v) uranyl acetate solution (pH 4.5) for 30 seconds. Grids were examined using a transmission electron microscope (Phillips, UK, CM10) operated at 60 kV. Magnifications were calibrated by measurement of T4 bacteriophage tails and virion dimensions established by measurement of at least 20 intact particles. Each bacteriophage isolate was assigned to a respective family in accordance with the recommended guidelines of the International Committee on Taxonomy of Viruses (ICTV), based upon examination of virion particle morphology (ICTV, 2005).

2.7 Determination of adsorption rate constants

Determination of adsorption rate constants for bacteriophage isolates followed the method described by Kropinski (2009). Briefly, host strains were grown in LB to an OD_{540} of 0.1, *circa* 5 x 10^7 cfu ml^{-1}, and enumerated using a spiral plating system (Don Whitley Scientific, UK). Bacteriophages were added to cultures to yield a final concentration of 5 x 10^4 pfu ml^{-1} (*t* = 0). At 1 minute intervals, 50 µl aliquots were transferred to 950 µl SM buffer saturated with chloroform and stored on ice. Upon completion of the sampling period, 10 minutes, samples were immediately titrated for unabsorbed bacteriophages by plating 100 µl using agar overlay plates. Absorption rate constants (*k*) were calculated as $-m/N$ where *N* represents the initial bacterial density and *m* the slope of the linear regression equation of the natural logarithm of the measured free phage titre over time.

2.8 One-step growth curves of bacteriophage isolates

The method for one step growth was adapted from that described by Ellis and Delbrück (1939). Shake flask cultures of the relevant bacterial host were grown in LB broth supplemented with 10 mmol L^{-1} $MgSO_4$ and 1 mmol L^{-1} $CaCl_2$ to an OD_{540} of c. 0.1, corresponding to 5 x 10^7 cfu ml^{-1}. Bacteriophages were added to cultures at a concentration calculated to yield an multiplicity of infection (MOI) of approximately 0.005. After 4 minutes incubation to allow adsorption of virions to host cells, the culture was centrifuged at 13,000 x *g* for 1 minute and the supernatant discarded in order to remove un-adsorbed bacteriophage particles. The pellet, containing infected cells, was re-suspended in an equal volume of pre-warmed LB broth, immediately diluted to 10^{-4} and placed in a static water bath at 37°C. Samples (100 µl) were subsequently withdrawn at 5 minute intervals over a period of 60 minutes to two series of tubes denoted S and L, each containing 900 µl SM buffer. S tubes represented a measure of the number of free phage particles and infected cells (infective centres) and were retained on ice until sampling was completed. Tubes in series L also contained 50 µl of chloroform and represented the number of free and intracellular phage particles. Samples added to L tubes were mixed briefly and retained at room temperature for at least 30 minutes to allow chloroform-mediated cell lysis. Each series time-point was titrated by triplicate overlay plaque assay plates and phage concentrations determined by counting plaques after overnight incubation at 37°C.

2.9 Single-burst experiments

Single burst experiments (Burnet, 1929, Delbrück, 1945) were performed in order to supplement and verify data obtained from one step growth curves. Phage infected bacterial cultures were prepared as described for one step growth curves. Free virions were removed from samples by centrifugation and pellets of bacterial cells re-suspended in RS. Infected cultures were serially diluted in RS so that 10 tubes containing approximately 10 cfu ml^{-1} were obtained. From these, 1 ml volumes were transferred to individual tubes (n = 100). Samples were incubated at 37°C for 60 minutes in order to allow lysis to occur and the entire contents of each tube (1 ml) subsequently plated using overlay agar plates.

2.10 Bacteriophage stability assays

2.10.1 Temperature

The effects of exposure to heat upon bacteriophage titres were assessed at temperatures of 50, 60 and 70°C. Bacteriophage suspensions were adjusted to yield a titre of c. 1 x 10^{10} pfu ml^{-1} and diluted 1:10 in pre-warmed PBSa. At each temperature, samples were taken at 15, 30, 60 and 120 minutes and enumerated using triplicate soft agar overlay plates.

2.10.2 Long-term storage

Following CsCl purification and dialysis, 5 ml aliquots of each bacteriophage were retained for the purposes of assessing storage stability. Stocks were stored in SM buffer at 4°C in polycarbonate screw-capped tubes and titrated by overlay plaque assay at monthly intervals over a total period of 12 months.

2.10.3 Bacteriophage host range: Spot plate assay

The host range of bacteriophage isolates was first assessed by the semi-quantitative spot plate technique (Mazzocco *et al.,* 2009, Kutter, 2009). Bacteriophage preparations were adjusted by dilution to yield a titre of 10^{11} pfu ml^{-1} on their respective propagating host. Square 120 mm plates containing LB agar were subdivided to yield a 6 x 6 grid, to which was added LB overlay agar containing 200 µl from a mid-exponential phase culture of the bacterial strain to be tested. To each section of the grid, 5 µl samples of bacteriophage from a log-fold dilution series were spotted onto the surface of the overlay agar so that each plate assessed a range of phage concentrations (Figure 7).

Phage1		10^{-1}	10^{-2}	10^{-3}	10^{-4}	
		10^{-5}	10^{-6}	10^{-7}	10^{-8}	10^{-9}
Phage 2		10^{-1}	10^{-2}	10^{-3}	10^{-4}	
		10^{-5}	10^{-6}	10^{-7}	10^{-8}	10^{-9}
Phage 3		10^{-1}	10^{-2}	10^{-3}	10^{-4}	
		10^{-5}	10^{-6}	10^{-7}	10^{-8}	10^{-9}

Figure 7. Arrangement of log-fold dilutions of bacteriophage upon spot plate assays of host range. Values in cells refer to the dilution factor of the phage preparations.

Phage samples were allowed to absorb into the overlay agar prior to overnight incubation at 37°C. In total, 50 serovars of *Salmonella* and 10 strains belonging to other Gram negative genera were assessed. Spot plate results were interpreted by use of a semi-quantitative score-card system (Figure 8).

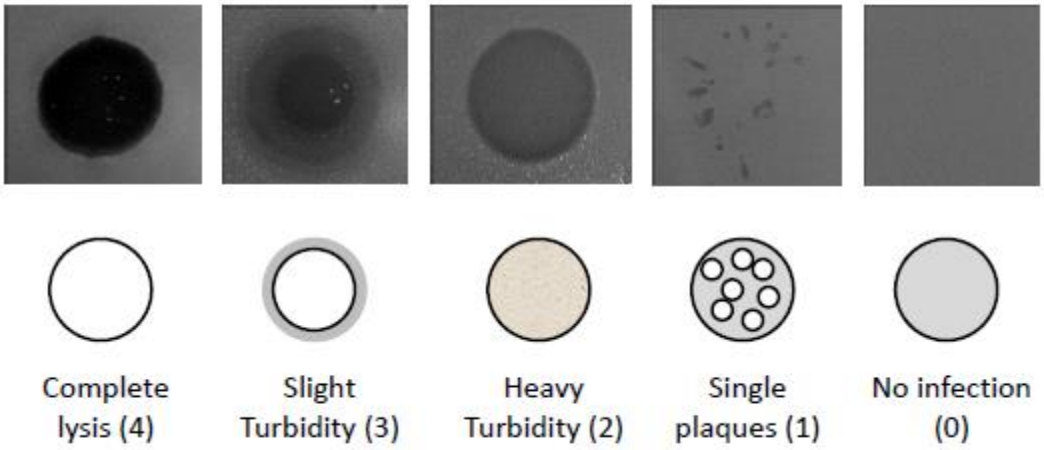

Figure 8. Score card for the visual assessment of plaques. The scoring system was adapted from that described by Rees and Dodd (2006b). Photographs of plaques formed by vB_SenS-Ent1 are provided for illustrative purposes.

2.10.4 Bacteriophage host range: Efficiency of plating

All bacterial isolates exhibiting the ability to form plaques on a particular bacterial isolate in spot plate assays were taken forward for analysis by efficiency of plating (EOP). Efficiency of plating was defined as the ratio of the mean values of two plaque titrations, calculated as;

$$\text{Relative EOP} = \frac{\text{Mean titre on propagating host (pfu ml}^{-1})}{\text{Mean titre on test isolate (pfu ml}^{-1})}$$

Thus, EOP was used to estimate the susceptibility of different bacterial isolates to productive infection by a particular phage preparation or isolate relative to that of the propagating host serovar.

2.11 Extraction of genomic DNA from CsCl purified bacteriophages

Bacteriophage DNA was obtained by phenol chloroform extraction (Sambrook, 2001). Briefly, a 5 ml sample of CsCl-purified bacteriophages was incubated at 37^{o}C for 1 hour in the presence of DNase I and RNase A in order to remove any exogenous DNA and RNA. DNase and RNase activity was halted by the addition of EDTA to a final concentration of 20 mmol l^{-1}. In order to release genomic DNA from capsids, virions were incubated at 56^{o}C for 1 hour in the presence of SDS (5 % w/v) and proteinase K (New England Biolabs, UK; 20 µg ml^{-1} in 10 mmol l^{-1} Tris pH 8.0 and 50 mmol l^{-1} EDTA). Samples were allowed to cool to room temperature before addition of an equal volume of equilibrated phenol (Sigma Aldrich, UK) and centrifugation at 13,000 x *g* for 5 minutes. This process was repeated using a 1:1 phenol:chloroform solution and then chloroform alone, transferring the aqueous phase to fresh Eppendorf tubes and discarding the interface and organic phase at each stage. DNA was precipitated from the aqueous phase by addition of sodium acetate (0.5 mol l^{-1}, pH 5.2) to a final concentration of 0.3 mol l^{-1} and two volumes of 100 % ice-cold ethanol. Samples were rapidly frozen using a -80^{o}C freezer (Sanyo, Japan) for 2 hours, after which samples were thawed on ice prior to centrifugation at

15,000 x *g* at 4°C for 30 minutes. The supernatant was removed and pellets washed and centrifuged (15,000 x *g*, 10 min, 4°C) twice with 70% v/v ethanol. Wash supernatants were removed to waste and residual ethanol removed from samples using a vacuum centrifuge (Vacufuge, Eppendorf, UK). Purified DNA was stored either in 100% ethanol or TE buffer at -20°C.

2.11.1 Concentration, purity and yield of bacteriophage genomic DNA

The concentration, yield and relative purity of extracted phage genomic DNA was assessed by ultraviolet spectroscopy. Measurements of absorbance at 230, 260, 280 and 320 nm were performed using a micro-volume spectrophotometer (Nanodrop 1000, Thermo Scientific, UK). The A_{260}/A_{280} ratio was employed as an estimate of DNA purity. Ratios were calculated post subtraction of the A_{320} value which represents absorbance caused by non-nucleic acid sample turbidity. A ratio of >=1.8 was considered as acceptable for use in downstream experiments.

$$\text{DNA Purity} = \frac{A_{260} - A_{320}}{A_{280} - A_{320}}$$

Sample concentrations were calculated by adjusting the A_{260} measurement for turbidity, multiplying by the sample dilution factor and using the assumptions that an A_{260} of 1.0 = 50 µg ml^{-1} under conditions of neutral pH and a G+C DNA content of 50%.

$$\text{DNA Concentration } \mu g\ ml^{-1} = (A_{260} - A_{320}) * \text{Dilution factor} * 50\ \mu g\ ml^{-1}$$

The total yield was obtained by multiplying the DNA concentration by the total volume of purified samples.

$$\text{DNA Yield } \mu g = \text{Sample concentration} * \text{Total Volume } (\mu l)$$

2.11.2 Estimation of bacteriophage genome size by pulsed field gel electrophoresis

Pulsed field gel electrophoresis (PFGE) was performed according to the method described by Lingohr et al. (2009). Bacteriophages, ~10^{10} pfu ml^{-1}, were immobilised in agar plugs (1 % w/v agarose) and lysed by treatment with proteinase K (20 mg ml^{-1} in 10 mmol l^{-1} Tris pH 8.0, 50 mmol l^{-1} EDTA, and 1 % w/v SDS) for 2 hours at 54°C. Agarose plugs were subsequently washed three times by soaking in TE buffer for 1 hour and stored at 4°C. Gels (1 % w/v agarose) were run in 0.5x TBE buffer (BioRad, France) at 6 V cm^{-1} for 15 hours at 14°C with pulses of 2.2 to 54.2 seconds using a CHEF-DR II Electrophoresis unit (BioRad, France). DNA size standards were provided by use of low range PFGE marker DNA (New England Biolabs, UK) and bands visualised by staining with 1 µg ml^{-1} ethidium bromide (EtBr). Gel images acquired using a FluorChem Q (ProteinSimple, USA) and analysed using ImageJ (Abramoff *et al.,* 2004).

2.11.3 Restriction digests of phage genomic DNA and gel electrophoresis

Phage genomic DNA was digested to completion by incubation for 1 hour at 37^{o}C with 20U of the dsDNA-specific restriction enzymes *Eco*RV and *Sma*I, and 5U of *Bam*HI, *HindIII* and *Xba*I in accordance with the manufacturer's instructions (New England Biolabs, UK). For genomic DNA immobilised in agar plugs, the restriction incubation time was extended to 4 hours. DNA fragments were separated by PFGE, as described in section 2.11.2, and conventional agarose electrophoresis gels (0.8 % w/v agarose containing 0.5 µg ml^{-1} EtBr) in TAE electrophoresis buffer (40 mmol l^{-1} Tris-HCl, 20 mmol l^{-1} sodium acetate and 50 mmol l^{-1} EDTA at pH 7.2) at 5 V cm^{-1}. Low-range PFGE ladder and 2-log DNA ladder (New England Biolabs, UK) were run alongside samples to provide size standards for PFGE and agarose gel electrophoresis, respectively.

2.11.4 Determination of phage genomic termini

To determine whether the genome termini were fixed or circularly permuted, purified genomic DNA was subjected to a time-limited digest with the exonuclease BAL-31 (M0231S, New England Biolabs, UK). Briefly, 10 µg was incubated with 10 U of BAL-31 and samples withdrawn at 0, 10, 20, 40 and 60 minutes. The DNA was then precipitated with ethanol, re-dissolved in TE buffer and digested with *Eco*RV before separation by agarose electrophoresis.

In order to test for the possibility of cohesive genome ends, one microgram of purified genomic DNA was digested to completion with *Eco*RV and heated to 80^{o}C for 15 minutes using a heating block. The samples were then divided into equal portions. One sample was rapidly cooled by placing in an ice bath while the other was allowed to cool to room temperature in the heating block. The resulting bands were separated by agarose gel electrophoresis.

2.12 Genome sequencing and bioinformatics analysis of bacteriophages

Purified bacteriophage genomic DNA was sequenced externally (MWG Operon, Germany) using GS FLX 454 sequencing and targeted Sanger sequencing for gap closure. Consensus sequences were examined using Consed (Gordon *et al.,* 1998) and opened upstream of the gene predicted to encode the small terminase subunit. *Ab initio* prediction of open reading frames (ORFs) used a combination of the GeneMark.hmm algorithm for prokaryotes (Besemer and Borodovsky, 1999), Glimmer 3.02 (Delcher *et al.,* 1999) and ORF Finder (htto://www.ncbi.nlm.gov/projects/gorf). Overlapping 10 kb sections of sequenced genomes were queried against non-redundant protein databases using tBLASTx for intrinsic prediction of ORFs. The results of evidence-based and *ab initio* gene predictions were compared in order to evaluate the best gene models and to resolve overlaps among ORFs. All ORFs were inspected for the presence of convincing purine-rich ribosome binding sites upstream of the start codon. Annotation of sequenced bacteriophage genomes was performed using Artemis (Rutherford *et al.,* 2000) and physical maps prepared using DNA plotter (Carver *et al.,* 2009), GView (Petkau *et al.,* 2010) and CGView (Stothard and Wishart, 2005).

Translated sequences from predicted ORFs were queried using BLASTP and PSI-BLAST against the non-redundant database (Altschul *et al.,* 1990, 1997). Functional annotation of gene products was performed by querying translated sequences against the conserved domain database (Marchler-Bauer *et al.,* 2011), Prosite (Sigrist *et al.,* 2010), Pfam (Punta *et al.,* 2012) and InterProScan (Quevillon *et al.,* 2005). The Hidden Markov Model search tool HHpred (Söding *et al.,* 2005) was used to query translated sequences against protein three dimensional structures held in the Protein Data Bank.

Translated ORFs were characterised by number of amino acids, molecular weight and isoelectric point using the ExPASy tool: Compute pI/Mw (Bjellqvist *et al.,* 1993). Prediction of transmembrane helices was performed using TMHMM 2.0 (Krogh *et al.,* 2001) and searches for structural motifs and signal peptides were carried out using COILS and SignalP (Petersen *et al.,* 2011). tRNAScan-SE (Schattner *et al.,* 2005) and ARAGORN (Laslett and Canback, 2004) were used to scan for tRNAs.

Next, intergenic regions were investigated for the presence of regulatory elements. Candidate promoter sequences and conserved intergenic motifs were identified by searches of 150 bp sequences upstream of ORFs using MEME (Bailey *et al.,* 2006) and the regulatory sequence analysis (RSAT) toolset (Thomas-Chollier *et al.,* 2011). Putative rho-independent terminators were predicted using TransTermHP (Kingsford *et al.,* 2007) and WebGester (Mitra *et al.,* 2010). Candidate terminators were assessed according to location, presence of a U-rich tail and stable predicted stem loop secondary structure ($\Delta G \leq -10$ kcal mol^{-1}) as calculated by RNAFold (Gruber *et al.,* 2008).

2.13 Comparative genomics

Comparisons of nucleotide sequences between phage genomes were performed using MAUVE (Darling *et al.,* 2010) and Gepard (Krumsiek *et al.,* 2007). Related proteins between *Salmonella* bacteriophages with completely sequenced genomes were identified by two complementary methods. Firstly, shared proteins were identified using CoreGenes3.5 using default settings (Mahadevan *et al.,* 2009). Secondly, custom BLAST databases comprising the nucleotide and protein sequences from 42 *Salmonella* phage genomes were prepared and all-versus-all BLAST comparisons performed. Protein sequences conserved among the vB_SenS-Ent and related phages were analysed using iterative PSI-BLAST (Altschul *et al.,* 1997) against the non-redundant databases and HHpred (Söding, 2005, Söding *et al.,* 2005) against the pdb70 database maintained by the Department of Protein Evolution at the Max Planck Institute for Developmental biology. Diagrammatic representation of BLASTP comparisons were prepared using Circoletto (Darzentas, 2010) and the CGview comparison tool (Grant *et al.,* 2012). Alignments were performed using ClustalX2 (Larkin *et al.,* 2007) and Neighbour-joining trees constructed using MEGA5 (Tamura *et al.,* 2011).

2.14 Bacteriophage structural proteins

2.14.1 Quantification of protein

Sample protein concentrations were quantified by the Bradford method using bovine serum albumin as standards (Bradford, 1976, de Moreno *et al.,* 1986). Bradford assays were performed in a 96-well microtitre plate format where samples were plated alongside standardised concentrations of bovine serum albumin. Measurements of absorbance at 600 nm were performed using a microplate reader (Genios Pro, Tecan, Switzerland). Solving the linear regression line equation for absorbance of standard concentrations of BSA allowed estimation of the sample protein concentration.

2.14.2 Extraction and analysis of bacteriophage structural proteins by SDS-PAGE

Structural proteins from CsCl purified virions were extracted and concentrated using methanol-chloroform and re-suspended in lithium dodecyl sulphate sample buffer (LDS) prior to analysis by one- and two-dimensional SDS-PAGE. For isoelectric focusing, linear IPG Zoom strips from pH 3 to 10 were rehydrated overnight with the solubilised proteins and separated using a ZOOM® IPGRunner™ system according to the manufacturer's instructions (Invitrogen, UK). Prior to electrophoresis in the second dimension, IPG strips were equilibrated twice for 15 minutes in 1x LDS sample buffer containing 1x reducing agent for the first equilibration step and 125 mmol l^{-1} iodoacetamide for the second step. Protein size separation was conducted alongside Novex® Sharp unstained protein standard marker using a NuPAGE mini-gel system and 4-12 % bis-tris gels in MES-SDS running buffer (Invitrogen, UK) at 200 V. Proteins were fixed (50 % v/v methanol, 10 % v/v acetic acid) for 1 hour at room temperature then stained using SimplyBlue™ Safestain (Invitrogen, UK) and images of gels acquired and analysed as described for PFGE (section 2.11.2).

2.15 Transformation of *Salmonella* with the *luxCDABE* operon

The construction of plasmids pGLITE and pMCS5-LITE containing the *luxCDABE* operon of *Photorhabdus luminescens* under constitutive control of the lac promoter have been described previously (Parveen *et al.,* 2001, Lewis *et al.,* 2006a). Plasmids were amplified by electroporation into *E. coli* DH5α (Invitrogen, UK) and purified using a Wizard SV Miniprep kit (Promega, USA, A1330) in accordance with the manufacturer's instructions. Purified plasmids were eluted in nuclease-free water and stored at -20°C. Plasmids contained a Kanamycin (Km) or Gentamicin (Gm) resistance marker for pGLITE and pMCS5-LITE, respectively (Kovach *et al.,* 1995) and appropriate concentrations of antibiotics were selected from results of broth dilution MIC assays for *Salmonella enterica* serovars. *Salmonella enterica* sv. Dublin, used as the propagating host of Felix O1a and Felix O1b, and *Salmonella enterica* sv. Enteritidis, the propagating host of Ent1, Ent2 and Ent3 were transformed to express the *lux* operon by electroporation (GenePulser, BioRad, France) using conditions of 3.0 kV, 25 µF capacitance and 200 Ω resistance (O'Callaghan and Charbit, 1990). After a 1 hour recovery period in SOC media (2 % w/v tryptone, 0.5 % w/v yeast extract, 20 mmol l^{-1} glucose, 10 mmol l^{-1} NaCL, 2.5

mmol l^{-1} KCl, 10 mmol l^{-1} $MgCl_2$, 10 mmol l^{-1} $MgSO_4$) at 37°C, transformants were selected by plating onto solid media containing the appropriate antibiotic and identified by examination with an EMCCD camera (iXON DV897+, Andor Technologies, UK) for evidence of light emission after 24 hours incubation at 37°C. Colonies exhibiting light emission were sub-cultured onto fresh media and identities confirmed by Gram stain morphology, plating onto selective media and biochemical characteristics (API 20E, Biomerieux, France).

2.15.1 Calibration of bioluminescence and cell density

For calibration of bioluminescence with viable counts, standard curves consisting of serial 10-fold dilutions of bacteria were prepared. Briefly, 10 ml batch cultures were grown to late exponential phase ($OD_{540} \geq 1.0$). Cells were pelleted by centrifugation at 10,000 x *g* for 5 minutes, washed twice and re-suspended in 10 ml of ¼ strength Ringers solution (RS). The resulting suspensions were serially diluted to 10^{-8}, plated onto LB agar and colonies counted after 24 hours incubation at 37°C. Each log-fold dilution of bacteria was assessed for light emission using a tube and a microtitre plate luminometer. Measurements of light emission using tube luminometers (Sirius FB-12, Berthold Detection Systems GmbH, Germany) were performed at room temperature, approximately 20°C and employed a 1 ml sample volume. Microtitre assays (Centro LB960 XS^3 Berthold Technologies GmbH, Germany) were performed at 37°C using a sample volume of 100 µl. All assays of bioluminescence included measurements of instrument and reagent blanks. Limits of detection and quantification were defined as 3 and 10 standard deviations of the reagent background, respectively. Calibration experiments were performed on 3 independent occasions for each bacterial isolate.

2.15.2 Calibration of light emission and growth in batch culture

Overnight batch cultures were diluted 1:1000 in Erlenmeyer flasks containing 50 ml of LB so that the initial concentration was approximately 1 x 10^6 cfu ml^{-1}. Bacterial growth at 37°C with orbital shaking (150 rpm) was recorded over a period of 10 hours by measurements of bioluminescence, OD_{540nm} and viable counts at hourly intervals. Measurements of bioluminescence were performed using a tube luminometer (Sirius FB-12, Berthold Detection Systems, Germany), a volume of 100 µl and an integration time of 1 second.

2.15.3 Measurement of bioluminescence spectra

Bioluminescent bacteria were grown in batch culture to OD_{540} 1.0, centrifuged and pellets re-suspended in Ringer's solution containing glucose at a final concentration of 10 mmol l^{-1}. The wavelength spectrum of light emission for each bacterial transformant was determined using a fluorescence spectrophotometer (Fluorosens, Gilden Photonics, UK) with the excitation monochromator port blocked. Data were recorded using an emission scan in 1 nm steps across a wavelength range of 400 to 700 nm.

2.15.4 Microplate broth lysis assay

Overnight batch cultures of bioluminescent *Salmonella* bacteria grown in LB containing the appropriate antibiotic were diluted 1:100 into fresh LB medium. Cultures were incubated until an OD_{540} of 1.0 was reached and then serially diluted in fresh LB media containing antibiotics, 10 mmol l^{-1} $MgSO_4$ and 1 mmol l^{-1} $CaCl_2$. Log-fold dilutions of bacteriophages in LB broth were prepared from purified stock solutions. Triplicate wells of a 96-well microtitre plate (Lumitrac200, Greiner Bio-One, Germany) were loaded with 180 µl and 20 µl of the appropriate dilution of bacteria and bacteriophages, respectively, such that each plate assessed a range of multiplicities of infection at different bacterial concentrations (Figure 9). Reagent background measurements comprised wells constituting media alone or media containing only bacteriophages. Bacteria grown in the absence of bacteriophage were used as positive controls.

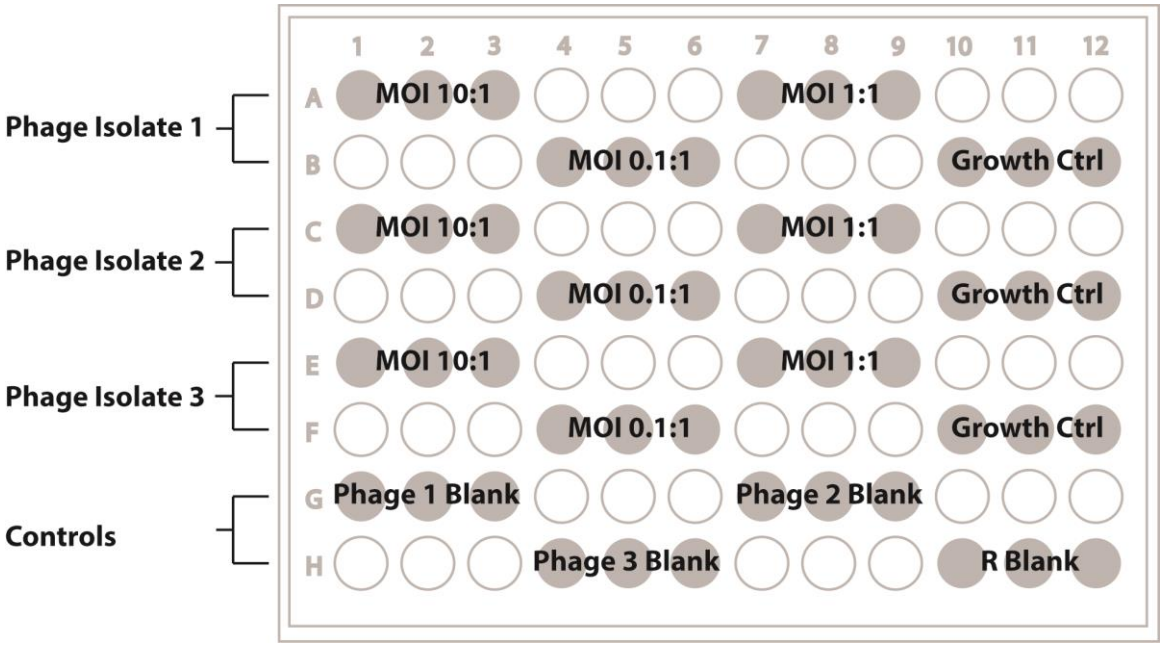

Figure 9. Layout of samples on 96 well microtitre plates. Wells containing samples are shown as grey filled circles while outlined wells were filled with sterile water. MOI, multiplicity of infection; R Blank, reagent background.

Measurements of light emission were recorded using a microplate luminometer programmed to measure each well using an integration time of 1 second at 5 minute intervals over a period of 12 hours. The contents of wells were mixed by orbital shaking for 2 seconds immediately prior to each measurement. Data were exported as tab-delimited text files and analysed using Prism 5 (GraphPad Software Inc., USA) and Excel (Microsoft Corporation, USA).

2.16 Bioluminescence imaging

2.16.1 EMCCD system characterisation

EMCCD camera (iXON DV897+) sensor fixed-pattern read noise was determined by capturing 100 images using an integration time of 1 µsec with the camera shutter closed to ensure that no external

light was captured. Thermal noise was recorded by capture of 100 images at exposure times of 1, 5, 10 and seconds and 1, 5, 10, 15 and 30 minutes. Exposures were then combined into stacks using Fiji ImageJ software (Schindelin, 2008), and z-plot images consisting of either the median value or standard deviation (r.m.s.) for each pixel across the 100 exposures produced. The procedure for obtaining sensor fixed-pattern read noise and thermal noise was repeated for electron multiplication gain values of 0, 100, 200 and 300 and horizontal sensor readout speeds of 1, 3, 5 and 10 MHz. The camera sensor was maintained at a temperature of -95^{o}C by liquid cooling for these and all subsequent experiments.

2.16.2 Limits of detection for bioluminescent bacteria using EMCCD imaging

Cells from overnight batch cultures were harvested by centrifugation at 11,000 x *g* for 10 minutes, washed in sterile Ringer's solution and re-suspended in pre-warmed nutrient broth. The resultant suspension was serially diluted in nutrient broth and immediately plated onto solid media. Colony counts were established after 24 hours incubation at 37^{o}C. Aliquots of 100 µl of each log-fold dilution were transferred to individual wells of a black 96-well microtitre plate (Greiner Bio-one, UK) in triplicate and images of bioluminescence acquired at integration times of 5, 10 and 30 seconds and 1, 5, 10 and 15 minutes at an EM gain value of x300.

2.17 Calibration of colony forming units and light emission in overlay agar

Batch cultures were grown until an OD_{540} of >1.0 was achieved and cells pelleted by centrifugation (10,000 x *g*, 10 minutes), washed twice and re-suspended in Ringers solution. The resultant cell suspensions were serially diluted, plated onto LB agar and colony counts recorded after 24 hours incubation at 37^{o}C. The same cell suspensions were serially diluted in LB overlay agar to 10^{-8} and 100 µl aliquots transferred to wells of a black, 96-well microtitre plate containing 100 µl LB agar. Measurements of light emission were recorded using a microplate reader (Berthold Technologies GmbH, Centro XS^3) and by EMCCD imaging. All assays included instrument and reagent blanks and the limit of detection was defined as 3 standard deviations of the reagent background. Calibration experiments were performed on three independent occasions for each bacterial isolate.

2.18 Bioluminescence imaging of plaque formation

Bacteriophages were diluted sufficiently in SM buffer to yield approximately 50 plaques on overlay agar plates. Briefly, plates were prepared by mixing 10 µl of the diluted bacteriophage sample with 150 µl of exponential phase bacterial culture (OD_{540nm} = 0.25, c. 1 x 10^8 cfu ml^{-1}). After a period of 1 minute, this mixture was diluted with 6 ml of LB-Miller overlay agar (0.6 % w/v bacteriological agar, 10 mmol l^{-1} $MgSO_4$, 1 mmol l^{-1} $CaCl_2$) supplemented with either 10 µg ml^{-1} Km or Gm. The overlay agar was poured onto the surface of LB agar plates also containing the appropriate antibiotic. Once the overlay had solidified, plates were transferred to a transparent Perspex incubator preheated to 37^{o}C and bioluminescence recorded using an EMCCD camera and macro lens (EF 100 mm f/2.8,

Canon, Japan) controlled using iQ 2.2 software (Andor Technologies, UK). Image acquisition used three different exposure times during the experimental timeframe; 300 seconds, 10 seconds and 5 seconds. An exposure time of 300 seconds was used for the first 160 minutes in order to facilitate detection of low levels of light emission. The exposure time was then altered to 10 seconds for a further 120 minutes before reducing to 5 seconds for the remaining experimental duration. Exposure times were reduced in order to prevent sensor saturation by the increased signal present at later points in the experimental timeframe. All exposures were acquired at 5 minute intervals over 20-hour periods. The EMMCD sensor was liquid cooled to -95^{o}C with device settings of 1 MHz horizontal shift speed, 16 bit A/D converter with a pre-amplifier gain of x4.9 and an electron multiplication factor of 300.

2.19 Processing and analysis of bioluminescence images

Initial analyses of time-lapse images were performed using the open-source software ImageJ (Abramoff *et al.,* 2004). Raw images were normalised by subtraction of dark frames and converted to counts per second by dividing pixel values by the exposure duration. Individual, isolated plaques were identified and cropped from the full-size images (Figure 10). Coarse particle descriptions were obtained for each image by thresholding, converting to binary and fitting regions of interest to the plaque boundary using ImageJ's inbuilt particle analysis function. A basic description of the rate of enlargement was obtained by calculating the radius of a circle equivalent to the area of the plaque and taking the slope of the radius versus time. In order to obtain a more accurate description of plaque expansion, a routine was also developed using Matlab (Wolfram Research, Germany) to detect the plaque edge perimeter (Figure 10). The centroid of the earliest image in which the plaque becomes visible was employed as a fixed origin to plot the detected edge in a polar co-ordinate system. This approach allowed determination of the distance from the plaque centroid to the edge along rays pointing outwards at regular angle increments.

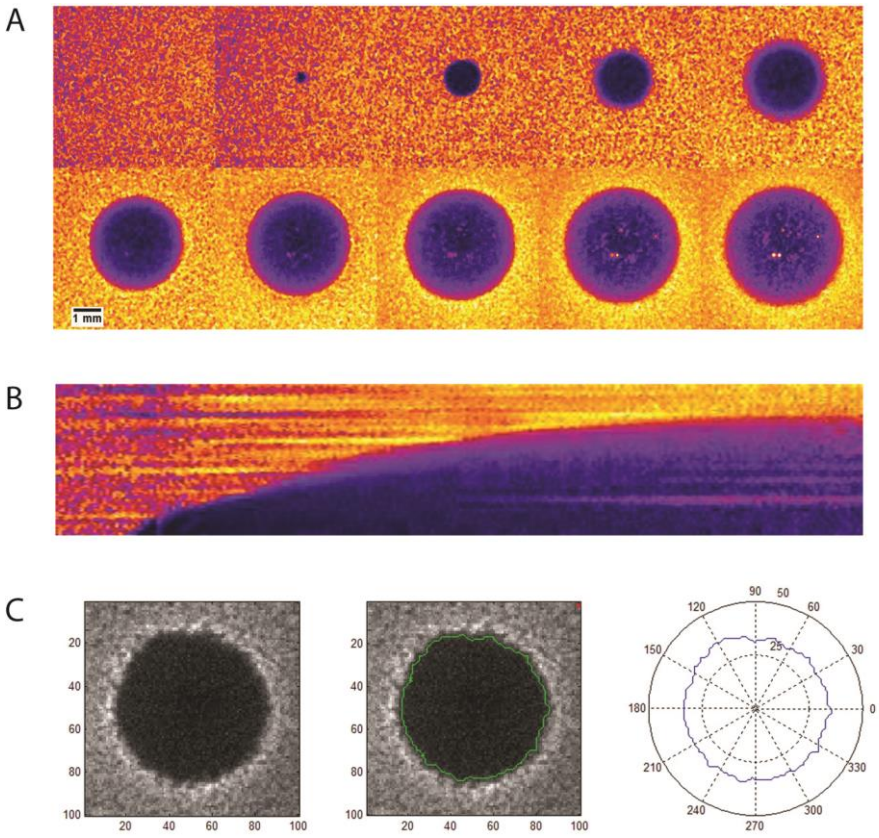

Figure 10. Detection of plaque formation by bioluminescence imaging. All images have been contrast adjusted for clarity. A. Montage of plaque formation by vB_SenS-Ent1. Moving from left to right, panels show the formation of a single plaque at intervals of 2.5 hours. B. Kymograph of a line of pixels extending through the plaque radius. The x-axis represents pixels comprising the line, coloured according to intensity of light emission. The y-axis represents time. C. Edge fitting and conversion to polar co-ordinates of a single frame.

2.20 Imaging of Plaques by CSLM and Live:Dead staining

Briefly, plaques and a surrounding area of the bacterial lawn were excised from plates after 24-hours incubation at 37^{o}C and the underlay layer carefully cut away using a sterile scalpel. Bacteria in the overlay agar were stained by flooding the cored plaques with 30 µmol l^{-1} propidium iodide and 6 µmol l^{-1} SYTO-9 (BacLITE, Invitrogen, UK) and incubating for 30 minutes at room temperature. The distribution of live and dead bacteria were examined at x20 magnification using an Ultraview ERS spinning-disk confocal microscope equipped with a 0.3 µm step z-stage (Perkin Elmer,UK), after excitation at 488 nm and 568 nm. Deconvolution of z-stacks was performed using the Volocity software package (Perkin Elmer, UK). Control samples consisted of examination of live:dead stained bacterial lawns grown in the absence of bacteriophages and overlay agar lacking both bacterial cells and bacteriophages.

2.21 Biocontrol of *Salmonella* Enteritidis in foodstuffs

2.21.1 Stability of bioluminescent reporters

Prior to beginning biocontrol experiments, the stability of plasmid retention by bioluminescent *S.* Enteritidis PT4 at 4°C and in the absence of selective agents was assessed. Briefly, an overnight culture was subcultured to fresh LB-Km broth and grown to OD_{540} 1.0. The culture was pelleted by centrifugation at 10,000 x *g* for 5 minutes and washed twice and resuspended in an equal volume of RS. After serial dilution and preparation of enumeration plates, the culture was stored at 4°C and enumerations performed daily for 7 days. After 24 hours incubation at 37°C, enumeration plates were examined using an EMCCD camera to identify numbers of bioluminescent colonies.

2.21.2 Food samples

The ability of bacteriophages to reduce pathogen loads in artificially contaminated food matrices was assessed. Four food matrices were tested, sourced from a local grocery store: mixed salad leaves; beansprouts; cooked and raw skinless chicken breast. Each food was first screened for contamination with *Salmonella* by ISO 6579:2002 protocols (Anonymous, 2002). A bulk quantity of 720 g of each food matrix was split between 9 sterile LDPE containers so that each contained 80 g. Three series of food samples were used for each experiment. For positive controls, a food sample was inoculated with bacteria only, whilst the stability of bacteriophages in the different food matrices was assessed using a food sample inoculated with the relevant bacteriophage isolate. The third series comprised food samples inoculated with both bacteria and bacteriophages.

2.21.3 Addition of *Salmonella* Enteritidis and bacteriophages

Batch cultures of bioluminescent *S.* Enteritidis PT4 were grown in LB-Km broth to an OD_{540} of 0.1, representing a concentration of 5×10^7 cfu ml^{-1}. The bioluminescent transformant was used as the presence of the plasmid provided an antibiotic resistance marker for selection and light emission for colony identification. Cultures were serially diluted in RS and enumeration plates prepared from two consecutive dilutions. Bacteria were added to foods to achieve a contamination level of approximately 10^3 cfu g^{-1}. For food samples assessing the action of bacteriophages, the sample was first inoculated with bacteria and a 10 g sample withdrawn immediately after mixing. The food samples were then incubated at 4°C for 2 hours in order to allow bacteria to equilibrate to storage conditions. Bacteriophages were added to a final concentration of 1×10^8 pfu g^{-1} and the food samples mixed for 2 minutes to ensure dispersal of bacteria and bacteriophages throughout the matrix. After inoculation of bacteriophages, the food was sampled for a second time and then stored at 4°C for 7 days.

2.21.4 Determination of bacterial and phage counts

Sampling was performed at daily intervals. Briefly, for each series 10 g of food was weighed into sterile bags (Seward, UK) and diluted 10-fold by addition of 90 ml maximum recovery diluent (MRD) (Oxoid, UK). Samples were homogenised for 30 seconds using a stomacher (Seward, UK) and titrated for the presence of *Salmonella* and bacteriophages as appropriate. For quantitative enumerations of bacteria, 500 µl and 100 µl aliquots were spread plated onto LB-Km and xylose lysine deoxycholate (XLD, Oxoid, UK) agar plates. Colonies present on LB-Km and XLD plates after overnight incubation at 37^{o}C were examined for light emission using an EMCCD camera. Infective virions recovered from foods were enumerated using the overlay plaque assay. Aliquots of 100 µl and 10 µl from log-fold dilutions of food homogenates were added to 200 µl of host cells prior to plating. Samples were held for 5 minutes prior to the addition of 6 ml LB overlay agar containing kanamycin.

Chapter 3 Characterisation of the vB_SenS-Ent *Salmonella* Bacteriophages

Data presented in this chapter are adapted from Turner *et al.,* (2012) *Journal of General Virology* 93: 2046-2056.

3.1 Introduction

The bacteriophages vB_SenS-Ent1, vB_SenS-Ent2 and vB_SenS-Ent3 (Ent1, Ent2 and Ent3, respectively) are members of a proposed genus, the *Setp3likevirus* that fall within the *Siphoviridae* family of tailed bacteriophages. These phages are characterised by their ability to infect and reproduce within a broad range of serovars of the enteric pathogen *Salmonella enterica*. Apparent differences in host range and susceptibility to restriction enzymes were investigated by taking forward each isolate for genome sequencing. This report details the microbiological characterisation and bioinformatics analysis of these three novel *Salmonella* bacteriophages, vB_SenS-Ent1, vB_SenS-Ent2 and vB_SenS-Ent3.

Nucleotide sequence accession number. The whole-genome sequence of phage vB_SenS-Ent1 has been deposited in the international nucleotide sequence database under accession number HE775250.

3.2 Results

3.2.1 Isolation of the vB_SenS-Ent phages

The vB_SenS-Ent bacteriophages were isolated from swine lagoon effluent and named according to the recommendations outlined by Kropinski *et al.,* (2009), with an additional mnemonic of Ent to denote the host *Salmonella* Enteritidis serotype. A total of four *Siphoviridae* were isolated from a single effluent sample of which three were taken forward for further study. All three phages propagated efficiently on *Salmonella* Enteritidis phage type 4 (PT4) and upon plating produced relatively large plaques, at least 5 mm in diameter (n=30). The morphology of plaques may be termed as 'bull's-eye', but are best described as consisting of at least three discrete zones. Plaque centres exhibited clearing but contained a number of small colonies. Moving outwards, the second zone consisted of a halo of reduced turbidity, extending to the plaque boundary with the bacterial lawn. A third zone, consisting of a ring of increased turbidity relative to the surrounding bacterial lawn, was observed occasionally just beyond the plaque boundary. Once purified, small stocks were propagated and each candidate phage isolate was taken forward to determine sensitivity to restriction digestion with *BamH*I, *EcoR*V, *Sma*I, *Xba*I and *Hind*III and for estimation of genome size by PFGE.

3.2.2 Propagation and Purification

For phage Ent1 growth of the bacterial culture appeared to be inhibited for around 90 minutes prior to lysis, a longer period than observed for phages Ent2 or Ent3 where lysis occurred after a period of >30 minutes incubation (Figure 11). Lysis was indicated by a significant drop in culture absorbance and was visually apparent by clearing of the bacterial culture. After 7 hours a slow increase in absorbance was observed for all lysates, probably representing population growth of resistant mutants. Growth of the phage-free control culture showed typical lag, exponential and stationary phases. The onset of stationary phase, indicated by a plateau in measured absorbance, was apparent after 8 hours.

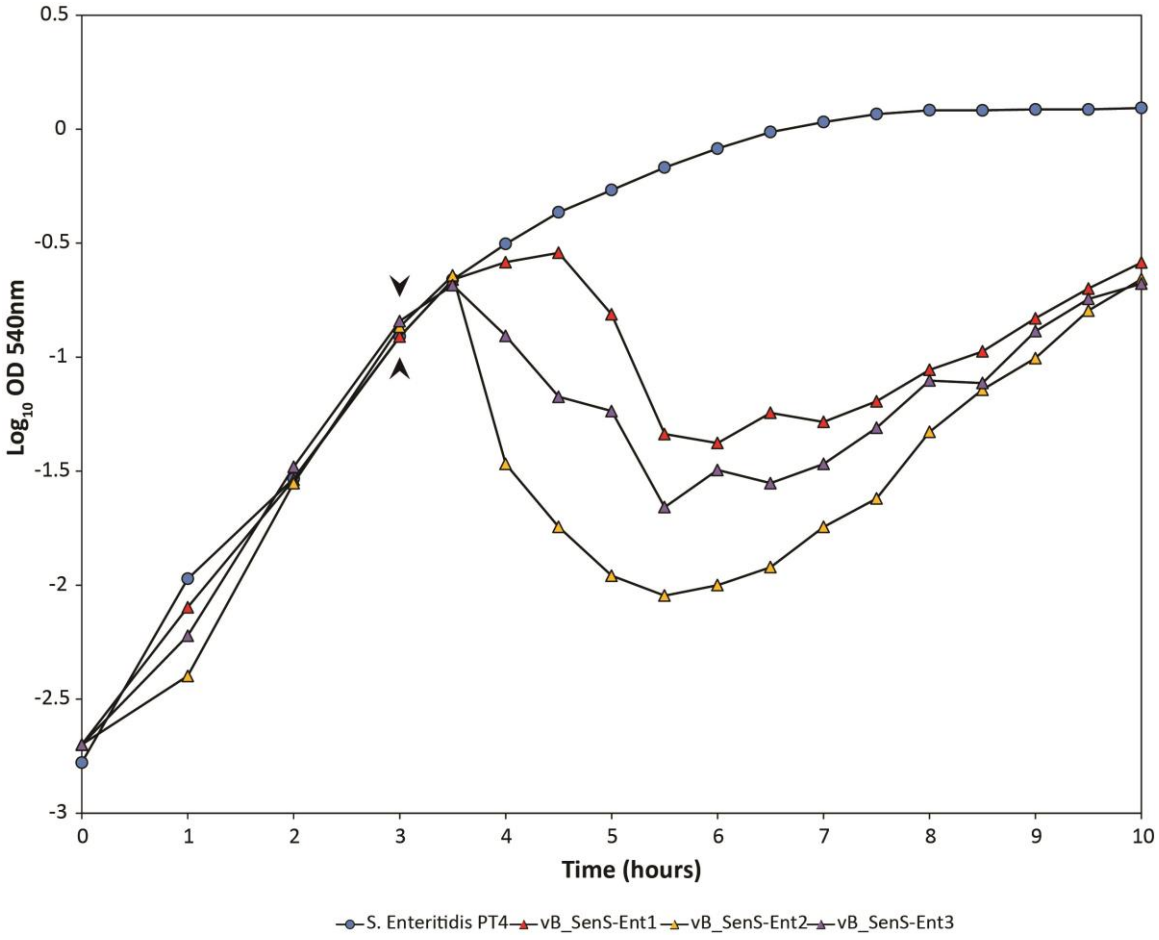

Figure 11. Propagation of bacteriophages vB_SenS-Ent1, Ent2 and Ent3 measured by optical density at 540nm. The chart represents a single propagation experiment. Host cells were grown in LB broth supplemented with 10 mmol l^{-1} $MgSO_4$ and 1 mmol l^{-1} $CaCl_2$ at 37°C with orbital shaking at 150 rpm. The time point of phage addition (3 hours) to bacterial cultures is marked on the graph by the arrows.

Propagation using *S. Enteritidis* as the host routinely yielded lysates containing 10^{10} pfu ml^{-1}, which after clarification and precipitation with polyethylene glycol, could be concentrated to >1 x 10^{11} pfu ml^{-1}. Purified virions were obtained using CsCl density gradient centrifugation (Figure 12).

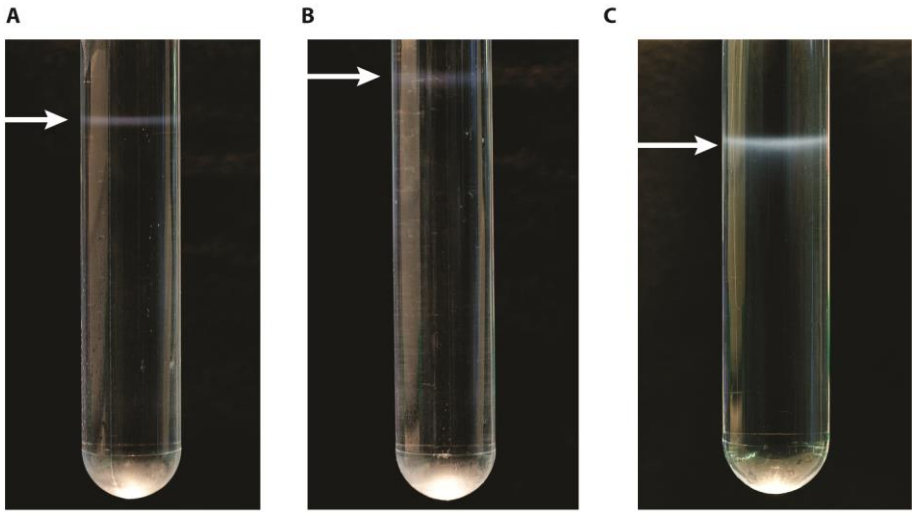

Figure 12. Bacteriophage bands recovered after isopynic CsCl density gradient centrifugation. A, Felix O1; B, vB_SenS-Ent1; C, vB_SenS-Ent1 band after equilibration centrifugation in CsCl (ρ = 1.5). The white arrows indicate the location of bacteriophage bands.

3.2.3 Restriction analysis and estimation of genome size

Estimations of genome size by PFGE suggested that the vB_SenS-Ent phages all possessed genomes of approximately 45 kb. DNA from phages Felix O1 and T4 were run alongside samples to provide controls and estimations of 85 and 170 kb agreed closely with the length of sequences deposited in the International Nucleotide Sequence Databases (INSD). Whilst the predicted genome sizes were similar for the Ent phages, their susceptibility to digestion by restriction enzymes differed considerably (Figure 13). Phage Ent1 was resistant to digestion by *Bam*HI whereas both Ent2 and Ent3 were susceptible to the activity of this enzyme. Conversely, both Ent2 and Ent3 were resistant to *Xba*I whereas Ent1 was not. Ent3 showed additional resistance to digestion by *Sma*I. On the basis of these differing restriction patterns, these three phages were taken forward for further characterisation and genome sequencing.

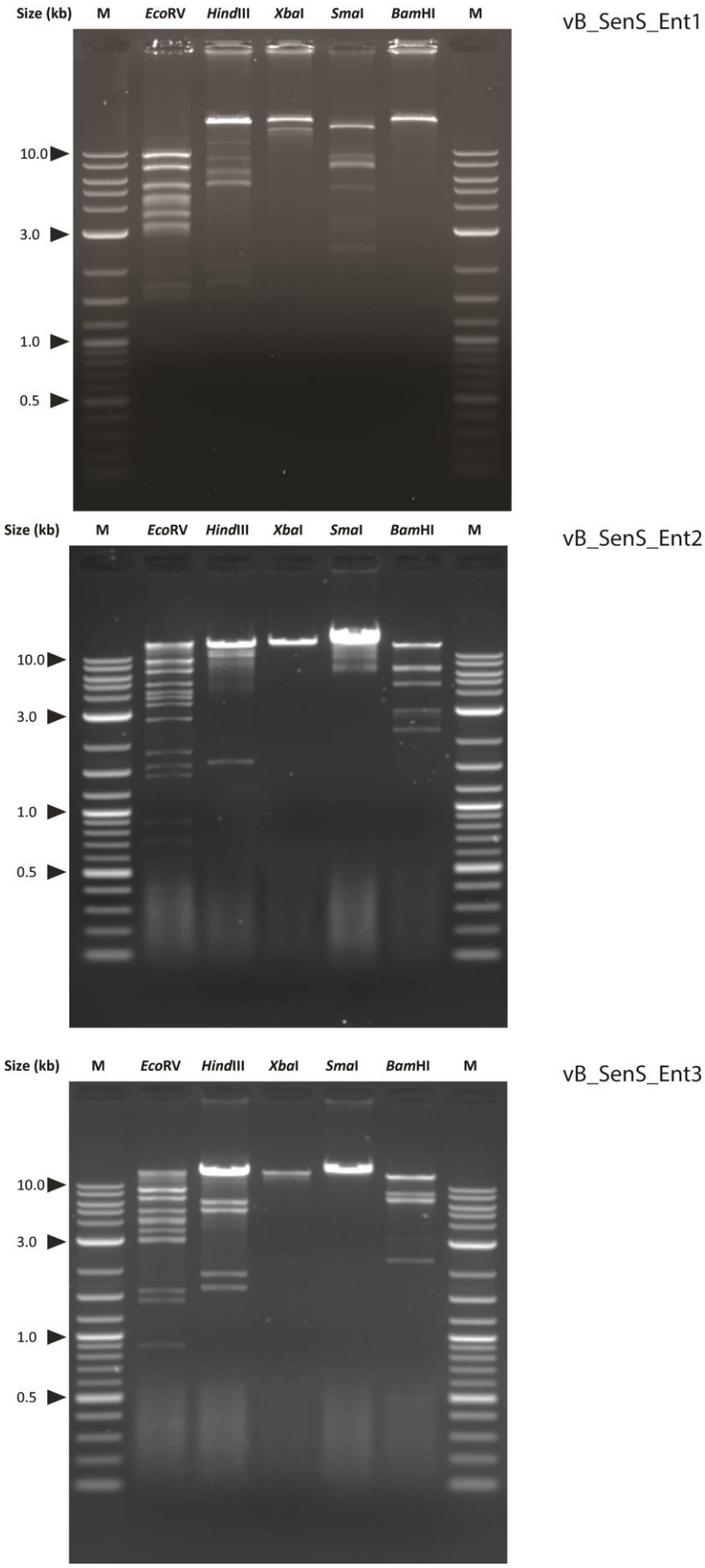

Figure 13. Sensitivity of the vB_SenS_Ent bacteriophage genomic DNA to restriction enzymes. Experiments were performed on at least 3 independent occasions to verify reproducibility of fragment banding patterns.

3.2.4 Virion morphology

Examination by transmission electron microscopy revealed the vB_SenS-Ent phages as members of the *Siphoviridiae* family of dsDNA bacteriophages (Figure 14), similar to the Jersey morphotype (Ackermann, 2007b). The phage particle consists of an isometric head of 64 nm mean diameter (n=20) and flexible, non-contractile tail 116 nm in length and 8.5 nm in width. The tail appears to have transverse striations and 6 short tear drop shaped tailspikes can be distinguished at the terminal end.

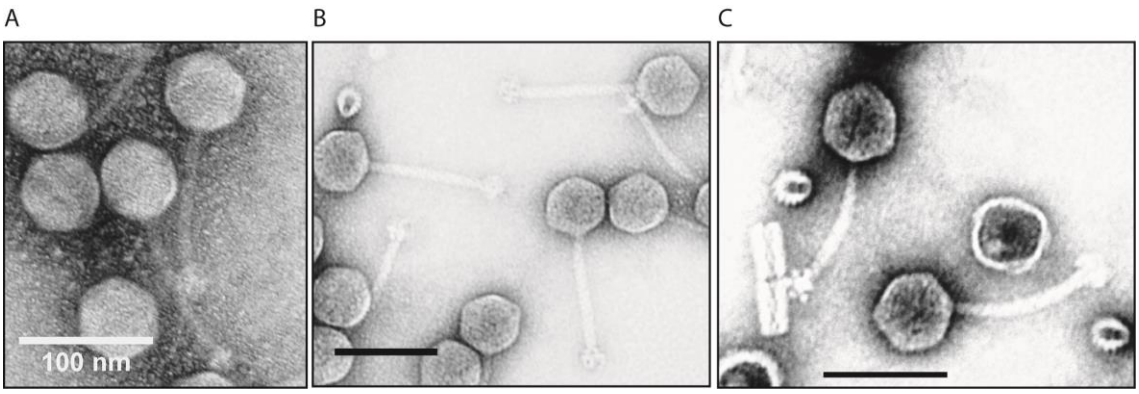

Figure 14. Transmission electron micrograph of A) vB_SenS-Ent1, B) vB_SenS-Ent2 and C) vB_SenS-Ent3 stained using 2 % aqueous uranyl acetate. Scale bars represent 100 nm.

3.2.5 Adsorption and one step growth

The infection process of the vB_SenS-Ent phages upon co-incubation with *S.* Enteritidis PT4 was investigated by standard adsorption and one-step growth assays. At 37^{o}C vB_SenS-Ent1 exhibited rapid adsorption, 6.73 x 10^{-9} ml min^{-1} (R^2 = 0.992), to cells of *S.* Enteritidis PT4. Adsorption rate constants were similar for vB_SenS-Ent2 and vB_SenS-Ent3 at 6.20 and 3.82 x 10^{-9} ml min^{-1} ($R^2 \geq$ 0.96), respectively (Figure 15).

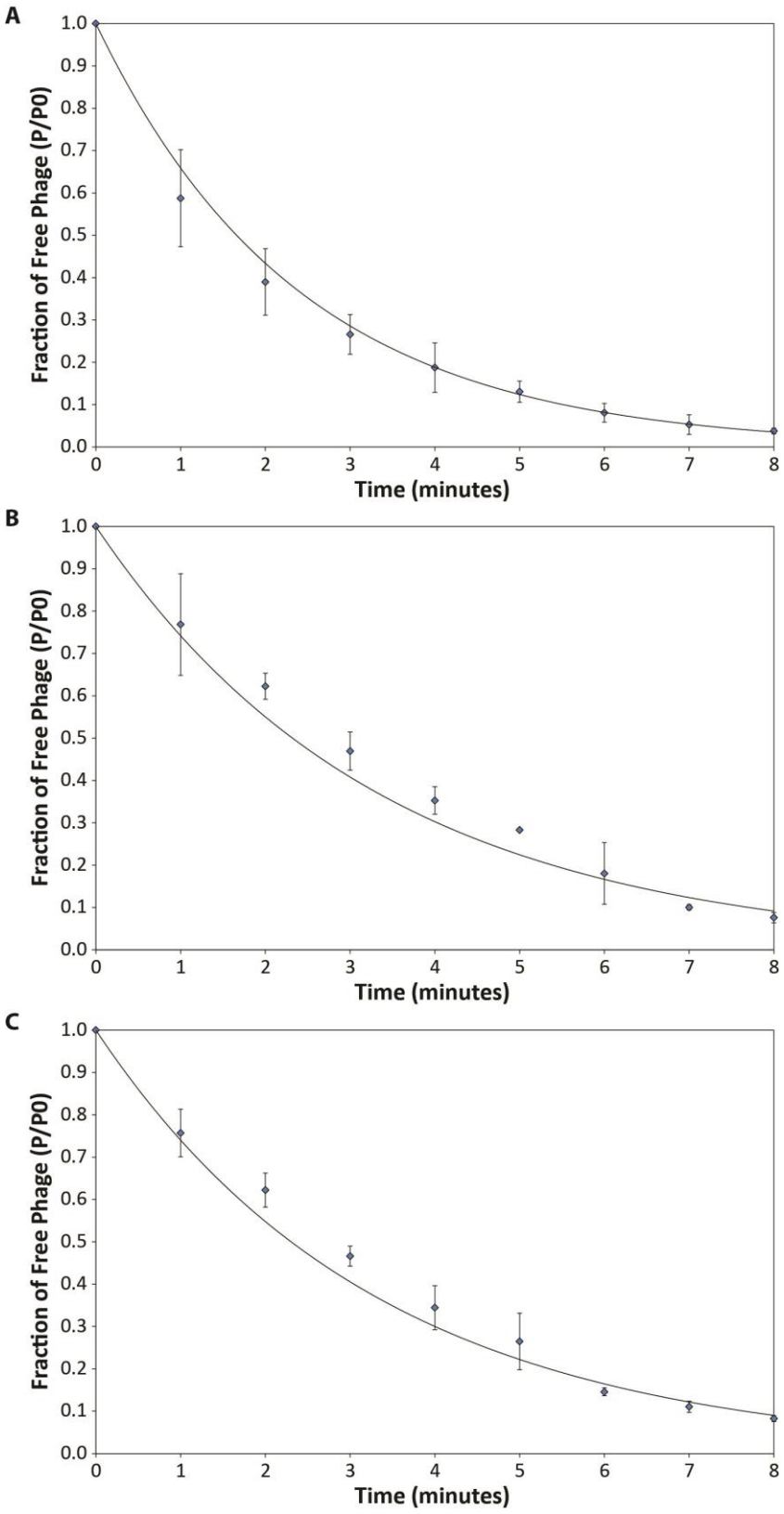

Figure 15. Adsorption of vB_SenS-Ent1 (A), vB_SenS-Ent2 (B) and vB_SenS-Ent3 (C) to cells of *Salmonella* Enteritidis shown as the fraction of free phages remaining over time. Results represent the mean and standard deviation of at least three independent experiments.

One step growth curves yielded identical results for vB_SenS-Ent1, -Ent2 and -Ent3 (Figure 16). Once adsorbed to host cells, the Ent phages exhibited latent and eclipse periods of 25 and 20 minutes, respectively. The rise period began after 25 minutes, with host cell lysis completed after 35 minutes

releasing 35 progeny virions per infected cell. Estimations of burst sizes were corroborated by single burst experiments comprising 150 samples for each bacteriophage.

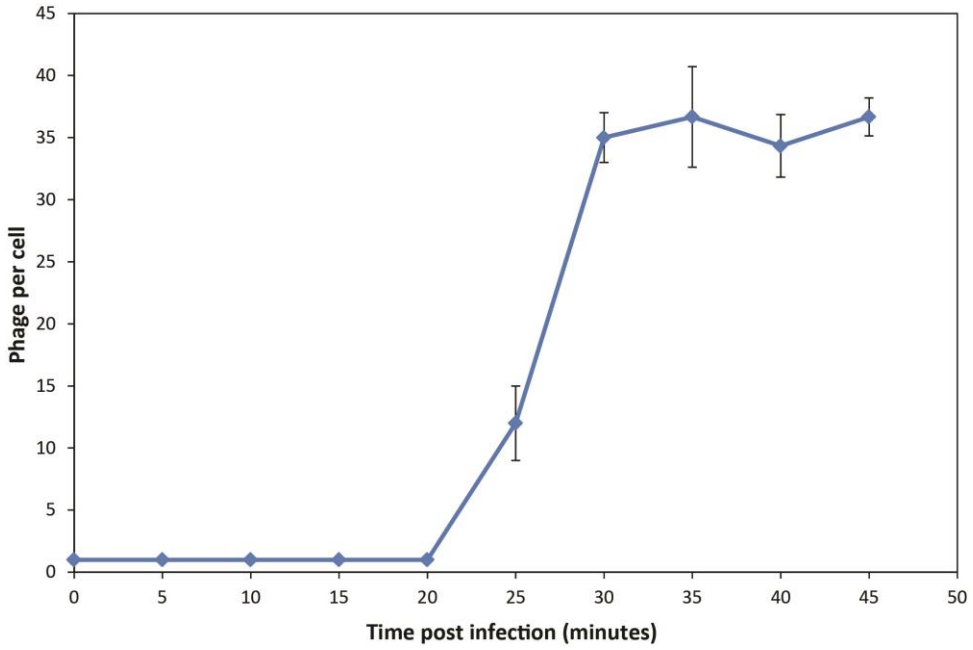

Figure 16. One step growth curve for vB_SenS-Ent1 using *S.* Enteritidis PT4 as host. Data presented are the mean and standard deviation of three independent experiments.

3.2.6 Host range and efficiency of plating

Host range was assessed by the ability of log-fold dilutions of vB_SenS-ENT phages to form plaques upon a library of *Salmonella* consisting of 48 different isolates. Serovars Typhimurium and Enteritidis were represented by 9 and 8 isolates, respectively (Table 6). At the highest dilution of bacteriophages, approximately 10^{10} pfu ml^{-1}, Ent1 formed plaques on 25 isolates (52 %), Ent2 on 23 isolates (48 %) and Ent3 on 24 isolates (50 %). The number of isolates showing formation of spot plaques reduced with increasing dilutions of bacteriophages (Figure 17).

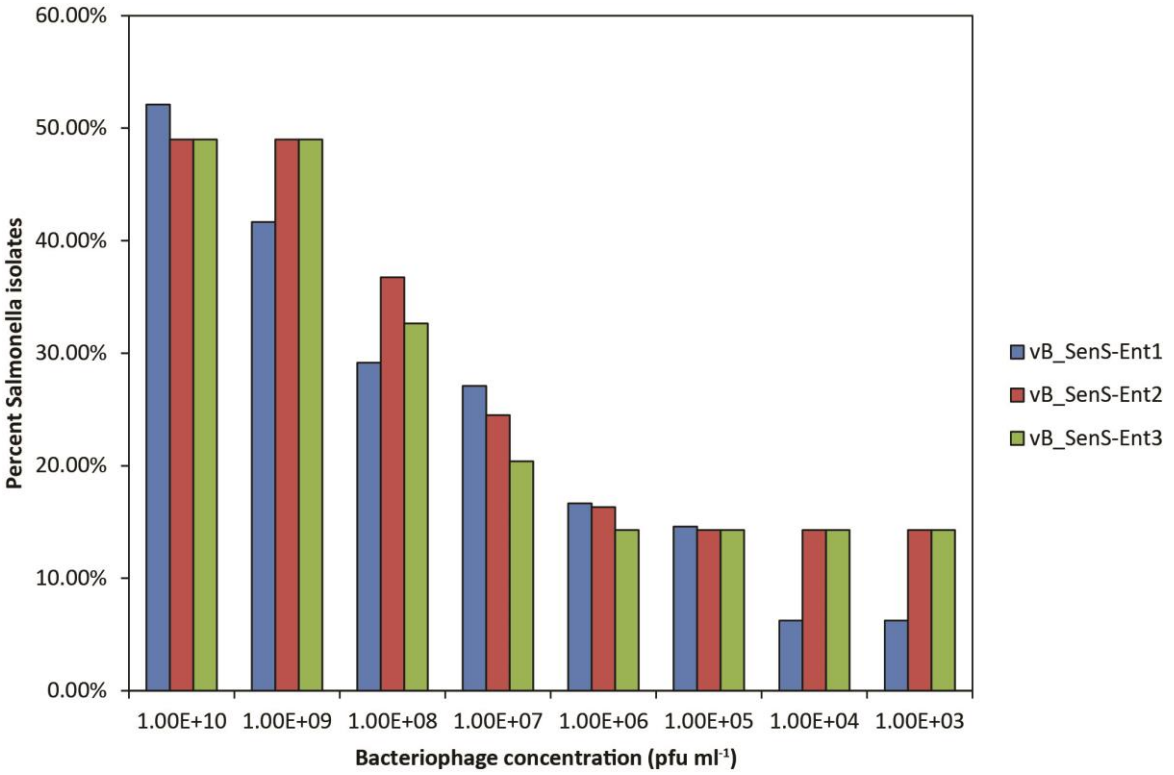

Figure 17. Percentage of *Salmonella* isolates forming plaques by spot plate assay with decreasing concentrations of bacteriophage.

Sensitive isolates were taken forward to ascertain the relative efficiency of plating (EOP). EOP represents a more rigorous analysis of the ability of a bacteriophage to form plaques as phage particles are allowed to adsorb to host cells at lower concentrations or are distributed throughout the overlay agar rather than presented at the lawn surface as a concentrated focal 'spot'. Hence, the formation of plaques results from productive infection of a bacterium by at least a single phage particle rather than by non-productive infection or lysis from without.

The ability of the Ent phages to form plaques under EOP assay conditions differed markedly from spot plates and the number of sensitive isolates was reduced substantially for each phage (Table 6). Productive lysis was reduced to 14 of 48 isolates (31.25 %) for Ent1, while Ent2 and Ent3 both showed productive lysis on 12 strains (25 %). Plating efficiencies ranged from 5.67×10^{2} to 3.94×10^{-9} for susceptible isolates. With the exceptions of *S.* Enteritidis CBRI 1944, which was resistant to infection, and a reduced EOP of 10^{-7} for *S.* Enteritidis PT13a, the Ent phages infected all isolates of *S.* Enteritidis at similar or greater efficiencies to the propagating strain. For *S.* Typhimurium, each of the Ent phages were able to form plaques on four of the nine isolates tested. Efficient infection relative to the host strain was observed for only one Typhimurium isolate, CBRI 1005. Only two isolates exhibited plaque formation with all three Ent phages, CBRI 1005 and S07519-07. Ent2 did not form plaques on *S.* Typhimurium isolate VLA S07541-07 while isolate VLA S07540-07 was not lysed by Ent3. Overall, each of the Ent phages showed broadly similar host specificity profiles and plating

efficiencies. It is notable that aside from serovar Napoli, only Ent1 formed plaques upon *Salmonella* serovars other than Enteritidis and Typhimurium.

Table 6. Host range of the vB_SenS-Ent bacteriophages. Spot plate results were scored visually where ++++, complete lysis; +++, slight turbidity; ++, heavy turbidity; + single plaques; 0, no plaque formation. The reader is referred to Figure for images of plaques corresponding to these scores. Efficiency of plating (EOP) values represents the ratio of plaques formed upon a bacterial isolate relative to the propagating host, *S.* Enteritidis PT4. NT, Not tested; 0, no plaque formation. All data were determined from three independent repeats.

		vB_SenS-Ent1		vB_SenS-Ent2		vB_SenS-Ent3	
Isolate	**Accession Number**	**Spot Plate**	**EOP**	**Spot Plate**	**EOP**	**Spot Plate**	**EOP**
***S. enterica serovar* Enteritidis**							
S. Enteritidis	VLA S07533-07	++++	2.64×10^{-1}	++++	9.40×10^{-1}	++++	6.2×10^{-1}
S. Enteritidis PT 13	VLA S04967-07	++	4.04×10^{-7}	++	2.86×10^{-2}	++	8.29×10^{-6}
S. Enteritidis PT1	CBRI 1937	++++	1.47×10^{-1}	++++	7.44×10^{-1}	++++	1.19
S. Enteritidis PT4	VLA S07544-07	++++	HOST	++++	HOST	++++	HOST
S. Enteritidis	CBRI 1869	++++	6.24×10^{-1}	++++	0.188034	++++	1.62×10^{-1}
S. Enteritidis	CBRI 1870	+++	10.4	++++	0.854701	++++	1.31
S. Enteritidis	CBRI 1951	++	567	++++	0.0598	++++	1.43×10^{-1}
S. Enteritidis	CBRI 1944	+++	0	-	NT	-	NT
***S. enterica serovar* Typhimurium**							
S. Typhimurium	VLA S07519-07	++	1.27×10^{-5}	++	3.87×10^{-2}	++	3.43×10^{-3}
S. Typhimurium	VLA S07540-07	++	1.64×10^{-5}	++	9.29×10^{-2}	++	0
S. Typhimurium	VLA S07541-07	++++	4.96×10^{-4}	-	NT	++	1.14×10^{-2}
S. Typhimurium DT104b	VLA S01523-08	++	0	++	0	++	0
S. Typhimurium	CBRI 1960	+++	0	++	4.71×10^{-7}	++	4.29×10^{-7}
S. Typhimurium	CBRI 1962	+++	0	++	0	++	0
S. Typhimurium	CBRI 1005	+++	1.34×10^{-1}	++++	1.0683	++++	9.05×10^{-1}
S. Typhimurium	CBRI 1006	++	0	++	0	++	0
S. Typhimurium	CBRI 1007	+++	0	++++	0	++++	0
Other Serovars							
S. Agona	NCTC 11377	++	0	++++	0	+++	0
S. Brandenburg	VLA S07530-07	-	NT	-	NT	-	NT
S. Braenderup	VLA S02130-08	-	NT	-	NT	-	NT
S. Braenderup	VLA S07531-07	-	NT	-	NT	-	NT
S. Concord	NCTC 6588	-	NT	-	NT	-	NT
S. Crossness	NCTC 11059	-	NT	-	NT	-	NT
S. Derby	HPA	++	0	+++	0	+++	0
S. Dublin	VLA S07539-07	+++	5.81×10^{-5}	-	-	-	-
S. enterica 4, 12: e, h: -	VLA S07521-07	+++	0	+++	0	+++	0
S. enterica 6, 8: -: e, n, x	VLA S07523-07	-	NT	+++	0	+++	0
S. enterica O-Rough: z10: -	VLA S07520-07	-	NT	-	NT	-	NT
S. enterica O-Rough: e, h: e, n, x, z15	VLA S07538-07	+	3.94×10^{-9}	-	-	-	NT
S. arizonae 6: 13, 14	NCTC 7308	-	NT	-	NT	-	NT
S. Heidelberg	VLA S07546-07	++	4.30×10^{-6}	+++	0	++	0
S. Heidelberg	VLA S07529-07	++	0	++	0	++	0
S. Infantis	CBRI 1037	-	NT	-	NT	-	NT
S. Inverness	NCTC 6591	-	NT	-	NT	-	NT
S. Jerusalem	NCTC 8146	-	NT	-	NT	-	NT
S. Mbandaka	VLA S07524-07	-	NT	-	NT	-	NT
S. Molade	VLA S07526-07	-	NT	-	NT	-	NT
S. Montevideo	CBRI 1030	-	NT	-	NT	-	NT
S. Napoli	NCTC 6853	++	4.30×10^{-6}	++	3.76×10^{-6}	++	4.55×10^{-6}
S. Orion var. 15+	VLA S07525-07	-	NT	-	NT	-	NT

S. Panama	CBRI 1045	-	-	+++	0	+++	0
S. Poona	NCTC 4840	-	NT	-	NT	-	NT
S. Seftenberg	VLA S07528-07	-	NT	-	NT	-	NT
S. Tennessee	NCTC 6388	-	NT	-	NT	-	NT
S. Typhisuis	NCTC 347	-	NT	-	NT	-	NT
S. Utrecht	NCTC 10077	-	NT	-	NT	-	NT
S. Virchow	CBRI 1012	-	NT	-	NT	-	NT
S. Virchow	CBRI 1010	-	NT	-	NT	-	NT
Other Gram-negative bacteria							
Escherichia coli Nissle 1917	Ardeypharm GmbH	-	NT	-	NT	-	NT
E. coli	NCTC 10418	-	NT	-	NT	-	NT
E. coli O157:H7	NCTC 12900	-	NT	-	NT	-	NT
Pseudomonas aeruginosa PAO1	ATCC 15692	-	NT	-	NT	-	NT
P. aeruginosa	NCTC 13359	-	NT	-	NT	-	NT
Citrobacter freundii	NCTC 6266	-	NT	-	NT	-	NT
Klebsiella aerogenes	NCTC 9660	-	NT	-	NT	-	NT

Genome sequencing results indicate that host specificity of the Ent phages is mediated by the presence of a P22-like tailspike. For P22, this protein binds to O-antigen 12, found in serogroups A, B and D1. From the panel of serovars tested, it is clear that all isolates allowing productive infection by the ENT phages possess the O-antigen 12. However, it was noted that vB_SenS-Ent1 formed plaques, albeit at low efficiency, upon the rough strain *S. enterica* e,h: e,n,x,z (VLA S07538-07) but did not plaque upon another rough isolate, *S. enterica* z10:- (VLA S07520-07). No lysis was observed when the vB_SenS-Ent phages were co-incubated with representatives of four other Gram-negative bacterial species.

3.2.7 Genome properties and architecture

A single consensus sequence for each Ent phage was obtained by 454 pyrosequencing at 30, 146 and 92-fold coverage for Ent1, Ent2 and Ent3, respectively. The vB_SenS-Ent1 particle encapsulates a linear dsDNA molecule 42,391 bp in length with an average G+C content of 49.79 %, slightly lower than the average of 52 % reported for serovars of *Salmonella enterica* (McClelland *et al.,* 2001, Reen *et al.,* 2005, Thomson *et al.,* 2008). The vB_SenS-Ent2 genome is 42,093 bp in length (49.92 % G+C) and for vB_SenS-Ent3 the size is 42,764 bp (49.79 % G+C). Genomes were opened upstream of the putative small terminase subunit, following the convention established for bacteriophages λ and P22. A total of 58, 56 and 60 open reading frames (ORFs) were predicted for Ent1, Ent2 and Ent3, respectively (Figure 18), accounting for a coding potential of >90 %. Each of the genomes may be structured into 4 clusters on the basis of transcriptional direction. The genes are tightly spaced at a density of 1.37 per kb and have an average length of 678 bp. Short overlaps between the stop codon of one gene and the start codon of the adjacent downstream gene are common and no tRNA genes were discovered with either tRNAscan-SE, WebGester or ARAGORN. As for many bacteriophages, only a limited number of protein functions could be predicted by sequence similarity and the

presence of conserved domains (Supplemental Tables 1 through 6). As such, many ORFs were annotated as hypothetical.

Whilst synteny of gene order is often preserved within arrays of genes, particularly those encoding structural and assembly proteins in the *Siphoviridae*, bacteriophage genomes are strikingly mosaic (Hatfull, 2008). Individual genes and gene segments are exchangeable by horizontal transfer with members of the population by a number of potential mechanisms (Hatfull and Hendrix, 2011). Where similarities in nucleotide sequence are no longer apparent, the comparison of amino acid sequences and predicted tertiary structures are useful tools to delineate common protein ancestries.

Like most phages, the genome structure of the vB_SenS-Ent phages exhibits a modular organisation with four gene clusters representing two early and two late transcriptional regions (Figure 18). Late clusters encompassed genes coding for proteins involved in genome packaging (gp01 to gp03), virion structure and morphogenesis (gp05 to gp19) super-infection immunity (gp20 to 24) and lysis (gp51 and gp52). With the exception of gp42, all early ORFs with inferred DNA replication (gp32 to gp45) or regulatory functions (gp20 to gp24) are encoded on the complementary strand. A relatively large noncoding region of approximately 1 kb is located between gp45 and gp46, and this region contains the minimum G+C skew, suggesting that it may contain the replication origin site. Full descriptions for predicted open reading frames and the presence of domains and motifs for the vB_SenS-Ent phages are provided in Appendix II.

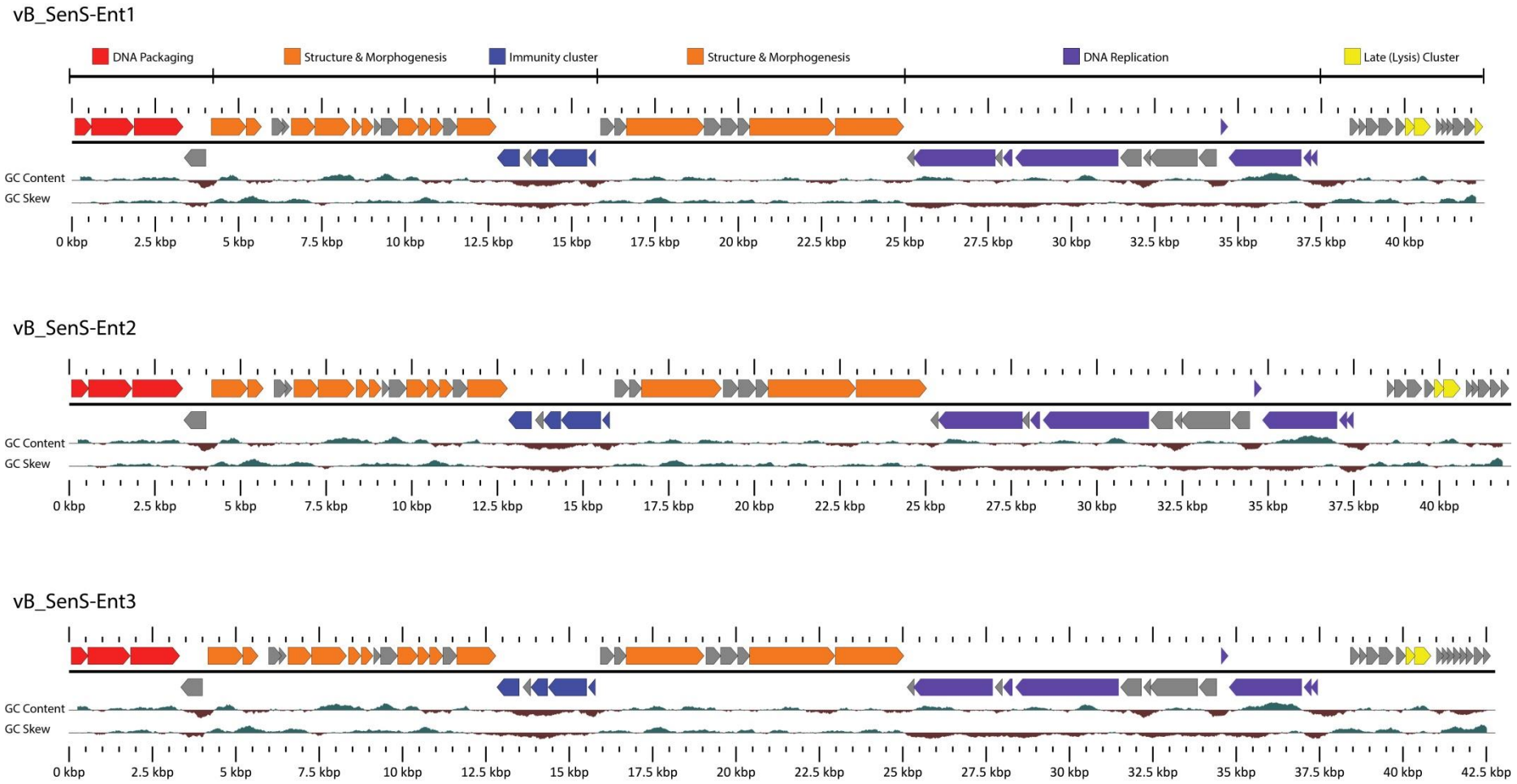

Figure 18. Linear map of the vB_SenS-Ent1, vB_SenS-Ent2 and vB_SenS-Ent3 genomes prepared using GView. Arrows denote coding sequences and have been coloured according the generalised function of each gene cluster. Grey arrows denote hypothetical proteins of unknown function.

3.2.8 Packaging, morphogenesis and structural proteins

Nearly half (48 %) of the Ent virion genomes are devoted to encoding proteins involved in packaging, structure and morphogenesis. These genes comprise two gene clusters totalling 27 ORFs, separated by an immunity region spanning genes gp20-24. The arrangement of genes encoding virion structural and morphogenesis proteins generally follows a conserved organisation in the *Siphoviridae* (Casjens, 2005; Hatfull, 2008) and have been characterised in detail for *Escherchia coli* phages λ and T5, *Bacillus subtilis* phage SPP1 and *Lactococcus* phages TP901-1 and p2. Both gene order and function appear highly conserved among the vB_SenS-Ent phages and related *Siphoviridae.*

One dimensional SDS-PAGE of CsCl purified vB_SenS-Ent virions yielded 10 bands consisting of 4 major bands at 72, 42, 38 and 13.5 kDa and 6 minor bands of 90, 56, 20, 18 and 9 kDa (Figure 19). Further proteins were identified on 2D SDS-PAGE gels and genes corresponding to spots were annotated on the basis of predicted molecular mass, isoelectric point and protein homologues from HHpred, BLASTP and PSI-BLAST queries.

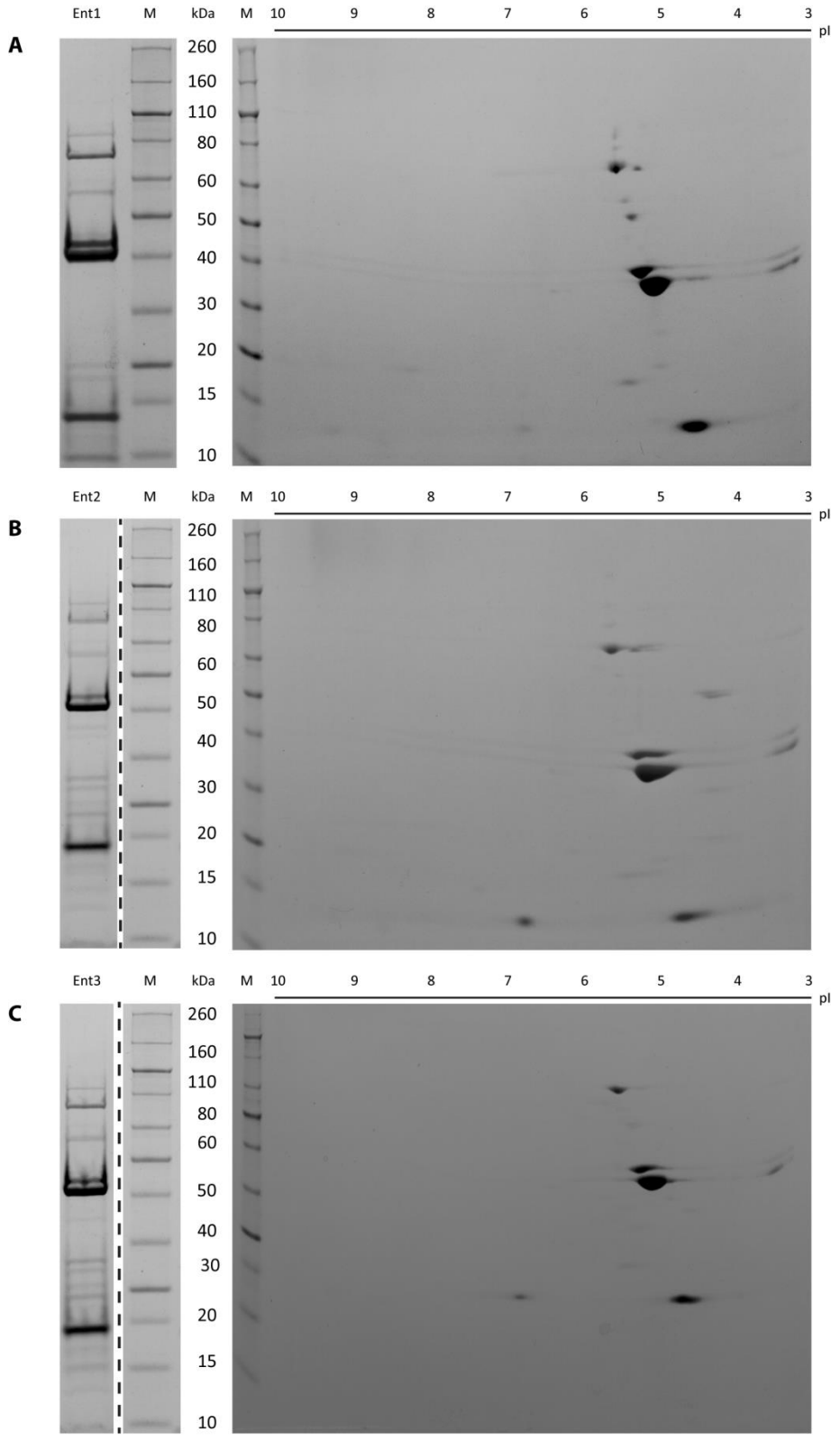

Figure 19. vB_SenS-Ent phage structural proteins resolved by 1D and 2D SDS-PAGE. A. vB_SenS-Ent1. B. vB_SenS-Ent2. B. vB_SenS-Ent3. Banding patterns were confirmed Two replicates were performed for 2D.

Gene gp01 was assigned as the small terminase subunit due to its position immediately upstream of the large terminase subunit, gp02. BLASTP results showed limited protein sequence identity (37 %) to gp01 of *Sodalis* phage SO-1, whilst PSI-BLAST analysis yielded hits to small terminase subunits of phage infecting both Gram positive and Gram negative bacteria and HHpred returned a strong hit to the crystal structure of the Sf6 small terminase (pdb: 3hef). A terminase 6 family domain (PF03237) spanning residues 24-406 was identified by Pfam analysis of Gp02. Gp03 was identified as the putative portal protein due to its position immediately downstream of the large terminase subunit. Supporting this assignment, a spot of 58 kDa, slightly larger than the predicted mass of 54 kDa, was observed on 1D and 2D SDS gels.

Gp05 was predicted to belong to the phage Mu protein F like family (PF04233). A member of this Pfam family is gp07 of phage SPP1, a non-essential minor protein participating in capsid assembly and DNA packaging (Dröge *et al.,* 2000). The presence of an immunoglobulin-like I-set domain (PF13895) in gp06 suggests that this gene encodes a head decoration protein. Head decoration proteins have been described for phages L, λ and ES18 and are thought to aid stabilisation of the capsid structure against disruption by chelating agents (Gilcrease *et al.,* 2005). Immunoglobulin-like domains are found widely within the *Caudovirales* and are predominantly associated with structural proteins. The precise role of such domains remains unclear but it has been suggested that they facilitate weak, non-specific binding to the cell surface or act to stabilise the virion structure (Fraser *et al.,* 2007).

No putative function could be assigned to either gp07 or gp08. However, gp08 has multiple potential start sites which would yield significant overlap with gp07 and gene calling routines showed disagreement as to the correct start codon, perhaps indicating that gp08 is expressed using a translational frameshift. A scaffold protein with a predicted mass of 25.7 kDa is encoded by gp09 immediately upstream of the major coat protein (MCP) gp10. The MCP appears as a strong band of 38 kDa on SDS gels. PSI-BLAST and HHpred results suggest that Gp11 is a distant homologue of the gp8.5 head fibre of *Bacillus* phage PZA and Phi-29, respectively. As second I-set domain (IPR007110) is found in gp12 and PSI-BLAST hits included Hoc and Wac proteins. The proximity to the MCP suggests that both these proteins are involved in head completion.

The six open reading frames (gp13-gp18) located downstream of gp12 probably constitute head to tail joining and tail scaffold proteins and of these, gp15, gp16 and gp17 are candidates for spots on 2D SDS-PAGE gels. Two ORFs, gp14 and gp16 can be linked by PSI-BLAST searches to proteins found in mature virions of the *Pseudomonas aeruginosa* phage vB_PaeS-Kakheti25 (Karumidze *et al.,* 2012). HHpred analysis of Gp18 identified SPP1 Gp17 and the λ GpU minor tail protein as homologs. No ORFs encoding candidate ejection proteins such as those reported for P22 and SPP1 were identified

through database searches. Gp19 was assigned as the major tail protein (MTP) on the basis of PSI-BLAST results and presence as a strong band of 41 kDa on SDS gels.

Genes comprising the second structural gene cluster encode the proteins forming the virion tail. No candidate slippery sequence associated with a programmed translational frameshift was identified within the coding regions of gp25 and gp26, though this may be due to inexperience (Xu *et al.,* 2004). Gp27 was assigned as the tail tape measure protein and a strong spot at 83 kDa corresponding to the predicted size of this gene product was observed on 2D gels. The length of the tape measure protein agreed precisely with the measured length of the virion tail from TEM images, assuming a ratio of 0.15 nm per amino acid residue as reported for λ (Katsura & Hendrix, 1984), and like other tape measure proteins gp27 is predicted to form a predominantly helical structure. Three ORFs separate gp27 from the putative tail fibre gene gp31. Referring to the organisation of the structural cassette in SPP1, P22 and phages infecting *Lactococcus* species it is plausible that these genes encode the distal tail baseplate (Casjens & Thuman-Commike, 2011; Mc Grath *et al.,* 2006; Veesler & Cambillau, 2011). PSI-BLAST analysis of gp31 revealed similarities to the GpJ host specificity protein of λ and p33 of phage T1. A tail spike, gp32, was identified with confidence due to the presence of a complete Pfam P22 tail spike domain (PF09251), indicating that adsorption of Ent1 to host cells involves recognition of the LPS O:12 antigen. BLASTN and BLASTP analyses revealed significant homologues in the *Siphoviridae*; SE2, KS7, SETP3, SETP5, SETP7, SETP12 and SETP13, and *Podoviridae*; P22, SE1, ST104, ST64T and SETP1, SETP14 and SETP15. A ClustalW alignment of Gp32 revealed an N-terminal sequence similar to other *Salmonella Siphoviridae* SE2, KS7 and SETP phages 3, 5, 7 and 12, but retaining significant conservation in the catalytic and C-terminal regions relative to P22. N-terminal sequences of P22-like tail spikes are involved in attachment to the virion tail structure and exhibit conservation between related phages within the *Podoviridae*, *Siphoviridae* and *Myoviridae* (Hooton *et al.,* 2011). Spots and bands corresponding to the predicted mass of the putative tape measure, tail fibre and tailspike were apparent on 1D and 2D SDS gels.

3.2.9 Regulatory proteins

Phage genomes usually encode of a number of regulatory proteins which, in concert with host proteins, co-ordinate the expression of early and late genes. The Ent phages possess a regulatory module consisting of 5 early genes encoded on the complementary strand, gp20 through gp24, dividing the array of genes responsible for virion morphogenesis. Gp20 showed strong sequence similarity to winged-helix DNA binding proteins from a number of different phage and bacteria and contains matches to two Pfam family domains; ANT (PF03374) and pRha (PF09669). In P22 *ant* encodes an anti-repressor which inhibits binding of the *c2* repressor to the P_L and P_R operators enabling the expression of genes necessary for lytic development (Byl & Kropinski, 2000). The pRha domain represents a family of proteins whose expression is detrimental for lytic growth in the

absence of integration host factor function (Henthorn & Friedman, 1995). Gp22 is predicted to encode a free standing HNH endonuclease (PF13392) and PSI-BLAST analysis of gp23 revealed similarities to recombination endonuclease subunits. Gp24 shares extended similarity to the inner membrane immunity (Imm) proteins effecting exclusion of superinfecting phage (Lu *et al.,* 1993). BLASTP homologues included phages JS98 (Zuber *et al.,* 2007), vB_EcoM-VR7 (Kaliniene *et al.,* 2011) and IME08 (Jiang *et al.,* 2011). Supporting the protein homologue evidence, Gp24 is predicted to localise at the cytoplasmic membrane (PSortb) and contain two transmembrane domains (TMHMM).

In addition to the regulatory gene cluster two ORFs, gp04 and gp42, interrupt the sequence of the structural and replication gene modules, in each instance encoded in the opposite orientation to the transcriptional direction of the respective module. The first, gp04, separates the structural genes gp03 and gp05. The sequence of gp04 exhibits negative GC skew in relation to neighbouring coding sequences, suggestive of a historical horizontal acquisition event. Protein homologues detected by PSI-BLAST suggest that gp05 encodes a KilA-like protein. Gp42 interrupts the sequence of the replicative gene cluster and is predicted to act as a transcriptional regulator, possibly involved in control of late gene expression, due to the presence of an N-terminal helix-turn-helix DNA binding domain similar to Cro/CI (PF12844).

3.2.10 The vB_SenS-Ent DNA replication module contains mobile elements

The Ent phages encode at least 12 genes involved in genome replication co-localised as a distinct module. This gene cluster comprises a primase, helicase, DNA polymerase, a restriction endonuclease, two putative DNA binding proteins, a uvsX homologue and 6 hypothetical products. Sequence similarity to other phage-encoded helicases suggested the presence of an in-frame insertion containing a DOD homing endonuclease motif within the sequence of *gp*34. The insertion sequence was identified as a large intein of 348 aa, satisfying the four criteria outlined by Perler *et al.,* (1997). Inteins are defined as internal protein elements that self-excise from their host protein and catalyse ligation of the flanking sequences with a peptide bond yielding two stable proteins, the mature protein and the intein. Searches conducted using BLASTP and the mature helicase resulted in significantly improved alignments to other bacteriophages. Notably, an intein is also present at an identical position within the helicase of the closely related SETP3 phage. Similarly, the DNA polymerase A encoded by gp37 contains a minimal intein, that is lacking an endonuclease domain, of 299 aa consistent with those predicted for the DNA polymerase gene of SETP3, SETP5 and SETP12. To date, 290 inteins are documented for Eubacteria within the InBase database, of which 36 are associated with phages or prophages (Perler, 2002).

Analysis with HHpred and PSI-BLAST suggests that Gp36, Gp38 and Gp40 encode a Holliday junction resolvase (pdb: 1hh1), helix-destabilising ssDNA-binding protein (pdb: 1je5) and RecE helicase subunit (pdb: 3h4r), respectively. Gp43 encodes a putative primease containing an AAA_28 Pfam

domain (PF13481) suggesting that, like *Enterobacteria* phages T4 and T5, Ent1 employs a primosome complex consisting of separate primase and helicase proteins (Ilyina *et al.,* 1992). A further DNA binding protein containing a helix-turn-helix 17 domain (PF12728) with low identity to transcriptional regulators of bacterial and phage origins is encoded by gp45. Of the remaining hypothetical proteins, no putative function could be assigned.

3.2.11 Host lysis and the late Gene Cluster

It is notable that the vB_SenS-Ent phages show the greatest degree of sequence variation within the late gene cluster which begins at gp46. For phages Ent1, Ent2 and Ent3 the late region is comprised of 13, 11 and 15 ORFs, respectively (Figure 20). With the exception of four gene products, common to each phage, no putative functions could be assigned to remaining genes in this region using PSI-BLAST or HHpred. The four common gene products comprise an ATP-dependant protease, class II holin, lysin and transcriptional regulator.

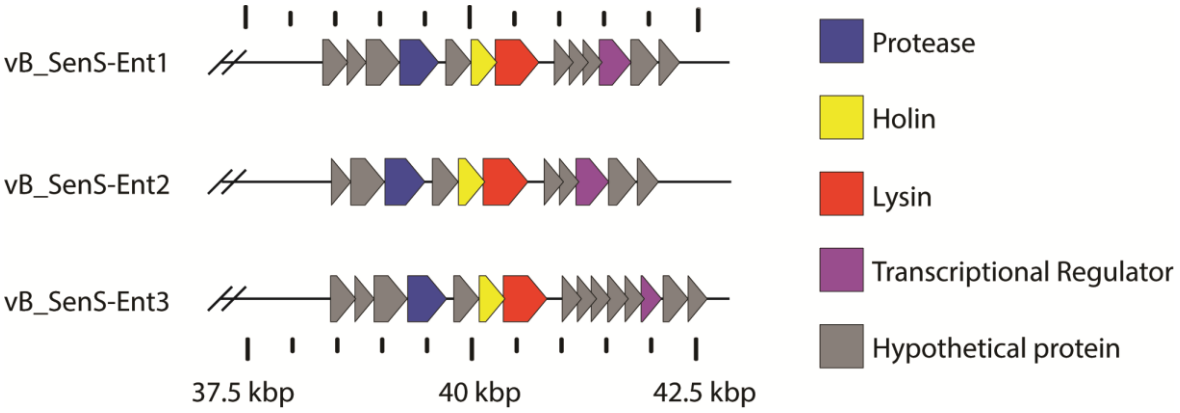

Figure 20. Late gene cluster of the vB_SenS-Ent phages. Genes encoding products with homology to proteins known function are coloured.

Phages of eubacteria employ a dual protein system comprised of a holin and lysin to effect host cell lysis (Young *et al.,* 2000). A lysin with inferred glycoside hydrolyase (lysozyme) activity (PF00959) and is immediately preceded by a protein of 95 aa, predicted to contain two transmembrane regions, a feature consistent with class II holins (Young, 2002). These two genes are separated from downstream genes by a putative rho-independent terminator.

The putative transcriptional regulator contains a PFAM AAA+ domain, representing a superfamily of ATPases. This family of proteins have a diverse range of functions. HHpred shows a short region with structural similarity to the sigma54 activator ZraR of *S.* Typhimurium (pdb: 1ojl).

3.2.12 Promoters

Analysis of 150 bp regions upstream of ORFs using MEME yielded a single candidate motif of 47 bp width (E value = 9.4 x 10^{-8}) containing regions resembling -10 and -35 elements (Figure 21). The RSAT toolset was used to convert the MEME output file to a position matrix and search upstream regions

for additional instances. Locations for the consensus motif were found at an average distance of 48 bases from the start codon, suggesting a role in transcriptional regulation (Tables 7 to 9). No candidate sequences were identified upstream of cluster starts gp04, gp05, gp25 or gp45 and the absence of promoter motifs in these areas suggests that additional sequences involved in transcriptional regulation remain to be found.

Table 7. Locations and DNA sequences of a MEME-identified motif in the vB-SenS-Ent1 genome.

Name	Coordinates	Strand	Sequence
P_{ORF20}	13457..13503	-	AGAATCTGATTTGAACGATAAGAATGTTCGAAGTTAAATATATCTAC
P_{ORF24}	15721..15767	-	AATAGCTTGCATAACCGTTAATAGTGTCCTATTATCTCTACGTCAAC
P_{ORF35}	27932..27978	-	AGAAACAGGTTGATAAATTAATAGAACACTATTATATTTAGTTCACA
P_{ORF38}	32142..32188	-	AAAATTCGGTTGACAAGTTAATAGTACTCTATTATATTCTTAATCAC
P_{ORF41}	34372..34418	-	AAAAAGTGCTTGCATAAATAATAGAGCACGATTATAGTTCTTATCAC
P_{ORF42}	34367..34413	+	AGTTGGTGATAAGAACTATAATCGTGCTCTATTATTTATGCAAGCAC
P_{ORF53}	40887..40933	+	AAATAATAGTTGACTAGTAACATTAACCCTATTATATTTAGTTCATC

Entries highlighted in red font indicate that this sequence overlaps with the 3' end of an upstream ORF.

Table 8. Locations and DNA sequences of a MEME-identified motif in the vB-SenS-Ent2 genome.

Name	Coordinates	Strand	Sequence
P_{ORF24}	15795..15811	-	TTAATAGTGTCCTATTA
P_{ORF25}	15794..15810	+	ATAATAGGACACTATTA
P_{ORF35}	28057..28073	-	TTAATAGAACACTATTA
P_{ORF38}	32267..32283	-	TTAATAGTACTCTATTA
P_{ORF41}	34497..34513	-	ATAATAGAGCACGATTA
P_{ORF42}	34496..34512	+	ATAATCGTGCTCTATTA
P_{ORF46}	38423..38439	+	ATAATAGGGTACTATTA
P_{ORF52}	40726..40742	+	ATAATAGTTGACTAGTA

Entries highlighted in red font indicate that this sequence overlaps with the 3' end of an upstream ORF.

Table 9. Locations and DNA sequences of a MEME-identified motif in the vB-SenS-Ent3 genome.

Name	Coordinates	Strand	Sequence
P_{ORF20}	13522..13568	-	AGAATCTGATTTGAACGATAAGAATGTTCGAAGTTAAATATATCTAC
P_{ORF24}	15786..15832	+	AATAGCTTGCATAACCGTTAATAGTGTCCTATTATCCCTACGTCAAC
P_{ORF35}	27997..28043	-	AGAAACAGGTTGATAAATTAATAGAACACTATTATATTTAGTTCACA
P_{ORF38}	32207..32253	-	AAAATTCGGTTGACAAGTTAATAGTACTCTATTATATTCTTAATCAC
P_{ORF41}	34437..34483	-	AAAAAGTGCTTGCATAAATAATAGAGCACGATTATAGTTCTTATCAC
P_{ORF42}	34432.34478	+	AGTTGGTGATAAGAACTATAATCGTGCTCTATTATTTATGCAAGCAC
P_{ORF53}	40952..40998	+	AAATAATAGTTGACTAGTAACACTAACCCTATTATATTTAGTTCATC

Entries highlighted in red font indicate that this sequence overlaps with the 3' end of an upstream ORF.

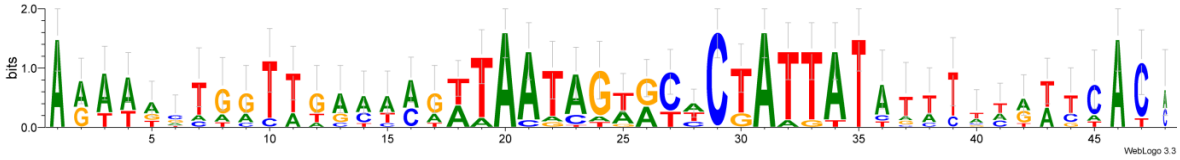

Figure 21. Weblogo of consensus motif from sequences identified using MEME and aligned with ClustalW for the vB_SenS-Ent phages.

3.2.13 Terminators

Seventeen intergenic sequences representing potential rho-independent transcription terminators were identified in each of the Ent phage genomes (Table 10, Table 11 and Table 12). Candidate terminators were assessed according to location, presence of a U-rich tail and stable predicted stem loop secondary structure (ΔG ≤ -10 kcal mol^{-1}) as calculated by RNAFold (Gruber *et al.,* 2008). Seven of these are predicted to be on early transcripts and ten on late transcripts. Of these, eight form four bi-directional terminators separating the 3' junctions of opposing transcriptional gene clusters.

Table 10. Putative rho-independent terminators identified in the vB_SenS-Ent1 genome.

Name	Coordinates	Strand	Sequence	Stability (ΔG)
T_{ORF03}	3342..3368	+	AAGGCCCCATGACGGGGCCTTAGTTTT	-15.7 kcal/mol
T_{ORF04}	3337..3362	-	AAGGCCCCGTCATGGGGCCTTTTGTT	-15.5 kcal/mol
T_{ORF06}	5691..5717	+	AAGGCCCCTTCAAGGGGCCTTAATTTT	-16.1 kcal/mol
T_{ORF08}	6540..6559	+	ACACCGGGAGGCCCGGTGTC	-13.4 kcal/mol
T_{ORF10}	8357..8378	+	GAGGGACTTCGGTCCCTCTTTT	-12.6 kcal/mol
T_{ORF12}	9056..9074	+	GCGGCCTCCGGGCCGCTTT	-13.7 kcal/mol
T_{ORF19}	12739..12764	+	AAGGCCCCGAAAGGGGCCTTAGTTTT	-16.6 kcal/mol
T_{ORF20}	12736..12758	-	AAGGCCCCTTTCGGGGCCTTTTT	-15.5 kcal/mol
T_{ORF21}	13515..13538	-	GCCCCTTTCGGGGCTTTTTTTTAT	-9.7 kcal/mol
T_{ORF32}	24974..25000	+	AAGGCCCCTTACGGGGCCTTAATTTAT	-15.7 kcal/mol
T_{ORF33}	24964..24993	-	AAGGCCCCGTAAGGGGCCTTTACTATTTAT	-16.4 kcal/mol
T_{ORF38}	31424..31447	-	GGCGGCTTCGGTCGCCTTTTCTAT	-10.0 kcal/mol
T_{ORF41}	33793..33811	-	GCGGCCTTCGGGCCGCTTT	-12.7 kcal/mol
T_{ORF42}	34693..34717	+	GGGGCCTGATGGCCCCTTTCTTTTT	-13.7 kcal/mol
T_{ORF43}	34692..34709	-	AGGGGCCATCAGGCCCCT	-14.1 kcal/mol
T_{ORF49}	39696..39735	+	TCTCCGAAGGATAAACCAACTTTCGGAGATTTTTTATTGT	-12.9 kcal/mol
T_{ORF52}	40842..40876	+	TCCCGGTAACTGACCCTACCGGGATTTTTTTTTAT	-12.8 kcal/mol

Nucleotides forming stem structures are underlined. Stability refers to the predicted minimum free energy of the entire sequence by RNAFold (http://rna.tbi.univie.ac.at/).

Table 11. Putative rho-independent terminators identified in the vB_SenS-Ent2 genome.

Name	Coordinates	Strand	Sequence	Stability (ΔG)
T_{ORF03}	3320..3346	+	AAGGCCCCATGACGGGGCCTTAGTTTT	-15.7 kcal/mol
T_{ORF04}	3315..3340	-	AAGGCCCCGTCATGGGGCCTTTTGTT	-15.5 kcal/mol
T_{ORF06}	5669..5695	+	AAGGCCCCTTCAAGGGGCCTTAATTTT	-16.1 kcal/mol
T_{ORF08}	6518..6537	+	ACACCGGGAGGCCCGGTGTC	-13.4 kcal/mol
T_{ORF10}	8335..8356	+	GAGGGACTTCGGTCCCTCTTTT	-12.6 kcal/mol
T_{ORF12}	9117..9135	+	GCGGCCTCCGGGCCGCTTT	-13.7 kcal/mol
T_{ORF19}	12800..12825	+	AAGGCCCCGAAAGGGGCCTTAGTTTT	-16.6 kcal/mol
T_{ORF20}	12797..12819	-	AAGGCCCCTTTCGGGGCCTTTTT	-15.5 kcal/mol
T_{ORF21}	13576..13599	-	GCCCCTTTCGGGGCTTTTTTTTAT	-9.7 kcal/mol
T_{ORF32}	25035..25061	+	AAGGCCCCGTAAGGGGCCTTAATTTAT	-16.6 kcal/mol
T_{ORF33}	25025..25054	-	AAGGCCCCTTACGGGGCCTTTACTATTTAT	-15.5 kcal/mol
T_{ORF38}	31536..31559	-	GGCGGCTTCGGTCGCCTTTTCTAT	-10.0 kcal/mol
T_{ORF41}	33905..33923	-	GCGGCCTTCGGGCCGCTTT	-12.7 kcal/mol
T_{ORF42}	34805..34829	+	GGGGCCTGATGGCCCCTTTCTTTTT	-13.7 kcal/mol
T_{ORF43}	34804..34821	-	AGGGGCCATCAGGCCCCT	-14.1 kcal/mol
T_{ORF49}	39531..39570	+	TCTCCGAAGGATAAACCAACTTTCGGAGATTTTTTATTGT	-12.9 kcal/mol
T_{ORF52}	40677..40711	+	TCCCGGTAACTGACCCTTACCGGGATTTTTTTTTT	-12.9 kcal/mol

Nucleotides forming stem structures are underlined. Stability refers to the predicted minimum free energy of the entire sequence by RNAFold (http://rna.tbi.univie.ac.at/).

Table 12. Putative rho-independent terminators identified in the vB_SenS-Ent2 genome.

Name	Coordinates	Strand	Sequence	Stability (ΔG)
T_{ORF03}	3324..3350	+	AAGGCCCCATAACGGGGCCTTATTTTT	-15.7 kcal/mol
T_{ORF04}	3317..3344	-	AAGGCCCCGTTATGGGGCCTTTTCTTT	-15.5 kcal/mol
T_{ORF06}	5673..5699	+	AAGGCCCCTTCAAGGGGCCTTAATTTT	-16.1 kcal/mol
T_{ORF08}	6522..6541	+	ACACCGGGAGGCCCGGTGTC	-13.4 kcal/mol
T_{ORF10}	8339..8360	+	GAGGGACTTCGGTCCCTCTTTT	-12.6 kcal/mol
T_{ORF12}	9121..9139	+	GCGGCCTCCGGGCCGCTTT	-13.7 kcal/mol
T_{ORF19}	12804..12829	+	AAGGCCCCGAAAGGGGCCTTAGTTTT	-16.6 kcal/mol
T_{ORF20}	12801..12823	-	AAGGCCCCTTTCGGGGCCTTTTT	-15.5 kcal/mol
T_{ORF21}	13580..13603	-	GCCCCTTTCGGGGCTTTTTTTTAT	-9.7 kcal/mol
T_{ORF32}	25039..25065	+	AAGGCCCCTTACGGGGCCTTAATTTAT	-15.7 kcal/mol
T_{ORF33}	25029..25058	-	AAGGCCCCGTAAGGGGCCTTTACTATTTAT	-16.4 kcal/mol
T_{ORF38}	31489..31512	-	GGCGGCTTCGGTCGCCTTTTCTAT	-10.0 kcal/mol
T_{ORF41}	33858..33876	-	GCGGCCTTCGGGCCGCTTT	-12.7 kcal/mol
T_{ORF42}	34758..34782	+	GGGGCCTGATGGCCCCTTTCTTTTT	-13.7 kcal/mol
T_{ORF43}	34757..34774	-	AGGGGCCATCAGGCCCCT	-14.1 kcal/mol
T_{ORF49}	39761..39800	+	TCTCCGAATGGTAAACCAACTTTCGGAGATTTTTTATTGT	-12.2 kcal/mol
T_{ORF52}	40907..40939	+	TCCCGGTAACTGACCCTACCGGGATTTTTTTTT	-12.8 kcal/mol

Nucleotides forming stem structures are underlined. Stability refers to the predicted minimum free energy of the entire sequence by RNAFold (http://rna.tbi.univie.ac.at/).

3.2.14 Physical genome ends

Heat treatment of restriction fragments followed by either rapid or slow cooling did not alter restriction patterns (data not shown), excluding the possibility of cohesive genome ends. Time limited treatment with the exonuclease BAL-31 resulted in even, simultaneous degradation of all restriction fragments (Figure 22). These data, combined with apparently circular consensus sequence assemblies, suggests that the vB_SenS-Ent genomes are terminally redundant and circularly permuted (Loessner *et al.,* 2000). Circularly permuted genomes are characteristic of head-full packaging strategy where the packaged DNA length is between 102-110 % of the total genome length and would account for the >1 kb discrepancy between genome sizes as estimated by PFGE and DNA sequencing.

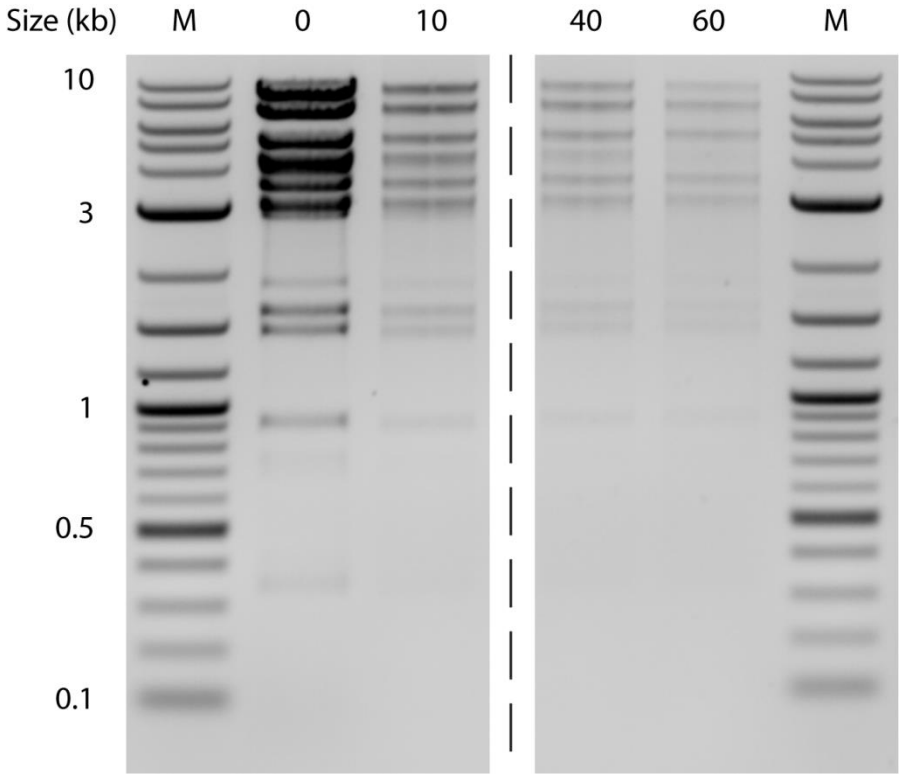

Figure 22. Time limited digestion of vB_SenS-Ent1 genomic DNA with the exonuclease BAL-31. The hashed line indicates the removal of the 20 minute digestion due to improper migration of DNA through the gel. M, marker lane; Numerical values refer to length of digestion with BAL-31 in minutes.

Discussion

The vB_SenS-Ent bacteriophages show a relatively broad host range, capable of infecting isolates from serogroups A, B and D1. While initially thought to be independent species due to differences in host range and susceptibility to digestion by restriction endonucleases, the extremely high nucleotide similarity, gene content and conserved location of putative promoters and rho-independent terminators suggest that these isolates may actually represent strains of the same parent species. It is noteworthy that these isolates are differentiated almost exclusively by differences in the number of candidate genes flanking the lysin and holin, suggesting that this late region is subject to high gene mobility.

As yet there is no evidence that the vB_SenS-Ent phages exhibit a temperate lifecycle. No gene products were found which exhibited homology to characterised integrases, resolvases or excisionases and preliminary results suggest that the growth of small colonies within plaques arises due to host resistance rather than by a phage-related immunity mechanism. In addition the related *Siphoviridae* SS3e, SETP3 and K1-Phages are reported to be lytic (Bull *et al.,* 2010, De Lappe *et al.,* 2009). In contrast, PHACTS analysis (McNair *et al.,* 2012) denotes that the vB_SenS-Ent1 lifestyle is temperate, but the result is marginal with only 0.51 of trees in the forest algorithm yielding this decision. However, without an absolute answer as to whether the vB_SenS-Ent phages possess a temperate lifecycle the use of these phage as either biocontrol or therapeutic agents *ex vitro* is precluded, a necessary condition due to the association of temperate phage with the horizontal transfer of bacterial virulence factors (Canchaya *et al.,* 2003a, Figueroa-Bossi *et al.,* 2001). Notwithstanding, the establishment of an efficient and productive lytic infection cycle depends upon the function and interaction of multiple early and late proteins with both self and host encoded proteins (for a review see (Roucourt and Lavigne, 2009). As such, and like other bacteriophage genomes, the vB_SenS-Ent phages may harbour multiple gene products that have potential for exploitation as antimicrobial agents (Liu *et al.,* 2004). Whilst much information still remains to be elucidated for the vB_SenS-Ent phages, the study reported here advances the annotation of a distinct genus of *Siphoviridae* infecting *Salmonella* serovars. The relationships between the vB_SenS-Ent phages and other fully sequenced *Salmonella* phages are explored in detail in the following chapter.

Chapter 4 A proposed new genus of bacteriophage: the "*Setp3likevirus*"

4.1 Introduction

4.1.1 Bacteriophage taxonomy and mosaicism

Under the latest revision of virus taxonomy by the ICTV, members of the order *Caudovirales* are segregated into three morphological families (King *et al.,* 2011): the *Siphoviridae* (9 genera) possessing flexible, non-contractile tails, the *Myoviridae* (3 subfamilies; 17 genera), characterised by complex, rigid contractile tails and the short-tailed *Podoviridae* (2 subfamilies; 11 genera). Bacteriophage taxonomy continues to be subject to lively debate and disagreements with Lawrence (2002) describing the field as a battle ground of phenetics versus cladistics.

Despite being considered as clonal organisms, bacteriophage genomes have been shown to be pervasively mosaic (Lawrence *et al.,* 2002). Each genome may be envisioned as a unique combination of modules representing individual and groups of genes (and intragenic segments) that are interchangeable between other viruses and host cells. The mosaic arrangement of phage genomes was recognised early on, due to the ability of P22 and λ to recombine to form functional hybrids (Susskind and Botstein, 1978). Several other phages have been shown to recombine including ES18, Fels-1 and P22 (Yamamoto, 1978, Yamamoto and McDonald, 1986) and a mechanism of homologous recombination occurring at linker sequences was initially proposed to explain these observations (Susskind and Botstein, 1978). It is now thought more likely that mosaicism arises at random positions in the genome through the a number of different mechanisms including homologous and illegitimate recombination, site-specific recombination, transposition and action of homing endonucleases (Hendrix *et al.,* 1999, Nilsson and Haggård-Ljungquist, 2001, Hatfull, 2008). The horizontal transfer of modules is constrained by at least three aspects. Firstly, the host preference of the infecting bacteriophage influences the potential for contact with prophages and other (co-infecting) bacteriophages. Second, that the loss, gain or exchange of modules does not render the phage replication-incompetent. Lastly, the viral genome should be of an appropriate size for packaging into the capsid (Lawrence *et al.,* 2002).

The availability of an increasing number of genome sequences and improvements in gene prediction methods has resulted in a sizeable shift towards the inclusion of genomic and proteomic data for the taxonomic/phylogenetic classification of bacteriophages (Lawrence *et al.,* 2002). A number of different approaches have been reported in the literature for the purposes of delineating

evolutionary relationships between the bacteriophages including the phage proteomic tree (Rohwer and Edwards, 2002), numbers of shared homologous/orthologous proteins (Lavigne *et al.,* 2009, Lavigne *et al.,* 2008) and reticulate classification based on gene content (Lima-Mendez *et al.,* 2011, Lima-Mendez *et al.,* 2008).

4.2 The *Salmonella* bacteriophages with completely sequenced genomes

The *Salmonella* bacteriophages are numerous and varied. The morphology of 177 *Salmonella* phages has been reviewed by Ackerman (2007b) and are predominantly represented by the *Siphoviridae*, *Myoviridae* and *Podoviridae*. A small number of phages representing filamentous and isometric phages have also been documented. Whilst a number of partial sequences are present for *Salmonella* bacteriophages within the INSD (e.g. MB78, ST4), this manuscript focuses solely upon those bacteriophages with completely sequenced genomes. At the time of writing, the complete genomes of 42 bacteriophages infecting *Salmonella* were held in the international nucleotide sequence data bases, far fewer than the total number of 170 reported in the literature by 2007 (Kropinski et al., 2007b). Of the 42 complete genomes, 20 fall into 8 genera as defined by the latest revision of virus taxonomy by the ICTV (Table 13). Several papers describing new genome sequences for *Salmonella* bacteriophages have recently been published and two proposals relevant to bacteriophages infecting *Salmonella* are currently awaiting ratification by the ICTV. The first proposes the creation of a new genus, the *Viunalikevirus* comprising *Salmonella* phages Vi01, SFP10, ϕSH19, and Escherichia, Shigella and Dickeya phages vB_EcoM_CBA120, PhaxI, ϕSboM-AG3 and vB_DsoM_LIMEstone1, respectively. The second concerns the inclusion of phage SPC35 (Kim and Ryu, 2011), reported to be capable of infecting both *Salmonella* Typhimurium and *Escherichia coli*, within the genus T5likevirus. In addition two further bacteriophages, vB_SenS-Ent2 and vB_SenS-Ent3 have recently been sequenced, both of which exhibit high nucleotide sequence similarity to phage vB_SenS-Ent1. Considering that all but one of the *Siphoviridae* infecting *Salmonella* are unclassified, a review of these bacteriophages is timely.

Table 13. *Caudovirales* infecting the genus *Salmonella* with complete genome sequences held in GenBank.

I. *Myoviridae*			
Genus	**Accession No.**	**Name**	**Reference**
Viunalikevirus[a]	JN126049.1	ϕSH19	(Hooton *et al.,* 2011a)
Viunalikevirus[a]	NC_016073.1	SFP10	(Park *et al.,* 2011)
Viunalikevirus[a]	NC_015296.1	Vi01	(Pickard *et al.,* 2010)
P2likevirus	NC_010463.1	Fels-2	(McClelland *et al.,* 2001)
P2likevirus	NC_005340.1	PsP3	(Bullas *et al.,* 1991)
Felixounalikevirus	NC_005282.1	Felix01	(Whichard *et al.,* 2010)
Unclassified	NC_016071.1	PVP-SE1	(Santos *et al.,* 2011b)
Unclassified	HM770079.1	RE-2010	(Hanna *et al.,* 2012)
Unclassified	JN641803.1	SPN3US	(Lee *et al.,* 2011)
II. *Siphoviridae*			
Genus	**INSD Accession**	**Name**	**Reference**
T5likevirus[c]	NC_015269.1	SPC35	(Kim and Ryu, 2011)
Unclassified	NC_016763.1	SE2	(Tiwari *et al.,* 2012)
Unclassified	NC_009232.1	SETP3	(De Lappe *et al.,* 2009)
Unclassified	JQ288021	SPN3UB	(Lee *et al.,* 2012)
Unclassified	NC_006940.2	SS3e	(Kim *et al.,* 2012b)
Unclassified	NC_018279.1	vB_SosS_Oslo	(Nelson *et al.,* 2012)
Unclassified	NC_010495.1	Vi II-E1	(Pickard *et al.,* 2008)
Unclassified	NC_006949.1	ES18	(Casjens *et al.*, 2005b)
Unclassified	JQ965645.1	SSU5	(Kim *et al.,* 2012a)
Unclassified	JX202565.1	wksl3	(Kang *et al.,* 2013)
Unclassified	HE775250.1	vB_SenS-Ent1	(Turner *et al.,* 2012)
Unclassified	PRIVATE	vB_SenS-Ent2	Unpublished
Unclassified	PRIVATE	vB_SenS-Ent3	Unpublished
Unclassified	NC_010583.1	EPS7	(Hong *et al.,* 2008)
Unclassified Prophage	NC_010391.1	Fels-1	(McClelland *et al.,* 2001)
Unclassified Prophage	NC_010392.1	Gifsy-1	(McClelland *et al.,* 2001)
Unclassified Prophage	NC_010393.1	Gifsy-2	(McClelland *et al.,* 2001)
III. *Podoviridae*			
Genus	**INSD Accession**	**Name**	**Reference**
epsilon15likevirus	NC_004775.1	ε15	(Kropinski *et al.,* 2007a)
P22likevirus	NC_002371.2	P22-pbi	(Byl and Kropinski, 2000)
P22likevirus	NC_004348.1	ST64T	(Mmolawa *et al.,* 2003b)
P22likevirus	NC_011976.1	ε34	(Villafane *et al.,* 2008)
P22likevirus	NC_013059.1	g341c	-
P22likevirus	NC_011802.1	SE1	(Llagostera *et al.,* 1986)
P22likevirus	NC_014900.1	ST160	(Price-Carter *et al.,* 2011)
P22likevirus	NC_018275.1	vB_SemP_Emek	(Nelson *et al.,* 2012)
P22likevirus	NC_005841.1	ST104	(Tanaka *et al.,* 2004)
Sp6likevirus	NC_004831.2	SP6	(Dobbins *et al.,* 2004)
T7likevirus	NC_010807.1	ϕSG-JL2	(Kwon *et al.,* 2008)
Unclassified	NC_015271.1	Vi06	(Pickard *et al.,* 2010)
Unclassified	NC_016761.1	SPN1S	(Shin *et al.*, 2012b)
Unclassified	NC_017985.1	SPN9CC	-

Unclassified	NC_015938.1	7-11	(Kropinski *et al.,* 2011)
Defective prophage	NC_004313.1	ST64B	(Mmolawa *et al.,* 2003a)

Key: [a]Proposed genus not yet ratified by ICTV. [b]Prophage. [c]Proposed inclusion within genus not yet ratified by ICTV.

4.3 Comparative genomics of the *Salmonella* bacteriophages

Dot plot analysis of the genomes of 42 *Salmonella* bacteriophages demonstrates that while significant genetic diversity exists between these phage, clusters may be delineated on the basis of nucleotide sequence similarity (Figure 23). Of the 42 sequenced phages, twenty fall into seven major clusters, which reflect current ICTV genera. A further thirteen phages form three additional clusters which are not yet represented by an official genus epithet. Excluding the unclassified prophages Gifsy-1, Gifsy-2 and Fels-1, six phage genomes, PVP-SE1, SPN3US, 7-11, SSU5, ST64B and ViII-E1 appear as 'singletons' which do not fall under any current taxonomic designation.

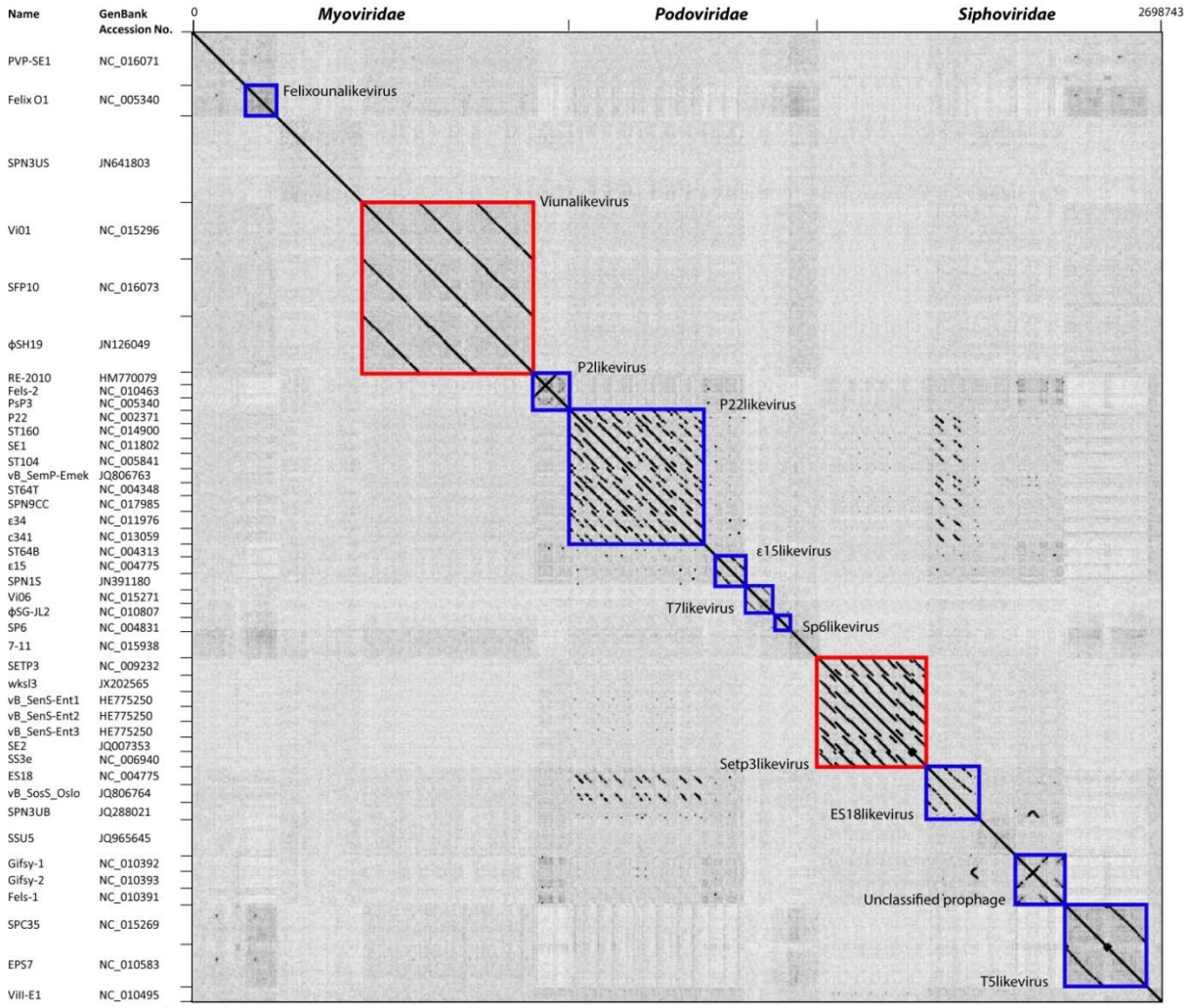

Figure 23. Nucleotide similarity dotplot of 42 *Salmonella* phage genomes. Clusters of nucleotide similarity corresponding to current ICTV genus designations are outlined in blue, with unclassified genera outlined in red. The reverse complement of the genomic sequences of phages SS3e and wksl3 were used.

The pairwise comparison of genomes using CoreGenes provides a measure of the total similarity at the protein level between pairs of bacteriophage genomes (Mahadevan *et al.,* 2009). The program returns pairs of proteins scoring above a predefined BLASTP score threshold allowing, where appropriate, the putative assignment of function for genes previously annotated as unknown or hypothetical. A total of 42 genomes were compared using the CoreGenes3.0 webserver (http://binf.gmu.edu:8080/CoreGenes3.0/), representing a total of 1764 comparisons. To facilitate this analysis a JavaScript was developed allowing the automated and iterative submission of pairs of genomes to the CoreGenes webserver (Turner *et al.*, 2013). Following the methods of Lavigne *et al.,* (2008, 2009), the output of each paired comparison was stored in a matrix, converted to relative (percentage) correlation values and reciprocally compared. A similarity threshold value of 40 % orthologous protein was employed to delineate high level relationships (Figure 24).

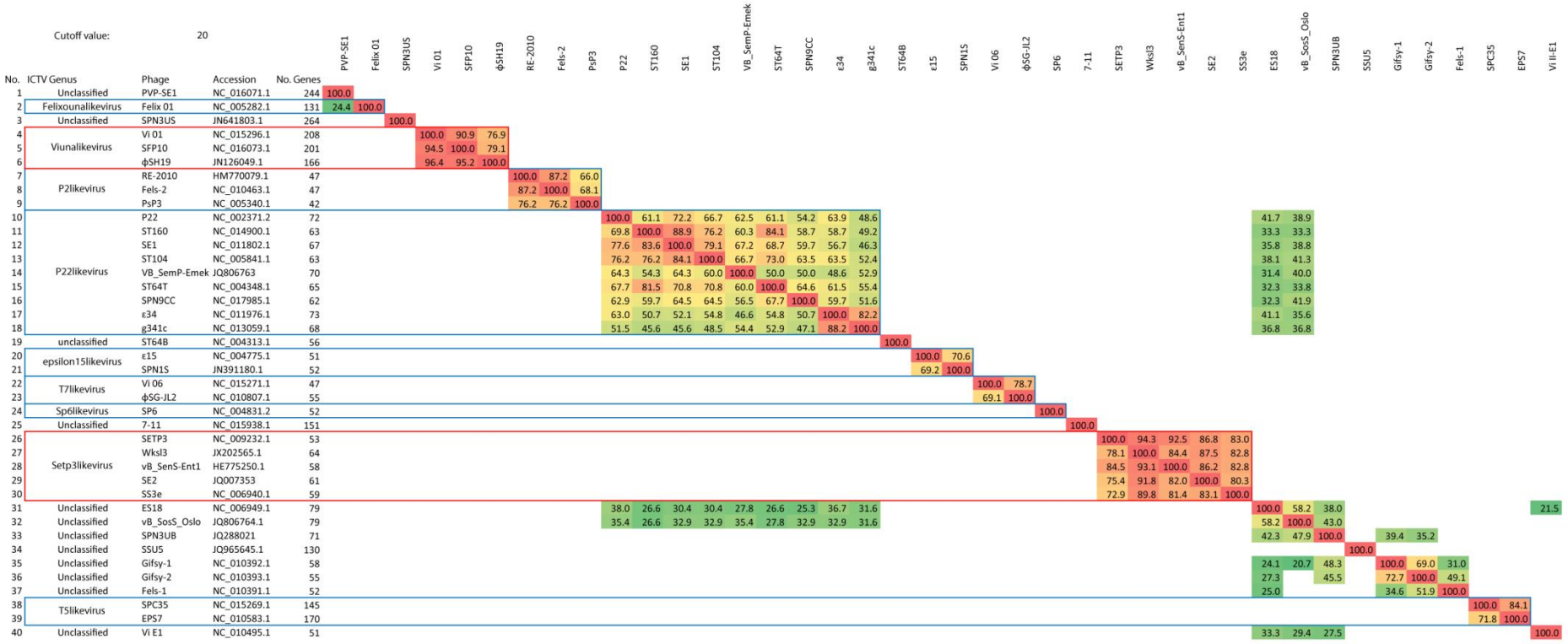

Figure 24. Hierarchical clustering of 40 bacteriophages by numbers of shared proteins determined by CoreGenes3.0. Relationships are shown for pairs of genomes which share at least 20 % homologous proteins. Current ICTV genus designations are outlined in blue, while proposed genera are outlined in red.

4.4 The *Setp3likevirus*

Comparative genomic analysis of the *Salmonella* phages reveals that 5 phages form a coherent group within the *Siphoviridae* and supports the establishment of a new genus, the *Setp3likevirus*. The proposed genus is comprised of virulent bacteriophages infecting members of genera *Salmonella*, SETP3, SS3e (KS7), SE2, wksl3 and vB_SenS-Ent1, *Escherichia coli,* K1ind1, K1ind2 K1ind3, K1G and K1H. The SETP3-like viruses are distinguished by a shared morphology, similar genome size with co-linear organisation of coding sequences and high numbers of protein homologues. These phages have not been shown to encode tRNAs and to date, none have been shown capable of lysogeny nor harbour homologues to known integrases, recombinases or excisionases. This lack of a temperate life-cycle presents members of this group as candidates for biocontrol applications.

4.5 Members of the proposed genus

4.5.1 SETP3

Bacteriophage SETP3 represents the only sequenced member of the *Salmonella* Enteritidis phage typing scheme (SETP) (Ward *et al.,* 1987) and is therefore presented as the type species of the genus proposed here. The SETP scheme consists of 16 bacteriophages denoted as SETP1 through to SETP16 (De Lappe *et al.,* 2009). Of these 6 are *Podoviridae* (SETP1, 8, 10, 14 & 15) and 6 *Siphoviridae* (SETP3, 5, 7, 11, 12 & 13) each with an estimated genome size of 45 kb as determined by PFGE. The remaining 4 belong to the order *Myoviridae*. All SETP phages adsorb to serovars expressing group B1 and D1 O-antigens. SETP3 is the only fully sequenced member of this group of typing phages, although partial sequences for other members are available. The genome of SETP3 is 42,575 bp in length (49.85 % G+C) with 53 annotated ORFs.

4.5.2 vB_SenS-Ent1, vB_SenS-Ent2 and vB_SenS-Ent3

Phage vB_SenS-Ent1 (Ent1), isolated from swine lagoon effluent in the UK, propagates efficiently on *S.* Enteritidis PT4 (Turner *et al.,* 2012). This phage was demonstrated to exhibit a broad host range activity against *Salmonella* serovars but unlike SS3e was not observed to lyse other genera of the *Enterobacteriaciae*. Ent1 harbours a 42.39 kb genome (49.79 % G+C) encoding 58 ORFs. Two further bacteriophages, vB_SenS-Ent2 and vB_SenS-Ent3, have been isolated from the same environmental sample and sequenced. These phages were originally selected for genome sequencing due to their exhibiting differences in genome size, as determined by PFGE, and restriction fragment banding patterns. The extremely high nucleotide sequence similarity for the vB_SenS-Ent phages is unsurprising considering that all three phages were isolated from the same environmental sample and are therefore most likely to be strains of the same species. Interestingly and notwithstanding minor sequence variations in proteins from the structural, immunity and replication gene clusters,

the primary locale for variation between these isolates appears to be confined to the late gene cluster containing the lysin and holin coding sequences.

4.5.3 SS3e

SS3e was isolated from poultry farm sewage in South Korea and the sequenced genome is 40.79kb (50.1 % G+C) encoding 58 ORFs (Kim *et al.,* 2012b). Notably, SS3e is reported to be capable of lysing other Enterobacteria, including *E. coli*, *Shigella sonnei*, *Enterobacter cloacae* and *Serratia marcescens*. As almost all the ORFs are annotated as hypothetical proteins a preliminary analysis of the SS3e genome was undertaken and confirmed that the same collinear arrangement of gene order and function in SETP3, wksl3, SE2 and vB_SenS-Ent1 is followed. However, it was noted that the SS3e genome appeared to lack an ORF corresponding to the major tail protein and was missing the immunity and regulation gene cluster. Sequence similarity searches located a truncated candidate for the major tail protein residing at bases 1 to 888 on the complementary strand and a further region (nucleotides 40165..40791), homologous to the first 208 amino acids of the vB_SenS-Ent1 putative recombination endonuclease subunit. The latter is located at the 3' end of the immunity cluster in vB_SenS-Ent1. These data suggest that the genome sequence of SS3e may be incomplete.

4.5.4 SE2

SE2 was also isolated from sewage samples from poultry farms in South Korea and is propagated on *S.* Enteritidis PT4. The genomic sequence is 43,221 bp in length (49.6 % G+C), and with 64 predicated ORFs, encodes the largest number of genes amongst the SETP3-like phages (Tiwari *et al.,* 2012). While, the arrangement of coding sequences follows the same collinear organisation as observed for other SETP3-like phages, SE2 shows some notable differences within both the immunity and replication gene clusters.

4.5.5 wksl3

The deposited sequence for phage wksl3 is 42.63 kb in length with a G+C content of 50.32 % and encodes 64 ORFs, maintaining the high coding potential (91.6 %) characteristic of the SETP3-like phages (Kang *et al.,* 2013). Sequence analysis and comparison to other phages strongly suggest that this isolate is a SETP3-like *Siphoviridae*. Core genes analysis demonstrates that wksl3 shares 50, 54, 56 and 53 proteins with SETP3, vB_SenS-Ent1, SE2 and SS3e, respectively.

4.5.6 *Escherichia coli* phages K1G, K1H, K1ind1, K1ind2 and K1ind3

The nomenclature of the K1 phages refers to the requirement for the presence of the K1 capsular antigen for productive infection. K1ind indicates that the phage does not require the presence of the K1 antigen for productive infection. In contrast K1-dep indicates that productive infection requires the presence of K1 antigen. This specificity is mediated by the presence of different tailspikes. Phages K1H and K1ind1 were isolated from sewage in Atlanta (Bull *et al.,* 2002). Phage K1G was isolated from sewage in Austin while K1ind2 and K1ind3 were selected due to high growth rates in

competition experiments (Bull *et al.,* 2010). Each of these phages uses *E. coli* O18:K1:H7 as the host (Table 14).

Table 14. Genome properties and aliases of phages K1G, K1H, K1ind1, K1ind2 and K1ind3.

Phage	Genome size (bp)	Mol %G+C	No. ORFs	Aliases
K1G	43,587	51.07	52	K1-dep(4)
K1H	41,632	51.17	50	ϕLH, K1-dep(1)
K1ind1	42,292	51.27	51	ϕLW, K1ind(1)
K1ind2	42,765	51.32	48	K1ind(2)
K1ind3	43,461	51.15	49	K1ind(3)

4.6 Virion morphology

The SETP3-like virion structure highly resembles the morphology of *Salmonella* Paratyphi B typing phage Jersey (Ackermann *et al.,* 1972). This group of *Siphoviridae* possess an icosahedral capsid, a relatively short flexible tail, for which horizontal striations are sometimes observed and six short tailspikes. vB_SenS-Ent1 is composed of an isometric capsid 64 nm in diameter and a flexible, non-contractile tail 116 x 8.5 nm. Wksl3 is reported to possess a 63 nm capsid, 121 x 7.9 nm tail and 20nm baseplate, similar to SETP3 which has a capsid 62.5 nm in diameter and 120 x 7 nm tail (De Lappe *et al.,* 2009). A similar morphology has also been described for phages 2 and 3 of the *S.* Heidelberg phage typing scheme (Demczuk *et al.,* 2004) and phage MB78 appears to be morphologically similar to phage Jersey (Joshi *et al.,* 1982). Binding to the LPS O-antigen of target host cells is facilitated by the presence of 6 tailspikes located at the tail terminus, suggesting that the baseplate or tail terminal protein has a six-folded symmetry. Two-dimensional SDS-PAGE analysis of vB_SenS-Ent1 suggests that the mature virion is composed of at least 12 proteins, though these results have not been confirmed using mass spectrometry.

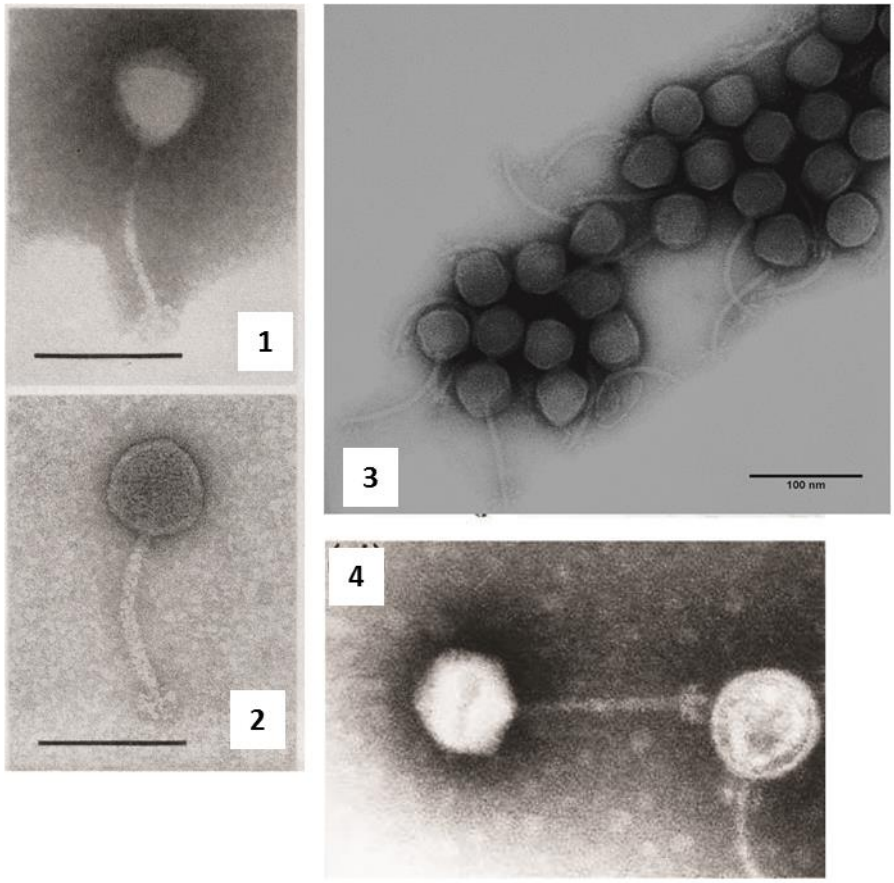

Figure 25. Morphology of the *Setp3likevirus*. Images represent electron micrographs of bacteriophages Jersey (1 & 2), vB_SenS-Ent1 (3) and Heidelberg typing phage 2 (4). Scale bars denote distances of 100 nm. Micrographs of phages 2 and Jersey were supplied by H.W. Ackermann and are reproduced with permission.

4.7 Host specificity

Host specificity is conferred by six tailspikes attached to end of the tail. The tailspike protein is characterised by the presence of a highly conserved N-terminal head binding domain, common to all members of the SETP3-like phages, and a P22-like catalytic C-terminal domain. Alignments using ClustalX2 demonstrates that the tailspikes of all *Setp3likevirus* possess a conserved N-terminal domain of 50 residues which, with the exception of wksl3 (residues 2-53), is located at residues 11-60 (Figure 26). Downstream of this region conservation is maintained, although to a lesser degree overall, with three conserved blocks of four residues (GGTL, VLWP and GGDG).

Figure 26. ClustalX2 alignments of the N-terminal region of the *Setp3likevirus* tailspike proteins. Conserved residues were shaded using Boxshade.

Several podoviral phage tailspikes, including P22, Sf6 and HK620, have been shown to exhibit a modular architecture consisting of N-terminal head binding and C-terminal catalytic domains. As such it is not unreasonable to suggest that the N-terminal domain identified for the *Setp3likevirus* is involved in attachment of the tailspike to the virion baseplate.

Each of the SETP3-like phages infecting the *Salmonella* encodes a P22-like tailspike. Phage P22 adsorbs to *Salmonella* O-antigen 12 which is found in serogroups A, B and D1 (Wollin *et al.,* 1981). The presence of repeating O-antigen subunits are required for adsorption as both rough and semi-rough strains are resistant to infection by P22 (Naide *et al.,* 1965). The mature P22 tailspike exists a homotrimer of the 72 kDa gp09 product and crystal structures have been determined for the N-terminal head binding and C-terminal catalytic domains (Steinbacher *et al.,* 1997, Steinbacher *et al.,* 1996, Steinbacher *et al.,* 1994). The tailspike forms a right handed parallel beta-helix structure first observed for a pectin lyase in *Erwinia chrysanthemi* EC16 (Weigele *et al.,* 2003). P22-like tailspikes exhibit endo-*N*-rhamnosidase activity (Wollin *et al.,* 1981). Consistent with P22 tailspike specificity, SETP3 infects members of serogroups B & D1. Examining host range data for vB_SenS-Ent1 and wksl3 suggests that productive infection by these phages is also limited to isolates of those serogroups. Unusually, SS3e is reported to lyse other genera of the *Enterobacteriacae* in addition to *Salmonella*, including *E. coli*, *Shigella sonnei*, *Enterobacter cloacae* and *Serratia marcescens*. No additional putative receptor binding proteins could be identified in SS3e, so perhaps this observation is due to these strains sharing a common LPS structure. Host range studies have not been reported for SE2 which is propagated on *S.* Enteritidis PT4.

Sequences coding for P22-like tail-spike proteins (PF09251) are widespread and highly conserved among *Podoviridae* and *Siphoviridae* but appear less frequently among the *Myoviridae* (Figure 27). To date, P22-like tailspikes have been reported for 3 *Myoviridae*; Det7 (Walter *et al.,* 2008), SFP10 (Park

et al., 2011) and ϕSH19 (Hooton *et al.,* 2011a). Despite reduced sequence identity (<50 %) the residues involved in the catalytic mechanism are preserved in all these TSPs. Of these, the Det7 TSP is most closely related to the SP6 P22-like fragment.

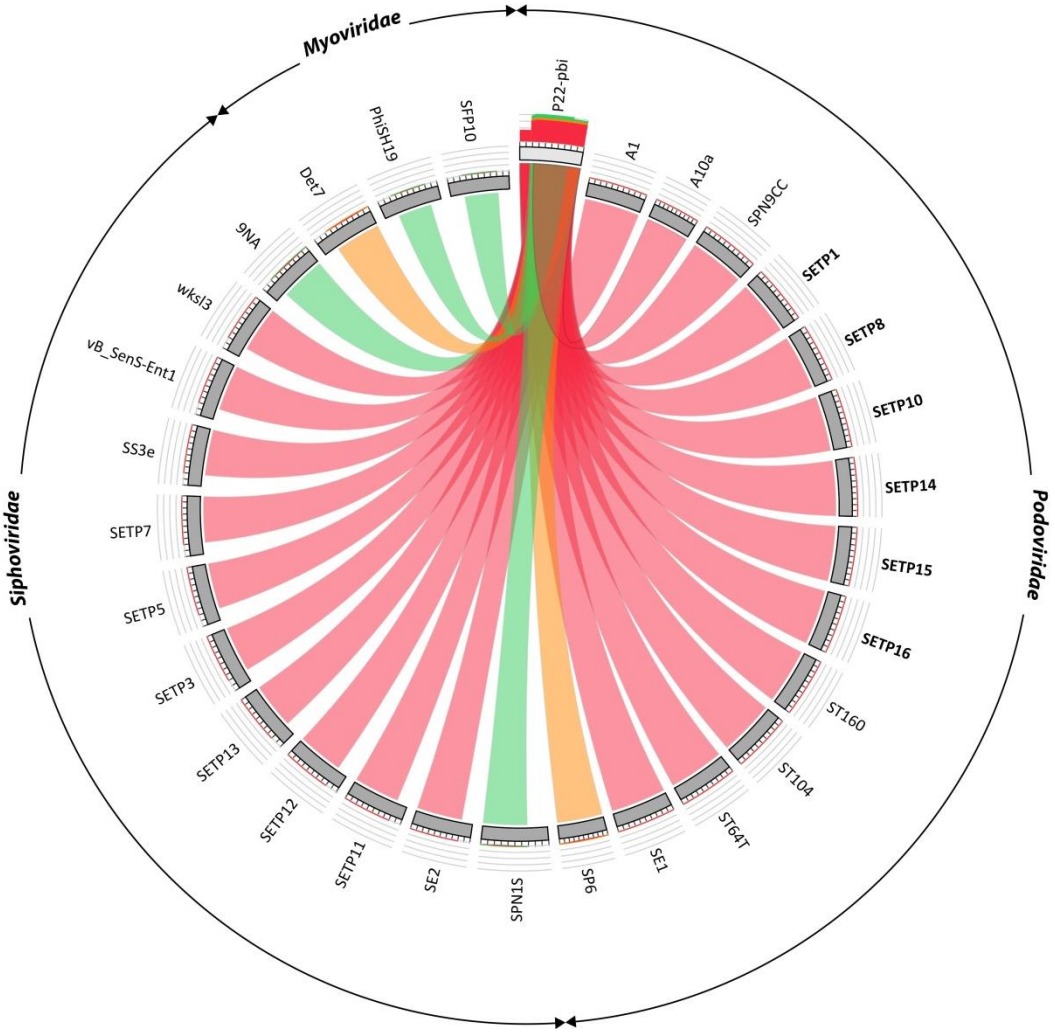

Figure 27. Sequence identity amongst the P22-like tailspikes of the *Salmonella* bacteriophages. The diagram was created using Circoletto from a BLASTP comparison (-e $1e^{-20}$) of *Salmonella* phage P22 gp22 against other P22-like tailspikes of *Salmonella* phages reported within the literature. Names of phages for which the tailspike sequence is annotated as partial are indicated in bold type. Ribbon colour indicates sequence identity ranging from low (green) to high (red).

Phylogenetic analysis of the sequenced P22-like tailspikes in *Myoviridae*, *Podoviridae* and *Siphoviridae* demonstrates that the SETP3-like bacteriophages form a discrete clade (Figure 28).

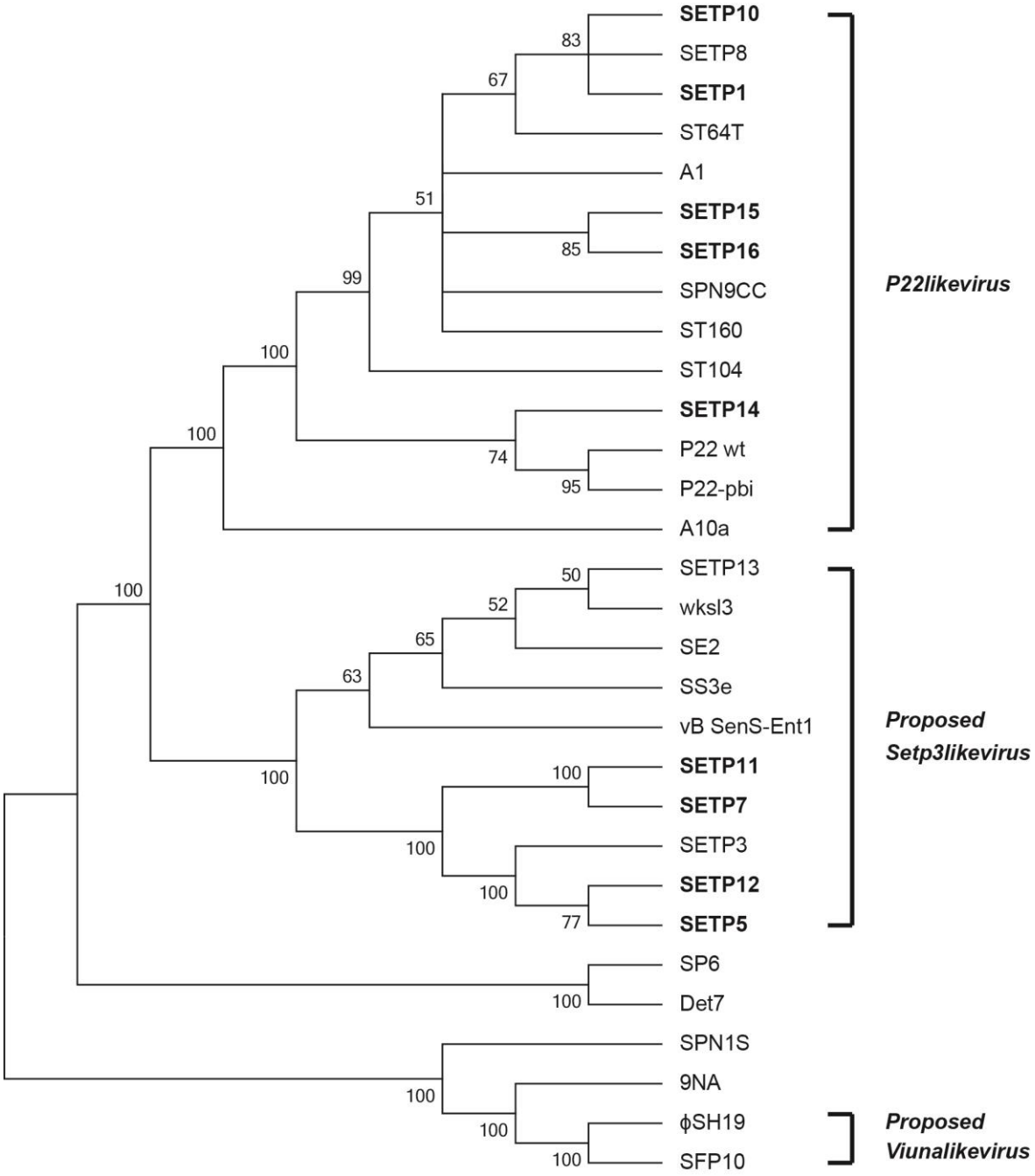

Figure 28. Condensed Neighbour joining tree of the P22-like tailspikes. Values at the nodes are the percentage results of 1000 bootstrap replicates. Names of phages for which the tailspike sequence is annotated as partial are indicated in bold type.

The *Escherichia* phages K1G, K1H, K1ind1, K1ind2 and K1ind3 possess tailspikes of similar size, which share the conserved N-terminal domain but possess different C-terminal domains indicative of separate host specificities. Tailspikes from K1ind phages exhibit high similarity to the HK620 tailspike (pdb:2x6w) and each returns matches to the pectate lysase 3 family (PF12708). The HK620 tailspike possess endo-*N*-acetylglucosaminidase activity that degrades the O-antigen of *E. coli* serotype O18A1 (Barbirz *et al.,* 2008). In contrast, K1 dependant phage tailspikes exhibit endo-*N*-acyl-neuraminidase (endosialidase) activity and are nearly identical to the tailspike of K1F (pdb:3ju4). Endosialidases bind to and degrade the K1 capsular polysaccharide, a homopolymer composed of α2,8-linked sialic acid

residues. Each of the K1 dependant tailspikes is predicted to contain a Peptidase_S74 domain (PF13884) suggesting that these tailspikes undergo a different maturation process to counterparts in the *Salmonella* and K1 independent SETP3-like bacteriophages.

4.8 Genome structure

The SETP3-like phages encapsulate a genome of approximately 43 kb and 50 % G+C, predicted to be circularly permuted and terminally redundant. The genomes show high nucleotide sequence identity (Figure 29) and encode at least 49 genes that follow a common clustered architecture, where the order and function of genes within each cluster is highly conserved. The genomes of all SETP3-like phages are organised into four clusters or modules of coding sequences which may be categorised according to the function of the component genes. These gene clusters represent two early and two late transcriptional regions.

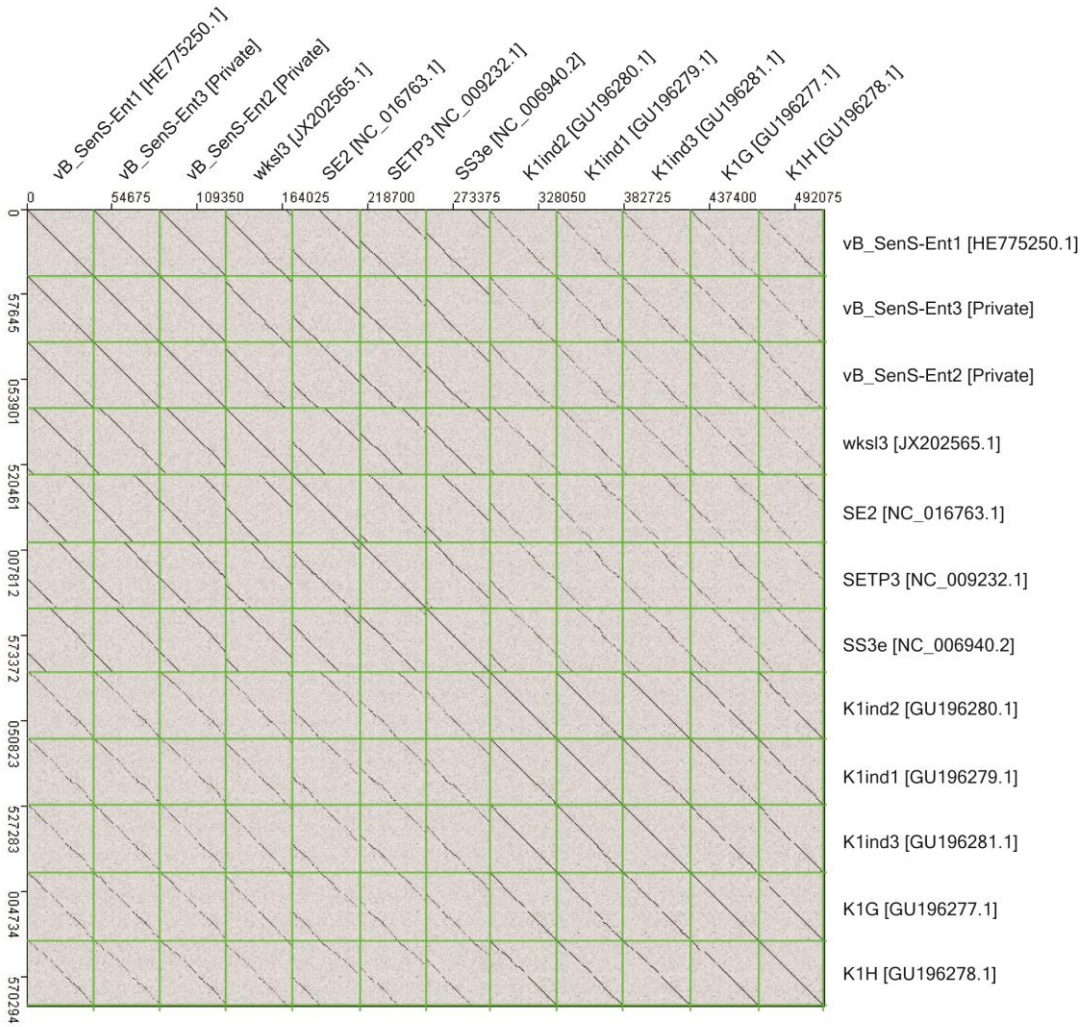

Figure 29. Clustering of the related SETP3-like *Salmonella* phage by nucleotide sequence similarity. The genome sequences of phages SS3e and wksl3 were reverse complemented to conform to convention of presenting structural genes on the forward strand.

4.8.1 Immunity and regulatory region

The first early gene cluster encodes proteins predicted to be involved in regulation and immunity to superinfecting phage. Each of the *Salmonella* phages encodes 5 proteins in this cluster, while the *Escherichia* phages encode four and no single protein is shared between all SETP3-like phages. For vB_SenS-Ent1 and wksl3, the regulatory cluster encodes a regulatory protein containing ANT and pRHa PFAM family domains, predicted to be involved within the regulation of lytic growth, a T4-like inner-membrane superinfection immunity protein, a HNH endonuclease and a recombination endonuclease subunit. SETP3 differs from vB_SenS-Ent1 and wksl3 in that it lacks the HNH endonuclease. Whilst SE2 retains the T4-like immunity protein and putative recombination endonuclease subunit, like SETP3 it lacks the HNH endonuclease. In its place SE2 encodes a DNA methylase (gp51) containing the PFAM family N6_N4_Mtase domain (PF01555). An additional annotated ORF is located on the opposite strand situated between the DNA methylase and putative transcriptional regulator (gp49). This protein appears to be unique to SE2 as it lacks known homologs in the non-redundant sequence databases. Furthermore, the SE2 regulatory protein (gp49) contains the ANT but not the pRHA domain. Only the immunity protein is annotated in SS3e, though this appears to be due to an incomplete genome sequence rather than an absence of further proteins in this region.

The *E. coli* SETP-like phages encode 4 proteins in the immunity and regulation gene cluster, two of which are shared with related phages infecting *Salmonella*. All except K1H possess the T4 superinfection immunity protein and putative recombination endonuclease subunit. The two remaining genes encode a putative polynucleotide kinase and a protein with inferred ATPase activity. In place of the immunity protein, K1H encodes a protein unique amongst the SETP3-like phages.

4.8.2 DNA maintenance and replication

The second early cluster is devoted to the maintenance and replication of the virion genome. The number of coding sequences in this region ranges from 9 ORFS in K1ind2 to 17 in SS3e. Each member of the SETP3-like phages encodes a replicative family A DNA polymerase, DEAD-box helicase-primase and helicase. Analysis of the replication gene cluster for the SETP3-like phages with HHpred provides additional evidence for the presence of a Holliday junction resolvase (pdb:1hh1), helicase subunit (pdb:3h4r) and a helix-destabilising ssDNA-binding protein similar to that encoded by gp2.5 of phage T7 (pdb:1je5). Each of the *Escherichia coli* SETP-like phages encodes two ORFs not found in the *Salmonella* phage, a putative cytosine-specific methylase which overlaps the complete sequence of a putative MTE-like protein. A number of other hypothetical proteins are found in this region in some, but not all, SETP3-like phages.

Several of the *Salmonella* SETP3-like phages are predicted to possess inteins in either the helicase or DNA-polymerase or both. Inteins are defined as protein sequences embedded within a precursor

protein sequence which upon translation self-excise from their host protein and catalyse ligation of the flanking sequences with a peptide bond yielding two stable proteins, the mature protein (extein) and the intein (Perler *et al.,* 1994). Each of the helicase and DNA-polymerase protein sequences from the SETP3-like phages were searched against the InBase intein database (Perler, 2002). A minimal intein is found in the helicase of wksl3 (gp36), SETP3 and vB_SenS-Ent1 but not SS3e or SE2. A second intein containing an endonuclease domain is found in the DNA polymerase of SETP3, vB_SenS-Ent1 and SE2. Phage SE2 exhibits notable differences within the replication gene cluster and of particular interest is the identification of two proteins, gp05 (200 aa) and gp06 (794 aa) with predicted DNA polymerase activity, suggesting that the SE2 DNA polymerase is composed of two subunits. The large subunit, gp06, is predicted to possess an intein similar to that found in SETP3 and vB_SenS-Ent1, spanning residues 447 to 747. Relative to the DNA polymerase of SETP3 and vB_SenS-Ent1, gp06 aligns across the first 783 residues with 95 % identities. A gap of 100 aa is then observed prior to the alignment of gp05 which spans residues 833 to 1032 at 99 % identity. Like SE2, the DNA polymerase of SS3e also appears to be split into two coding sequences (gp41 and gp43) although in this case the subunits are interrupted by an additional gene (gp42). Notably gp41, gp42 and gp43 show short matches to the SETP3 intein. A 91 residue sequence with 88 % identity to the SETP3 intein is located at the N-terminal end of gp42 spanning residues 2-92. Searches conducted using this gene product and HHpred suggests the presence of a C-terminal HNH endonuclease domain while BLASTP returns a hit to gp39 of Sodalis phage SO-1. Of the two subunits identified as the SS3e DNA polymerase, gp41 shows a sequence spanning residues 447-459 at the C-terminal end which aligns to the beginning of the SETP polymerase intein. Conversely, gp43 returns a 21 aa match across N-terminal residues 1-21 which aligns with the C-terminal end of the intein sequence (Figure 30). No inteins were identified in the genomes of K1H, K1G, K1ind1, K1ind2 or K1ind3.

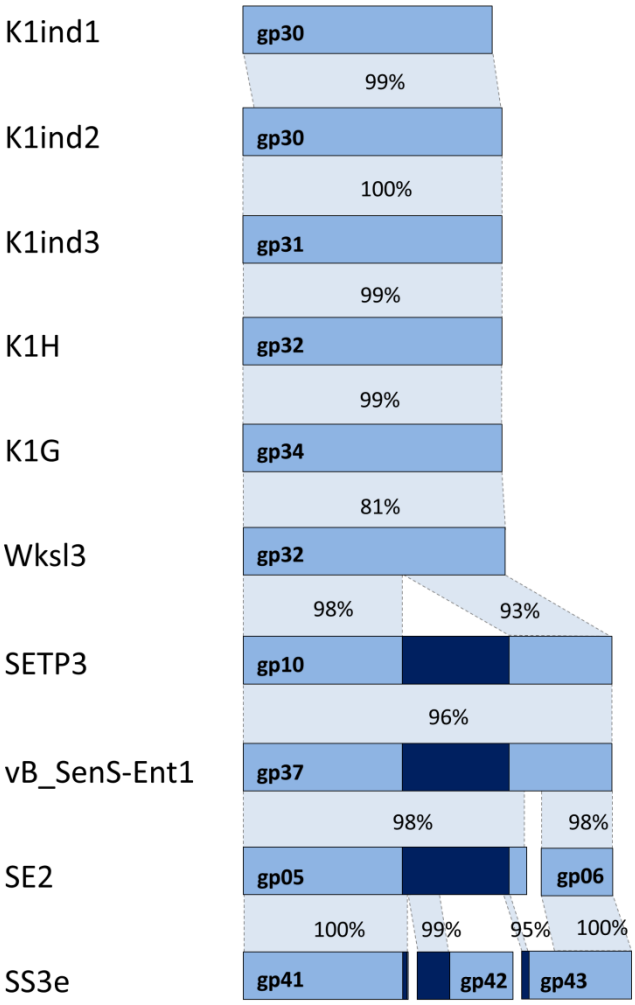

Figure 30. Presence and location of inteins in the DNA polymerases of the *Setp3likevirus*. The blue rectangles delineate proteins with inteins represented in dark blue. Regions of homology are represented in light blue where values indicate percentage identities from results of alignments using BLASTP and InBase.

4.8.3 Structural and morphogenesis regions

The first of the late gene clusters contains the coding sequences facilitating genome packaging and the structural components necessary to form mature progeny virions. The structural and morphogenesis cluster is large, comprising up to 26 ORFs, and accounts for almost 50 % of the genome. The cluster follows a strongly conserved gene order, encoding the DNA packaging apparatus followed by the virion capsid, tail and terminal tail structures (Figure 31). The structural genes are split into two sections, divided after the major tail protein by the early regulation and immunity gene cluster.

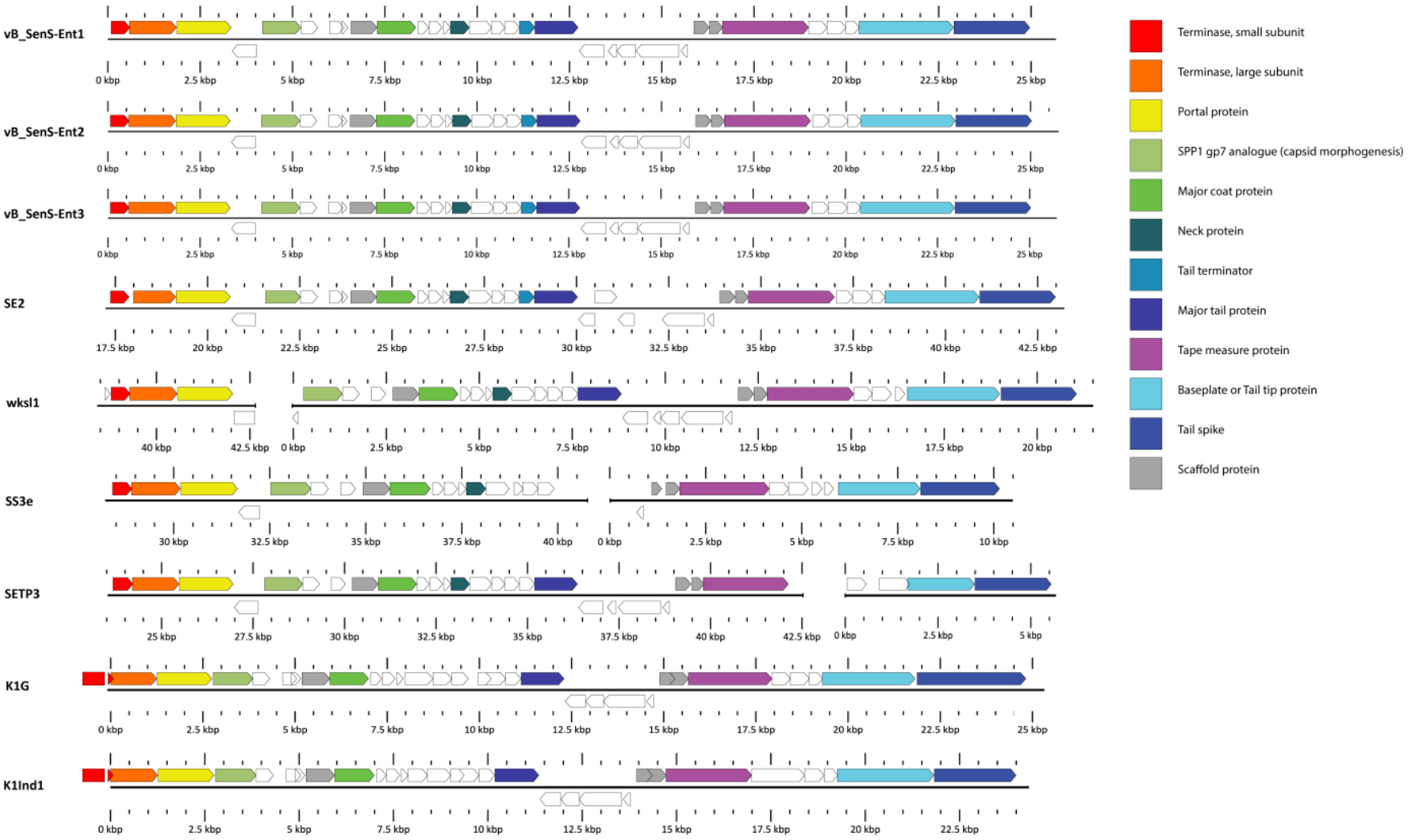

Figure 31. Synteny of gene order and function in the structural and immunity regions of the SETP3-like phage genomes. Genes are coloured according to putative function using data obtained from Blastp, HHpred, Pfam and InterProScan. The ruler beneath each gene map denotes the location within the genome sequence.

The three genes facilitating genome packaging in all *Salmonella* SETP3-like phages are separated downstream of the portal from the capsid structural and assembly genes by a single gene encoded on the opposite strand. This gene product has been annotated as an amidase in SETP3 (gp32), SE2 (gp33) and wksl3 (gp01) and as a hypothetical protein for vB_SenS-Ent1 (gp04) and SS3e (gp14). Analysis with HHpred against the conserved domain database returns a single significant hit to the PFAM KilA-N domain (PF04383) and iterative searches performed using PSI-BLAST confirm a relationship to other phage proteins encoding this domain suggesting a role in DNA-binding. These results do not however, return homologues with known amidase activity. This description has stemmed from SETP3 where gp32 is annotated as "similar to amidase of *Arabidospsis thaliana*". BLASTP of this sequence does result in a low scoring hit to this protein, but the alignment is not significant. Notably, this protein is absent from the *Escherichia* phages and exhibits negative GC skew in relation to neighbouring coding sequences, suggesting a past horizontal acquisition event. Three proteins are unique to the *Escherichia* phages within the structural gene cluster, two hypothetical proteins in K1H (ORF13) and K1ind3 (ORF4) and a HNH endonuclease with low identity to MobE of phage T6 in K1G (ORF12).

The identity of the capsid morphogenesis, major capsid, major tail, tape measure and tailspike proteins are apparent in each phage using PSI-BLAST and BLASTP. HHpred provides additional evidence allowing the tentative identification of neck, tail terminator and baseplate proteins. Using vB_SenS-Ent1 as an example, gp14 returns a match to the head-tail connector protein gp6 from HK97 (pdb:3jvo) and this association is reflected with HHpred searches against the Conserved Domain Database where several domains involved in head to tail joining are returned (cd08023, cd08054). The product of gp18 shows similarity to the minor tail protein U or tail terminator of phage λ (Pell *et al.,* 2009b). Lastly, gp44, a large ORF directly upstream of the tailspike shows a region of similarity to the baseplate protein of phage Mu (pdb:1wru).

4.8.4 Lysis cluster

The second late gene cluster contains proteins facilitating lysis of the host cell, allowing egress of newly formed virion particles into the environment. The function of only two proteins in the late lysis region have been inferred, the lysin and holin. The phage lysin is a glycoside hydrolase, easily identified by the presence of a conserved lysozyme catalytic domain with searches of PFAM and the conserved domain database. Holins are categorised as Class I or Class II depending upon the presence of three or two transmembrane domains, respectively (Young and Bläsi, 1995, Young, 2002). Phage SE2 is predicted to encode a holin-independent lytic system (Tiwari *et al.,* 2012). However, an analysis of the lysis gene cluster identifies gp021, encoded immediately upstream of the lysin, as a candidate holin. Searches conducted using PSI-BLAST with gp21 returns matches to gene products annotated as holins in all SETP3, wksl3, vB_SenS-Ent1, Shigella phage EP23, Enterobacteria

phages HK578 and JL2, Sodalis phage SO-1. Furthermore, three trans-membrane domains are predicted by TMHMM v2.0 and HHpred shows some similarity to an ion transport membrane protein in *Bacillus weihenstephanensis* (pdb:3vou). Similarly, no candidate genes for either a lysin or a holin have been identified in SS3e. Analysis of the genome sequence identifies gp25 as a putative lysozyme (PF00959) and gp26 as a putative class II holin due to the predicted presence of two transmembrane domains by TMHMM. On the basis of predicted transmembrane domains using TMHMM v2.0, phages SE2 and wksl3 are presumed to encode Class I holins while Class II holins are encoded by SETP3, SS3e and vB_SenS-Ent1. Each of the *Escherichia coli* phages encode both a class I and class II holin.

While the functions of the majority of genes are unknown, the lysis cluster appears to represent an area of significant diversity amongst these phages. Each of the SETP3-like phages encode between 8 and 13 proteins from a total pool of 19. Of these, 10 and 3 are exclusive to those phages infecting *Salmonella* and *Escherichia*, respectively, but aside from the holin and lysin only one other hypothetical protein is shared amongst all SETP-like phage in this cluster. Searches with HHpred using a ClustalX2 alignment returns a match to Phage_NinH pfam domain (PF06322).

4.8.5 Regulatory sequences

DNA sequences (150bp) upstream of ORF start codons were extracted using Artemis and submitted for analysis using MEME (Bailey *et al.,* 2006). A single motif is found within all *Salmonella* SETP3-like phages with sequence TAATA[N5]CTATTA, although further experimental investigation is required to ascertain whether this motif truly represents a promoter or operator binding sequence. This motif is not shared by members infecting *Escherichia coli*.

4.9 CoreGenes

At the protein level, analysis with CoreGenes demonstrates that the *Salmonella* SETP3-like phages share at minimum 44 homologous proteins relative to the proposed type species SETP3 (Table 15). This number is reduced to 34 for members infecting *Escherichia coli*. A detailed listing of the proteins shared between members of the proposed genus is provided in Appendix II.

Table 15. Number and percentage of shared proteins between the *Setp3likevirus* relative to the proposed type species, SETP3.

Phage	No of Shared Proteins	% Similarity
SETP3	53	100
wksl3	50	94
vB_SenS-Ent1	49	92
SE2	46	87
SS3e	44	83
K1ind1	35	66
K1ind2	34	64
K1ind3	35	66
K1H	34	64
K1G	36	68

The high degree of similarity between proteins encoded by the SETP3-like phages is clearly visible in graphical representations of whole genome BLASTP protein similarity searches (Figure 32), conducted using the CGView Comparison Tool (Grant *et al.,* 2012).

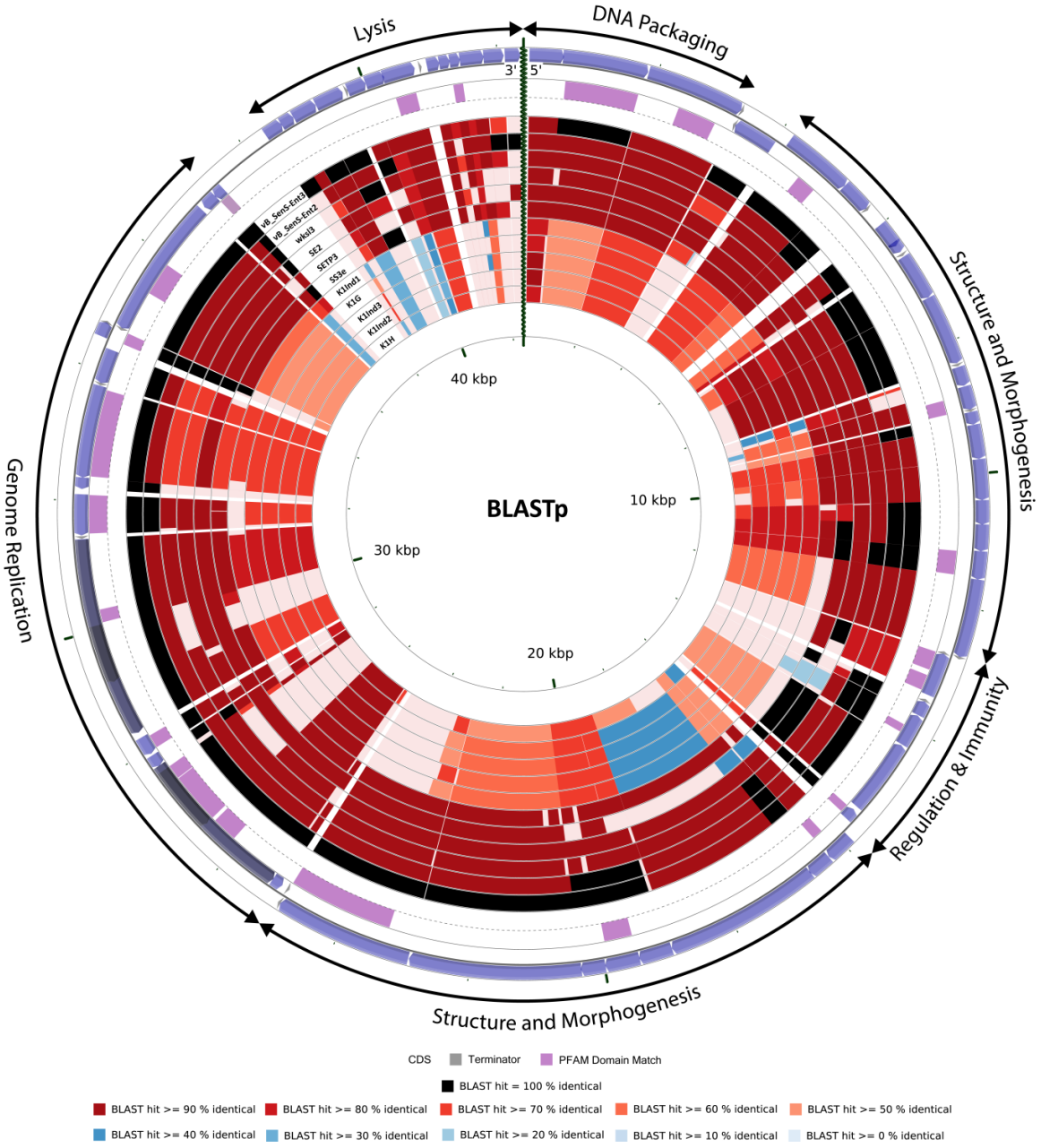

Figure 32. CGView Comparison Tool map comparing vB_SenS-Ent1 to other bacteriophages belonging to the predicted *Setp3likevirus* genus. Starting from the outermost ring the feature rings depict forward strand coding sequences, reverse strand sequence features. The remaining rings show regions of sequence similarity detected by BLASTP comparisons conducted between translated coding sequence translations from the reference genome and comparison genomes.

4.10 Phylogenetic analysis

Phylogenetic analysis was performed by construction of neighbour-joining trees using MEGA5 using the large terminase subunits, major capsid proteins and DNA polymerases of the *Setp3likevirus* and those of species representing other phage genera (Figure 33, Figure 34 and Figure 35). The results for each protein support the proposal that *SETP3likevirus* represents an independent genus within the family *Siphoviridae*.

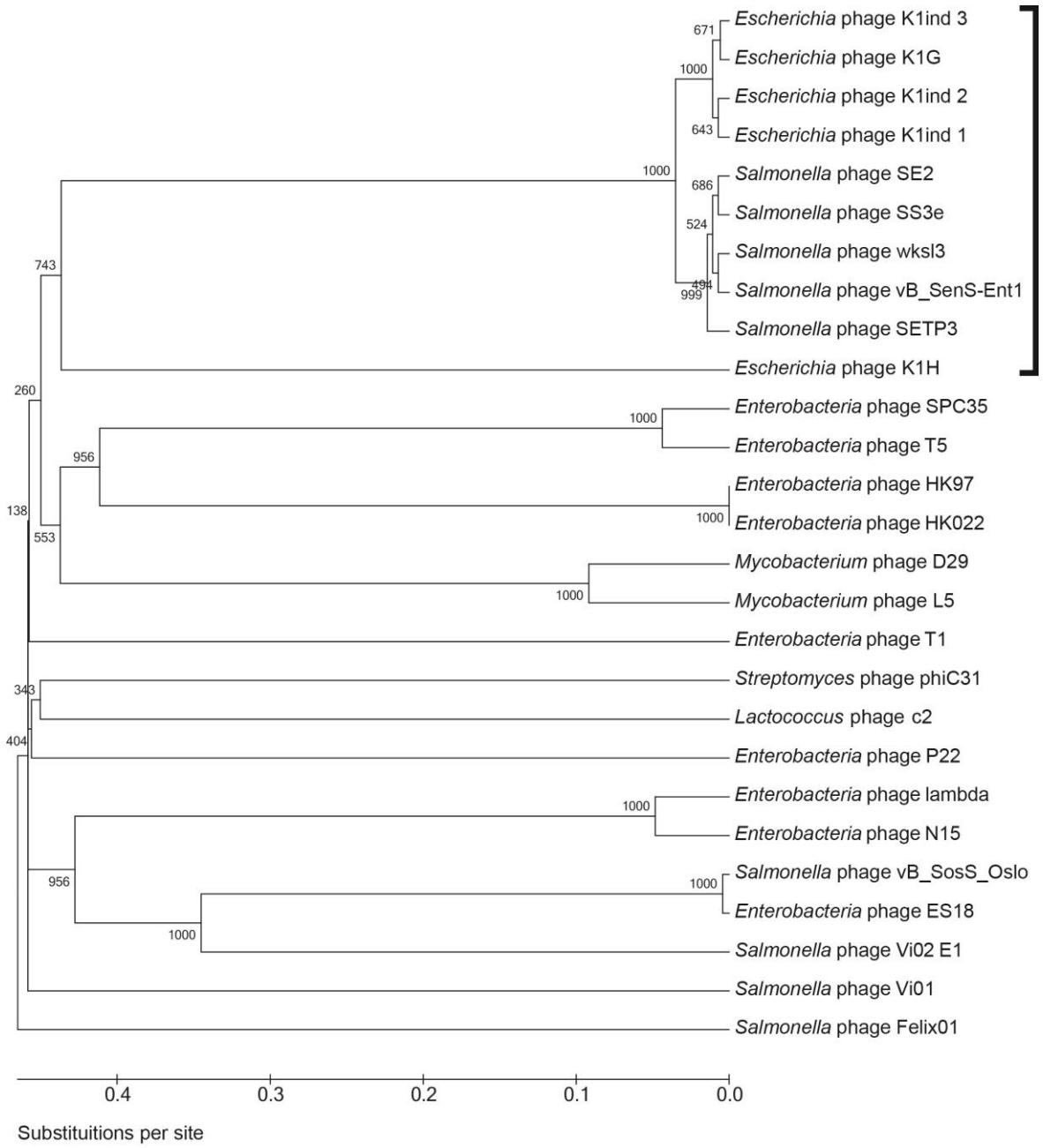

Figure 33. Neighbour-joining phylogenetic tree of major capsid proteins from the *Setp3likevirus* and representatives of other bacteriophage genera. The proposed *Setp3likevirus* are indicated by square brackets.

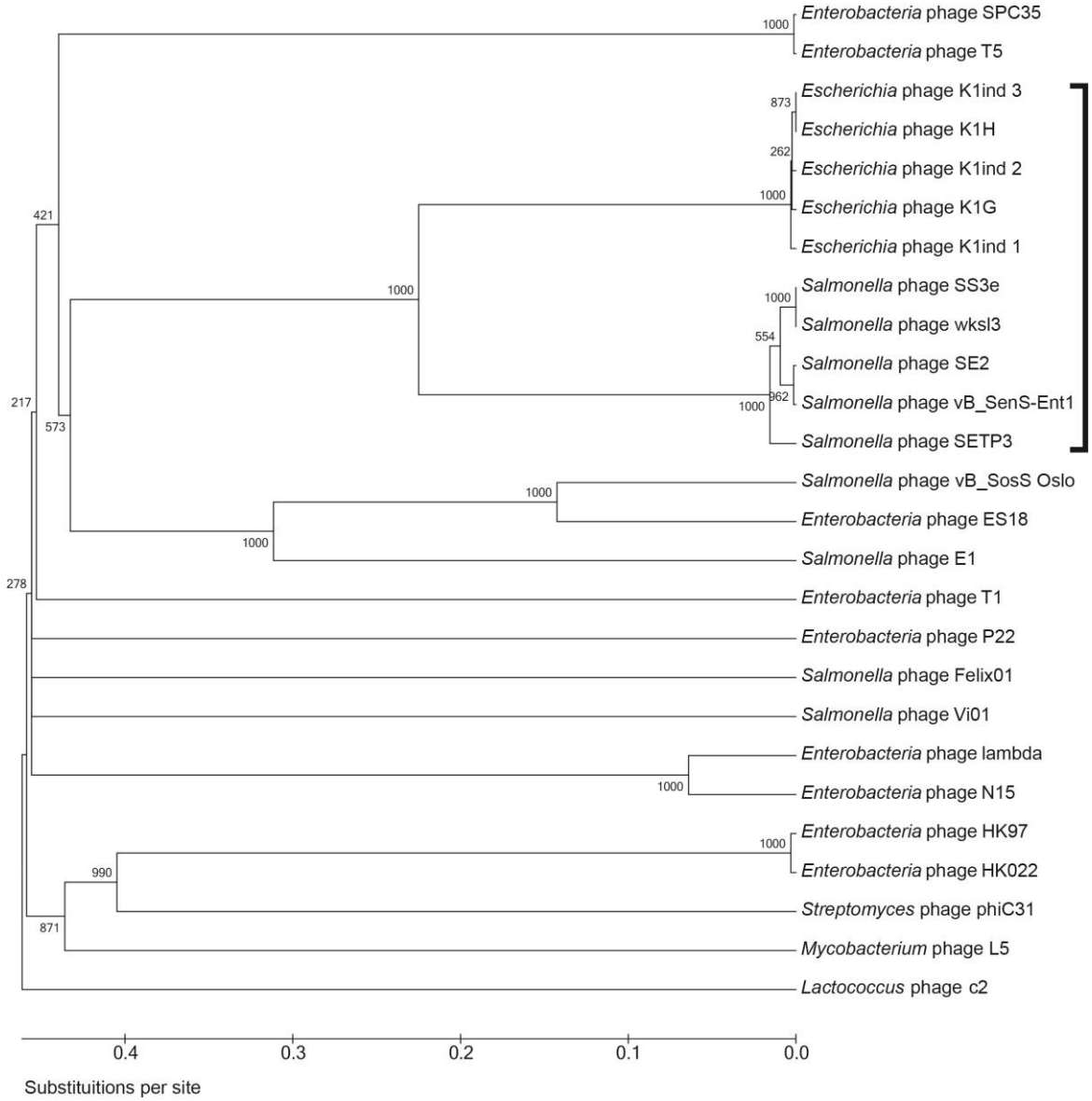

Figure 34. Neighbour-joining phylogenetic tree of the large terminase subunit from the *Setp3likevirus* and representatives of other bacteriophage genera. The proposed *Setp3likevirus* are indicated by square brackets.

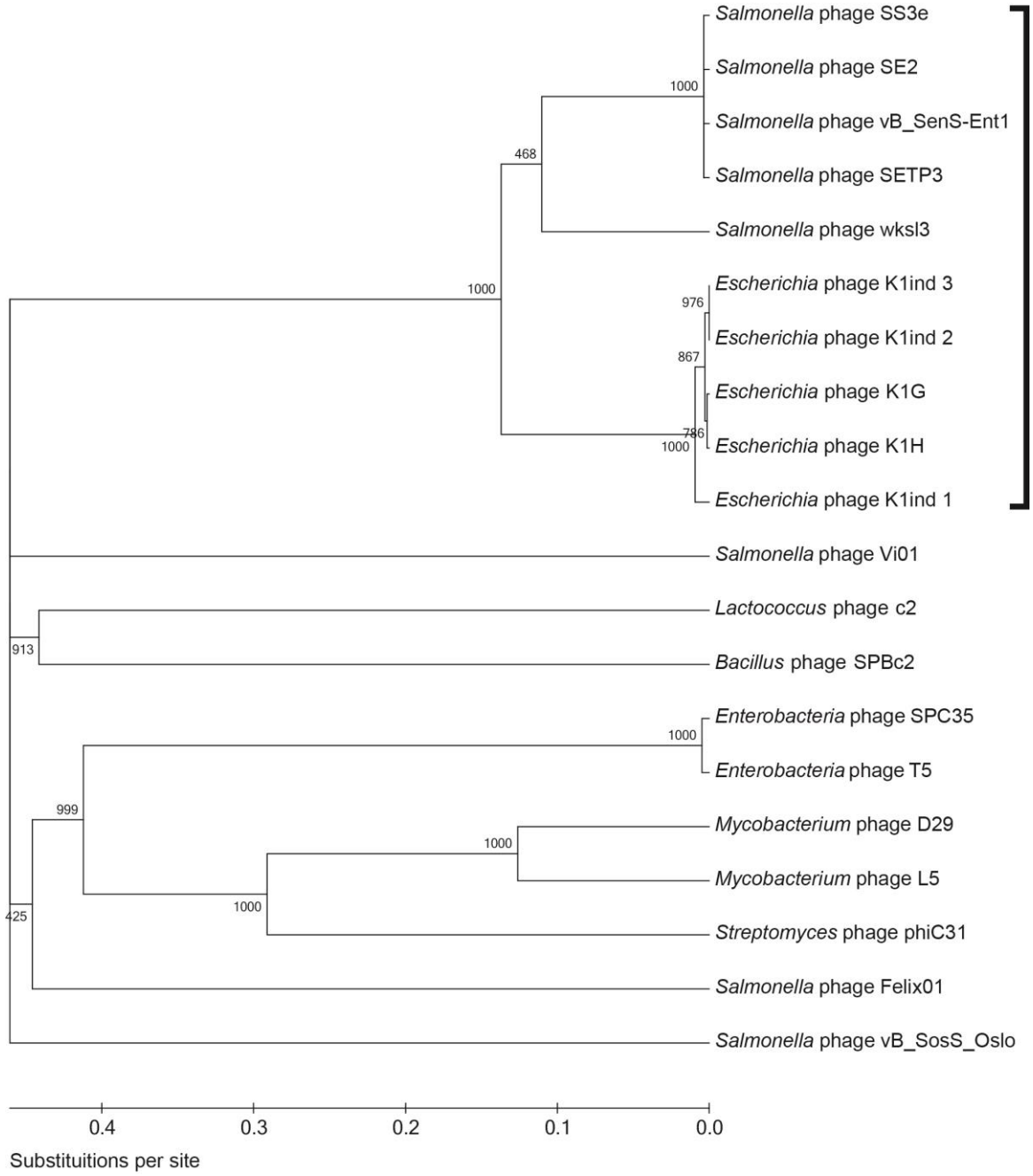

Figure 35. Neighbour-joining phylogenetic tree of the DNA polymerases from the *Setp3likevirus* and representatives of other bacteriophage genera. The proposed *Setp3likevirus* are indicated by square brackets.

4.11 Discussion

Analysis of the *Salmonella* bacteriophages held in international nucleotide sequence databases with CoreGenes showed broad agreement with current ICTV designations and reinforce current proposals for the *Viunalikevirus* (Adriaenssens *et al.,* 2012) and designation of SPC35 as a member of the *T5likevirus* (Kim and Ryu, 2011). These data also strongly supports the creation of a novel genus; the *Setp3likevirus*, consisting of 5 *Salmonella* and 5 *Escherichia* phage. Members of the *Setp3likevirus* share a common morphology, consisting of an isometric head, relatively short flexible tail and six terminal tailspikes. Bacteriophages of *Setp3likevirus* morphology appear to be restricted to enteric bacteria, predominantly *Salmonella* (Ackermann, personal communication) and the literature contains a number of additional bacteriophages which may belong to the *Setp3likevirus* but for which no or only partial genome sequences are available. Additional defining features of the group are a high degree of nucleotide homology, near identical organisation of coding sequences within the genome and at least 64 % shared proteins relative to SETP3. Comparisons between the SETP3-like bacteriophages indicate several historical insertion events, a feature which may aid in delineating the evolutionary lineage of these bacteriophages. Inteins are present in the DNA polymerase and helicase encoding genes of some, but not all members. The presence of inteins is an interesting finding and one which would be worth confirming with *in vitro* studies. Of particular note is the apparent fragmentation of the DNA polymerase of SE2 and SS3e. Similarly, homing endonucleases are present in some members but absent in others. Host specificity is conferred by the tailspike protein. The tailspike N-terminal sequence is conserved amongst all proposed members of the *Setp3likevirus* while the C-terminal varies dependent upon the host. The C-terminal region for each of members infecting the *Salmonella* encodes a P22-like catalytic domain. For members infecting *Escherichia*, two C-terminal regions are present, representing a differentiation between the requirements for the K1 capsular antigen for infection by these phages. It may also be that different tailspike C-terminal domains remain to be found in as yet un-sequenced *Salmonella* bacteriophages.

Data obtained using CoreGenes3.5 indicates an additional number of high level relationships amongst other *Salmonella* bacteriophages which are summarised but not discussed in detail. For the *Myoviridae*, the data suggests the assignment of RE-2010 to the genus *P2likevirus.* RE-2010, termed ELϕS in the associated publication, was isolated from *S.* Enteritidis PT8 strain LK5 by induction with mitomycin C (Hanna *et al.,* 2012). The genome is 34.11 kb flanked by 84 bp direct repeats and encodes 46 ORFs, three of which are unique to this phage. Several features suggest that RE-2010 is a P2-like virus. Firstly, RE-2010 shares 41, 31 and 27 proteins with Fels-2, PSP3 and P2, respectively. Secondly, RE-2010 has been demonstrated capable of forming functional lysogens and the *attB* site overlaps the respective sites for SopEϕ and Fels-2 within the tmRNA gene *ssrA* (Hanna *et al.,* 2012, Pelludat *et al.,* 2003). Lastly, RE-2010 encodes a significant number of structural homologues with P2.

With no observed relationships to other phages, PVP-SE1, Felix O1 and SPN3US remain singletons amongst the *Salmonella Myoviridae*.

For the *Podoviridae*, the genus *P22likevirus* is expanded to 10 members infecting *Salmonella* with the proposed additions of vB_SemP_Emek and SPN9CC. These designations are in agreement with recommendations outlined in the associated literature (Nelson *et al.,* 2012). In addition, SPN1S and Vi06 are predicted to belong to genera *epsilon15likevirus* and *T7likevirus*, respectively. Two genomic orphans remain within the *Salmonella Podoviridae,* ST64B and 7-11, while SP6 remains the sole representative of the *Sp6likevirus* genus.

Phages ES18, SPN3UB and vB_SosS_Oslo may also form a novel genus within the *Siphoviridae*, although the relationship is not as distinct for the *Setp3likevirus*. Relative to ES18, vB_SenS_Oslo shares 46 proteins (58 % similarity) and SPN3UB 30 (38 %). Each of these phages encodes a number of proteins also found in Enterobacteria phage ʎ and P22. Strikingly, ES18 and vB_SosS_Olso share a large number of proteins, at least 20 %, with members of the *P22likevirus*. For ES18 these include genes within the integration, recombination and lysis gene clusters. This relationship is less pronounced for SPN3UB which shares only 7 proteins for P22 but retains the ʎ-like tail structural genes. This number is reduced for SPN3UB which shares 7 proteins with P22. SPN3UB also shares a significant number of proteins, 39 % and 35 %, with the prophages Gifsy-1 and Gifsy-2, respectively. Lastly, EPS7 joins SPC35 as a *T5likevirus* with 122 proteins shared between the two genomes (71.8/84 %) including the pre-early proteins encoded within a large terminal repetition at right end of genome analogous to T5. Phages SSU5, Vi II-E1 and the siphoviral prophages Gifsy-1, Gifsy-2 and Fels-1 remain unclassified.

The clustering performed here represents a simple method to identify and investigate groups of related genes among viral isolates, although the caveat of Lavigne *et al.,* (2008) still stands. Specifically the validity of this analysis is dependent upon correct annotation of coding sequences and crucially, the correct determination of gene boundaries. However, with the exponential increase in bacteriophage sequences deposited in the international sequence databases, the value of storing such data in relational databases, an approach exemplified by ACLAME and Phamerator, cannot be under-estimated. With the implementation of appropriately coded script pipelines, relational databases have the ability to include additional sequence data and analyses and update this data dynamically. In contrast, the approach presented here represents but a single snapshot in time.

SETP3, Vi01 and ViII-E1 represent the only members of the *Salmonella* phage typing sets that are publically available within the INSD, though we note that sequences for the Vi phages are available via FTP (ftp://ftp.sanger.ac.uk/pub/pathogens/Phage/). Whilst the phages used for typing of serovars Enteritidis and Typhimurium have been described (De Lappe *et al.,* 2009, Schmieger, 1999), it would

be of value to sequence and annotate more members comprising the international phage typing sets for *Salmonella* given that at least a partial record of their genealogy exists.

With an estimated 10^{31} bacteriophages present in the biosphere, and considering the striking example of the Mycobacteriophages, it is assured that the diversity of *Salmonella* phages is even greater than that represented by the current set of sequenced genomes. Similarly, extension of the analysis reported here to all sequenced bacteriophage genomes would likely reveal relationships for the genomic orphans amongst the *Salmonella* phages. Despite these limitations it is hoped that this review will provide a useful starting point for the future investigation of relationships between *Salmonella* bacteriophage genomes. Given the improvement of existing genome sequencing technologies and rapid development of new approaches, the number of sequenced phage genomes deposited in EMBL and GenBank will continue to increase exponentially.

4.12 Addendum

This study was limited to sequences deposited in Genbank and the INSD prior to the 17th of September 2012. Since then an additional three *Salmonella* phage sequences have been deposited, SKML-39 (JX181829.1), STML-198 (JX181825.1) and SSE-121 (JX181824.1). An extension of the core genes analysis to include these phages suggests that SKML-39 is a member of the *Viunalikevirus*, SSE-121 is highly related to PVP-SE1 with 221 shared proteins (91 % similarity), while STML-198 shows little similarity to other characterised *Salmonella* phages.

Chapter 5 Measuring bacteriophage-mediated lysis of *Salmonella* using bioluminescence

5.1 Introduction

The use of microtitre plate assays is attractive for studies of bacteriophage-mediated lysis. Microtitre plate readers allow for automated and regular measurement of many samples under controlled conditions of temperature and agitation. Several microtitre assays for phage lysis have been described in the literature using either absorbance or colorimetric methods. Decreases in culture absorbance due to phage-mediated lysis have been monitored in a microtitre format for a number of host and phage combinations (Niu *et al.,* 2009, Fridholm and Everitt, 2005, Cooper *et al.,* 2011). However, measurements of absorbance are limited to relatively high host cell concentrations, generally between greater than 10^5 and 10^6 cfu ml^{-1}, and can be influenced by the presence of cell debris. Colorimetric methods using the reduction of tetrazolium dyes have been applied for the study of bacteriophages upon *Salmonella* serovars (McLaughlin, 2007), *Bacillus anthracis* (Henry *et al.,* 2012) and *Pseudomonas aeruginosa* (Knezevic and Petrovic, 2008). Tetrazolium redox dyes scavenge electrons from microbial redox reactions and are intracellularly reduced to form insoluble coloured formazan precipiates, which may be measured at specific wavelength (Mosmann, 1983). Differential fluorescent stains, such as SYTO-9 and propidium iodide, may also be employed to provide endpoint measurements of live and dead bacterial cells (Jassim and Griffiths, 2007).

Despite the widespread use of the *lux* operon in bacteria as a biosensor and reporter of gene expression, the application of bioluminescent bacterial reporters in conjunction with bacteriophages is limited. Several groups have reported the construction of recombinant reporter bacteriophage engineered to encode the *luxAB* genes. These bacteriophages are designed to deliver the *luxAB* genes to a specific host, which are subsequently translated alongside expression and replication of the phage genome. The addition of an aldehyde substrate results in the generation of a bioluminescent signal should the target host be present. This approach has been employed for the detection of *Yersinia pestis* (Schofield *et al.,* 2009), *Bacillus anthracis* (Schofield and Westwater, 2009) and *Listeria* (Loessner *et al.,* 1996, Loessner *et al.,* 1997). Detection of the enteropathogenic *E. coli* serotype O157:H7 has also been achieved using phage transformed to encode the *luxI* quorum sensing signal transducing molecule (Brigati *et al.,* 2007). Infection results in expression of this gene which can then be detected by a phage-insensitive reporter harbouring the *luxCDABE* operon. Only a single manuscript could be found in the literature detailing the use of constitutively bioluminescent *E. coli* DH5α with T4 phage at different multiplicities of infection. Lysis was monitored using light

emission at 40 minute intervals for a period of 13 hours. The authors suggest that decreases in light emission at 5.3 and 3.3h after infection correlates to phage concentration (Kim *et al.,* 2009).

This chapter details the transformation of *Salmonella* serovars Typhimurium and Enteritidis to a bioluminescent phenotype by introduction of a plasmid encoding the *luxCDABE* operon of *Photorhabdus luminescens* under control of the constituitive *lac* promoter. Light emission was correlated with log-fold dilutions of batch cultures, growth in batch culture and optical density. Finally, the effects of applying the bacteriophages vB_SenS-Ent1 –Ent2 and –Ent3, at different multiplicities of infection and host cell concentrations were determined using bioluminescent *S.* Enteritidis within a microtitre plate broth assay.

5.2 Results

5.2.1 Calibration curves

Calibration curves were constructed to relate optical density at 540nm, bioluminescence and colony forming units. Values of optical density at 540nm, bioluminescence and viable counts were transformed to base 10 logarithms prior to analysis by linear regression (Figure 36). Absorbance increased linearly with viable counts between OD_{540nm} values of 0.05 and 1.200. Values of R^2 were 0.994 and 0.989 for *S.* Typhimurium and *S.* Enteritidis, respectively. Regression line equations from calibration curves were subsequently used for the estimation of bacterial numbers when preparing inocula. Light emission increased linearly with absorbance and colony forming units until a concentration 1 x 10^8 cfu ml^{-1}, after which the intensity of light emission was at a level causing saturation of the photo-multiplier tube.

S. Typhimurium DT104 LITE

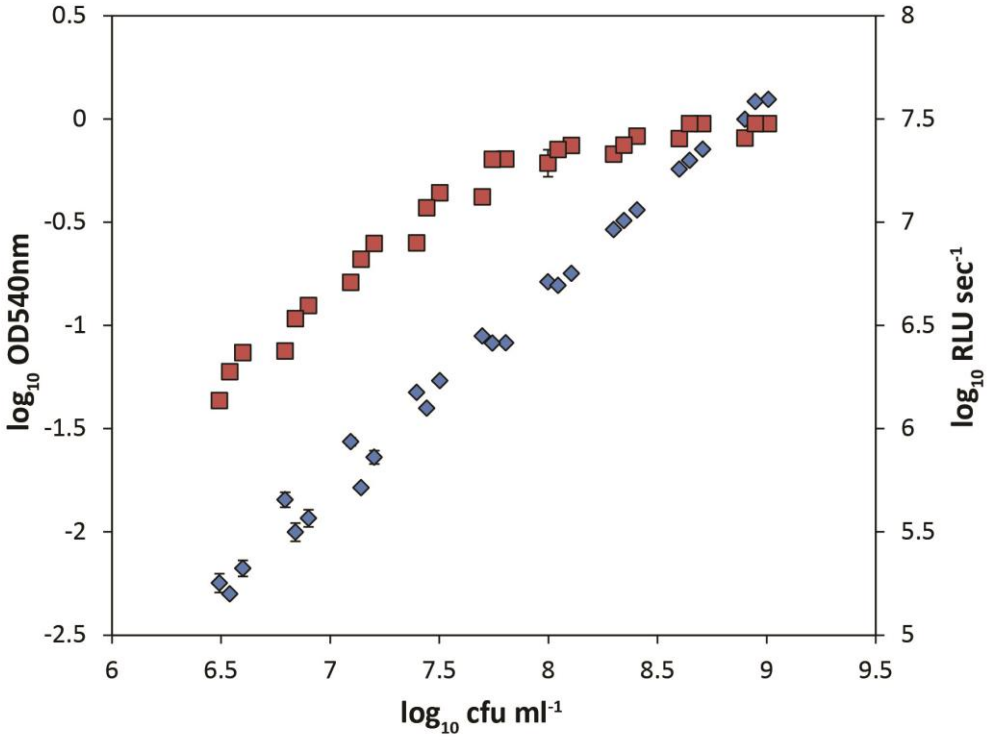

S. Enteritidis PT4 LITE

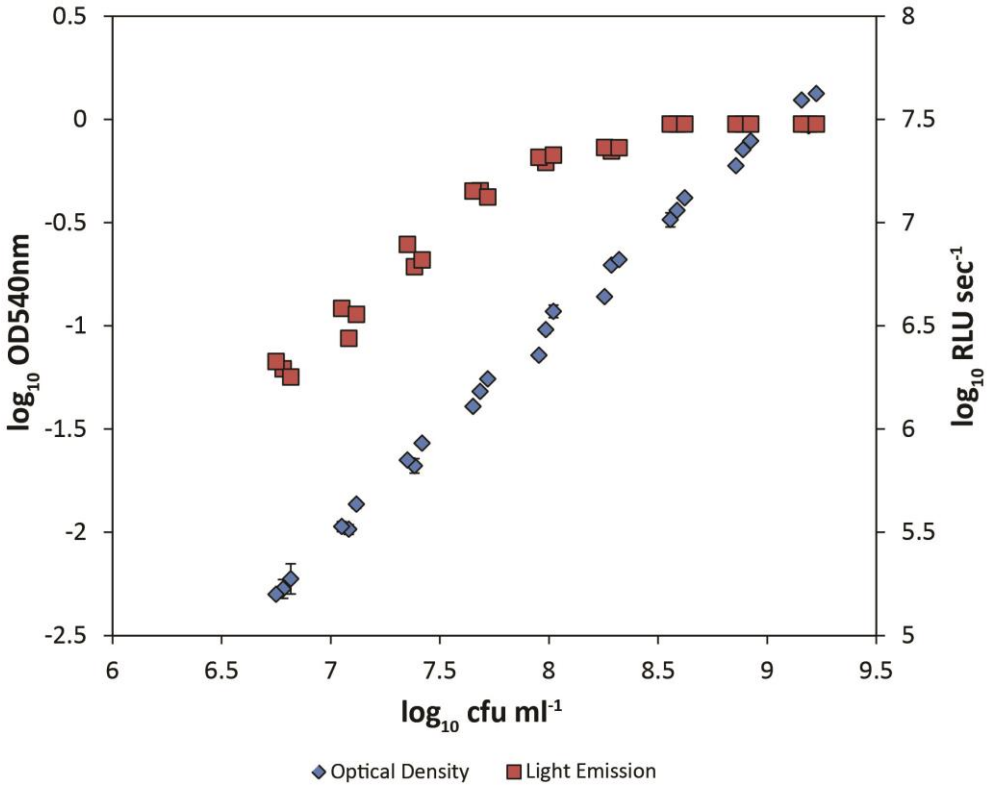

Figure 36. Calibration curves of optical density at 540 nm, light emission and colony forming units. One ml samples from a two-fold dilution series of batch cultures of *S.* Enteritidis and *S.* Typhimurium expressing the *luxCDABE* opron were measured. Data represent the mean of triplicate samples from three independent experiments. Error bars indicate standard deviation.

Since optical density at 540 nm could not detect bacterial concentrations less than 10^6 cfu ml^{-1} a second set of calibration curves were constructed measuring bioluminescence against 10-fold

dilution series of batch cultures of *S.* Enteritidis and *S.* Typhimurium. Units of relative light emission (RLU) and viable counts were transformed to $\log_{10}$ values. The detection limit was defined as the $\log_{10}$ value of the mean plus 3 standard deviations of the reagent blank control while the limit of quantification was defined as the 10 standard deviations above the reagent blank control (Mosmann, 1983). Light emission exhibited strong correlation with viable counts from log phase batch cultures with R^2 values of 0.98 and 0.99 for *Salmonella* serovars Enteritidis PT4 LITE and Typhimurium DT104 LITE, respectively (Figure 37). Slope values from linear regression were 1.22 and 1.26 suggesting that the relationship between light emission and viable counts is not perfectly linear. Most photocathode based detection systems show two non-linear response regions: at or below the limit of detection of the sensor and the onset of non-linear gain at levels near to sensor saturation. Linearity might be improved by excluding values that fall within the non-linear regions of the response detector. Using bioluminescence, limits of detection were established at 2.18×10^2 and 5.76×10^2 cfu ml^{-1} and limits of quantification at 8.71×10^2 and 2.39×10^3 cfu ml^{-1} for serovars Enteritidis and Typhimurium, respectively.

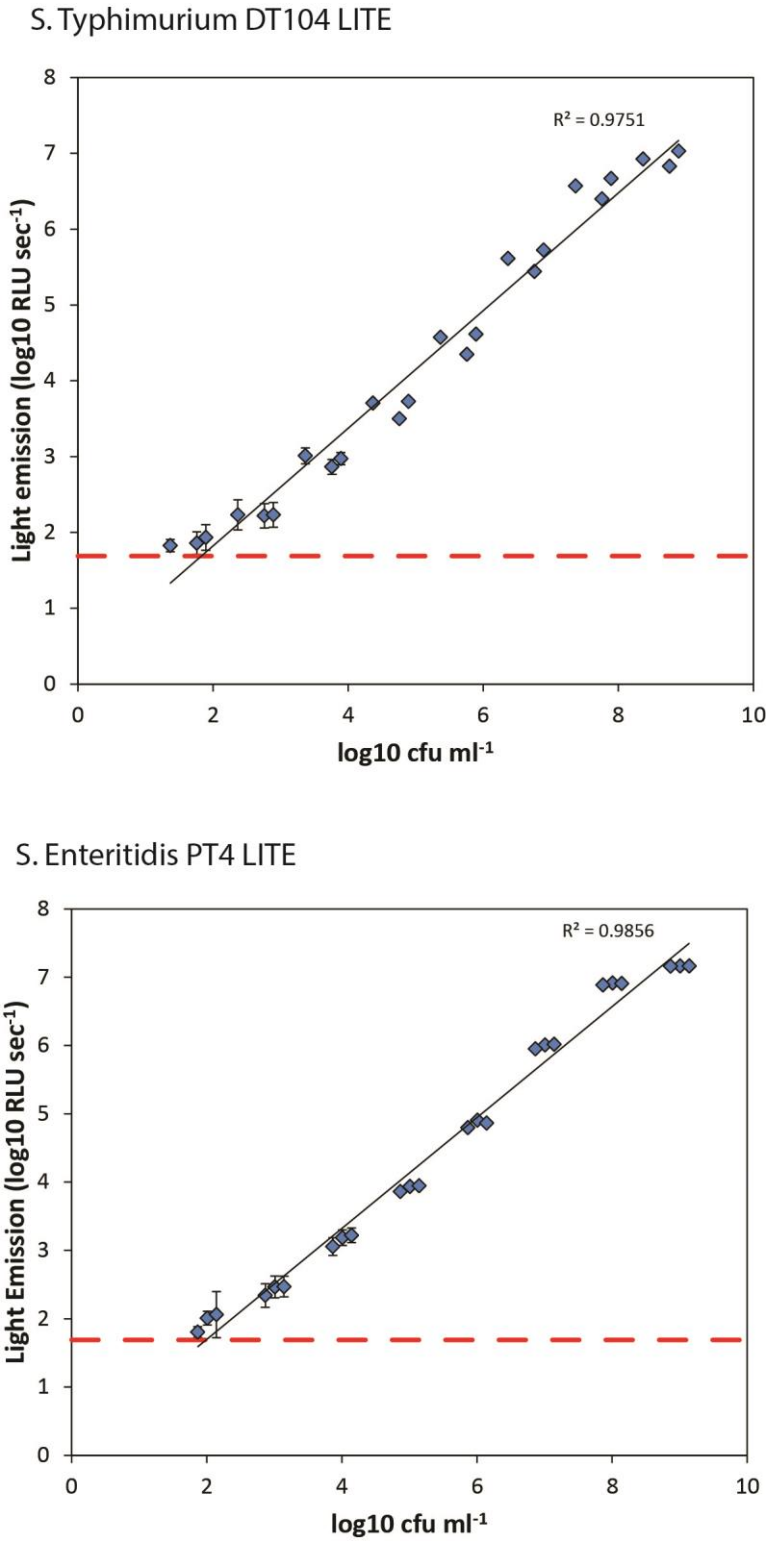

Figure 37. Calibration curves of light emission versus bacterial cell concentrations performed on batch cultures of *S.* Enteritidis and *S.* Typhimurium expressing the *luxCDABE* operon. Measurements were performed using 100 µl samples from log-fold dilutions of exponential phase batch cultures. Data represent the mean of triplicate samples from three independent experiments. The red dotted line denotes the limit of detection, representing the mean reagent blank plus 3 standard deviations.

Comparisons of growth curves of wildtype and bioluminescent *Salmonella* serovars Enteritidis and Typhimurium in batch culture were performed to establish whether expression of the *lux* operon resulted in any significant alteration to the growth characteristics of these serovars (Figure 38).

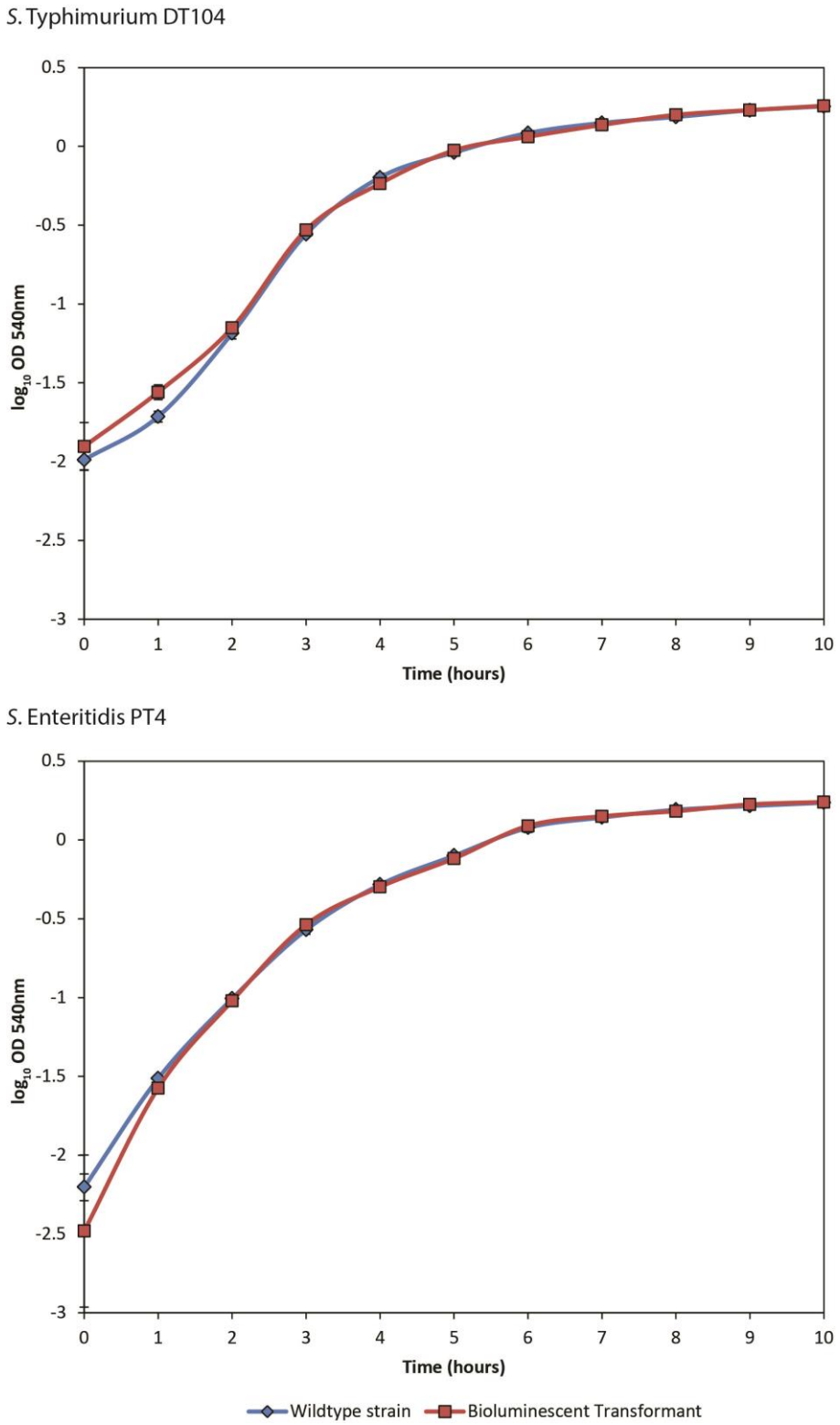

Figure 38. Growth of wild-type and bioluminescent *S.* Enteritidis and *S.* Typhimurium in batch culture. Data presented are the mean and standard deviation of absorbance measurements of three independent cultures.

No significant difference (Student's t-test, P = 0.05) was observed for growth of wild-type and bioluminescent transformants in batch culture.

5.2.2 Bioluminescence emission spectra

Bioluminescence emission, measured using a monochromator-based fluorometer with the excitation port blocked (Fluorosens, Gilden Photonics, UK), was observed as a single peak for bacteria transformed with the *lux* operon (Figure 39) ranging from approximately 410 nm to 640 nm. Area under curve analysis identified peak emissions at 482 nm for *S.* Enteritidis PT4 and 481 nm for *S.* Typhimurium DT104. The diluent control was constant with a mean emission value of 3952 ± 347.8 (s.d.). The accuracy of wavelengths reported by the instrument was confirmed by water Raman. The peak wavelength values reported differs from that reported in the literature for bacterial luciferase, which is 490 nm (Meighen, 1991). This apparent lack of agreement could be due to scattering caused by the turbidity of the bacterial culture, or by the association of proteins with the bacterial luciferase.

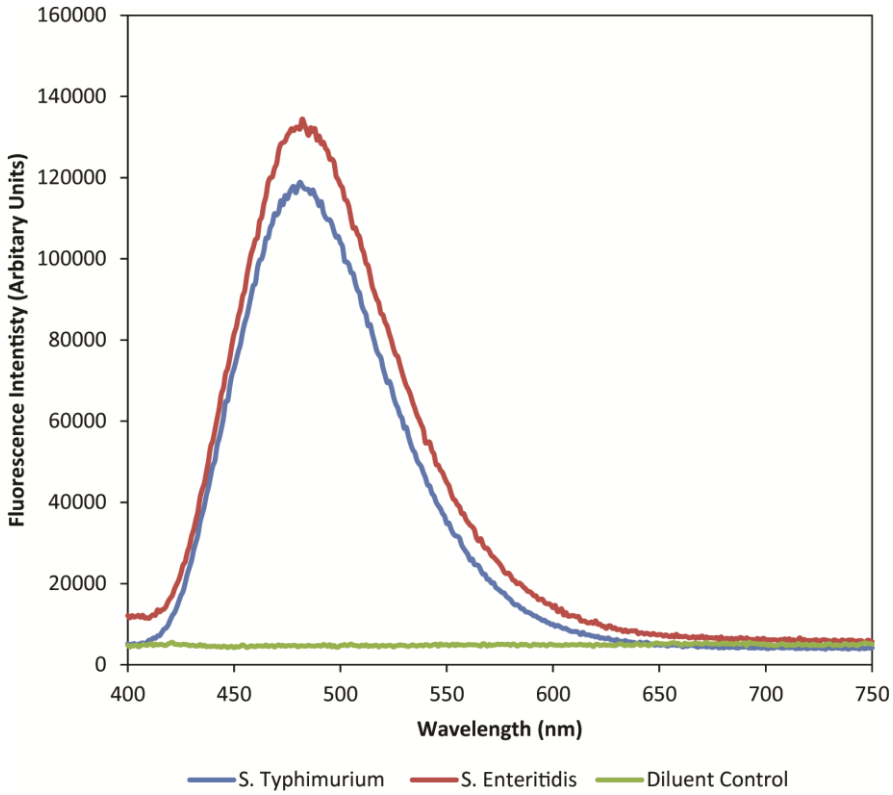

Figure 39. Emission spectra across 400 to 750 nm for bioluminescent reporters *S.* Enteritidis and *S.* Typhimurium. Emission values were obtained for 1nm steps using an integration time of 1 second.

5.2.3 Growth of bioluminescent bacteria

Overnight cultures were diluted 1:1000 upon addition into fresh pre-warmed LB broth to yield a starting concentration of approximately 1 x 10^6 cfu ml^{-1}. LB broth was supplemented with appropriate antibiotics to maintain plasmid selection. Growth curves were ascertained by measurement of optical density at 540nm, bioluminescence and viable counts over a 10 hour period. All bioluminescent bacterial reporters exhibited lag, exponential and stationary phases (Figure 40). All cultures exhibited a lag phase for the first hour after inoculation, where viable counts either remained stationary or increased very slightly. In contrast to viable counts, values of absorbance increased during this period, perhaps indicating an increase in cell biomass with little or no increase in population number. Exponential phase growth was characterised by rapid, exponential increase in viable counts and OD_{540nm}. The onset of stationary phase was indicated by a deceleration of the rate of increase of absorbance and viable counts. Stationary phase was characterised as a constant or very slow increase in absorbance and viable counts. Growth rates and generation times for the exponential phases of bioluminescent reporters were calculated from log_{10} mean values of viable counts (n=3). Of the bioluminescent reporters, *S.* Enteritidis exhibited the fastest generation time at just over 20 minutes with an observed growth rate (*k*) of 2.89 generations per hour. Growth of the bioluminescent serovar Typhimurium was somewhat slower, with a generation time of 25 minutes.

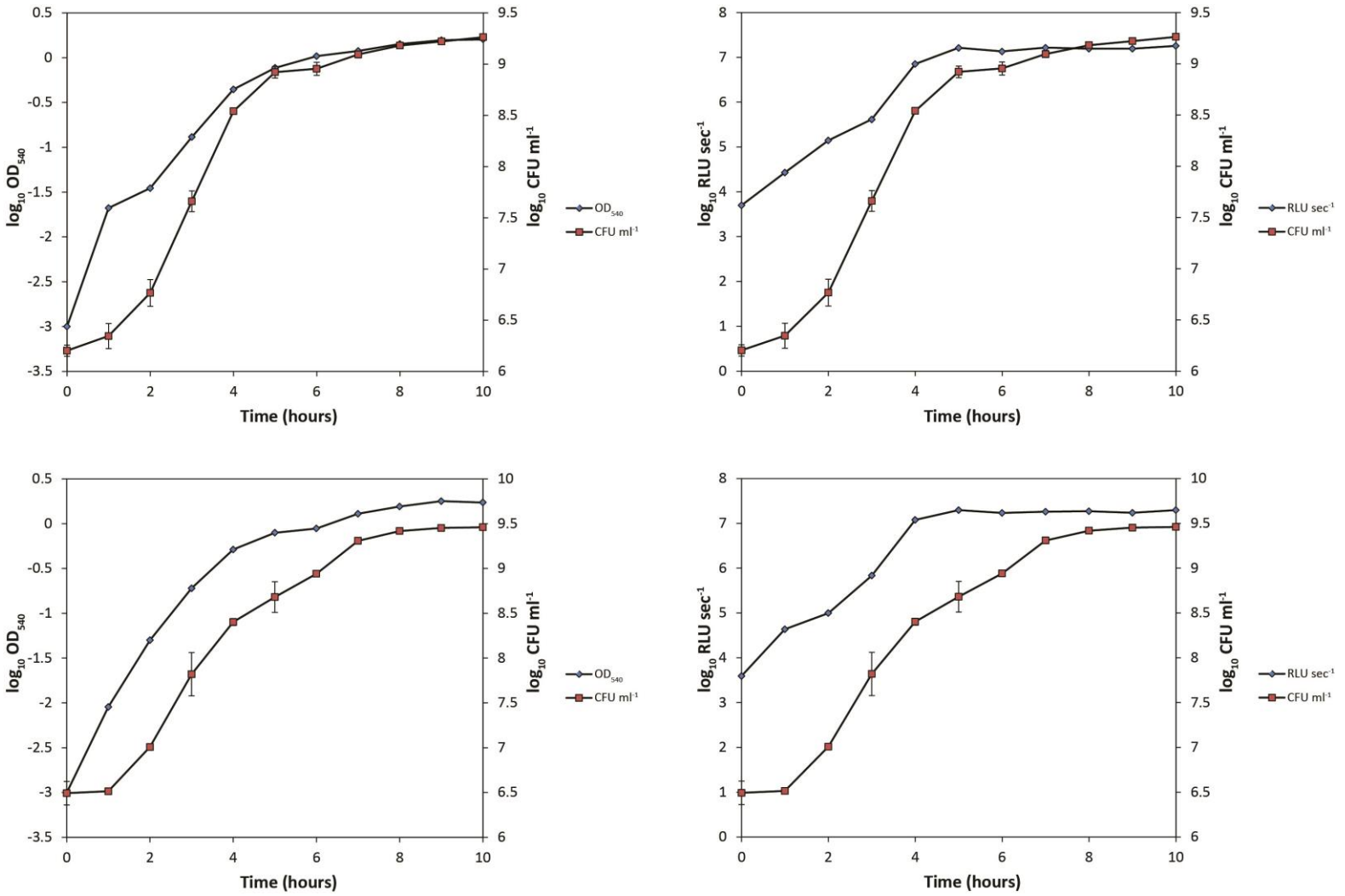

Figure 40. Growth of bioluminescent *Salmonella* serovars Enteritidis (top) and Typhimurium (bottom) over time in batch cultures measured by colony counts, absorbance at 540nm and relative light emission. Data represent mean and standard deviation of triplicate measurements of three independent batch cultures.

5.2.4 Multiplicity of infection

The effects of co-incubation of the vB_SenS-Ent bacteriophages and their host bacteria, *S.* Enteritidis PT4, at 37^{o}C and varying multiplicities of infection were investigated using a broth microplate assay format. Initially these effects were to be measured using both absorbance and bioluminescence. Bioluminescence was chosen as light emission from *S.* Enteritidis PT4 showed high correlation with cell numbers and yielded typical growth curves not significantly different to that observed with the wild-type strain. Additionally, bioluminescence afforded a lower limit of detection than that obtainable by measurements of absorbance. Unfortunately, the use of dual luminescence and absorbance readings was precluded due to the effects of sample evaporation when plates were incubated at 37^{o}C in the instrument for periods greater than 4 hours. Attempts to mitigate this effect using plate sealing films resulted in skewed absorbance data due to the formation of droplets by condensation on the inner surface of the sealing film. As such bioluminescence was measured using a single-mode microplate reader (Centro XS^{3}, Berthold GmBH, Germany) where the heating system did not result in such extensive evaporation.

Bacteriophages were added to bacterial cultures to yield multiplicities of infection (MOI) of approximately 10, 1 and 0.1. As at the time of addition of bacteriophages bacterial counts were estimated from calibration curves of optical density, actual multiplicities of infection were not exactly 10, 1 and 0.1 (Table 16).

Table 16. Multiplicity of Infection (MOI) ratios employed for microtitre broth lysis experiments. The MOI, as used here, is the ratio of plaque forming units to colony forming units, established from triplicate enumerations performed in tandem.

Phage Isolate	Bacterial concentration (cfu ml^{-1})	Multiplicity of Infection (MOI)		
vB_SenS-Ent1	1.50 x 10^{7}	11.53	1.53	0.14
	2.22 x 10^{5}	7.78	0.78	0.08
	2.64 x 10^{3}	6.54	0.66	0.07
vB_SenS-Ent2	1.50 x 10^{7}	12.67	1.27	0.13
	2.22 x 10^{5}	8.14	0.82	0.07
	2.64 x 10^{3}	6.86	0.69	0.07
vB_SenS-Ent3	1.50 x 10^{3}	10.47	1.05	0.11
	2.22 x 10^{5}	7.06	0.71	0.06
	2.64 x 10^{3}	5.95	0.58	0.06

Profiles of bioluminescence for control cultures of *S.* Enteritidis showed typical bacterial growth curves consisting of exponential, deceleration and stationary phages. In contrast, growth in the presence of bacteriophages resulted in substantially different profiles of light emission.

At low host cell concentrations in the region of 1 x 10^3 cfu ml^{-1}, light emission for bacteria grown in the presence of bacteriophages increased initially at a similar rate to cells grown in the absence of phage (Figure 41). Light emission began to decline at different times dependent upon the multiplicity of infection employed, with the highest MOI resulting in earliest declines. At the highest MOI, bioluminescence began to plateau after 60 minutes and reduce at 120 minutes. For MOIs of 1 and 0.1, declines in bioluminescence began after 160 and 180 minutes, respectively. Bioluminescence in all phage treated samples fell to levels at or below the reagent blank control after 200, 240 and 260 minutes for MOIs of 10, 1 and 0.1, respectively, representing declines of 1.1 to 1.7 $\log_{10}$ RLU sec^{-1}. With the exception of vB_SenS-Ent3 at an MOI of 0.1, regrowth was observed for all samples after 300 minutes by a slow rate of increase in light emission that continued for the remainder of the experimental duration.

vB_SenS-Ent1

1 x 10^3 cfu ml^{-1}

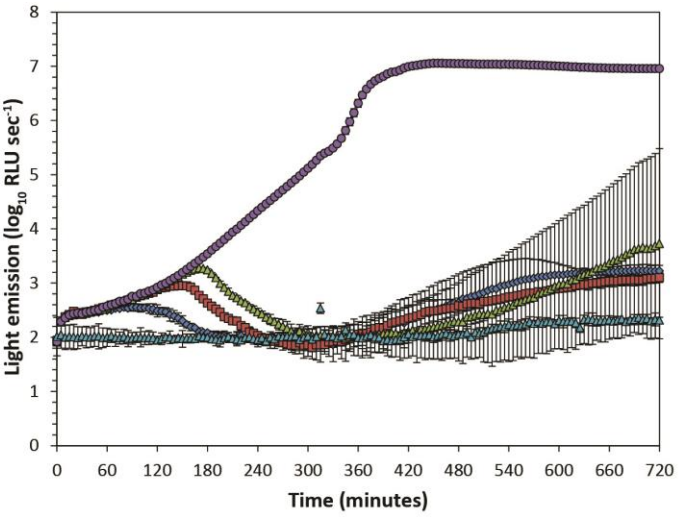

vB_SenS-Ent2

1 x 10^3 cfu ml^{-1}

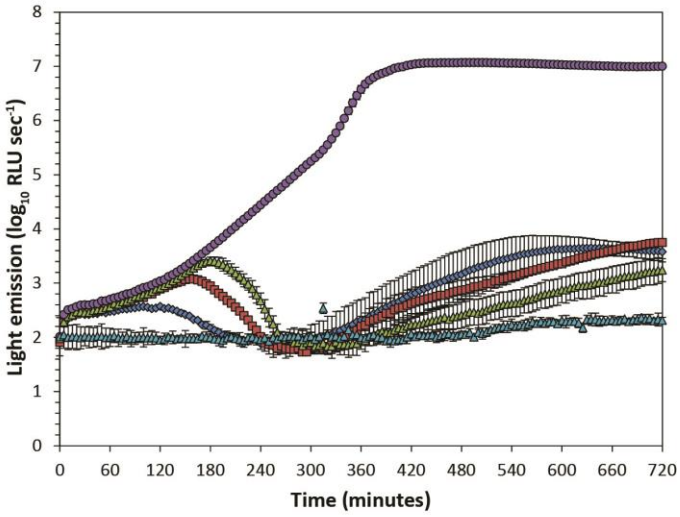

vB_SenS-Ent3

1 x 10^3 cfu ml^{-1}

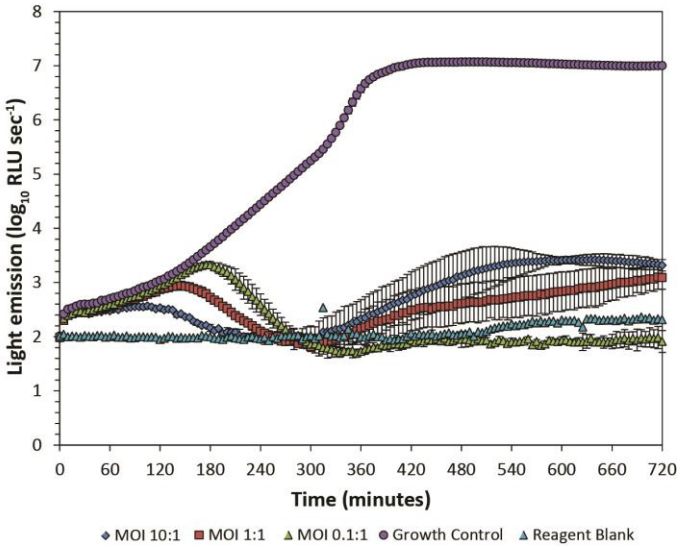

Figure 41. Bioluminescence for *S.* Enteritidis at low density (10^3 cfu ml^{-1}) incubated in the presence and absence of vB_SenS-Ent bacteriophages. Light emission was recorded every 5 minutes for a total duration of 12 hours using an integration time of 1 second. Data points represent the mean and standard deviation from measurements of triplicate wells.

At a concentration of 1 x 10^5 cfu ml^{-1} samples treated with bacteriophages showed a near immediate decline in light emission, beginning after 35 minutes (Figure 42). The rate of decline decreased after 120 minutes, reaching a minimum between 260 and 300 minutes. At the minimum, light emission levels remained three times greater than the reagent control mean. All wells showed reductions in bioluminescence of 3.0 $\log_{10}$ RLU sec^{-1}, but after 300 minutes increasing levels of light emission were observed at all multiplicities of infection. The control culture showed evidence of a prolonged lag phase in the data presented here, lasting for around 2 hours, during which light emission exhibited a slow rate of increase.

vB_SenS-Ent1

1 x 10^5 cfu ml^{-1}

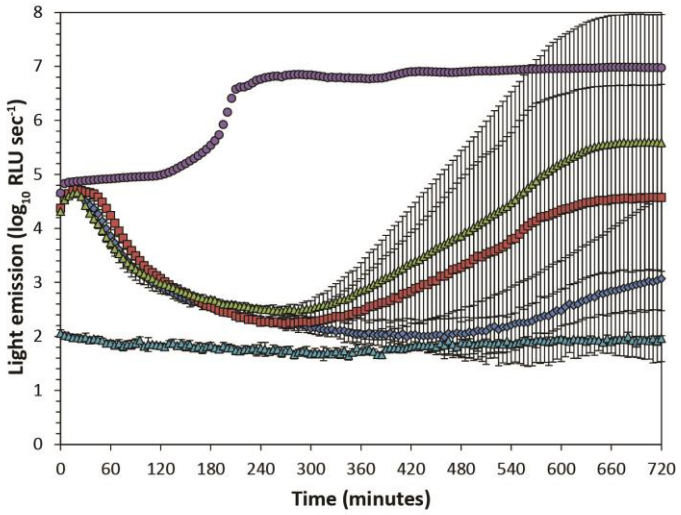

vB_SenS-Ent2

1 x 10^5 cfu ml^{-1}

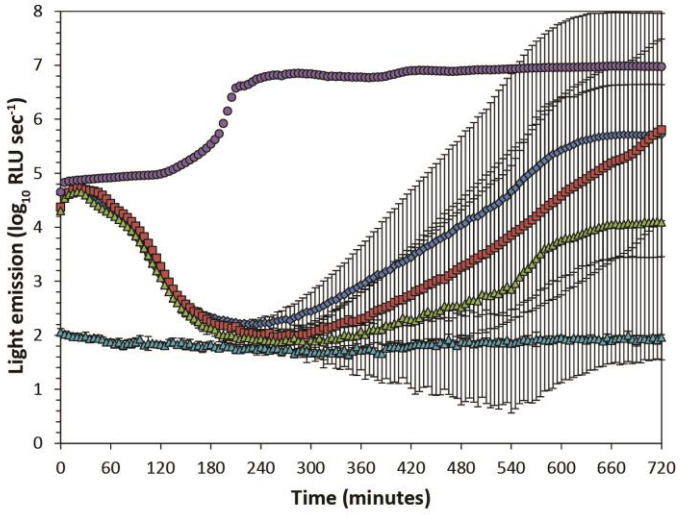

vB_SenS-Ent3

1 x 10^5 cfu ml^{-1}

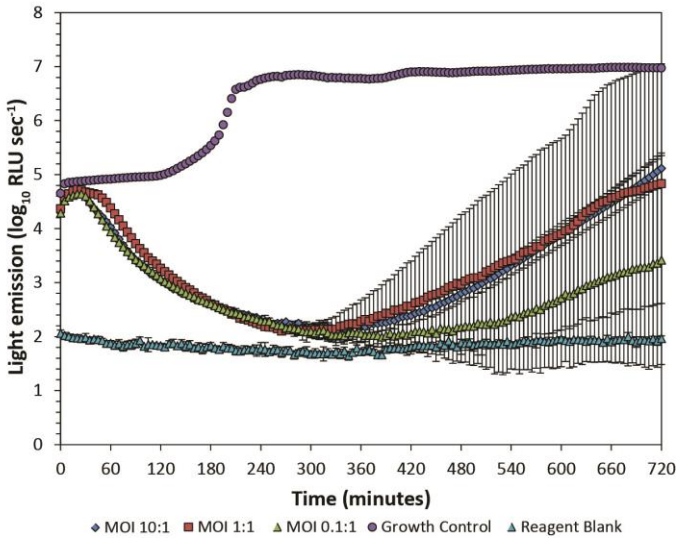

Figure 42. Bioluminescence for *S.* Enteritidis at medium density (10^5 cfu ml^{-1}) incubated in the presence and absence of vB_SenS-Ent bacteriophages. Light emission was recorded every 5 minutes for a total duration of 12 hours using an integration time of 1 second. Data points represent the mean and standard deviation from measurements of triplicate wells.

At concentrations of greater than 1 x 10^7 cfu ml^{-1}, control cultures grown in the absence of bacteriophage showed initial increases in bioluminescence, followed by a period of near constant light emission for the entire duration of experiments (Figure 43). At this high concentration of host cells, the addition of the vB_SenS-Ent phages to yield different MOIs resulted in a near immediate reduction in bioluminescence. In all phage treated samples bioluminescence initially declined by approximately 2 log_{10} RLU sec^{-1}, reaching a minimum between 240 and 300 minutes. As for other host cell densities, after 300 minutes each of the cultures incubated with the vB_SenS-Ent phages showed a recovery of light emission which, after 480 minutes, achieved levels equivalent to that of untreated growth controls.

vB_SenS-Ent1

1 x 10^7 cfu ml^{-1}

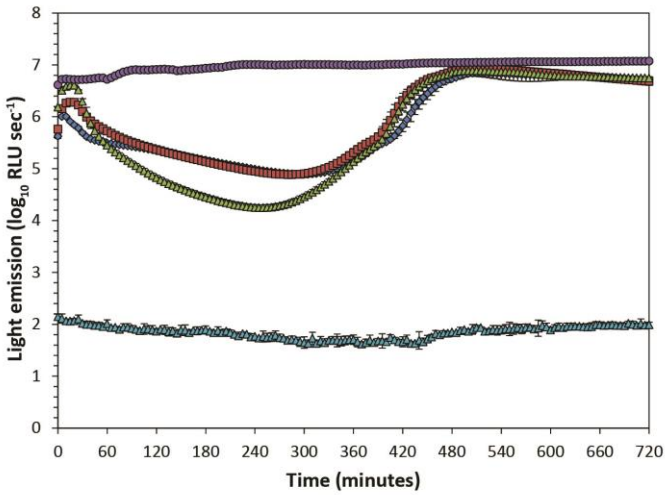

vB_SenS-Ent2

1 x 10^7 cfu ml^{-1}

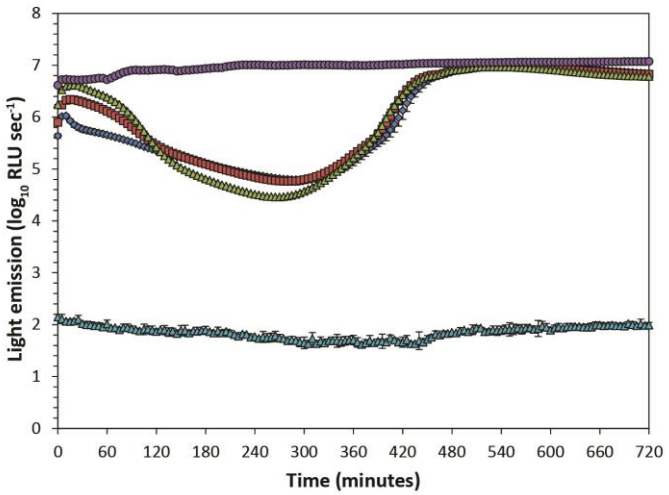

vB_SenS-Ent3

1 x 10^7 cfu ml^{-1}

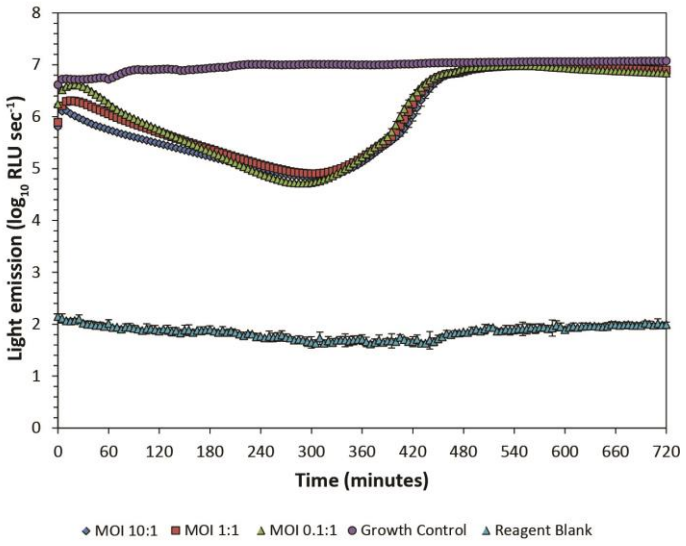

Figure 43. Bioluminescence for *S.* Enteritidis at high density (10^7 cfu ml^{-1}) incubated in the presence and absence of vB_SenS-Ent bacteriophages. Light emission was recorded every 5 minutes for a total duration of 12 hours using an integration time of 1 second. Data points represent the mean and standard deviation from measurements of triplicate wells.

5.3 Discussion

Salmonella serovars Typhimurium and Enteritidis were transformed to stably express a bioluminescent phenotype by expression of plasmid-borne *luxCDABE* operon of *Photorhabdus luminescens*. Light emission showed linear correlation with bacterial cell concentration and growth in batch culture. The limit of detection is three orders of magnitude lower for light emission than for optical density making this reporter system ideal for investigating the effects of bacteriophages at relatively low host cell concentrations. Profiles of light emission over time clearly demarked bacterial lysis in all phage-treated samples, represented by a plateau followed by diminishing bioluminescence intensity. As such, the use of bioluminescent reporter bacteria within a microplate format provides a high-throughput system (up to 96 samples) for the indirect monitoring of bacteriophage mediated lysis. Continuous and automated measurement is maintained throughout the assay time period. Moreover, this approach could be further employed to investigate combinatorial applications of bacteriophages with other antimicrobial agents.

The differences in light emission observed for lysis at different host concentrations appears to be a function of the dilution of host cells and bacteriophages. In simplistic terms, mass action kinetic theory dictates that higher concentrations of phage and bacteria within a fixed volume are more likely to randomly encounter one another, whereas the presence of lower concentrations in the sample volume reduces the probability of these encounters. At low host concentrations, bacteriophages must replicate sufficiently and produce enough progeny virions to reach a critical mass where the number of productive infection events surpasses the rate of bacterial replication. This critical mass of infection is observed in these assays by a plateauing and decline in bioluminescence and has been described as the 'innundation threshold' (Payne and Jansen, 2001). The data presented here suggests that time to this event is function of the initial concentration of bacteriophages added to the sample, at least between multiplicities of 10 and 0.1, which would account for the increasing time delay before the reduction in light emission for the different MOIs.

With the singular exception of vB_SenS-Ent3 incubated with 1 x 10^3 cfu ml^{-1} *S.* Enteritidis at a MOI of 0.01, it is highly notable that for every combination of host and bacteriophage concentration, individual replicates showed evidence of regrowth, as evidenced by increasing light emission after an initial period of suppression and decline. At high host concentrations, every replicate well exhibited regrowth regardless of the multiplicity of infection, a phenomenon reproducible across independent experiments. While the mean value of triplicate wells are presented in graphs, individual wells treated with bacteriophages showed different profiles of light emission, resulting in large variation as shown by error bars depicting standard deviation. Two possible reasons may be presented to explain this variation. Firstly that the concentration of bacteriophages added to wells was not consistent caused either by pipetting errors or by inhomogeneous distribution within dilution tubes. Second,

that wells contained different numbers of cells of *S.* Enteritidis that were or became resistant to infection by the vB_SenS-Ent phages. Numerous studies have highlighted the growth of bacteriophage insensitive mutants (BIMs) after challenge with lytic bacteriophages. A purely lytic phage forces clonal selection and thus acts towards the generation of resistant mutants. In many cases these BIMs have resulted from mutations to the host surface receptor used by the bacteriophage for adsorption and show altered properties in comparison to the parental strain. For example, BIMs resistant to the *Salmonella* phage ϕAB2 and *E. coli* O:157 phages e11/2, e4/1c and pp01 were demonstrated to exhibit a rough phenotype and possess a smaller coccoid shape in comparison to the rod shape of parental strains (Berchieri Jr *et al.,* 1991, O'Flynn *et al.,* 2004). Whilst the characteristics of resistant populations observed after exposure to the vB_SenS-Ent phages were not established, a likely explanation is the conversion to a rough LPS phenotype. Several mechanisms conferring resistance to infection by bacteriophages have been characterised including alteration or blocking of cell surface receptors, DNA restriction-modification, the CRISPR-Cas (clustered regularly interspaced palindromic repeats) system, abortive infection systems and the acquisition of lysogens encoding superinfection immunity or antigen modification systems (Labrie *et al.,* 2010). Parallels have been drawn between the occurrence of phage and antibiotic resistance, specifically with regard to the mutation selection hypothesis (Cairns and Payne, 2008). The mutation selection hypothesis which describes the development of antibiotic resistance in relation to dose concentrations (Zhao and Drlica, 2001). The development of resistance to antimicrobials requires two events; firstly mutations generating resistant mutants and secondly, the presence of a selective pressure allowing for enrichment of the mutant population. In clinical therapy, the susceptibility of a bacterial isolate is established to determine the minimum concentration of antibiotic required to prevent growth of the bacteria at the site of infection, termed the minimum inhibitory concentration or MIC. The mutation selection hypothesis defines a window of selection that ranges from the MIC to a greater concentration, termed the mutation prevention concentration (MPC). Delivery of antibiotic concentrations above the MIC results in suppression of susceptible bacteria but provides a selective pressure for single mutations conferring resistance. For antibiotic concentrations at or above the mutation prevention concentration, multiple mutations are required to confer resistance. Since spontaneous mutations occur at low frequency, between 10^{-6} and 10^{-8}, the probability that an individual cell will incur multiple mutations conferring resistance is greatly decreased.

The interpretation of data from lux^{+} reporters is not trivial, due in part to the complexity of the pathway to light emission and also to the metabolic rate of the bacteria. Differences in the intensity of light emission between different bioluminescent reporters may arise due to plasmid copy number, processes involved in transcription or translation, choice of promoter and the availability of substrates and precursors. While it is well established in the literature that good correlation with viable counts may be achieved within exponential growth of bacterial cultures but that this

correlation is lost upon entry into stationary phase (Koga *et al.,* 2005, Duncan *et al.,* 1994). The extent that expression of the lux genes has upon cell physiology, specifically the metabolic load exerted upon the cell, is unclear. In fact, it is a major assumption that introduction of the *lux* genes have little or no effect upon cell physiology. Chen *et al.,* (2008) have reported alterations to Gram-positive bacterial surface hydrophobicity in luminescent transformants of *Lactobacillus casei* ATCC 11578, *Streptococcus mitis* ATCC 9456 and *Micrococcus luetus* ATCC 15176. Considering that the formation of aldehyde by *luxCDE* is dependent upon endogenous ATP, NADPH and the availability of an appropriate fatty acid substrate, expression of the *lux* operon is likely to represent a metabolic burden upon the recipient cell. Moreover, the utilisation of $FMNH_2$, a part of the electron transport chain, and the requirement for ATP and NADPH for generation of the fatty acid aldehyde suggests a diversion of energy to different components of electron transport systems for the production of luminescence. Similarly, substrates utilised by the *luxCDE* reductase are involved within the critical processes of lipid biosynthesis. However, it is also this requirement for $FMNH_2$, NADPH and ATP that demonstrates that the production of light from recombinant bacteria containing the *lux* genes depends upon an intact and functional intracellular redox potential and herein lays the power of this system as an analytical tool; any physico-chemical or environmental factor that impairs the redox potential or results in alterations to cellular viability leads to a change in light emission. Stewart defines this as the "capacity of cells to supply high energy biochemical intermediates during or after some form of cellular insult" (Stewart, 1990). The application of intact luminescent reporters presents a number of analytical advantages. Firstly, cells present a high and steady signal allowing continuous and non-destructive measurements of a single population. Secondly, light emission may be constitutive or induced, providing a means to measure viability or transcriptional activation of genes and operons. In this capacity the *lux* genes have provided an invaluable tool to microbiologists since the early 1980s, providing flexible, sensitive and non-destructive methods by which to investigate bacterial physiology and transcriptional responses to stimuli. A recent development has extended the application of this system even further, with the announcement that the *lux* operon is expressed and fully functional within mammalian cells after codon optimisation (Close *et al.,* 2010a).

This chapter demonstrates that the *lux* operon may be employed as a rapid, sensitive and non-destructive measure of the effects of lytic bacteriophage upon bacterial populations in batch culture. Moreover, this approach enabled measurement of regrowth of resistant bacterial populations over time. These data suggest that *S.* Enteritidis PT4 is able to acquire resistance to infection by the vB_SenS-Ent phages, an important consideration with regard to the design of biocontrol strategies using these phages. One shortcoming of the data reported here were that titres of bacteria and phages over time were not established. Therefore, the precise levels of bacterial regrowth in terms of colony forming units are not known. Similarly, the concentration of bacteriophage remaining after the initial period of lysis observed, and any decay effects caused by phage loss also remain

undetermined. Future experiments should seek to include such enumerations to provide a secondary measure of growth and loss of bacteria and bacteriophages, however the time-consuming nature of such measurements would reduce throughput.

Chapter 6 Control of *Salmonella* in raw and ready-to-eat foods by the vB_SenS-Ent bacteriophages

6.1 Introduction

The control of *Salmonella* within the food chain is essential for both minimising the risk of illness to consumers and alleviating the detrimental economic effects associated with lost labour productivity, cost of clinical treatment and impact of product recalls and media health scares (Santos *et al.,* 2011a). *Salmonella enterica* serovar Enteritidis remains the most common serovar associated with human gastroenteritis in the UK comprising 30 % of cases, followed by serovars Typhimurium, Newport and Infantis at 25.9, 2.0 and 1.9 %, respectively, from a total of 8,937 isolations in 2011 (Lawes and Kidd, 2011). Over the same period 1,978 incidents were reported within animal husbandry in the UK.

It is now widely accepted that the use of antibiotics in agriculture and animal husbandry has led to an increase in the emergence and dissemination antibiotic resistance amongst food-borne pathogens (Marshall and Levy, 2011). Antibiotics are used with livestock for three main purposes: to provide a prophylactic treatment in order to prevent disease in flocks and herds; for the veterinary treatment of diseased animals; as growth promoters to improve the digestion and utilisation of feed. Due to the association with resistance, the use of antibiotics agents for agricultural purposes has come under increased scrutiny and is subject to a number of restrictions in the EU. However, the same restrictions are not practised internationally. Animal usage still accounts for the majority of antibiotics produced in the USA, estimated to represent 80 % of all produced antibiotics (FDA, 2009).

Antibiotic resistance in the *Salmonella*e is now widespread in developed and undeveloped countries (Rowe *et al.,* 1997, Rowe *et al.,* 1990) and of key concern is the resistance to key antimicrobials such as the flouroquinones (Herikstad *et al.,* 1997), extended spectrum β-lactamases (Vahaboglu *et al.,* 2001) and cephalosporins (Gray *et al.,* 2004). Of particular note has been the emergence and spread of multiple drug resistant strains of *S.* Typhimurium DT104, which now has a worldwide distribution (Helms *et al.,* 2005). The *S.* Typhimurium DT104 pandemic arose in the 1980s with isolates in the UK characterised as resistance type ACSSuT with resistance to ampicillin (A), chloramphenicol (C), streptomycin (S), sulfonamide (Su) and tetracycline (T). This resistance type was found to be chromosomally encoded within *Salmonella* genomic island 1 (Mulvey *et al.,* 2006). The same genomic island has also been identified in other serovars including Agona, Paratyphi B, Albany, Newport and Infantis, suggesting that this genomic island has undergone horizontal gene transfer (Levings *et al.,* 2005). Notably this genomic island confers resistance to four of the five main classes of antimicrobials frequently employed within veterinary medicine: tetracyclines, β-lactams, aminoglycosides and sulphonamides.

The control of pathogens in the food chain is addressed by hazard analysis and the implementation of critical control points in order to minimise the risk of contamination at all stages of production. This HACCP strategy has become known as the "farm to fork" approach. In the EU approaches to the statutory control of zoonoses and zoonotic agents have been harmonised under the European Council Directive 2003/99/EC. The directive outlines bacteriological surveillance of animals, animal feeds, foods, human infections in addition to antimicrobial resistance in *Salmonella* and other foodborne pathogens such as *Campylobacter spp.* The poultry industry represents the only food animal production sector in the UK that has a structured bacteriological surveillance programme for *Salmonella* due to imposed statutory testing requirements (Lawes and Kidd, 2011).

The *Salmonella*e appear to be unsuitable targets for clinical phage therapy in humans for two reasons. Firstly, infections by non-typhoidal *Salmonella* serovars are generally self-limiting and are managed by supportive therapy. Secondly, a trait of typhoidal and some other serovars is the intracellular invasion of cells of the host immune system. This tactic of immune evasion renders intracellular *Salmonella* resistant to infection by bacteriophages. However, bacteriophages infecting *Salmonella* can be employed at different stages of the production and processing of food products. This concept of using bacteriophages for the specific targeting of bacterial pathogens in foods is not new and a number of reviews have been published on the subject (Rees and Dodd, 2006b, Hagens and Loessner, 2010, Mahony *et al.,* 2010, Stone, 2002, Sulakvelidze and Barrow, 2004). Bacteriophages represent an attractive alternative to conventional methods for the control of foodborne pathogens. Phages are highly specific for their target host, and unlike antibiotics, host specificity does not usually cross species boundaries. Infection with lytic phages results in lysis and death of host cells with a concurrent increase in the number of bacteriophages, representing a process of site specific replication. Finally, phages are highly abundant in the environment and are easily isolated using standard methods. Two broad areas are identified for intervention strategies using bacteriophages; pre-harvest and post-harvest (Hagens and Loessner, 2010). In the first instance, phages may be used to reduce intestinal colonization of live, agriculturally important animals that act as reservoirs for foodborne pathogens. In the second instance, phages may be applied directly onto carcasses during slaughter, onto raw and ready-to-eat foods, or upon environmental surfaces used in food processing.

It is clear that virulent or obligatory lytic phages are a prerequisite for biocontrol applications. Phages with this lifestyle lack the array of genetic factors required for integration of the viral genome into the bacterial chromosome and infection. Disregarding the presence of host- and prophage-encoded immunity systems, infection with lytic phages always leads to lysis and death of the host cell. In contrast, many temperate phages have been shown to carry toxins, effector proteins or regulatory factors that play a role in the development of host pathogenicity (Allison, 2007, Canchaya *et al.,*

2003a, Brussow *et al.,* 2004). Similarly, phages which exhibit generalised transduction, that is where host DNA is packaged into a functionally viable virion, should be avoided due to the potential for horizontal transfer of new genes into target hosts. Hagens and Loessner (2010) outline several properties that are desirable or prerequisite for phages to be employed as biocontrol agents. Absolute requirements, in addition to those described above, include genome sequencing and stability studies encompassing storage, thermal stability and pH tolerance. Desirable properties include the ability to propagate the phage on a non-pathogenic host and evidence that preparations exhibit no toxicity in animal feeding studies. Of late, several bacteriophage-based products have gained accreditation from the US Food and Drug Administration for use as food additives. The *Listeria* bacteriophage preparation ListShield (www.intralytix.com), consisting of a cocktail of 6 bacteriophages, was approved in 2006 for use with ready to eat foods (Bren, 2007, Hagens and Loessner, 2010). Similar products for *Listeria*, *Salmonella*, *E. coli* O157 and plant pathovars of *Pseudomonas putida* are available (www.micreos.com, www.omnilytics.com).

Several studies have been published that investigate the efficacy of bacteriophage preparations upon the control and removal of *Salmonella* from animal hosts and food produce destined for human consumption. The use of bacteriophages to reduce colonisation of livestock by *Salmonella* has been investigated in pigs and poultry, applied by oral ingestion of water and feed or by aerosol dispersal. In order to be effective, orally administered bacteriophages must be able to survive transit through the acidic environment of the gastric fluid in order to reach the digestive tract. This requires either the selection of bacteriophages with known acid-tolerance or encapsulation of the virions in a protective material. For example, phages ST104a and Felix O1 exhibited good tolerance to porcine gastric juice adjusted to pH 2.5 over 120 minutes while, conversely, phage ST104b could not be detected by plaque assay after only 30 minutes exposure to this environment (O'Flynn *et al.,* 2006). Clearly different phages show different tolerances to pH and temperature. Encapsulation of Felix O1 within chitosan-alginate microspheres has been demonstrated to aid survival of this phage from exposure to gastric fluid, presenting a method for the improved delivery of bacteriophages to the digestive tract of livestock animals (Ma *et al.,* 2008, Saez *et al.,* 2011). A microencapsulated phage cocktail provided with feed or by gavage was shown to reduce concentrations of *S.* Typhimurium in swine ileal and caecal contents compared to a control group, although this effect was only determined at 6 hours after the bacterial challenge (Saez *et al.,* 2011).

Much focus has been placed on the control of *Salmonella* in the breeding and raising of poultry destined for meat production. Treatment with bacteriophages by aerosol or oral application has been shown to reduce levels of colonisation of broiler chickens by *S.* Enteritidis (Borie *et al.,* 2008, Borie *et al.,* 2009, Fiorentin *et al.,* 2005). Oral application of the phage ϕSG-JL2 showed significant protective effects when applied orally prior to inoculation of broiler chickens with *S.* Gallinarum, the

causative agent of fowl typhoid (Kwon *et al.,* 2008). Another Gallinarum specific bacteriophage curtailed the rate of horizontal transmission from infected birds to a contact group treated with the phage before and during the contact period (Lim *et al.,* 2011). In a similar study, the phage ϕCJ07 resulted in a reduction in bacterial burden of *S.* Enteritidis for infected birds and frequency of horizontal transfer to contact birds (Lim *et al.,* 2012). Treatment of chicks inoculated with *S.* Enteritidis with the phages CB4ϕ and WT45ϕ resulted in a reduction in viable bacteria recovered from caecal tonsils at 24h. However, this reduction was transient and after 48 hours no significant difference was observed relative to untreated controls (Andreatti Filho *et al.,* 2007).

A variety of different food types have been used in phage biocontrol studies including raw and cooked meats, eggs, fresh fruit, cheese, and sprouting seeds (Goode *et al.,* 2003, Leverentz *et al.,* 2001, Modi *et al.,* 2001, Pao *et al.,* 2004, Whichard *et al.,* 2003, Guenther *et al.,* 2012). The contamination of ready to eat foods by *Salmonella* represents a major hazard as these food types are not subject to the sterilising effects of cooking prior to consumption. The broad host range myovirus Felix O1 was shown to suppress growth of *S.* Typhimurium DT104 in broth and frankfurter sausages, resulting in a 2 $\log_{10}$ suppression of growth compared to bacteria incubated in the absence of this bacteriophage (Whichard *et al.,* 2003). Similarly, Felix O1-E2, a variant possessing a 2 kb deletion, reduced viable numbers of *Salmonella* in turkey deli meat, chocolate milk, hot dogs, egg yolk and seafood at 8^{o}C and retarded growth at 15^{o}C (Guenther *et al.,* 2012). However, the same study highlighted the recovery of *Salmonella* from foods which had developed resistance to infection by this phage after 6 days incubation at 15^{o}C. Phages P22 and 29C were shown to elicit up to a 2 $\log_{10}$ reduction in recoverable numbers of *S.* Enteritidis over 48 hours when phages were added at MOIs of >100 to chicken skin (Goode *et al.,* 2003). However, P22 is both lysogenic and a generalised transducer, precluding the use of this phage within a commercial context. Hooten *et al.,* (2011b) investigated the application of a cocktail comprising three bacteriophages, ϕSH17, ϕSH18 and ϕSH19 upon pig skin artificially contaminated with *S.* Typhimurium. Addition of this phage cocktail, containing a combined concentration of 10^{8} pfu ml^{-1}, resulted in significant reductions of *Salmonella* when the MOI was in excess of 10. Reductions have also been reported for bacteriophage treated broiler caracasses and carcass rinse water (Higgins *et al.,* 2005)

In this chapter, the positive action of bacteriophages in reducing numbers of contaminating *Salmonella* in foods appears to occur when bacteriophages are added to excess, that is, at a high multiplicity of infection. Bigwood *et al.,* (2009) investigated the inactivation of *S.* Typhimurium by phage P7 as a function of MOI and host concentration and suggest that lysis from without may represent the predominant decontamination effect. Payne and Jansen (2001) outline the activity of bacteriophages in biocontrol applications as a density dependant kinetic process and define the action of bacteriophages as passive or active. Passive therapy is defined as a net reduction in

bacterial numbers caused by high concentrations of bacteriophages resulting in lysis from without and no increase in phage population. Active therapy is defined as where the bacteriophages actively replicate and the subsequent infection of bacteria by progeny virions outweighs the rate of phage decay.

In this chapter, the application of three closely related individual bacteriophages vB_SenS-Ent1, -Ent2 and -Ent3 and their effect at high MOI upon viable numbers of *Salmonella* artificially spiked food matrices are reported. Additionally, in order to ascertain the suitability of these phages for biocontrol applications, the stability over long term storage and upon exposure to different temperatures was established.

6.2 Results

6.2.1 Long term storage of bacteriophages

Each of the vB_SenS-Ent phages exhibited a slow decline in infectious titre over a 12 month period (Figure 44). After purification by CsCl density gradient centrifugation, the starting titres for each phage were approximately 5 x 10^{12} pfu ml^{-1}. Ent1 showed the greatest decrease in titre, representing a 1.91 log reduction, though recorded titres showed variability after 8 months. One possibility accounting for the observed variation might be the aggregation of virion particles which were not fully dispersed by mixing prior to titration. Decreases in titre were less pronounced for Ent2 and Ent3, which exhibited reductions of 1.21 and 0.37 log_{10} pfu ml^{-1}, respectively.

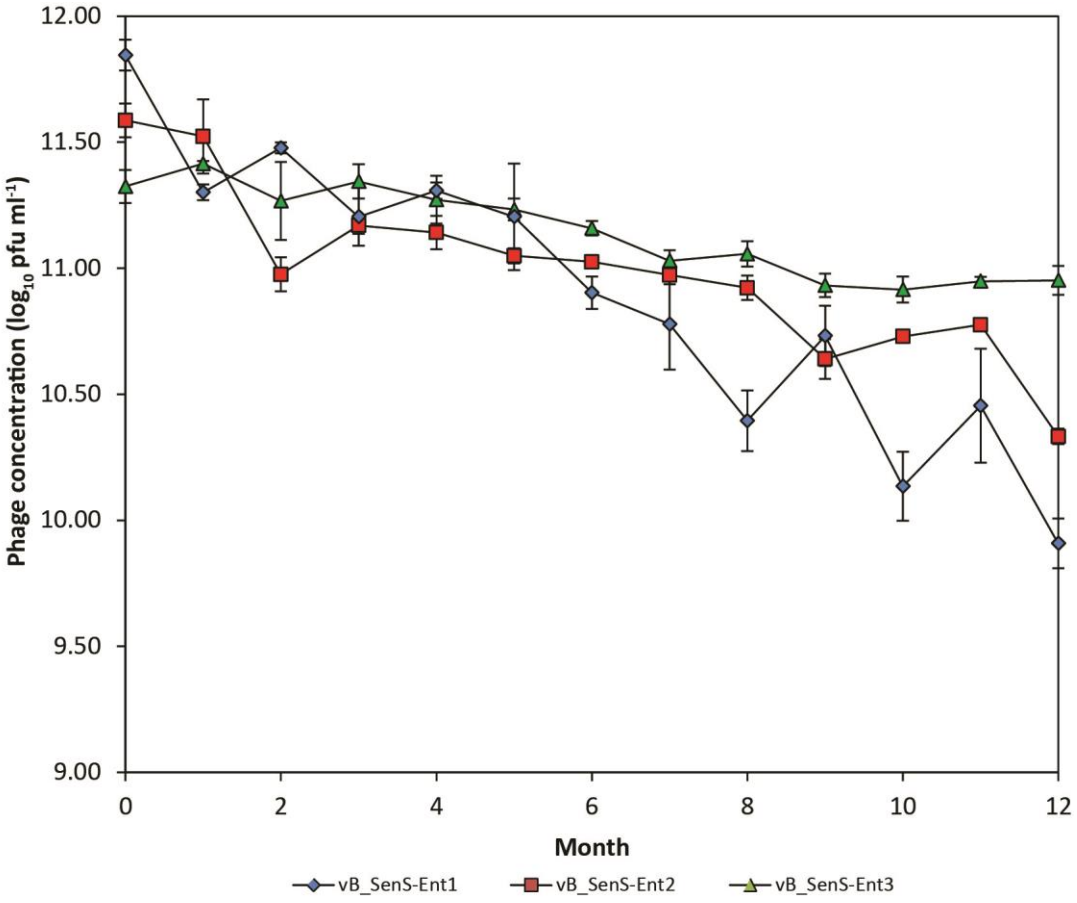

Figure 44. Stability of bacteriophage titres stored at 4°C in SM buffer over a 12 month period measured by overlay plaque assay. Data points represent weighted mean of triplicate counts for two consecutive dilutions.

6.2.2 Thermostability of bacteriophages

Each of the vB_SenS-Ent phages showed identical thermal tolerance profiles. Titres were unaffected by incubation at temperatures of 50 and 60°C. At 70°C a 5 log_{10} reduction in infective titre was observed after 120 minutes.

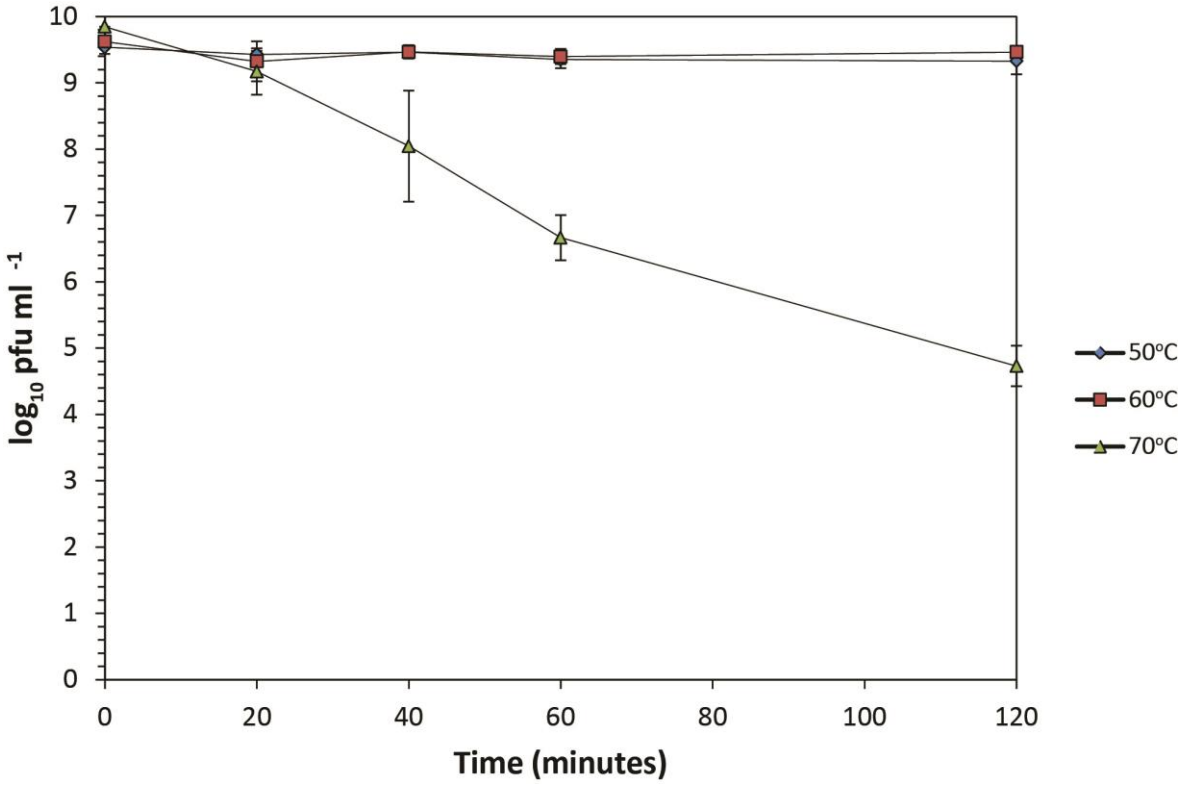

Figure 45. Thermal stability profile for vB_SenS-Ent1. Data presented are the mean and standard deviation of replicates (n=3) from three independent experiments.

6.2.3 Stability of *lux* plasmid retention by *Salmonella* at 4°C

Resuspended pellets of *S*. Enteritidis PT4 LITE stored at 4°C in PBS buffer were enumerated at daily intervals by plating diluted samples onto LB agar with and without the plasmid selective agent, kanamycin (10 µg ml^{-1}). No significant decline in cell numbers was observed over the 7 day period. The examination of both plate types by bioluminescence imaging did not identify any non-bioluminescent colonies nor was the relative emission diminished for colonies on non-selective agar.

6.2.4 Inoculation and recovery of bacteriophages and bacteria

Salmonella present on spiked matrices were recovered using two selective media from log-fold dilutions of sample homogenates prepared using a stomacher. LB agar, supplemented with 10 µg ml^{-1} kanamycin, was employed to suppress growth of the endogenous microflora native to the food matrix and to actively select for *S.* Enteritidis harbouring the lux plasmid. The second media, Xylose-Lysine-Desoxylcholate agar (XLD) is commonly used within the international standard horizontal culture method for the qualitative detection of *Salmonella* in food matrices, ISO 6579 (2002). Colonies of *Salmonella* are differentiated on the basis of their ability to ferment xylose, decarboxylate lysine and produce hydrogen sulphide, appearing on this medium as red colonies with back centres (Figure 46).

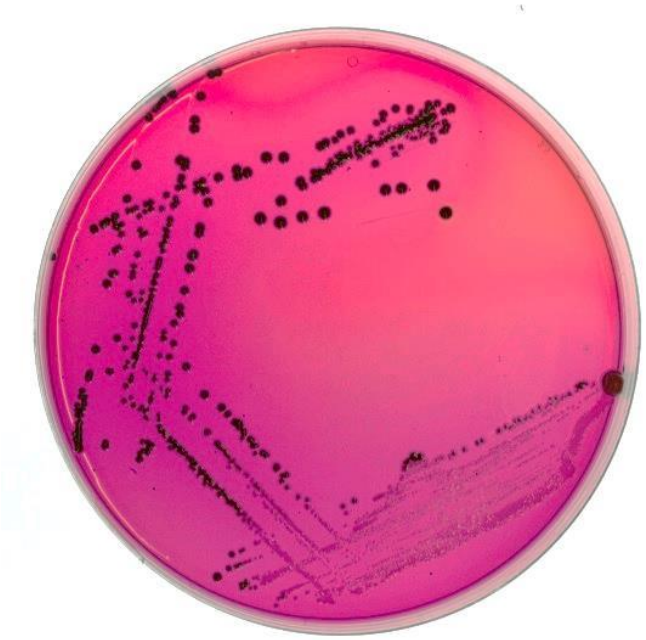

Figure 46. Typical colonies of *Salmonella* Enteritidis PT4 grown on XLD agar. Growth of *Salmonella* on this agar results in the decarboxylation of lysine and increased alkalinity, shown as a change in medium colour surrounding colonies by the indicator phenol red. The black colouration of colonies arises from the production of hydrogen sulphide.

To further aid in the identification of *Salmonella* colonies on solid media, each agar plate was examined using an EMCCD camera to detect bioluminescent colonies (Figure 47).

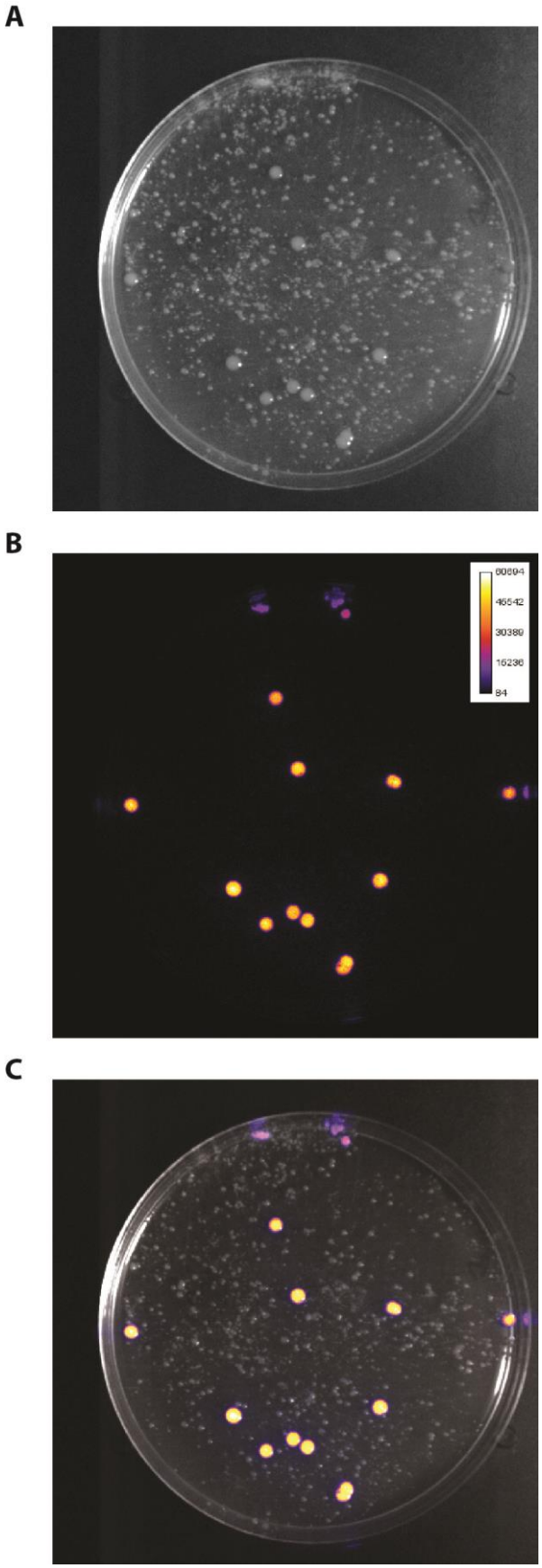

Figure 47. Example of identification of bioluminescent *S.* Enteritidis in mixed cultures recovered from fresh mixed salad on plate count agar supplemented with 10 ug ml^{-1} kanamycin. A) light photography and B) bioluminescence imaging. C) Merged light and bioluminescence images demonstrating the location of colonies of bioluminescent *S*. Enteritidis PT4.

The detection limit of the recovery method used here is dependant firstly upon the requirement to dilute and homogenise the solid sample matrix and, secondly, upon the volume used for plating. Two plating volumes, 1.0 and 0.5 ml were used, representing detection limits of 10 and 20 cfu g^{-1}, respectively, after a 10-fold dilution of the sample matrix. Bacteriophages were enumerated from log-fold dilutions of the sample matrix homogenate using the standard overlay plaque titration method, but employed media containing kanamycin as a selective agent. Counts of bacteria and bacteriophages are presented as the weighted mean calculated from triplicate plates from two consecutive dilutions.

6.2.5 Food Matrix 1 – Bean sprouts

Control series of *S.* Enteritidis inoculated onto fresh bean sprouts in the absence of bacteriophages exhibited a consistent decline in numbers of colony forming units recovered over the experimental period (Figure 48). In contrast, relatively stable titres were recovered from control series of the vB_SenS-Ent phages after addition and storage in this food matrix. Bacterial concentrations similar to the predicted spike density of 1.15 x 10^3 cfu ml^{-1} were recovered from food samples prior to the addition of bacteriophages. After the addition of bacteriophages and storage for 24 hours, no *Salmonella* colonies were recovered above the assay detection limit, representing nearly a 2 $\log_{10}$ reduction in phage treated samples in comparison to the untreated control. No further counts of *Salmonella* were obtained from samples performed on consecutive days.

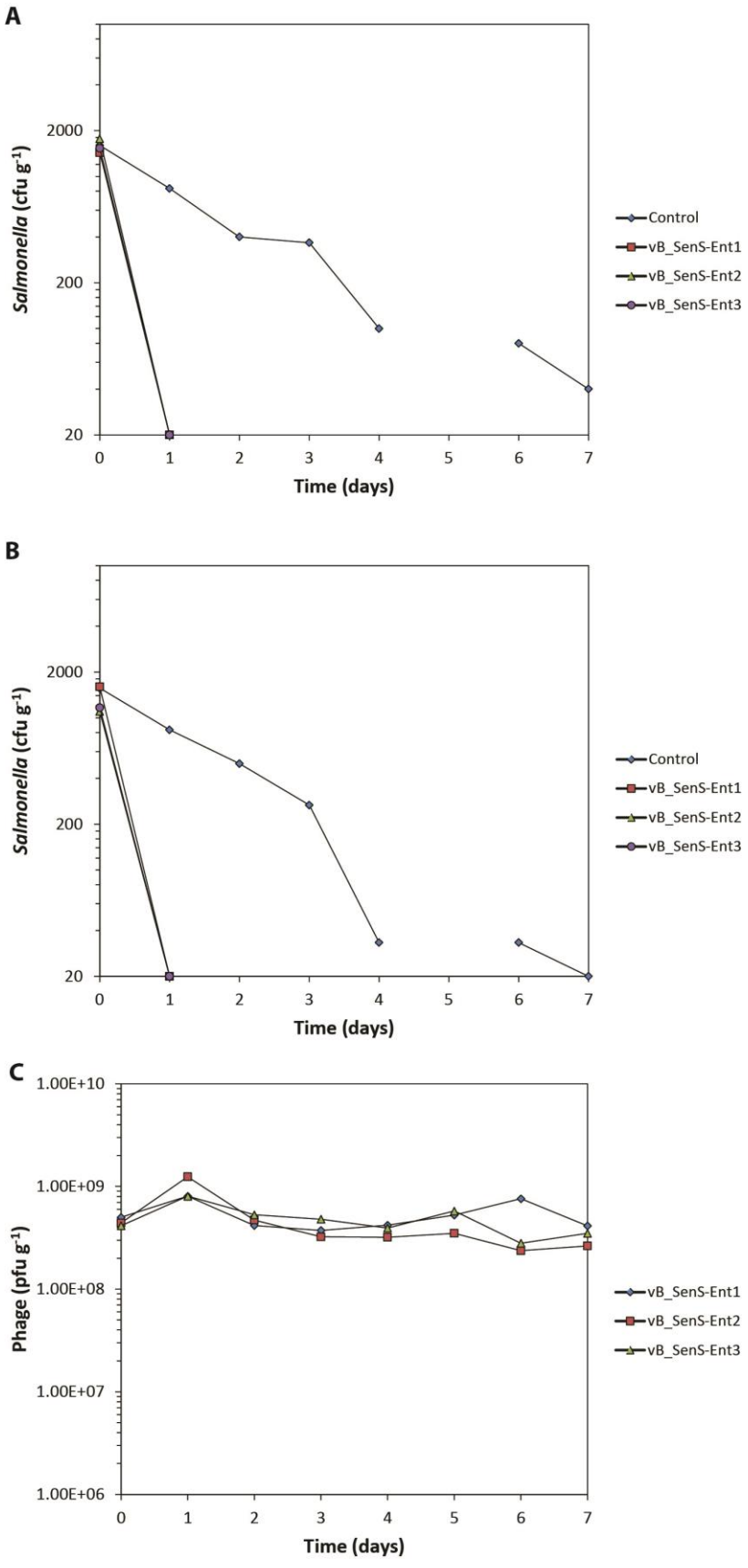

Figure 48. Recovery of *Salmonella* Enteritidis and bacteriophages from artificially contaminated raw beansprouts. Bacterial concentrations recovered using A) LB agar supplemented with kanamycin and B) XLD. C) Concentration of bacteriophage recovered as pfu g^{-1}. The y-axis is limited to 20 cfu g^{-1} to reflect the limit of detection imposed by sampling.

6.2.6 Food Matrix 2 – Mixed salad

During this period, control stability series of the vB_SenS-Ent phages added to mixed salad in the absence of *S.* Enteritidis appeared to show declining titres, representing losses of between 1 and 1.5 log_{10} pfu ml^{-1} over 7 days (Figure 49). No *Salmonella* were recovered from samples after treatment with bacteriophages on days 1 and 2. However, on day 3, colonies of *S.* Enteritidis were again recovered from all phage-treated samples. For vB_SenS-Ent1, *S.* Enteritidis was recovered on days 3 through 6 but not on day 7. For samples treated with vB_SenS-Ent2, *S. Enteritidis* was recovered on days 3 through 7, while for vB_SenS-Ent3, colonies recovered on days 3, 4, 6 and 7. These data might suggest that food samples were improperly mixed upon addition of bacteriophages meaning that some bacteria would not come into contact with bacteriophages or alternatively, may indicate a problem with the sampling method employed.

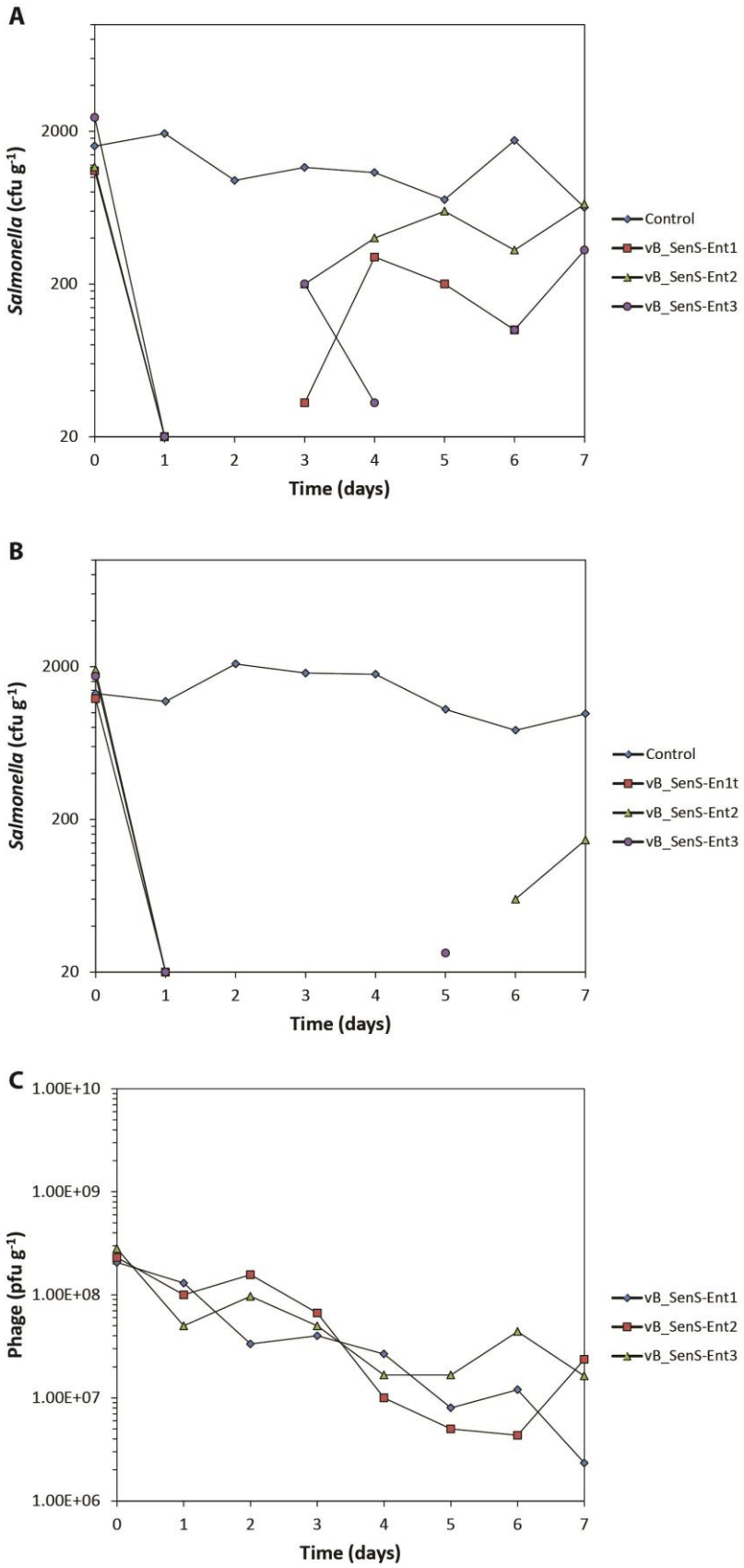

Figure 49. Recovery of *Salmonella* Enteritidis and bacteriophages from artificially contaminated mixed salad leaves. Bacterial concentrations recovered using A) LB agar supplemented with kanamycin and B) XLD. C) Concentration of bacteriophage recovered as pfu g^{-1}. The y-axis is limited to 20 cfu g^{-1} to reflect the limit of detection imposed by sampling.

6.2.7 Food Matrix 3 – Cooked skinless chicken breast

Numbers of *S.* Enteritidis and bacteriophages recovered from skinless cooked chicken breast remained relatively stable for the experimental duration (Figure 50). Similar to trials performed using other food types, plating onto XLD exhibited a lower overall recovery of *Salmonella* than for LB agar supplemented with kanamycin. No colonies of *S.* Enteritidis were recovered above the assay detection limit within 24 hours after the addition of bacteriophages, representing a decline of 2 $\log_{10}$ cfu ml^{-1}.

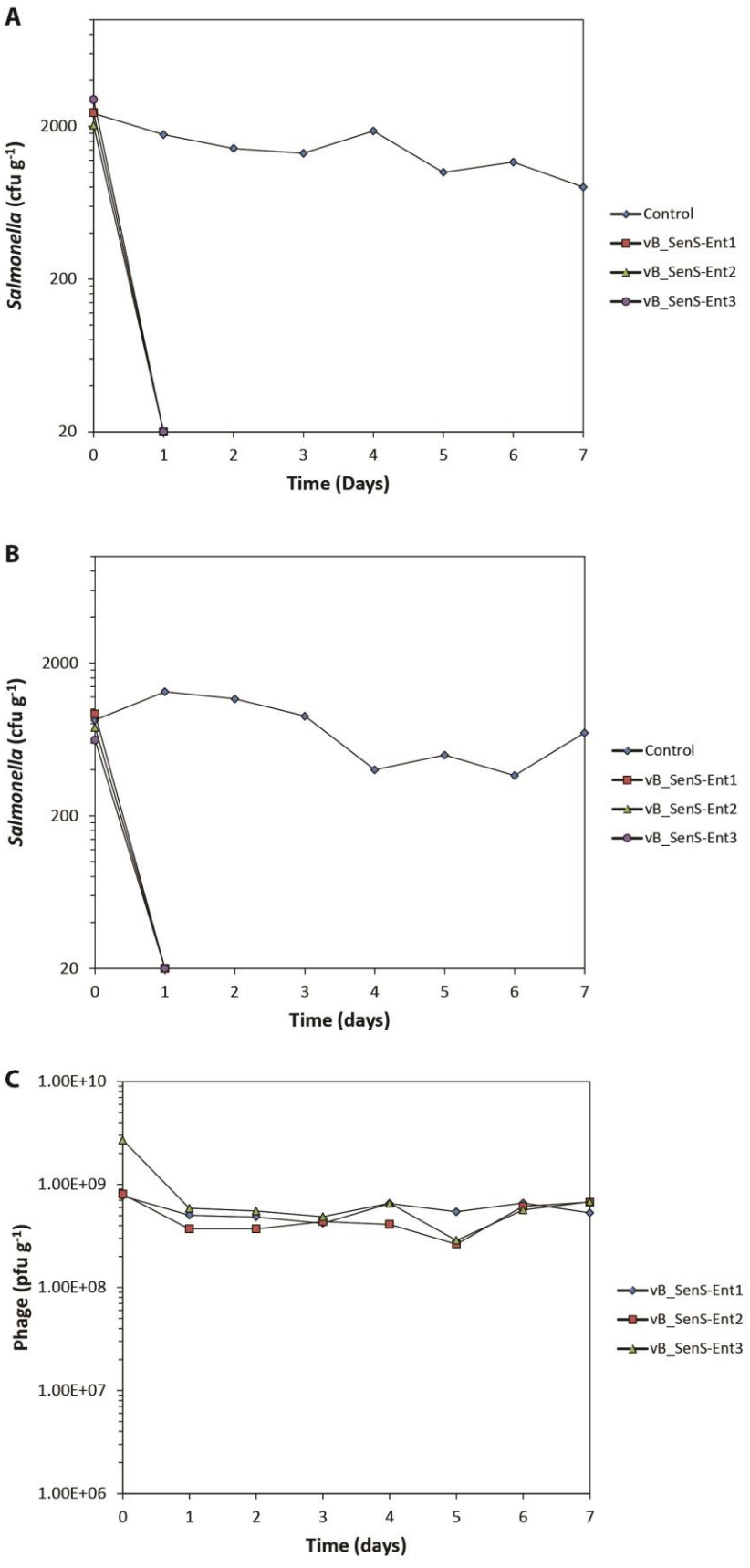

Figure 50. Recovery of *Salmonella* Enteritidis and bacteriophages from artificially contaminated cooked chicken breast. Bacterial concentrations recovered using A) LB agar supplemented with kanamycin and B) XLD. C) Concentration of bacteriophage recovered as pfu g^{-1}. The y-axis is limited to 20 cfu g^{-1} to reflect the limit of detection imposed by sampling.

6.2.8 Food Matrix 4 – Raw skinless chicken breast

Controls series demonstrated that numbers of *S.* Enteritidis stored in the absence of bacteriophages remained stable and that each of the vB_SenS-Ent bacteriophages retained the ability to infect host cells over 7 days in raw skinless chicken breasts (Figure 51). The reduction in *S.* Enteritidis appeared to occur in an identical manner to that observed for beansprouts and cooked chicken with no colonies recovered after 24 hours incubation at $4^{o}C$, representing a 1.75 $\log_{10}$ reduction from the calculated spike of 1.13×10^{3} cfu g^{-1}.

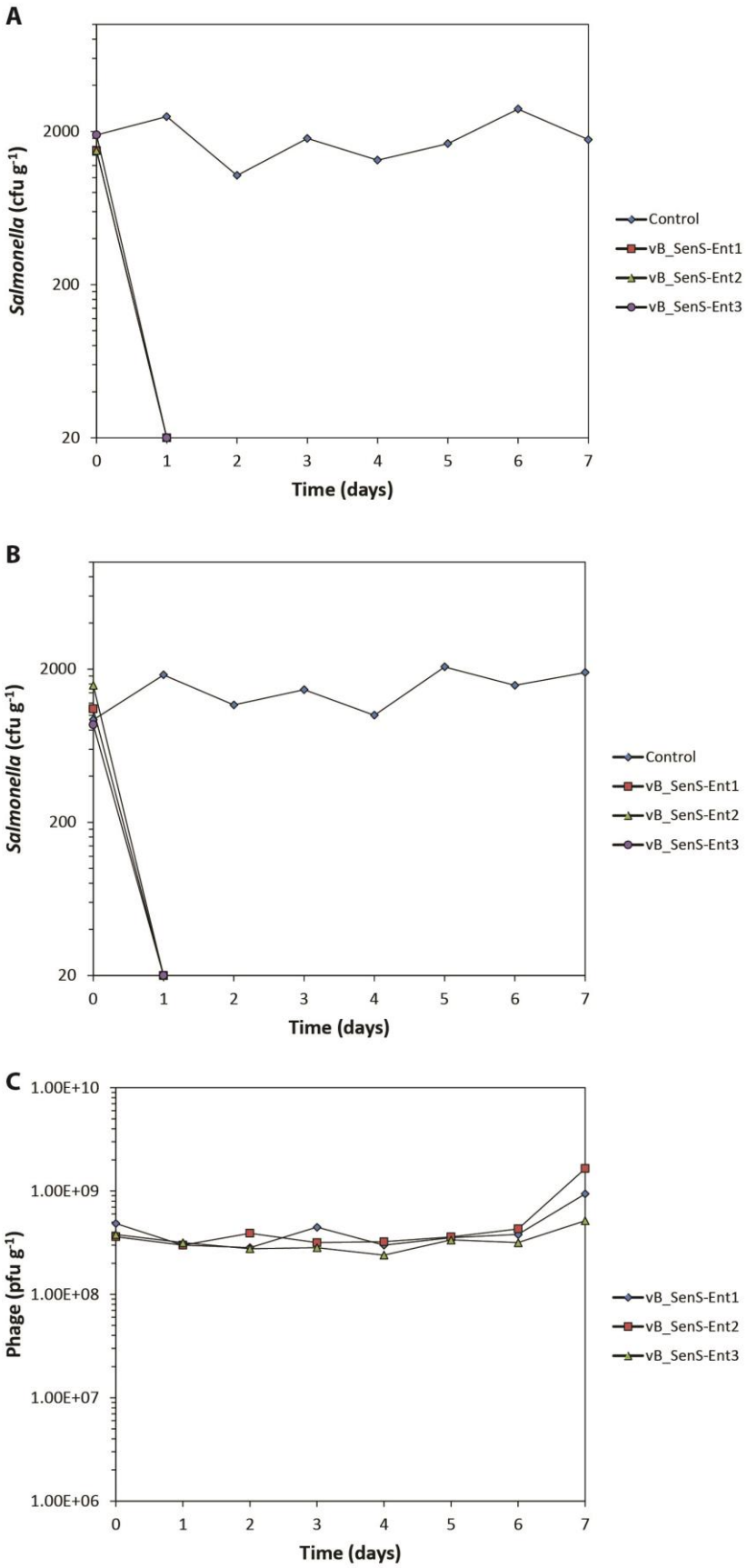

Figure 51. Recovery of *Salmonella* Enteritidis and bacteriophages from artificially contaminated raw chicken breast. Bacterial concentrations recovered using A) LB agar supplemented with kanamycin and B) XLD. C) Concentration of bacteriophage recovered as pfu g^{-1}. The y-axis is limited to 20 cfu g^{-1} to reflect the limit of detection imposed by sampling.

6.3 Discussion

The bacteriophages vB_SenS-Ent1, vB_SenS-Ent2 and vB_SenS-Ent3 show promise as putative biocontrol agents for *Salmonella* contaminating raw and ready to eat food matrices. With the exception of mixed salad leaves, the application of each bacteriophage elicited up to a 2 $\log_{10}$ reduction in viable bacteria within 24 hours at an incubation temperature of 4^{o}C. Due to the high nucleotide and protein similarity of the vB_SenS-Ent phages it was decided to investigate each bacteriophage individually rather than as a mixed cocktail. However, considering that the host range of these phages is limited to *Salmonella* serogroups A, B, and D1 the inclusion of additional phages in any treatment formulation would be required to extend coverage to other serogroups.

In food matrices other than mixed salad leaves, the reduction in *Salmonella* by the vB_SenS-Ent phages mirror the observations of Guenther *et al.,* (2012) who monitored reductions in foods of *S.* Typhimurium after challenge with the lytic Myovirus Felix O1-E2. Similarly this study demonstrated no significant losses in phage infectivity for storage with different food matrices. At an incubation temperature of 8^{o}C, Felix O1-E2 reduced counts of *S.* Typhimurium by 3 $\log_{10}$ cfu g^{-1} to below the detection limit within 24 hours. However, at 15^{o}C bacterial counts reduced by 2 $\log_{10}$ cfu g^{-1} over an initial period of two days prior to exhibiting recovery, although to levels below that of untreated control samples. As for other studies, the authors report the occurrence of bacteriophage-insensitive mutants after 6 days incubation. Pure cultures of *Salmonella* Enteritidis show evidence of the development of resistance to the vB_SenS-Ent phages in both semi-solid and liquid media, hence it cannot be discounted that similarly resistant mutants could arise in food matrices. However, the detection of such mutants is made difficult by conventional culture methods which show at best an inherent limit of detection of 10 cfu g^{-1}. Additionally, the low storage temperature used in this study effectively inhibits growth of these bacteria (Smith, 1985). It would be interesting to determine the effect of a 4^{o}C incubation temperature upon bacteriophage replication under one-step growth conditions. Considering that growth of *Salmonella* under these conditions is greatly reduced or halted, it is likely that the phage replication cycle would be either considerably extended or, alternatively, not begin to proceed until there is an increase in ambient temperature allowing the commencement of bacterial growth. For these reasons, a particularly high multiplicity of infection of bacteriophages to bacteria was employed, approximately 10,000:1. The presence of high concentrations of bacteriophages serves to ensure appropriate distribution and coverage of the food matrix but may also lead to 'lysis from without' (Abedon, 2011b). Lysis from without is a phenomenon whereby the sheer number of infecting bacteriophages attaching to the bacterial cell surface results in destabilisation of the cell membrane leading to osmotic disruption and ultimately, lysis. Distinct from lysis from without is that high multiplicities of infection may also render the cell incapable of producing functional progeny due to overwhelming numbers of phage competing for the same cellular machinery (Molineux, 2006). In both scenarios the bacteriophage infection is

unproductive, in that the cell is lysed prior to an infecting bacteriophage being able to replicate its genome and form progeny virion particles. The reduction in viable numbers of *Salmonella* observed here occurs within the first 24 hours and might suggest that unproductive infection is the predominant killing mechanism in the study reported here. As such, it would be of interest to establish the kill kinetics of *Salmonella* by these bacteriophages over the first 12 or 24 hours of incubation and determine whether there is any increase in phage titre during this period. Establishing whether or not phage titre alters could elucidate whether the action of the vB_SenS-Ent phages is active or passive, that is whether the killing effect occurs with or without phage replication.

The use of constitutively bioluminescent bacteria allowed for rapid and simple quantification of target species within mixed cultures composed of microflora endogenous to the food matrix being tested and the spike isolate. The *lux* system provides the benefits of a dual marker system. Firstly, the presence of the antibiotic resistance marker allows for selection of cell recovery whilst inhibiting susceptible background flora. Secondly, light emission allows the identification of colonies within mixed cultures on agar plates with the use of EMCCD cameras or equivalent technologies. Unfortunately, the selected spike concentration was below the limit of detection using the EMCCD camera system, otherwise it would have been interesting to follow kill kinetics of the bacteriophages directly *in situ*. This type of approach has been employed to assess the effects of heat inactivation and recovery of *Salmonella* Typhimurium DT104 inoculated at high cell densities upon the surface of a range of food matrices (Lewis *et al.,* 2006b). Additionally, whilst *S.* Enteritidis PT4 LITE showed good plasmid stability over 7 days at 4^{o}C in the absence of selective antibiotics, it does not preclude the possibility that some plasmid loss may occur in the competitive environment of the food matrix.

However, the data presented here shows only one independent trial per food matrix. Whilst some of the variations observed for enumerations may be the result of heterogeneous distribution of phages and bacteria in the sample matrix, additional trials are required to confirm and consolidate the results presented here. In hindsight, the methodology could be further improved upon by the use of larger diameter Petri dishes for plating, facilitating the plating of sample volumes 1 ml or greater. Secondly, additional data could be provided by performing a paired analysis using the standard ISO methodology, which would provide a qualitative gold standard indicating the presence or absence of *Salmonella* at each sampling time.

Chapter 7 Bioluminescence Imaging of Bacteriophage Plaque Expansion

7.1 Introduction

Over 75 years after its introduction the overlay agar plaque assay, accredited to Gratia, continues to constitute a primary technique within the research of bacteriophages (Adams, 1959). The method is used for titration, the identification of bacteriophage isolates from environmental sources, to investigate physiological characteristics such as adsorption, burst size and host range, and to test for phage viability. Plaques are defined as localised, visible zones of clearing within otherwise confluent bacterial lawns that arise after a primary adsorption and productive infection event that initiates the focal infective centre (Koch, 1964).

Phage population expansion following the primary infection event is mediated by multiple rounds of adsorption to individual bacteria. The release of progeny particles with lysis of individual host cells acts to offset diffusion mediated declines in local phage particle densities, and population growth continues so long as sufficient quantities of susceptible bacteria are present. Thus, the expansion of plaques may be envisioned as a travelling wave of infection that moves radially outwards in three dimensions from the focal infective centre, leaving lysed, resistant or shielded bacterial cells in its wake (Abedon and Yin, 2008, Rabinovitch *et al.,* 2003). Several theoretical models that seek to describe this travelling wave of infection by reaction-diffusion mechanisms have been presented (Koch, 1964, Kaplan *et al.,* 1981, John, 1991, Yin and McCaskill, 1992, Yin, 1994, You and Yin, 1999, Fort and Méndez, 2002, Ortega-Cejas *et al.,* 2004). These models have been summarised in comprehensive reviews by Abedon and co-workers (Abedon and Culler, 2007b, Abedon and Culler, 2007a, Abedon and Yin, 2008, Abedon and Yin, 2009, Krone and Abedon, 2008).

Since environmental mixing, virion diffusion, and host-cell mobility are more limited in solid than for liquid media, the formation of plaques in agar overlays provides a useful, simple and cost effective *in vitro* model for the approximation of the localised infection, expansion and spread of bacteriophage populations within semi-structured environments, such as biofilms (Abedon and Yin, 2009, Gallet *et al.,* 2009, Abedon, 2011a, Abedon and Thomas-Abedon, 2010, Jouenne *et al.,* 1994). As the formation and enlargement of plaques is a spatial process, empirical assessment requires visualisation and localisation of bacteriophages, intact bacteria, or bacterial lysis.

Classically, visual assessment of the reduction in turbidity of the bacterial lawn has been used to delineate the plaque. A number of hours must elapse before the bacterial lawn becomes visible to the naked eye, which precludes accurate measurements at the initial and early stages of plaque formation. Recent methods of recording plaque enlargement kinetics have comprised automated measurements using time-lapse photography and fluorescence microscopy (Alvarez *et al.,* 2007, Lee

and Yin, 1996b). An imaging modality not explored within the literature is bioluminescence imaging (BLI). Over the past decade reports detailing the use of BLI have increased significantly due to technological advancements, resulting in the widespread commercial availability of highly sensitive, intensified and electron multiplying CCD image acquisition systems. BLI has predominantly found use within the study of bacterial pathogenesis *in vivo* due, in part, because it allows non-invasive longitudinal monitoring and visualisation of individual test subjects. For bacterial pathogens, BLI has been employed to follow localisation and dissemination *in vivo* and for the quantification of antibiotic pharmacodynamics (Rocchetta *et al.*, 2001, Contag, 2008, Kadurugamuwa and Francis, 2008, Sanz *et al.*, 2008b).

The requirement of the light-emitting reaction for ATP, NADPH and $FMNH_2$ means that the ability of a cell to emit light is dependent upon an intact intracellular redox potential. Any physico-chemical factor affecting bacterial metabolism results in an alteration in relative light emission, presenting a rapid, sensitive and non-destructive means of monitoring bacterial cell metabolic viability. These characteristics have led to the widespread use of bioluminescent reporter bacteria across a range of applications including studies upon the pharmacodynamics of antibiotics, biocide kill kinetics, biofilm models and the design of biosensors for the detection and quantification of environmental pollutants (Ulitzur, 1986, Ben-Israel *et al.,* 1998, Alloush *et al.,* 2003, Ulitzur and Ulitzur, 2006, Kadurugamuwa and Francis, 2008, Robinson *et al.,* 2011). Bacteria transformed to constitutively express the *lux* operon thus present a means to study the effects of co-incubation of lytic bacteriophages or recombinant bacteriophage proteins, such as lysins, with bacterial populations in broth, semi-solid media or associated with solid substrata as biofilms.

The aim of this study was to employ bioluminescent bacterial reporters to investigate the effects of co-incubation of bacteria and bacteriophages under conditions of plaque formation. Experimental objectives included the transformation of *Salmonella enterica* serovars Dublin and Enteritidis, used as the propagating hosts of the myovirus Felix O1 and siphovirus vB_SenS-Ent1 respectively, to constitutively express the *luxCDABE* operon of *Photorhabdus luminescens*. Secondly, these bioluminescent serovars were utilised in conjunction with an EMCCD imaging system to record plaque formation in agar overlays. Lastly, an image processing workflow was developed, based on that reported by Lee and Yin (1996b), to allow quantification of plaque expansion and to provide descriptions of plaque morphology in relation to light emission from host cells.

7.2 Results

7.2.1 Calibration of cell density and light emission

Serovars *S.* Enteritidis PT4 and *S.* Dublin were successfully transformed to stably express a bioluminescent phenotype. For calibration curves, the detection limit (LOD) was defined as 3 standard deviations of the reagent blank control and the limit of quantification (LOQ) as 10 standard deviations of the reagent blank control. Light emission of log-fold dilutions of bacteria immobilised in overlay agar within microtitre plate wells showed strong correlation with colony forming units (R^2 > 0.95), affording a detection limit of approximately 1 x 10^3 cfu per well for *S.* Dublin and *S.* Enteritidis, respectively (Figure 52). The dynamic range of detection was reduced using BLI and detection limits were 1 x 10^4 cfu per well for *S.* Dublin and *S.* Enteritidis, respectively.

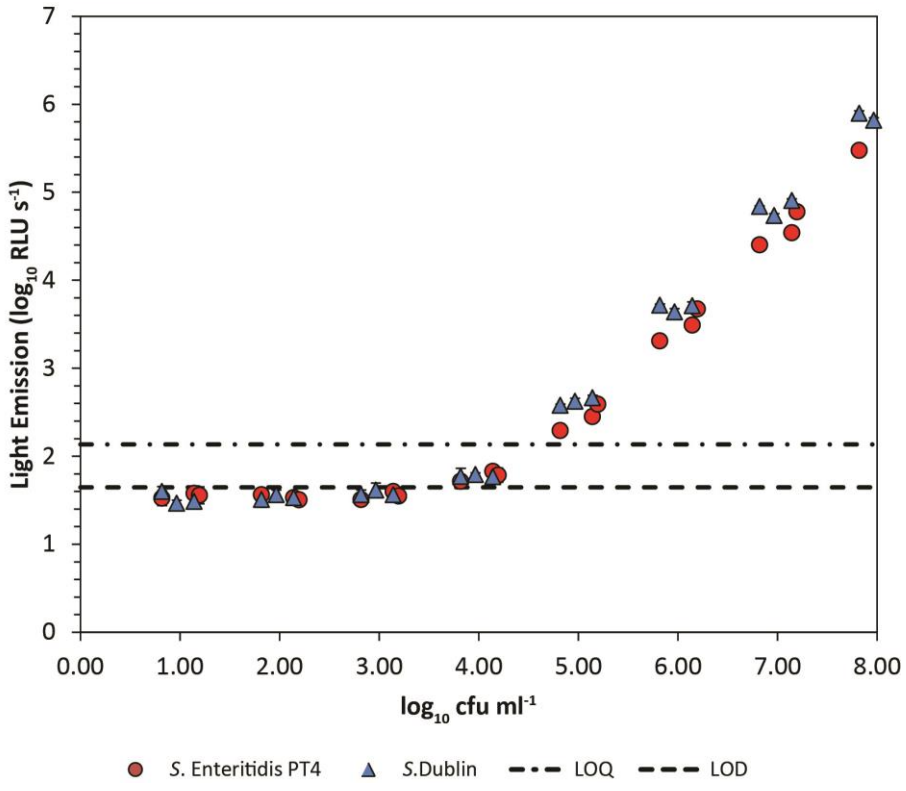

Figure 52. Calibration curve of log-fold dilutions of bioluminescent bacteria immobilised in overlay agar using a microplate luminometer. Values represent mean RLU/s of triplicate readings from three independent experiments.

Lawns of bioluminescent reporters grown in overlay agar in both microtitre plates and 90 mm petri dish formats exhibited similar trends of light emission to those grown in liquid batch culture. After an initial lag phase, logarithmic phase growth was characterized by a rapid exponential increase in light emission. Stationary phase onset was indicated by a deceleration of the rate of increase of bioluminescence, followed by a period of constant then reducing light emission (Figure 53).

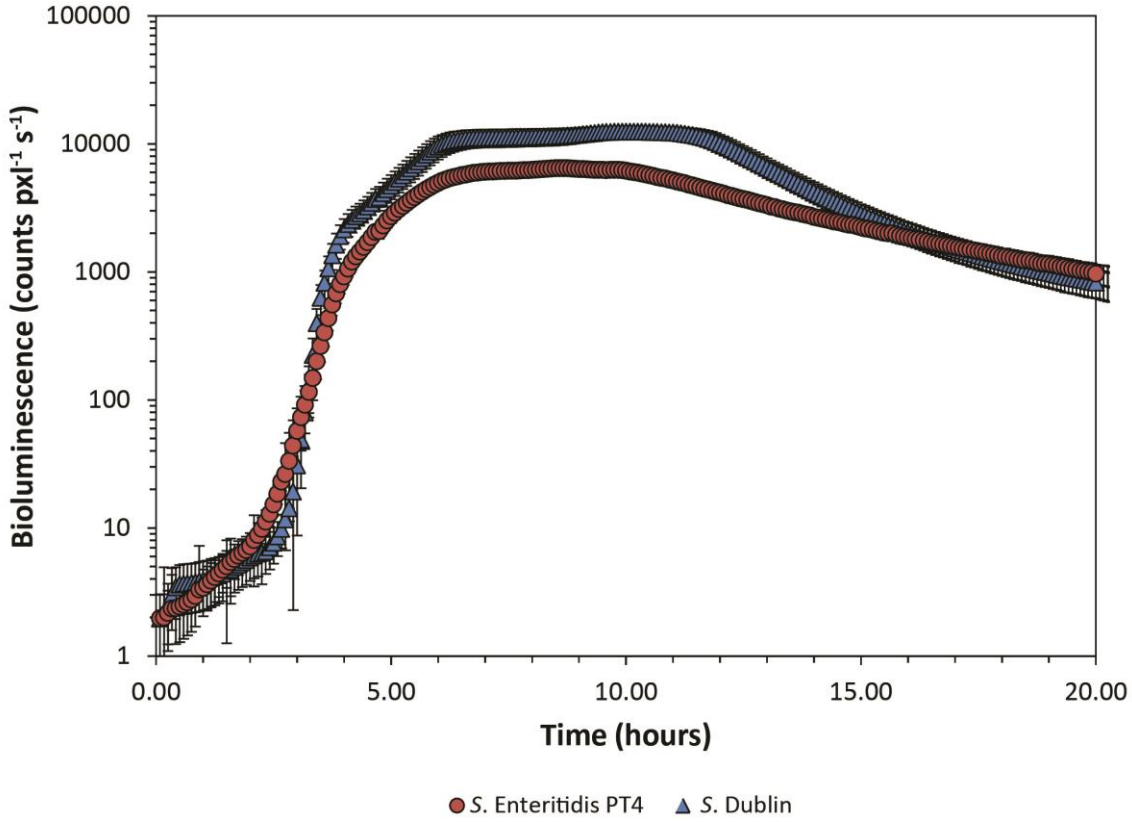

Figure 53. Bioluminescence imaging of a growing lawn of *S.* Enteritidis absent of bacteriophages. Values represent the mean and standard deviation of three independent platings, determined using a square region of interest comprising an area of 100 pixel^2. Bacterial lawns were incubated within a clear Perspex incubator at 37^{o}C and imaged at 5 minute intervals over a period of 20 hours.

7.2.2 Plaque morphology

The siphovirus vB_SenS-Ent1 produces relatively large plaques (mean diameter 5.69 ±1.72 mm, n=10) when titrated upon *S.* Enteritidis. Visually, plaques on overlay plates were best described as consisting of three discrete zones. Moving outwards from the plaque centre, the first zone consists of a region of clearing with little or no visible turbidity. The second zone is represented by an area of slight turbidity extending to the third zone; the boundary between the plaque and the bacterial lawn. Elution of bacteriophages in SM buffer from individual excised plaques yielded a mean productive titre of 8.6 ± 9.6 x 10^9 pfu ml^{-1} (n=15). Plaques formed by the myovirus Felix O1 were smaller (mean diameter 2.15 ±0.34 mm, n=10) but morphologically similar to plaques formed by vB_SenS-Ent1. Plaques formed by Felix O1 yielded a mean titre of 2.68 ± 2.56 x 10^8 pfu ml^{-1} (n=15) and consisted of a small central zone of clearing, zone of turbidity and a boundary at the junction with the bacterial lawn (Figure 54).

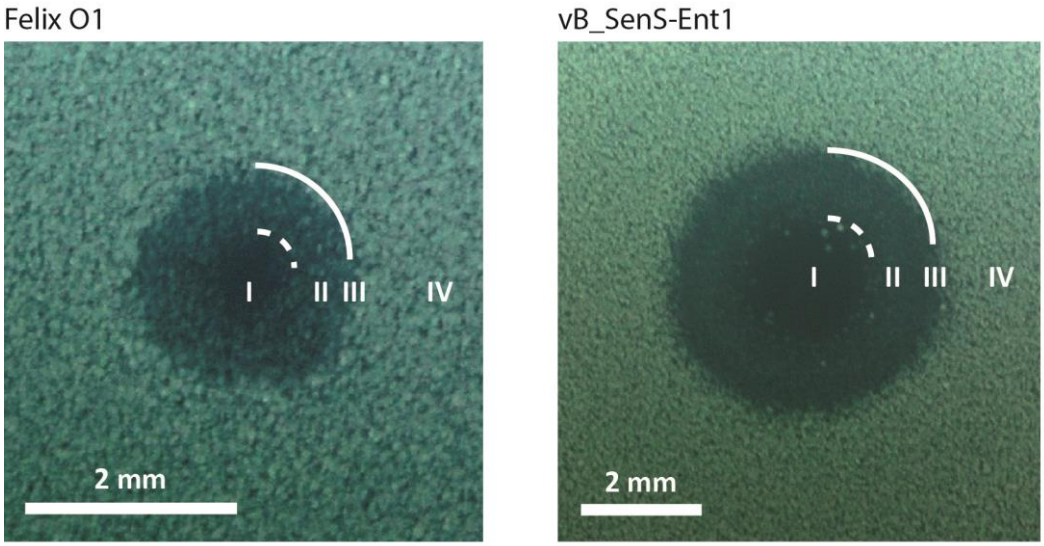

Figure 54. Photographs of plaques formed by Felix O1 and vB_SenS-Ent1. Roman numerals refer to regions of plaque morphology; I) zone of clearing; II) zone of turbidity; III) plaque boundary; IV) bacterial lawn. Dashed lines indicate the boundary between the zone of clearing and turbidity and solid lines the boundary between the plaque edge and the bacterial lawn.

7.2.3 Plaque development

Using bioluminescence imaging, developing plaques could be identified within a period of 2 to 4 hours. Profile plots of lines extending through the plaque centroid and into the bacterial lawn showed a distinct profile. The plaque centre is present as a region of low light emission and the plaque boundary as a gradient of increasing light emission rising to that emitted by the bacterial lawn. Histograms of plaque images exhibited a bimodal distribution. The mean and standard deviation of pixel grey values of control regions within the bacterial lawn were used to create coarse threshold values (TRH) which were subsequently used to segment images of plaques. After 12 hours the segmentation process resulted in images representing three regions (Figure 55).

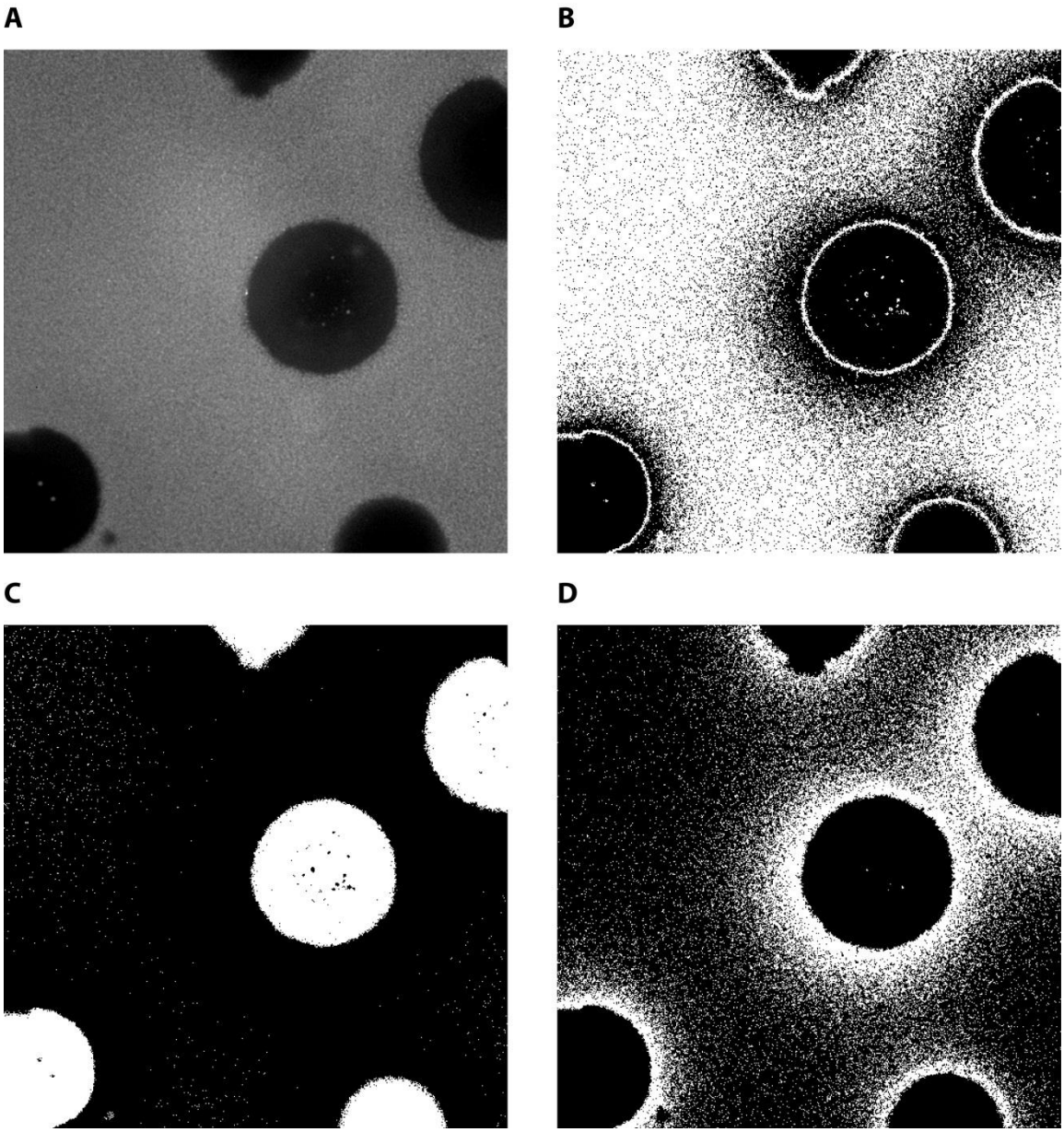

Figure 55. Thresholding of plaques. A) Light photograph of plaques formed by vB_SenS-Ent1. Bioluminescence imaging: B) Pixels of value equal to the mean ± 2sd light emission of the bacterial lawn. C) Pixels of value less than mean - 2sd light emission of the bacterial lawn D) Pixels of value greater than the mean + 2sd light emission of the bacterial lawn.

Using segmented images it is envisaged that region I (TRH1 ≤ mean -2σ) encompasses an area containing lysed bacterial cells where the infective process is predominantly finished and a region of on-going bacterial lysis, where a gradient of light emission represents increasing bacterial cell density as one moves outwards towards the plaque periphery. Region II (TRH2 = mean ±2σ) represents the average (±2σ) bioluminescence of the bacterial lawn. Region III (TRH3 > mean +2σ) corresponds to an area around the visible plaque boundary where light emission is greater than the bacterial lawn. This region, observed for both vB_SenS-Ent1 and FelixO1, is absent initially and becomes more pronounced after 12 hours. The increased emission from region III could arise due to two possible scenarios. Firstly, that the number of cells remained constant but with increased metabolism resulting in a greater number of RLU produced per cell. Second, that the bacteria in this region were

actively multiplying and the observed light emission reflects increasing cell density. The localisation of this region relative to the plaque boundary suggests that either scenario could arise from the presence of increased nutrient density in regions where plaque formation has suppressed bacterial growth (Lorian and Strauss, 1966). An alternative conjecture might be that this regions contains cells infected with bacteriophages and that the increased bioluminescence reflects increases in metabolism associated with the production of progeny virions. In order to test this possibility separate 1 µl spots of bacteriophages in SM buffer, representing a dose of 10^8 pfu, SM buffer alone and fresh LB media were applied to the surface of mature lawns of stationary phase bacteria and light emission monitored over a period of 2 hours (Figure 56).

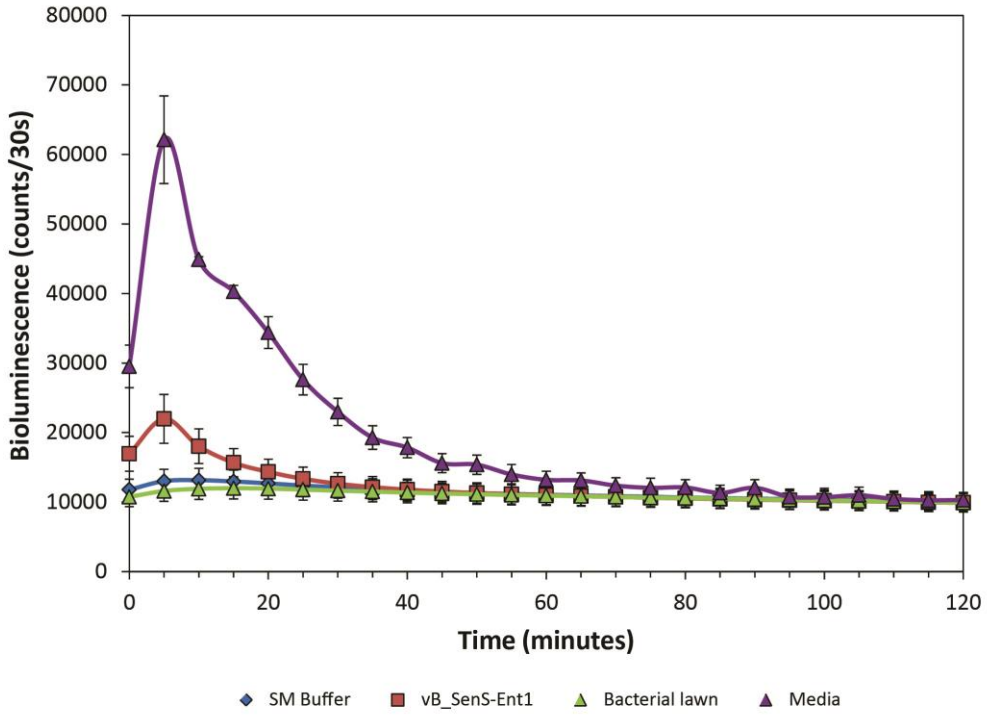

Figure 56. Profiles of bioluminescence from stationary phase lawns (24 hours old) after application of 1 µl spots of fresh LB media and SM buffer with and without bacteriophages.

Application of media to mature lawns resulted in a rapid increase of bioluminescence to a peak six times greater than the untreated bacterial lawn, which then decayed over 90 minutes. Notably, applying SM buffer containing bacteriophages resulted in a transient increase in bioluminescence to a peak level twice that of the bacterial lawn. Light emission decayed more rapidly than for addition with fresh LB medium. In contrast spots of SM buffer alone resulted in only a very slight rise in bioluminescence. However, analysis of peak emission by one-way ANOVA suggests the difference after addition of phages is not significant. The transient increase in bioluminescence caused by application of bacteriophages to stationary phase bacterial lawns is interesting, but as to how and why this phenomenon arises remains undetermined. Further experiments, representing a more

thorough examination are required to ascertain whether this effect is due to the presence of bacteriophages or diffusion of nutrients.

7.2.4 Examination of plaques with confocal microscopy

Examination of mature lawns by confocal microscopy demonstrated that bacterial cells were not homogenously distributed in the volume of overlay agar. Individual cells and smaller aggregates of bacteria were predominantly located at the surface of the overlay agar. Bacteria at the upper surface of agar overlays also exhibited motility, suggesting that these bacteria might act as an additional transit mechanism for the dispersal of bacteriophages within the overlay layer. However, this observation could be an artefact arising from hydration of the agar layer during the staining process. At depth, bacteria were distributed as numerous micro-colonies of varying sizes. For plaques, regions of clearing were characterised by an overt absence of bacteria. The boundaries of plaques initiated by Felix O1 were well defined with a high density of dead aggregates meeting a high density of live aggregates. In contrast, the plaque boundary was less definite for vB_SenS-Ent1, appearing as a gradual reduction in the density of micro-colonies stained with propidium iodide (Figure 57).

A

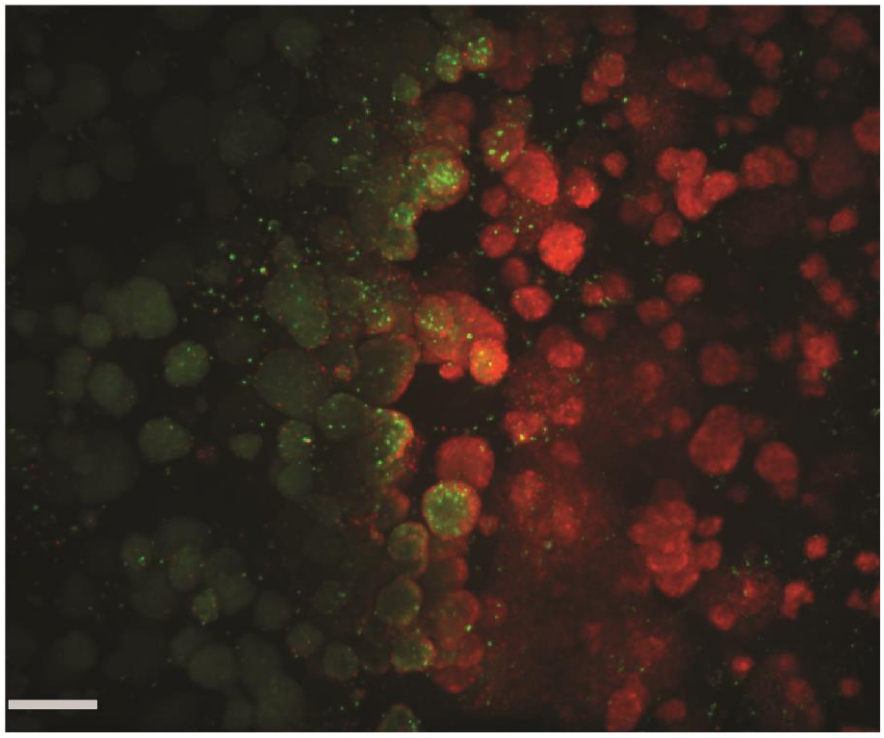

B

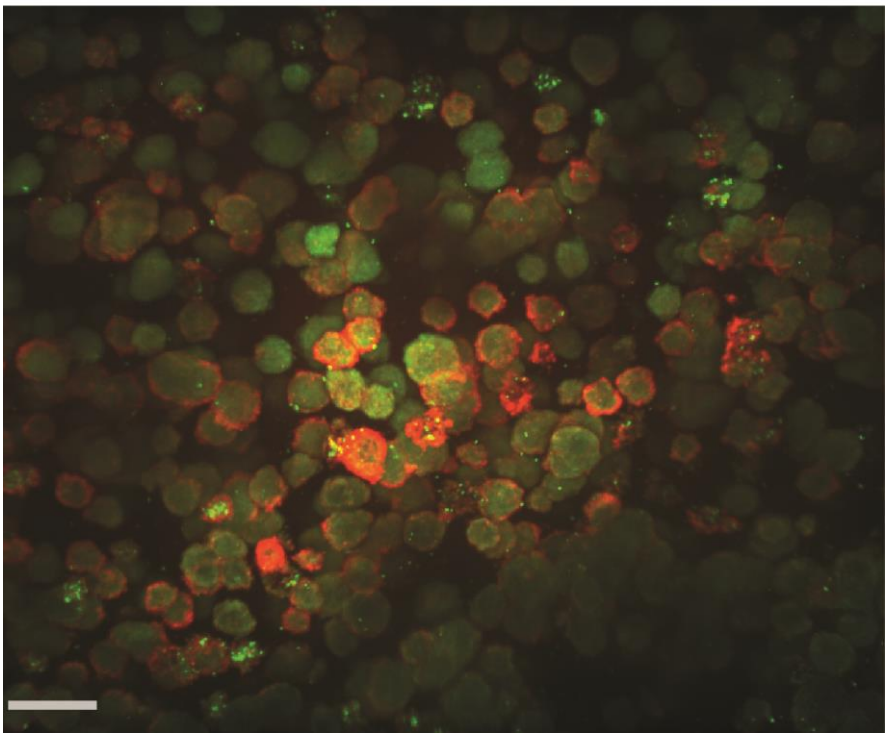

Figure 57. Spinning disk confocal images (extended focus) of microcolonies at the plaque boundary of A) Felix O1 and B) vB_SenS-Ent1 at x20 magnification. The scale bar represents a distance of 40 µm. Red denotes dead bacteria stained with propidium iodide. Green denotes live bacteria stained with SYTO-9.

7.2.5 Plaque enlargement

The rate of expansion was first measured by taking the slope of the area equivalent radius (R_e) over time. The area equivalent radius provides a coarse estimate of the rate plaque expansion and takes as an assumption that the plaque is a perfect circle and hence provides no indication of asymmetries at the plaque boundary. Using the area equivalent radius two distinct phases of enlargement were observed, common to both vB_SenS-Ent1 and Felix O1. In the first phase, which lasted up to 10 hours, the plaque radius expands at a near constant linear rate. This is followed by a period of deceleration into the second phase where the rate of expansion is greatly reduced and becomes near stationary (Table 17, Figure 58).

Table 17. Rates of enlargement, size and circularity after 20 hours for plaques formed by bacteriophages Felix O1 and vB_SenS-Ent1. Plaque numbers correspond to labels shown in figure 58.

vB_SenS-Ent1	**Adsorption:**	6.73×10^{-9} ml min^{-1}	**Latent Period:**	35 minutes
			Burst Size:	35 virions
Plaque	**Velocity (mm hr^{-1})**[1.]	**Velocity (mm hr^{-1})** [2.]	**Diameter (mm)** [3.]	**Circularity**[3.]
1	0.2102	0.0163	4.90	0.82
2	0.2182	0.0273	4.67	0.58
3	0.1828	0.0180	3.97	0.76
4	0.1382	0.0082	3.09	0.76
Felix O1	**Adsorption:**	5.4×10^{-9} ml min^{-1}	**Latent Period:**	40 minutes
			Burst Size:	46 virions
Plaque	**Velocity (mm hr^{-1})**[1.]	**Velocity (mm hr^{-1})** [2.]	**Diameter (mm)** [3.]	**Circularity**[3.]
1	0.1548	0.0083	2.08	0.54
2	0.1467	0.0041	2.38	0.31
3	0.1622	0.0056	2.33	0.49
4	0.1316	0.0116	2.54	0.84
5	0.1505	0.0136	2.71	0.76

[1.] Velocity determined from slope of the area equivalent radius between 5 and 9 hours.

[2.] Velocity determined from slope of the area equivalent radius between 15 and 19 hours.

[3.] Determined after 20 hours incubation

Felix O1

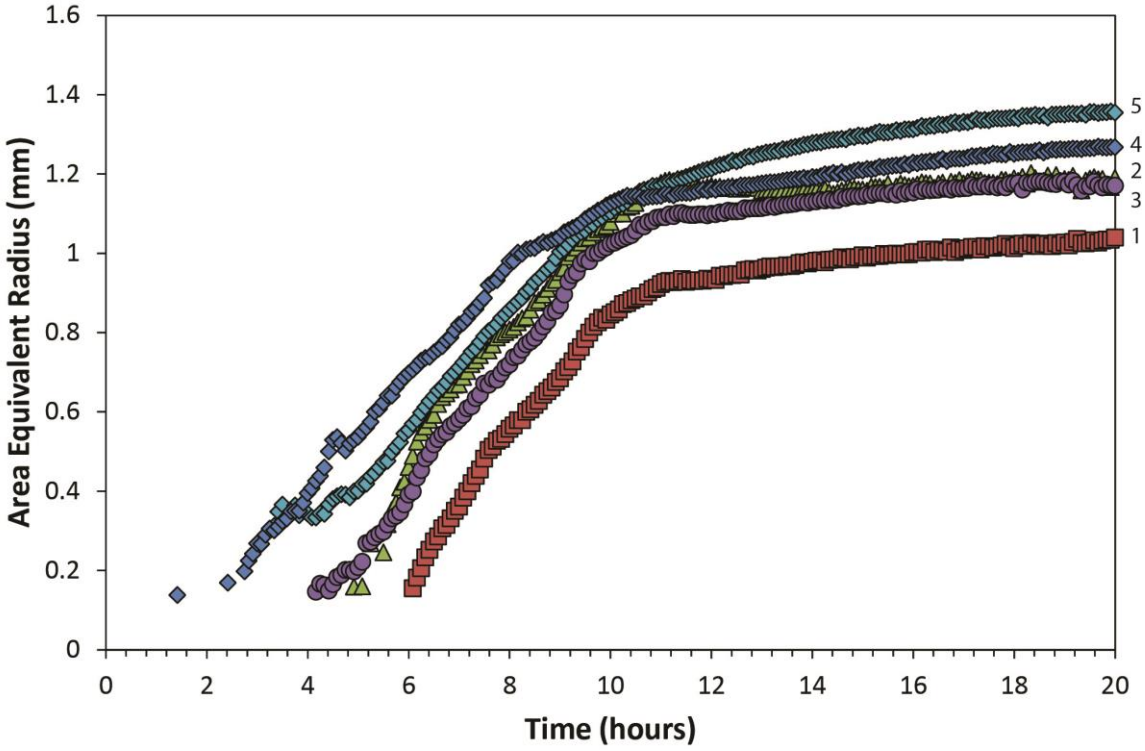

vB_SenS-Ent1

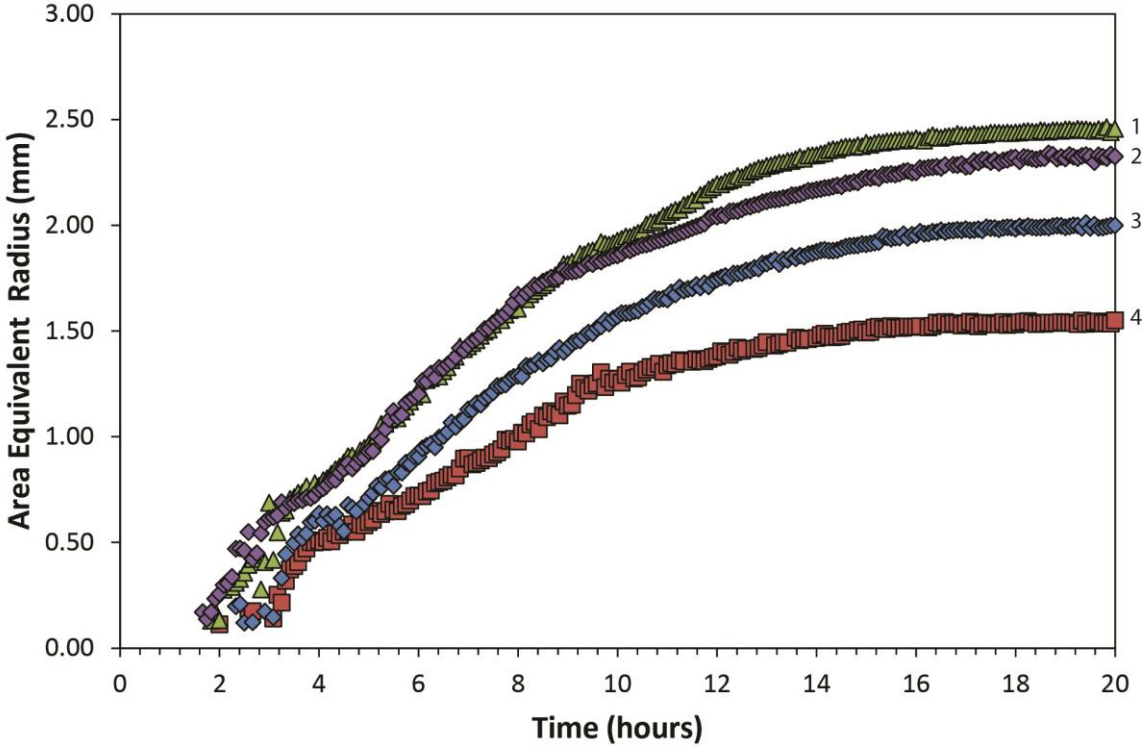

Figure 58. Increases in area equivalent radius with time for *Salmonella* phages Felix O1 (n=5 plaques) and vB_SenS-Ent1 (n=4 plaques). Data are plotted at 5 minute intervals.

For the first phase of enlargement, increases in the plaque area equivalent radius occurred at an average rate of 0.148±0.011 mm h^{-1} and 0.186±0.035 mm h^{-1} between 5 and 9 hours for Felix O1 (n=5) and vB_SenS-Ent1 (n=4), respectively. A period of deceleration preceded the second phase

where rates of expansion reduced to 0.019±0.021 mm h^{-1} and 0.017±0.008 mm h^{-1} between 15 and 20 hours for Felix O1 and vB_SenS-Ent1, respectively.

The observed differences in final plaque size are due to the limited time allowed for adsorption of virion particles to bacteriophages prior to mixing in the overlay agar. After one minute, only a limited proportion of the bacterial population would have undergone adsorption and injection by bacteriophages and a significant fraction of bacteriophages would be free in the agarose matrix. Bacteria encountering these extracellular phages, either by the expansion of microcolonies through cell division or by diffusion of the bacteriophages, would do so at later time points meaning that the initiating infection event would occur at different times.

Taking velocity as the difference of the average plaque radius across 360 angular orientations at hourly intervals demonstrates that the rate of plaque enlargement changes with time (Figure 59). It appears that plaque enlargement shows high initial values of velocity, which decreases over time in conjunction with growth of the bacterial lawn. However the accuracy of the data presented here are likely to be influenced by differences between the times of the plaque initiating infection.

Felix O1

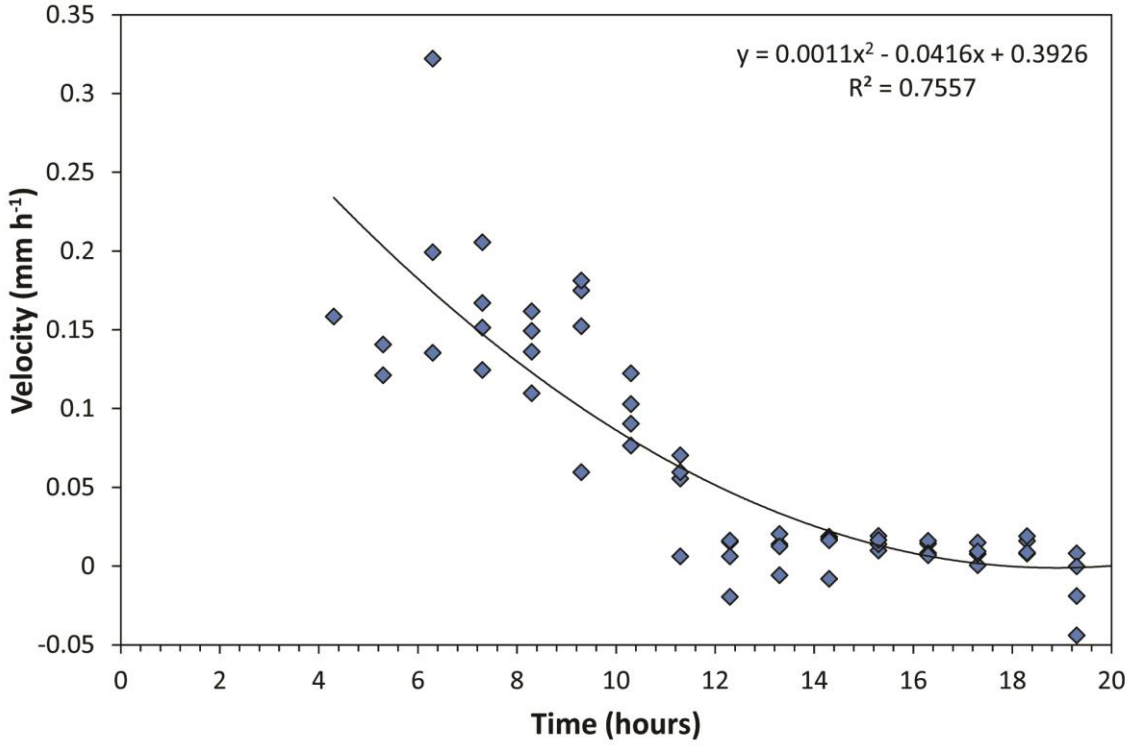

vB_SenS-Ent1

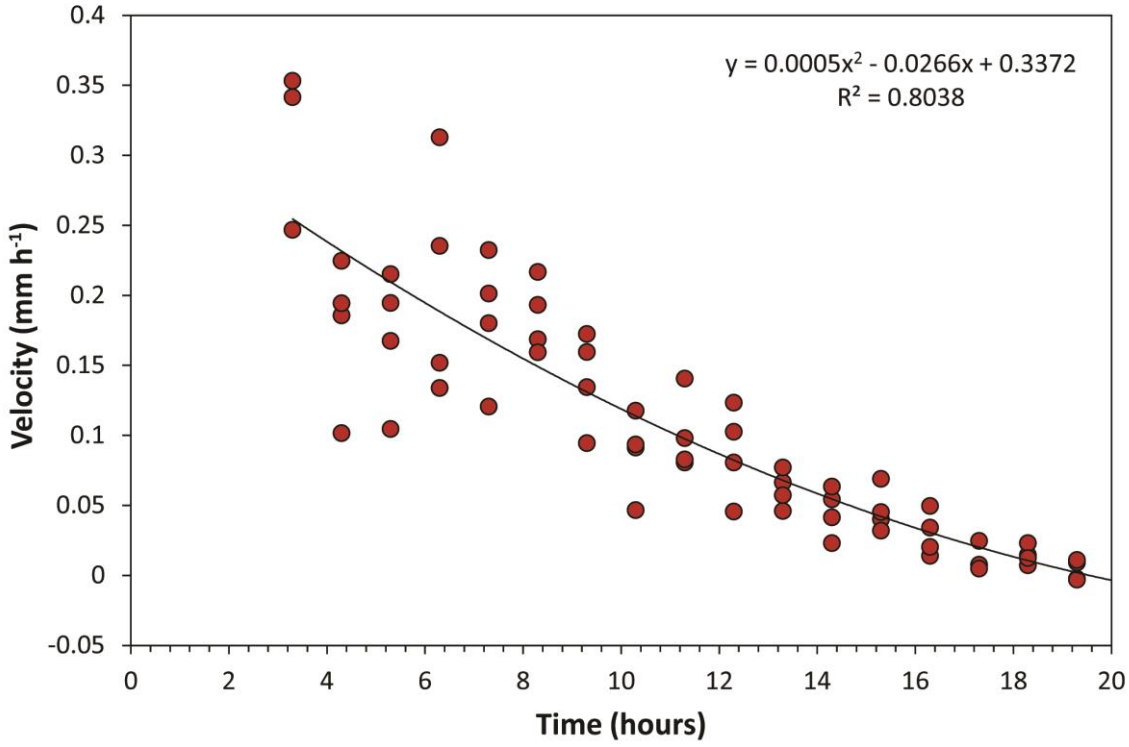

Figure 59. Velocity of plaque expansion by *Salmonella* bacteriophages Felix O1 and vB_SenS-Ent1 on lawns of *Salmonella* serovars Dubin and Enteritidis, respectively. Velocity was determined at hourly intervals. Quadratic lines of best fit are illustrated.

7.2.6 Resistant bacteria

The survival and subsequent growth of bacteria within plaques is clearly visible using bioluminescence imaging. These resistant bacteria are present as small circular regions of light emission that arise within the plaque zones of clearing and turbidity (Figure 60). These microcolonies were observed frequently within plaques formed vB_SenS-Ent1 and infrequently within plaques of Felix O1.

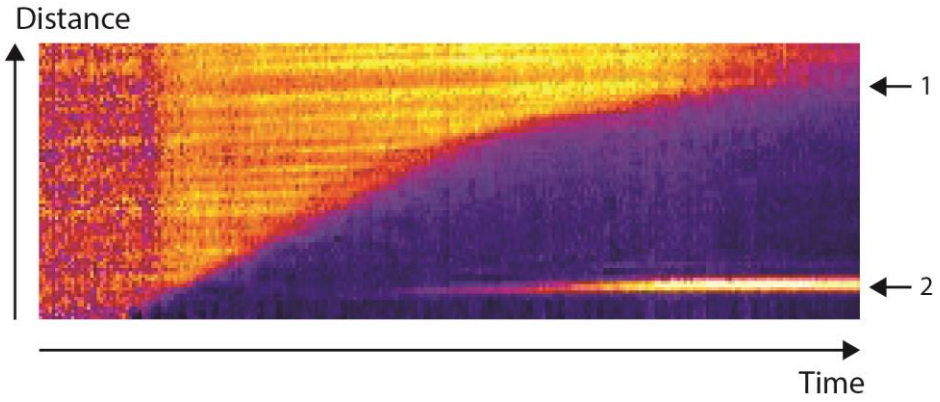

Figure 60. Kymograph of a line extending through the plaque boundary and a resistant bacterial microcolony for vB_SenS-Ent1. Arrow 1 indicates the plaque boundary. Arrow 2 indicates the location of the microcolony.

7.3 Discussion

The use of bioluminescent bacteria is a novel approach facilitating continuous high resolution imaging of plaque formation in agar overlays. This methodology presents two significant advantages in comparison to traditional methods. First, the growing bacterial lawn may be detected prior to becoming visible to the naked eye and earlier than afforded by turbidometric methods. Second, the intensity of light emission around the plaque, at and within the plaque boundary may be used to provide insights into the host's metabolic rate in addition to yielding geometric descriptions and rates of enlargement. For bacteriophages Felix O1 and vB_SenS-Ent1, plaques could be visualised within a period of between two and four hours incubation. However, whilst light emission from the bacterial lawn could be detected immediately, the boundary detection routine did not robustly detect the plaque at early stages of formation. However, it is worth noting that the use of BLI required a somewhat lengthy optimisation of exposure time for each reporter serotype and that using the methods reported here, the presence of individual plaques within the imaging area is not guaranteed. Additionally, early time frames using long exposure times run the risk of sensor saturation, at which point the correlation between bioluminescence and cell density is lost. In hindsight, this methodology could be further improved by the use of a triggered light source to facilitate light photography in addition to measurements of bioluminescence. Providing an appropriately modified reporter bacteriophage, fluorescence could also be employed to form a tri-

modal imaging approach facilitating detection of both bacteria and bacteriophages during the course of plaque formation.

Descriptions of plaque morphology are either quantitative or qualitative (Abedon and Yin, 2008, Abedon, 2011a). Quantitative differences describe the geometric characteristics of the plaque, for example; size, area, perimeter and circularity, whereas qualitative differences are descriptive and may include plaque turbidity, morphological variations, the presence of debris or resistant colonies. It has been proposed that plaques may be separated into at least four regions extending outwards from the plaque centre (Krone and Abedon, 2008). These regions comprise an area of clearing (i), an area of reduced turbidity (ii), a narrow periphery constituting the plaque boundary (iii) and the bacterial lawn (iv). Using bioluminescence imaging the zone of clearing is clearly apparent as an area of low light emission and the zone of turbidity as an area of reduced light emission. The plaque boundary is represented as a region where, moving outwards, bioluminescence increases until the bacterial lawn is reached. The reasons for an additional area of increased bioluminescence existing around and beyond the plaque boundary are unclear. It is pure speculation that this is a result of interactions with bacteriophages which have diffused beyond the visible plaque boundary; a further and more extensive investigation is required to elucidate the cause of this phenomenon. As yet, no accurate technique exists for assessing the very early stages of plaque formation, that is, the chain of infection events beginning with the focal infection and encompassing the first hours of expansion. It would be interesting to ascertain whether these primary stages exhibit fast initial velocities or accelerates as the turnover of infection and lysis events gathers momentum and the bacteriophage population increases.

The visual assessment of plaques has long been used to denote differences within viral populations; changes in gross plaque morphology allow the identification of rapid lysis mutants, minute and large plaque-forming mutants as well as temperate phage mutants producing clear rather than turbid plaques (Adams, 1959). Similarly, descriptions of plaque geometry can provide evidence of phage population heterogeneity within a single plaque. For example, Lee and Yin (Lee and Yin, 1996a) employed circularity as an indicator of population heterogeneity by proposing that asymmetries at the plaque perimeter arise from the emergence of mutant strains at the expanding region of infection. Using recombinant *E.* coli transformed to express the T7 RNA polymerase, it was found upon plating that with increasing distance from the centre of the plaque, mutant T7 bacteriophages were detected which had undergone deletions within the genome region encoding the RNA polymerase (Yin, 1993). This study clearly demonstrates that evolution occurs within expanding populations of bacteriophage during plaque formation.

The expansion of plaques is described as a travelling wave, that is, an expanding front of infection moving radially outwards where diffusion-mediated declines in phage concentration are offset by

continued lysis and release of progeny virions. Plaque wavefront velocity can be measured empirically by determining plaque size as a function of time. Plaque fecundity, also referred to as plaque productivity or yield, is defined as the total number of virions produced during plaque formation (Abedon and Culler, 2007b). Plaque productivity is thus a function of the number of bacteria infected, average burst size and those virions lost to decay, non-productive infection and secondary infections of host cells. A number of reaction-diffusion model have been developed to provide simulations of plaque formation in order to determine estimates of plaque wavefront velocity, in response to different physiological characteristics of bacteriophages. Each of the published models of plaque expansion has been systematically reviewed in terms of plaque wavefront velocity and productivity by Abedon and colleagues (Abedon and Culler, 2007b, Abedon and Culler, 2007a, Abedon and Yin, 2009).

As a general rule, plaque wavefront velocity directly influences plaque size, with faster velocities resulting in larger plaques. However, despite an apparent simplicity, the formation of plaques is subject to a number of physiological and environmental factors, all of which form a complex interplay impacting both upon wavefront velocity and plaque productivity. Physiological factors can be divided between bacteriophage and host, though are not altogether independent of each other. For the bacteriophage isolate these factors comprise rates of diffusion, adsorption (and desorption) rates during the extracellular phase, while the intracellular phase is represented by the latent or lysis time and burst size.

In the extracellular phase of plaque development, phages are governed by their diffusion coefficient and rate of adsorption to host cells. Since bacterial cells are immobile within the agar matrix, plaque size increases as a quadratic function of the virion diffusion coefficient (Gallet *et al.,* 2011). In addition to rates of diffusion, the time taken by a phage to find a host cell for infection is defined by the adsorption rate constant and the density of available host cells. In liquid cultures high adsorption rates are to be preferred, at least in order to minimise the time spent seeking a new host cell. Those bacteriophages exhibiting slow rates of adsorption will take significantly longer to obtain new host cells, effectively limiting the available time for production of progeny. However, a high adsorption rate can be detrimental to plaque formation. Using isogenic mutants of phage λ exhibiting different adsorption rates and marked by the addition of the lacZ gene to the viral genome, Gallet *et al.,* (2009) demonstrated that the phages with higher adsorption rates settled more rapidly on lawns of host cells but resulted in smaller plaques. It was suggested that diffusion of virions within the plaque is retarded due to the high affinity for host cells. These observations and further studies suggest that, for plaque formation, an adsorption optimum exists, above which plaque size and productivity is negatively impacted (Shao and Wang, 2008, Abedon and Culler, 2007b, Abedon and Yin, 2009).

Burst size is a measure of virion progeny yield per infected host cell, usually determined from one-step growth experiments in a liquid medium. With increasing burst size, greater numbers of progeny virions are released into the environment. Intuitively, greater burst sizes should result in larger plaques and or, greater plaque productivity (Abedon and Culler, 2007b). However this effect diminishes, as for some bacteriophages at least, there is a positive linear relationship between lysis time and burst size (Wang, 2006). Hence, the more time spent replicating progeny before lysis, the less time is available in the extracellular phase (Shao and Wang, 2008). The antagonism between these two factors has led to the suggestion that an optimal latent period exists which maximises plaque size and productivity (Abedon and Culler, 2007b, Abedon and Culler, 2007a).

Physiological factors pertinent to the host bacterial cell include the growth phase and initial concentration of the seed culture, specific growth rate, and duration of the exponential phase as well as final cell concentrations. Environmental factors are represented by variables of incubation temperature, available nutrients for the host lawn, pH, agar concentration and the availability of cofactors for the adsorption of virions to host cells.

Gallet *et al.,* (2011) describe an elegant study where a library of isogenic mutants of phage λ exhibiting altered morphology, rates of adsorption and latent periods, were used to ascertain how different virion traits impacted upon plaque formation. Plaque sizes and productivities from experimental observations were compared against the available models but none could quantitatively reproduce the experimentally observed data. Plaque size and productivity was found to diminish with increasing adsorption rates while lysis time exhibited a concave relationship with plaque size. Whilst this study made no attempt to empirically test the various mathematical models, we suggest that combining the use of isogenic phages exhibiting different physiological characteristics with bioluminescence or multi-modal imaging of plaque formation would form a useful tool for assessing discrepancies between experimental observations and estimates of plaque wavefront velocities by current models. Perhaps one reason for a lack of systematic experimental studies assessing the proposed models of plaque expansion for different bacteriophage isolates arises from the difficulty, perceived or otherwise, in obtaining accurate measurements of bacteriophage diffusion coefficients. Recently, Hu *et al.,* reported a simple modification of a two-chamber Stokes diffusion apparatus to allow the quantification of virion particle diffusion rate through agarose gel membranes for the myovirus T4 and filamentous phage fNEL (Hu *et al.,* 2010). The same group have recently extended this method to study the effects of adsorption and proliferation to phage diffusion coefficients (Hu *et al.,* 2012). Fluorescence correlation spectroscopy has also been used to characterise the diffusion of the *Lactobacillus* phage C2 in biofilms of *Stenotrophomonas maltophilia* (Lacroix-Gueu *et al.,* 2005). Additionally, while it is easy to adjust

phage traits within model equations, it is not always such a simple process to modify these *in vitro* (Gallet *et al.,* 2009).

The plaque assay represents a batch culture system, that is, a finite pool of resources is available to support bacterial population expansion. Bacterial cells entering stationary phase undergo pronounced changes in cell morphology and physiology (Navarro Llorens *et al.,* 2010, Nyström, 2004). The entry into stationary phase is highly regulated, resulting in patterns of gene expression which serve to prepare the bacterial cell for survival in a growth-limiting or hostile environment. Cells reduce in size, become more spherical and exhibit significant alterations to all structures of the cell envelope. Not only does this reduced size effectively reduce the cell surface area available for phage adsorption, the increased thickness of the peptidoglycan cell wall and reduced fluidity of the inner membrane may well serve to present a more difficult barrier for the injection of phage DNA. Stationary phase bacteria show reduced protein synthesis and the production of both rRNAs and tRNAs is decreased, a feature which is likely to impact upon phage lysis time. Similarly, aerobic metabolism is decreased while expression of fermentative enzymes is increased. The results reported here of reducing rates of expansion coinciding with entry of the bacterial population into stationary phase demonstrates that, for phages Felix O1 and vB_SenS-Ent1, bacteriophage genome replication and assembly of progeny requires that sufficient resources and synesthetic capability are available in the host cell to satisfy these requirements. This intuitive concept has been documented in several studies where it was shown that latent period, burst size and proliferation rates of bacteriophages are influenced by the growth conditions of the host (Hadas *et al.,* 1997, Los *et al.,* 2007, Corbin *et al.,* 2001, Webb *et al.,* 1982, You *et al.,* 2002, Middelboe, 2000, Kokjohn and Sayler, 1991). In general, bacteriophages infecting hosts with slow rates of growth due to starvation, nutrient limitation or sub-optimal carbon sources exhibit extended latent periods and slower formation of progeny virions leading to reduced burst sizes (Abedon *et al.,* 2001, Abedon, 2011a). However, notable exceptions to these observations exist, for example the bacteriophage T7 results in plaques that continuously expand, albeit at a greatly reduced rate, in stationary phase hosts (Yin, 1993).

Due to restrictions in mobility imposed by semi-structured environments, replicating bacteria form spatial arrangements termed microcolonies, which Abedon describes succinctly as a “closely associated collection of especially clonally related bacteria that is sufficiently small so as to be not readily discernible individually by the naked eye; a highly localised three-dimensional array of bacteria” (Abedon, 2012b). As the bacterial lawn grows to higher densities, there is a corresponding increase in the number of bacterial cells within a microcolony and its overall size. Such clusters of bacterial cells are clearly apparent within the confocal micrographs presented here. Abedon has considered the impact of group living, as exemplified by microcolonies, upon bacteria exposed to infection by lytic bacteriophages (Abedon, 2012a). It is suggested that microcolonies represent larger

spatial targets for phage adsorption than individual cells and secondly that, by virtue of their proximity and shared susceptibility, bacteria in the immediate vicinity of an infected cell are much more vulnerable to infection (Abedon, 2012a). Bacteriophages which infect cells present within the same microcolony as the parental infection can be described as settler phages, while those that which diffuse and infect cells in spatially separate microcolonies as scout phages (Abedon, 2011a). It seems intuitive to hypothesise that as microcolonies expand, the proportion of progeny phages which settle will increase, as there are more bacteria in the direct vicinity of the infected cell. Thus, a microcolony could act as a sponge, adsorbing those bacteriophages that would, at earlier times and with reduced microcolony size perhaps be more likely to diffuse away from the microcolony to become scouts. Increased microcolony size might also result in multiple infection events occurring for a single host cell. For the T-even phages, secondary infections can lead to lysis inhibition which, while resulting in extended latent periods, also results in larger burst sizes (Abedon, 1990, Paddison *et al.,* 1998). Lysis inhibition also has the added advantage of preventing the release of phage when there are few uninfected cells. In contrast, the adsorption of many phages to a cell surface may also induce destabilisation of the bacterial cell envelope, leading to lysis from without, effecting either non-productive infection or premature lysis.

To date, relatively few studies have employed the *lux* operon as a reporter within studies of microbial populations exposed to bacteriophages *in vitro.* With the exception of a microplate broth assay for T4 (Kim *et al.,* 2009) and a phage-based biosorbent (Sun *et al.,* 2001), applications of bacterial luciferases with bacteriophages have primarily focused upon the detection of specific bacterial pathogens present within mixed microbial communities in food, cosmetic, pharmaceutical and environmental matrices (Rees and Dodd, 2006a). Following Ulitzer and Kuhn (1987), several groups have reported the construction of recombinant bacteriophage encoding the *luxAB* genes for the transduction and subsequent detection of a target bacteria such as *Bacillus anthracis, E. coli* O:157, *Listeria spp.* and *Yersinia pestis* (Loessner *et al.,* 1997, Schofield and Westwater, 2009, Waddell and Poppe, 2000). A number of further applications for the use of bioluminescent bacterial reporters within bacteriophage research may be envisioned. The use of bioluminescent reporters in conjunction with EMCCD imaging systems might allow temporal and spatial discrimination of the effects of applying bacteriophage preparations to bacteria present on surfaces as biofilms or colonising food or material surfaces, presenting a quantitative measurement to supplement traditional enumerations of plaque and colony forming units. Moreover, and perhaps more importantly for biocontrol applications within industry, extended longitudinal measurements of this kind may allow for the identification of bacterial population recovery post-exposure to bacteriophages. This latter point is clearly demonstrated by this study with the observation of colonies of resistant bacteria which form within plaque regions of clearing.

7.4 Acknowledgements

Thanks are due to David Corry for confocal spinning disc microscopy. The work was performed by D. Turner and J. Sun developed the boundary detection routine.

Chapter 8 Discussion

The goal of this thesis was to isolate, identify, select and characterise bacteriophages specific for the genus *Salmonella*. Three novel *Siphoviridae*, vB_SenS-Ent1, vB_SenS-Ent2 and vB_SenS-Ent3 were isolated, sequenced and annotated using bioinformatics tools. The physiological characteristics, including host range, rate of adsorption, burst size and latent and eclipse periods of these phages were determined. Using bioluminescent bacterial reporters, the effects of co-incubation of these phages with *S.* Enteritidis PT4 were investigated in batch culture, agarose matrices and foods.

Each of the vB_SenS-Ent bacteriophages demonstrated broad host range specificity within *Salmonella* subspecies *enterica*. No single bacteriophage alone exhibited lysis of all *Salmonella* isolates tested when assessed using overlay spot or plaque assays. Such an observation is not surprising considering there are currently more than 2,500 designated serovars of *Salmonella* detailed within the LeMinor-Kauffmann-White serological typing system (Grimont and Weill, 2007). Analysis of those isolates lysed by these bacteriophages, and the presence of a P22-like tailspike protein inferred from genome sequence analysis, indicates that the vB_SenS-Ent bacteriophages display a host range limited to those *Salmonella* that display the LPS O:12 antigen. Notably, different isolates of the same serotype exhibited different susceptibilities which might be attributed to the presence of resident prophages or distinct immunity systems comprising CRISPR-Cas, restriction-modification and abortive infection. The differences in susceptibility to bacteriophages by a particular bacterial isolate forms the basis of phage typing. Phage typing is used to supplement epidemiological data, where, after biochemical confirmation and serotyping, the isolate is infected via the spot plate method with a range of different bacteriophages that comprise the typing set. Phage types are differentiated on the basis of lysis patterns, providing additional traceability for those isolates recovered from different patients or environmental sources. Phage typing schemes have been described for *S.* Typhi, *S.* Paratyphi, *S.* Typhimurium (Callow, 1959, Anderson *et al.,* 1977, Mitchell *et al.,* 1989), *S.* Enteritidis (Ward *et al.,* 1987), *S.* Heidelberg (Demczuk *et al.,* 2003), *S.* Bareilly (Jayasheela *et al.,* 1987) and those serovars carrying the Vi capsular antigen (Craigie and Felix, 1947, Felix and Callow, 1951). A short-coming of the data presented for the vB_SenS-Ent phages is the failure to obtain mass spectrometry data from proteins purified from 2D SDS-PAGE gels. Data from mass spectrometry would have provided additional evidence for inferences made from bioinformatics analyses and strengthened the case for the designation of structural proteins. It would also been of interest to investigate temporal gene expression using RT-PCR, to provide experimental evidence for the allocation of gene expression to early, middle or late stages of infection.

In order to place the phages vB_SenS-Ent1, vB_SenS-Ent2 and vB_SenS-Ent3 within the known *Salmonella* bacteriophages with completely sequenced genomes, a comparative genomics study was

undertaken, representing a continuation of the approach first detailed by Lavigne *et al.,* (Lavigne *et al.,* 2008, Lavigne *et al.,* 2009). This study, based upon the numbers of shared homologous or orthologous proteins between pairs of bacteriophage genomes, provided evidence for a significant updating of the relationships between the *Salmonella* bacteriophages. The vB_SenS-Ent phages are placed within a discrete clade of 10 members, which is proposed to constitute a novel genus within the *Siphoviridae*. However, the degree of similarity between the vB_SenS-Ent bacteriophages is unusual, considering the numerous and diverse bacteriophages reported to infect *Salmonella* in the literature, and is likely to be a direct result of enrichment and isolation from the same environmental sample. The high degree of relatedness between the vB_SenS-Ent phages, specifically that 95-100 % similarity is found in the majority of predicted genes, raises the question as to whether they are examples of separate species or merely three strains of one species. Under current ICTV definitions a 95% nucleotide sequence identity is used to differentiate between phage species. Nevertheless, the differences in susceptibility to different restriction enzymes, gene 'cargo' and host range present an image of evolutionary flux in these bacteriophages.

The control of *Salmonella* within the food chain and agriculture has become an increasingly important issue in recent years, particularly with the increasing resistance to antibiotics displayed by members of this genus. The use of bacteriophages for the specific recognition and eradication of this pathogen offers an attractive alternative approach to the use of conventional antimicrobial agents. Specifically, the advantages of bacteriophages include a high degree of specificity for the target host and the ability to increase exponentially with productive infection at the site of host infection or colonisation. To date, biocontrol methods involving bacteriophages have been limited to either the application of intact whole virions and, for Gram positive bacteria, the use of phage endolysins. While this thesis only considered the application of whole virions to bacterial populations in broth, foods and semi-structured environments (agar overlays), the efficiency by which bacteriophages subvert the host synthetic machinery suggests that further proteins with potential for exploitation as antimicrobial agents remain to be found. Indeed, a significant gap still exists between available sequence data and biological function; many phage proteins have no assigned function and are described only as 'hypothetical proteins'. Several concerted efforts are underway to attempt to reduce the number of hypothetical proteins, approaches exemplified by Phamerator and ACLAME (Leplae *et al.,* 2010, Cresawn *et al.,* 2011). These approaches rely upon sequence data to generate clusters of orthologous proteins. Recently, an efficient system based on the recombineering of electroporated phage DNA has been described for directed mutagenesis of the mycobacteriophages was described, a process which may be extended to other phages (van Kessel *et al.,* 2008, Marinelli *et al.,* 2012). This technique allows the construction of phage mutants which can be used to assess the function of individual genes and their requirement within infection. It is anticipated that

functional characterisation of phage-encoded proteins will provide for interesting tools and applications in the future.

With the exception of detection systems for the presence of specific bacteria using recombinant bacteriophages, bacterial luciferases are under-used as a reporter in studies of infection and lysis by bacteria. For *in vitro* assays of bacteriophage lysis, bioluminescence of the host bacterial species undergoes a distinct reduction in the presence of bacteriophages. However, for all combinations of bacteriophage and host bacteria, bioluminescence recovers after treatment with each of the vB_SenS-Ent bacteriophages. The growth of phage-resistant mutants is not surprising and appears many times within the literature (Labrie *et al.,* 2010). In effect, the addition of lytic bacteriophage to bacterial cultures acts as a strong selective pressure. Predation by bacteriophages is predicted to help maintain microbial species diversity within the environment through a process termed 'killing the winner' (Thingstad, 2000). This model proposes that the winner population, that is a microbial species displaying a competitive advantage and hence high densities within a mixed population, are more susceptible to bacteriophages. Thus any corresponding increase in host population is associated with a corresponding increase in phage predation leading to increased rates of phage-mediated killing. Phage suppression of the winner population leaves a vacuum, allowing room for other, potentially less competitive members of the host population to expand and fill this remaining niche within the prokaryotic community. The generation of resistance within the suppressed winner population ensures the survival of these bacteria, but it is assumed that resistance is associated with decreased fitness. Horizontal transfer of genes by lysogenic bacteriophage can also augment fitness by conferring morphological, metabolic or resistance characteristics (Weinbauer and Rassoulzadegan, 2004). This interaction between active virus host pairs is supported by evidence from marine environments where the abundance of specific phage varied in seasonal cycles while the overall density of bacteria and bacteriophages remained relatively stable (Wommack *et al.,* 1999a, Wommack *et al.,* 1999b).

Proof of principle studies performed on a range of foods demonstrated that the vB_SenS-Ent phages have the potential to control *Salmonella* in foods, at least for a limited number of serotypes. The design of phage biocontrol strategies requires careful consideration and candidate bacteriophages must be extensively characterised. The concentration of bacteriophages within any preparation must be optimised to ensure adequate coverage of the matrix to be treated and to restrict the potential for development of resistance in target bacterial populations. Due to the limitations imposed by host specificity, and the potential for selection of bacteriophage insensitive mutants, it is suggested that for biocontrol applications, the vB_SenS-Ent bacteriophages should be delivered in a cocktail containing other bacteriophages that employ distinct host receptors. The *Salmonella* phages show a great diversity of distal tail morphologies and have been demonstrated to utilise a wide variety of

targets for primary adsorption, including the O-antigen and core polysaccharide of LPS (Andres *et al.,* 2012, Bayer *et al.,* 1980, Lindberg and Holme, 1969, Shin *et al.,* 2012a), Vi capsular antigen (Pickard *et al.,* 2010), flagella (Shin *et al.,* 2012a) and the outer membrane proteins OmpC (Ho and Slauch, 2001), FepA, FhuA (Casjens *et al.,* 2005a) and BtuB (Hong *et al.,* 2008, Kim and Ryu, 2011). During the initial stages of infection, bacteriophages recognise and bind to bacterial cell surface components in an adsorption process mediated by diverse tail fibre, tail spike and tail tip proteins. Once bound, a signal is transmitted by an unknown mechanism along the tail resulting in conformational changes and ejection of the virion nucleic acid (Tavares *et al.,* 2012). This unidirectional process is poles apart from eukaryotic viruses, where the virion envelope fuses with the plasma membrane prior to release of the virion genome within the cell cytosol by dissociation of the proteinaceous capsid. In contrast, bacteriophages infecting Gram-negative bacterial hosts must overcome two hydrophobic barriers; the outer and inner membranes. Furthermore, the ejected genomic DNA must navigate the periplasmic space and the rigid peptidoglycan cell wall whilst avoiding degradative enzymes. The structure and properties of the proteins facilitating adsorption thus play a critical primary role in the determination of host specificity and initiation of infection. The identification of host receptors, phage adhesins and the elucidation of binding mechanisms has potential to provide insights into the development of phage resistance and inform the design of phage cocktails to achieve appropriate coverage for decontamination or biocontrol applications. Additionally, phage receptor binding proteins may provide alternatives to the use of antibodies as ligands within selective capture workflow components of assays for the detection of bacterial pathogens. In addition, whilst it is predicted that the *Setp3likevirus* are virulent phages, further studies are required to elucidate the mechanisms or mutations leading to host resistance before their potential as biocontrol agents can be fully realised.

In addition to the use of bioluminescence alone as a quantitative measure to describe the effects of bacteriophage, future assays necessitate the inclusion of an additional quantitative measure, either by viable counts, absorbance or by titration of bacteriophages, in order to demonstrate that the observed decrease in light emission occurs from a reduction in viable cells, via lysis and a concurrent expansion of bacteriophage population, as opposed to metabolic inhibition or abortive infection. While an additional, automated, measure of viability might be provided by use of absorbance, the dynamic range of detection is limited, spanning approximately 10^6 to 10^9 cfu ml^{-1} and therefore provides no information of lysis at concentrations lower than 10^6 cfu ml^{-1}. Viable counts would have provided a more sensitive, if time-consuming, alternative measure. However, viable counts are potentially subject to carry-over of bacteriophage, when performed in the absence of neutralising serum, which could cause an under-estimation of bacterial numbers. Bioluminescent bacterial reporters could potentially be used in future studies within classical one-step growth experiments to investigate the responses of bacterial metabolism during eclipse and latent phases of bacteriophage

replication. An alternative approach might be employed whereby promoter-coupled plasmid constructs containing the lux operon might be utilised to investigate the expression of particular sets of genes for host or bacteriophage upon infection.

The application of bioluminescent *Salmonella* serovars and sensitive photon counting EMCCD cameras represents a novel and hitherto unreported technique that allowed early detection and rate determination for the formation of plaques in spot and overlay assays. Light output from micro-colonies present within the plaque demonstrates the generation of metabolically viable, phage resistant mutants. The formation of plaques in overlay agar represents the processes of expansion and spread of bacteriophage populations within a semi-structured environment. Several authors have suggested that overlay plaque assays provide a useful model for approximating conditions within biofilms (Jouenne *et al.,* 1994, Abedon and Yin, 2009). The use bioluminescent imaging could be extended in future work to ascertain the effects of lytic bacteriophage within steady-state biofilm models (Gilbert *et al.,* 1989, Hodgson *et al.,* 1995, Gander and Gilbert, 1997, Greenman *et al.,* 2005, Thorn and Greenman, 2009). The advantages of employing a steady state biofilm system are two-fold. First, the agarose matrix is replaced by the polysaccharide matrix produced by the bacteria, which is likely to represent a much more heterogeneous environment, than that represented by purified agarose. Second, nutrients required for bacterial growth may be controlled, allowing direct modulation of bacterial growth rates within the biofilm environment. Such an approach could be used to more accurately represent the physiological state of bacteria within the environment. Moreover, the use of imaging systems provides an additional layer of spatial information which could be used to model the expansion and spread of bacteriophage populations within the biofilm matrix.

This thesis represents but a modest contribution to knowledge the *Salmonella* phages. However, considering the stunning morphological and genetic diversity of the bacteriophages, much still remains to be learned about phages infecting this genus of bacteria. The proposal that vB_SenS-Ent1, -Ent2 and –Ent3 belong to a distinct clade is being taken forward as part of an international collaboration with other phage researchers, led by Dr Hany Anany of the Canadian Research Institute for Food Safety at the University of Guelph.

Since their discovery, bacteriophages have underpinned the foundations of molecular biology. Now, with an ever increasing volume of genetic information we are just beginning to appreciate the evolution of bacteriophages and their prominent roles in natural ecosystems. This truly is the third age of phage (Mann, 2005).

References

ABEDON, S. T. 1990. Selection for lysis inhibition in bacteriophage. *Journal of Theoretical Biology,* 146**,** 501-511.

ABEDON, S. T. 2011a. *Bacteriophages and Biofilms: Ecology, Phage Therapy, Plaques*, Nova Science Publishers.

ABEDON, S. T. 2011b. Lysis from without. *Bacteriophage,* 1**,** 46-49.

ABEDON, S. T. 2012a. Spatial Vulnerability: Bacterial Arrangements, Microcolonies, and Biofilms as Responses to Low Rather than High Phage Densities. *Viruses,* 4**,** 663-687.

ABEDON, S. T. 2012b. Thinking about microcolonies as phage targets. *Bacteriophage,* 2**,** 200-204.

ABEDON, S. T. & CULLER, R. R. 2007a. Bacteriophage evolution given spatial constraint. *Journal of Theoretical Biology,* 248**,** 111-119.

ABEDON, S. T. & CULLER, R. R. 2007b. Optimizing bacteriophage plaque fecundity. *Journal of Theoretical Biology,* 249**,** 582-592.

ABEDON, S. T., HERSCHLER, T. D. & STOPAR, D. 2001. Bacteriophage Latent-Period Evolution as a Response to Resource Availability. *Applied and Environmental Microbiology,* 67**,** 4233-4241.

ABEDON, S. T. & THOMAS-ABEDON, C. 2010. Phage therapy pharmacology. *Current Pharmaceutical Biotechnology,* 11**,** 28-47.

ABEDON, S. T. & YIN, J. 2008. Impact of spatial structure on phage population growth. *In:* ABEDON, S. T. (ed.) *Bacteriophage Ecology: Population Growth Evolution and Impact of Bacterial Viruses.* Cambridge University Press.

ABEDON, S. T. & YIN, J. 2009. Bacteriophage Plaques: Theory and Analysis. *Bacteriophages.*

ABRAMOFF, M. D., MAGALHAES, P. J. & RAM, S. J. 2004. Image Processing with ImageJ. *Biophotonics International,* 11**,** 36-42.

ACHESON, D. & HOHMANN, E. L. 2001. Nontyphoidal Salmonellosis. *Clinical Infectious Diseases,* 32**,** 263-269.

ACKERMANN, H.-W. 1987. Bacteriophage taxonomy in 1987. *Microbiological Sciences,* 4**,** 214-218.

ACKERMANN, H.-W. 1996. Frequency of morphological phage descriptions in 1995. *Archives of Virology,* 141**,** 209-218.

ACKERMANN, H.-W. 2001. Frequency of morphological phage descriptions in the year 2000. *Archives of Virology,* 146**,** 843-857.

ACKERMANN, H.-W. 2007a. 5500 Phages examined in the electron microscope. *Archives of Virology,* 152**,** 227-243.

ACKERMANN, H.-W. 2007b. *Salmonella* Phages Examined in the Electron Microscope. *Methods in Molecular Biology,* 394**,** 213-234.

ACKERMANN, H.-W. 2009a. Phage Classification and Characterization. *Methods in Molecular Biology,* 501**,** 127-140.

ACKERMANN, H.-W. 2009b. Basic phage electron microscopy. *Methods in Molecular Biology,* 501**,** 113-126.

ACKERMANN, H.-W., BERTHIAUME, L. & KASATIYA, S. S. 1972. Morphologie des phages de lysotypie de *Salmonella paratyphi* B (schéma de Felix et Callow). *Canadian Journal of Microbiology,* 18**,** 77-81.

ACKERMANN, H.-W. & EISENSTARK, A. 1974. The Present State of Phage Taxonomy. *Intervirology,* 3**,** 201-219.

ACKERMANN, H.-W. & PRANGISHVILI, D. 2012. Prokaryote viruses studied by electron microscopy. *Archives of Virology,* 157**,** 1843-1849.

ADAMS, M. H. 1959. *Bacteriophages,* New York, Interscience.

ADRIAENSSENS, E., ACKERMANN, H.-W., ANANY, H., BLASDEL, B., CONNERTON, I., GOULDING, D., GRIFFITHS, M., HOOTON, S., KUTTER, E., KROPINSKI, A., LEE, J.-H., MAES, M., PICKARD, D., RYU, S., SEPEHRIZADEH, Z., SHAHRBABAK, S., TORIBIO, A. & LAVIGNE, R. 2012. A suggested new bacteriophage genus: "Viunalikevirus". *Archives of Virology,* 157**,** 2035-2046.

AGIRREZABALA, X., VELÁZQUEZ-MURIEL, J. A., GÓMEZ-PUERTAS, P., SCHERES, S. H. W., CARAZO, J. M. & CARRASCOSA, J. L. 2007. Quasi-Atomic Model of Bacteriophage T7 Procapsid Shell: Insights into the Structure and Evolution of a Basic Fold. *Structure,* 15**,** 461-472.

AKSYUK, A. A. & ROSSMANN, M. G. 2011. Bacteriophage Assembly. *Viruses,* 3**,** 172-203.

ALLISON, H. E. 2007. Stx-phages: drivers and mediators of the evolution of STEC and STEC-like pathogens. *Future Microbiology,* 2**,** 165-174.

ALLOUSH, H. M., SALISBURY, V., LEWIS, R. J. & MACGOWAN, A. P. 2003. Pharmacodynamics of linezolid in a clinical isolate of *Streptococcus pneumoniae* genetically modified to express *lux* genes. *Journal of Antimicrobial Chemotherapy,* 52**,** 511-3.

ALTSCHUL, S., MADDEN, T., SCHAFFER, A., ZHANG, J., ZHANG, Z., MILLER, W. & LIPMAN, D. 1997. Gapped BLAST and PSI-BLAST: a new generation of protein database search programs. *Nucleic Acids Research,* 25**,** 3389 - 3402.

ALVAREZ, L. J., THOMEN, P., MAKUSHOK, T. & CHATENAY, D. 2007. Propagation of fluorescent viruses in growing plaques. *Biotechnology and Bioengineering,* 96**,** 615-621.

ANDERSON, E. S., WARD, L. R., SAXE, M. J. & DE SA, J. D. 1977. Bacteriophage-typing designations of *Salmonella* Typhimurium. *The Journal of Hygiene,* 78**,** 297-300.

ANDREATTI FILHO, R. L., HIGGINS, J. P., HIGGINS, S. E., GAONA, G., WOLFENDEN, A. D., TELLEZ, G. & HARGIS, B. M. 2007. Ability of Bacteriophages Isolated from Different Sources to Reduce *Salmonella enterica* Serovar Enteritidis *In Vitro* and *In Vivo*. *Poultry Science,* 86**,** 1904-1909.

ANDRES, D., ROSKE, Y., DOERING, C., HEINEMANN, U., SECKLER, R. & BARBIRZ, S. 2012. Tail morphology controls DNA release in two *Salmonella* phages with one lipopolysaccharide receptor recognition system. *Molecular Microbiology,* 83**,** 1244-1253.

ANDREU, N., ZELMER, A., FLETCHER, T., ELKINGTON, P. T., WARD, T. H., RIPOLL, J., PARISH, T., BANCROFT, G. J., SCHAIBLE, U., ROBERTSON, B. D. & WILES, S. 2010. Optimisation of Bioluminescent Reporters for Use with Mycobacteria. *PLoS ONE,* 5**,** e10777.

ANDREWES, F. W. 1922. Studies in group-agglutination I. The *Salmonella* group and its antigenic structure. *The Journal of Pathology and Bacteriology,* 25**,** 505-521.

ANJUM, M. F., MAROONEY, C., FOOKES, M., BAKER, S., DOUGAN, G., IVENS, A. & WOODWARD, M. J. 2005. Identification of Core and Variable Components of the *Salmonella enterica* Subspecies I Genome by Microarray. *Infection and Immunity,* 73**,** 7894-7905.

ANONYMOUS 2002. EN ISO 6579:2002 Microbiology of food and animal feeding stuffs -- Horizontal method for the detection of *Salmonella*. European Committee for Standardisation.

ANONYMOUS 2003. EN ISO 4833:2003 Microbiology of food and animal feeding stuffs -- Horizontal method for the enumeration microorganisms -- Colony-count technique at 30 degrees C. European Committee for Standardisation.

BAILEY, T. L., WILLIAMS, N., MISLEH, C. & LI, W. W. 2006. MEME: discovering and analyzing DNA and protein sequence motifs. *Nucleic Acids Research,* 34**,** W369-W373.

BAKER, M. L., JIANG, W., RIXON, F. J. & CHIU, W. 2005. Common Ancestry of Herpesviruses and Tailed DNA Bacteriophages. *Journal of Virology,* 79**,** 14967-14970.

BARAK, Y., SCHREIBER, F., THORNE, S., CONTAG, C., DEBEER, D. & MATIN, A. 2010. Role of nitric oxide in *Salmonella typhimurium*-mediated cancer cell killing. *BMC Cancer,* 10**,** 146.

BARBIRZ, S., MÜLLER, J. J., UETRECHT, C., CLARK, A. J., HEINEMANN, U. & SECKLER, R. 2008. Crystal structure of *Escherichia coli* phage HK620 tailspike: podoviral tailspike endoglycosidase modules are evolutionarily related. *Molecular Microbiology,* 69**,** 303-316.

BAYER, M. E., TAKEDA, K. & UETAKE, H. 1980. Effects of receptor destruction by *Salmonella* bacteriophages ϵ15 and c341. *Virology,* 105**,** 328-337.

BEARD, S. J., SALISBURY, V., LEWIS, R. J., SHARPE, J. A. & MACGOWAN, A. P. 2002a. Expression of lux Genes in a Clinical Isolate of *Streptococcus pneumoniae*: Using Bioluminescence To Monitor Gemifloxacin Activity. *Antimicrobial Agents and Chemotherapy,* 46**,** 538-542.

BEARD, S. J., SALISBURY, V., LEWIS, R. J., SHARPE, J. A. & MACGOWAN, A. P. 2002b. Expression of *lux* Genes in a Clinical Isolate of *Streptococcus pneumoniae*: Using Bioluminescence To Monitor Gemifloxacin Activity. *Antimicrobial Agents and Chemotherapy,* 46**,** 538-542.

BEN-ISRAEL, O., BEN-ISRAEL, H. & ULITZUR, S. 1998. Identification and quantification of toxic chemicals by use of *Escherichia coli* carrying lux genes fused to stress promoters. *Applied and Environmental Microbiology,* 64**,** 4346-52.

BERCHIERI JR, A., LOVELL, M. A. & BARROW, P. A. 1991. The activity in the chicken alimentary tract of bacteriophages lytic for *Salmonella typhimurium*. *Research in Microbiology,* 142**,** 541-549.

BESEMER, J. & BORODOVSKY, M. 1999. Heuristic approach to deriving models for gene finding. *Nucleic Acids Research,* 27**,** 3911-3920.

BIGWOOD, T., HUDSON, J. A. & BILLINGTON, C. 2009. Influence of host and bacteriophage concentrations on the inactivation of food-borne pathogenic bacteria by two phages. *FEMS Microbiology Letters,* 291**,** 59-64.

BIRAN, A., YAGUR-KROLL, S., PEDAHZUR, R., BUCHINGER, S., REIFFERSCHEID, G., BEN-YOAV, H., SHACHAM-DIAMAND, Y. & BELKIN, S. 2010. Bacterial genotoxicity bioreporters. *Microbial Biotechnology,* 3**,** 412-427.

BJELLQVIST, B., HUGHES, G., PASQUALI, C., PAQUET, N., RAVIER, F., SANCHEZ, J., FRUTIGER, S. & HOCHSTRASSER, D. 1993. The focusing positions of polypeptides in immobilized pH gradients can be predicted from their amino acid sequences. *Electrophoresis,* 14**,** 1023-1031.

BLASER, M. J. & NEWMAN, L. S. 1982. A Review of Human Salmonellosis: I. Infective Dose. *Review of Infectious Diseases,* 4**,** 1096-1106.

BLISSETT, S. J. & STEWART, G. S. A. B. 1989. *In vivo* bioluminescent determination of apparent K_m's for aldehyde in recombinant bacteria expressing *luxA/B*. *Letters in Applied Microbiology,* 9**,** 149-152.

BORIE, C., ALBALA, I., SÀNCHEZ, P., SÁNCHEZ, M. L., RAMÍREZ, S., NAVARRO, C., MORALES, M. A., RETAMALES, J. & ROBESON, J. 2008. Bacteriophage Treatment Reduces *Salmonella* Colonization of Infected Chickens. *Avian Diseases,* 52**,** 64-67.

BORIE, C., SÁNCHEZ, M. L., NAVARRO, C., RAMÍREZ, S., MORALES, M. A., RETAMALES, J. & ROBESON, J. 2009. Aerosol Spray Treatment with Bacteriophages and Competitive Exclusion Reduces *Salmonella* Enteritidis Infection in Chickens. *Avian Diseases,* 53**,** 250-254.

BOYD, E., LI, J., OCHMAN, H. & SELANDER, R. 1997. Comparative genetics of the *inv-spa* invasion gene complex of *Salmonella enterica*. *Journal of Bacteriology,* 179**,** 1985-1991.

BOYLE, R. 1672. Some Observations about Shining Flesh, Both of Veal and of Pullet. *Philosophical Transactions of the Royal Society of London,* 7.

BRADFORD, M. M. 1976. A rapid and sensitive method for the quantitation of microgram quantities of protein utilizing the principle of protein-dye binding. *Analytical Biochemistry,* 72**,** 248-254.

BRADLEY, D. E. 1967. Ultrastructure of bacteriophage and bacteriocins. *Bacteriological Reviews,* 31**,** 230-314.

BREN, L. 2007. Bacteria-eating virus approved as food additive. *FDA Consumer,* 41**,** 20-22.

BRIGATI, J. R., RIPP, S. A., JOHNSON, C. M., IAKOVA, P. A., JEGIER, P. & SAYLER, G. S. 2007. Bacteriophage-Based Bioluminescent Bioreporter for the Detection of Escherichia coli O157:H7. *Journal of Food Protection,* 70**,** 1386-1392.

BRON, P. A., MONK, I. R., CORR, S. C., HILL, C. & GAHAN, C. G. M. 2006. Novel Luciferase Reporter System for In Vitro and Organ-Specific Monitoring of Differential Gene Expression in *Listeria monocytogenes*. *Applied and Environmental Microbiology,* 72**,** 2876-2884.

BRUSSOW, H., CANCHAYA, C. & HARDT, W.-D. 2004. Phages and the evolution of bacterial pathogens: from genomic rearrangements to lysogenic conversion. *Microbiology and Molecular Biology Reviews,* 68**,** 560-602.

BRÜSSOW, H., CANCHAYA, C. & HARDT, W.-D. 2004. Phages and the Evolution of Bacterial Pathogens: from Genomic Rearrangements to Lysogenic Conversion. *Microbiology and Molecular Biology Reviews,* 68**,** 560-602.

BUCHWALD, D. S. & BLASER, M. J. 1984. A Review of Human Salmonellosis: II. Duration of Excretion Following Infection with Nontyphi *Salmonella*. *Review of Infectious Diseases,* 6**,** 345-356.

BULL, J., LEVIN, B., DEROUIN, T., WALKER, N. & BLOCH, C. 2002. Dynamics of success and failure in phage and antibiotic therapy in experimental infections. *BMC Microbiology,* 2**,** 35.

BULL, J. J., VIMR, E. R. & MOLINEUX, I. J. 2010. A tale of tails: Sialidase is key to success in a model of phage therapy against K1-capsulated *Escherichia coli*. *Virology,* 398**,** 79-86.

BULLAS, L. R., MOSTAGHIMI, A. R., ARENSDORF, J. J., RAJADAS, P. T. & ZUCCARELLI, A. J. 1991. *Salmonella* phage PSP3, another member of the P2-like phage group. *Virology,* 185**,** 918-921.

BURNET, F. M. 1929. A Method for the Study of Bacteriophage Multiplication in Broth. *The British Journal of Experimental Pathology,* 10**,** 109-115.

BURNS-GUYDISH, S. M., OLOMU, I. N., ZHAO, H., WONG, R. J., STEVENSON, D. K. & CONTAG, C. H. 2005. Monitoring Age-Related Susceptibility of Young Mice To Oral *Salmonella enterica* Serovar Typhimurium Infection Using an *In Vivo* Murine Model. *Pediatric Research,* 58**,** 153-158.

BURNS-GUYDISH, S. M., ZHAO, H., STEVENSON, D. K. & CONTAG, C. H. 2007. The Potential *Salmonella aroA*– Vaccine Strain Is Safe and Effective in Young BALB/c Mice. *Neonatology,* 91**,** 114-120.

BYL, C. V. & KROPINSKI, A. M. 2000. Sequence of the Genome of *Salmonella* Bacteriophage P22. *Journal of Bacteriology,* 182**,** 6472-6481.

CAIRNS, B. J. & PAYNE, R. J. H. 2008. Bacteriophage Therapy and the Mutant Selection Window. *Antimicrobial Agents and Chemotherapy,* 52**,** 4344-4350.

CALLOW, B. R. 1959. A new phage-typing scheme for *Salmonella* Typhimurium. *The Journal of Hygiene,* 57**,** 346-359.

CAMPBELL, Z. T. & BALDWIN, T. O. 2009. Fre Is the Major Flavin Reductase Supporting Bioluminescence from *Vibrio harveyi* Luciferase in *Escherichia coli*. *Journal of Biological Chemistry,* 284**,** 8322-8328.

CANCHAYA, C., FOURNOUS, G., CHIBANI-CHENNOUFI, S., DILLMANN, M.-L. & BRÜSSOW, H. 2003a. Phage as agents of lateral gene transfer. *Current Opinion in Microbiology,* 6**,** 417-424.

CANCHAYA, C., PROUX, C., FOURNOUS, G., BRUTTIN, A. & BRÜSSOW, H. 2003b. Prophage Genomics. *Microbiology and Molecular Biology Reviews,* 67**,** 238-276.

CARDARELLI, L., PELL, L. G., NEUDECKER, P., PIRANI, N., LIU, A., BAKER, L. A., RUBINSTEIN, J. L., MAXWELL, K. L. & DAVIDSON, A. R. 2010. Phages have adapted the same protein fold to fulfill multiple functions in virion assembly. *Proceedings of the National Academy of Sciences,* 107**,** 14384-14389.

CARVER, T., THOMSON, N., BLEASBY, A., BERRIMAN, M. & PARKHILL, J. 2009. DNAPlotter: circular and linear interactive genome visualization. *Bioinformatics,* 25**,** 119-20.

CASJENS, S. 2003. Prophages and bacterial genomics: what have we learned so far? *Molecular Microbiology,* 49**,** 277-300.

CASJENS, S., GILCREASE, E., WINN-STAPLEY, D., SCHICKLMAIER, P., SCHMIEGER, H., PEDULLA, M., FORD, M., HOUTZ, J., HATFULL, G. & HENDRIX, R. 2005. The generalized transducing *Salmonella* bacteriophage ES18: complete genome sequence and DNA packaging strategy. *Journal of Bacteriology,* 187**,** 1091 - 1104.

CASPAR, D. L. D. & KLUG, A. 1962. Structure and intracellular localisation of viruses: Physical Principles in the Construction of Regular Viruses. *Cold Spring Harbor Symposia on Quantitative Biology,* 27**,** 1-24.

CERRITELLI, M. E., CONWAY, J. F., CHENG, N., TRUS, B. L. & STEVEN, A. C. 2003. Molecular Mechanisms In Bacteriophage T7 Procapsid Assembly, Maturation, And DNA Containment. *In:* WAH, C. & JOHN, E. J. (eds.) *Advances in Protein Chemistry.* Academic Press.

CHANG, H. R., LOO, L. H., JEYASEELAN, K., EARNEST, L. & STACKEBRANDT, E. 1997. Phylogenetic Relationships of *Salmonella typhi* and *Salmonella typhimurium* Based on 16S rRNA Sequence Analysis. *International Journal of Systematic Bacteriology,* 47**,** 1253-1254.

CHEN, G., SRINIVASA RANGA, V. P., MAO, Y., CHEN, K. & QIAO, H. 2008. Impact of *lux* gene insertion on bacterial surface properties and transport. *Research in Microbiology,* 159**,** 145-151.

CHRISTENSEN, H., NORDENTOFT, S. & OLSEN, J. E. 1998. NOTE: Phylogenetic relationships of *Salmonella* based on rRNA sequences. *International Journal of Systematic Bacteriology,* 48**,** 605-610.

CIRILLO, D. M., VALDIVIA, R. H., MONACK, D. M. & FALKOW, S. 1998. Macrophage-dependent induction of the *Salmonella* pathogenicity island 2 type III secretion system and its role in intracellular survival. *Molecular Microbiology,* 30**,** 175-188.

CLOSE, D. M., PATTERSON, S. S., RIPP, S., BAEK, S. J., SANSEVERINO, J. & SAYLER, G. S. 2010a. Autonomous Bioluminescent Expression of the Bacterial Luciferase Gene Cassette (*lux*) in a Mammalian Cell Line. *PLoS ONE,* 5**,** e12441.

CLOSE, D. M., XU, T., SAYLER, G. S. & RIPP, S. 2010b. *In Vivo* Bioluminescent Imaging (BLI): Noninvasive Visualization and Interrogation of Biological Processes in Living Animals. *Sensors,* 11**,** 180-206.

COHN, D. H., MILEHAM, A. J., SIMON, M. I., NEALSON, K. H., RAUSCH, S. K., BONAM, D. & BALDWIN, T. O. 1985. Nucleotide sequence of the *luxA* gene of *Vibrio harveyi* and the complete amino acid sequence of the alpha subunit of bacterial luciferase. *Journal of Biological Chemistry,* 260**,** 6139-6146.

CONTAG, C. H., CONTAG, P. R., MULLINS, J. I., SPILMAN, S. D., STEVENSON, D. K. & BENARON, D. A. 1995. Photonic detection of bacterial pathogens in living hosts. *Molecular Microbiology,* 18**,** 593-603.

CONTAG, P. R. 2008. Bioluminescence imaging to evaluate infections and host response in vivo. *Methods in Molecular Biology,* 415**,** 101-18.

COOPER, C. J., DENYER, S. P. & MAILLARD, J. Y. 2011. Rapid and quantitative automated measurement of bacteriophage activity against cystic fibrosis isolates of *Pseudomonas aeruginosa*. *Journal of Applied Microbiology,* 110**,** 631-640.

CORBIN, B. D., MCLEAN, R. J. C. & ARON, G. M. 2001. Bacteriophage T4 multiplication in a glucose-limited Escherichia coli biofilm. *Canadian Journal of Microbiology,* 47**,** 680-684.

CORDOVA, A., DESERNO, M., GELBART, W. M. & BEN-SHAUL, A. 2003. Osmotic Shock and the Strength of Viral Capsids. *Biophysical Journal,* 85**,** 70-74.

CRAIGIE, J. & FELIX, A. 1947. TYPING OF TYPHOID BACILLI WITH Vi BACTERIOPHAGE: SUGGESTIONS FOR ITS STANDARDISATION. *The Lancet,* 249**,** 823-827.

CRANEY, A., HOHENAUER, T., XU, Y., NAVANI, N. K., LI, Y. & NODWELL, J. 2007. A synthetic *luxCDABE* gene cluster optimized for expression in high-GC bacteria. *Nucleic Acids Research,* 35**,** e46.

CRESAWN, S., BOGEL, M., DAY, N., JACOBS-SERA, D., HENDRIX, R. & HATFULL, G. 2011. Phamerator: a bioinformatic tool for comparative bacteriophage genomics. *BMC Bioinformatics,* 12**,** 395.

CROSA, J. H., BRENNER, D. J., EWING, W. H. & FALKOW, S. 1973. Molecular Relationships Among the Salmonelleae. *Journal of Bacteriology,* 115**,** 307-315.

DAI, T., TEGOS, G. P., LU, Z., HUANG, L., ZHIYENTAYEV, T., FRANKLIN, M. J., BAER, D. G. & HAMBLIN, M. R. 2009. Photodynamic Therapy for Acinetobacter baumannii Burn Infections in Mice. *Antimicrobial Agents and Chemotherapy,* 53**,** 3929-3934.

DAI, W., HODES, A., HUI, W. H., GINGERY, M., MILLER, J. F. & ZHOU, Z. H. 2010. Three-dimensional structure of tropism-switching *Bordetella* bacteriophage. *Proceedings of the National Academy of Sciences,* 107**,** 4347-4352.

DARLING, A. E., MAU, B. & PERNA, N. T. 2010. progressiveMauve: Multiple Genome Alignment with Gene Gain, Loss and Rearrangement. *PLoS ONE,* 5**,** e11147.

DARZENTAS, N. 2010. Circoletto: visualizing sequence similarity with Circos. *Bioinformatics,* 26**,** 2620-2621.

DE LAPPE, N., DORAN, G., O'CONNOR, J., O'HARE, C. & CORMICAN, M. 2009. Characterization of bacteriophages used in the *Salmonella enterica* serovar Enteritidis phage-typing scheme. *Journal of Medical Microbiology,* 58**,** 86-93.

DE MORENO, M. R., SMITH, J. F. & SMITH, R. V. 1986. Mechanism studies of coomassie blue and silver staining of proteins. *Journal of Pharmaceutical Sciences,* 75**,** 907-911.

DELBRÜCK, M. 1945. The Burst Size Distribution in the Growth of Bacterial Viruses (Bacteriophages). *Journal of Bacteriology,* 50**,** 131-135.

DELCHER, A. L., HARMON, D., KASIF, S., WHITE, O. & SALZBERG, S. L. 1999. Improved microbial gene identification with GLIMMER. *Nucleic Acids Research,* 27**,** 4636-4641.

DEMCZUK, W., AHMED, R. & ACKERMANN, H.-W. 2004. Morphology of *Salmonella enterica* serovar Heidelberg typing phages. *Canadian Journal of Microbiology,* 50**,** 873-875.

DEMCZUK, W., SOULE, G., CLARK, C., ACKERMANN, H.-W., EASY, R., KHAKHRIA, R., RODGERS, F. & AHMED, R. 2003. Phage-Based Typing Scheme for *Salmonella enterica* Serovar Heidelberg, a Causative Agent of Food Poisonings in Canada. *Journal of Clinical Microbiology,* 41**,** 4279-4284.

DEVEAU, H., LABRIE, S. J., CHOPIN, M. C. & MOINEAU, S. 2006. Biodiversity and classification of lactococcal phages. *Applied and Environmental Microbiology,* 72**,** 4338-4346.

DOBBINS, A. T., GEORGE, M., JR., BASHAM, D. A., FORD, M. E., HOUTZ, J. M., PEDULLA, M. L., LAWRENCE, J. G., HATFULL, G. F. & HENDRIX, R. W. 2004. Complete genomic sequence of the virulent *Salmonella* bacteriophage SP6. *Journal of Bacteriology,* 186**,** 1933-1944.

DUNCAN, S., GLOVER, L. A., KILLHAM, K. & PROSSER, J. I. 1994. Luminescence-based detection of activity of starved and viable but nonculturable bacteria. *Applied and Environmental Microbiology,* 60**,** 1308-1316.

ECDC 2010. Annual Epidemiological Report on Communicable Diseases in Europe 2010. Stockholm: European Centre for Disease Prevention and Control.

ELLIS, E. L. & DELBRÜCK, M. 1939. The Growth of Bacteriophage. *The Journal of General Physiology,* 22**,** 365-384.

ENGELSMAN, A. F., VAN DER MEI, H. C., FRANCIS, K. P., BUSSCHER, H. J., PLOEG, R. J. & VAN DAM, G. M. 2009. Real time noninvasive monitoring of contaminating bacteria in a soft tissue implant infection model. *Journal of Biomedical Materials Research Part B: Applied Biomaterials,* 88B**,** 123-129.

EPPLER, K., WYCKOFF, E., GOATES, J., PARR, R. & CASJENS, S. 1991. Nucleotide sequence of the bacteriophage P22 genes required for DNA packaging. *Virology,* 183**,** 519 - 538.

FDA 2009. 2009 Summary report on antimicrobials sold or distributed for use in food-producing animals.: Food and Drug Administration (FDA), Department of Health and Human Services.

FELIX, A. & CALLOW, B. 1951. PARATYPHOID-B Vi-PHAGE TYPING. *The Lancet,* 258**,** 10-14.

FIGUEROA-BOSSI, N., UZZAU, S., MALORIOL, D. & BOSSI, L. 2001. Variable assortment of prophages provides a transferable repertoire of pathogenic determinants in *Salmonella*. *Molecular Microbiology,* 39**,** 260-272.

FIORENTIN, L., VIEIRA, N. D. & BARIONI, W. 2005. Oral treatment with bacteriophages reduces the concentration of *Salmonella* Enteritidis PT4 in caecal contents of broilers. *Avian Pathology,* 34**,** 258 - 263.

FISHER, A. J., THOMPSON, T. B., THODEN, J. B., BALDWIN, T. O. & RAYMENT, I. 1996. The 1.5-Å Resolution Crystal Structure of Bacterial Luciferase in Low Salt Conditions. *Journal of Biological Chemistry,* 271**,** 21956-21968.

FOKINE, A., LEIMAN, P. G., SHNEIDER, M. M., AHVAZI, B., BOESHANS, K. M., STEVEN, A. C., BLACK, L. W., MESYANZHINOV, V. V. & ROSSMANN, M. G. 2005. Structural and functional similarities between the capsid proteins of bacteriophages T4 and HK97 point to a common ancestry. *Proceedings of the National Academy of Sciences of the United States of America,* 102**,** 7163-7168.

FORT, J. & MÉNDEZ, V. 2002. Time-Delayed Spread of Viruses in Growing Plaques. *Physical Review Letters,* 89**,** 178101.

FOUCAULT, M. L., THOMAS, L., GOUSSARD, S., BRANCHINI, B. R. & GRILLOT-COURVALIN, C. 2010. In vivo bioluminescence imaging for the study of intestinal colonization by Escherichia coli in mice. *Applied and Environmental Microbiology,* 76**,** 264-74.

FRANCIS, K. P., JOH, D., BELLINGER-KAWAHARA, C., HAWKINSON, M. J., PURCHIO, T. F. & CONTAG, P. R. 2000. Monitoring Bioluminescent Staphylococcus aureus Infections in Living Mice Using a Novel luxABCDE Construct. *Infection and Immunity,* 68**,** 3594-3600.

FRANCIS, K. P., YU, J., BELLINGER-KAWAHARA, C., JOH, D., HAWKINSON, M. J., XIAO, G., PURCHIO, T. F., CAPARON, M. G., LIPSITCH, M. & CONTAG, P. R. 2001. Visualizing Pneumococcal Infections in the Lungs of Live Mice Using Bioluminescent Streptococcus pneumoniae Transformed with a Novel Gram-Positive lux Transposon. *Infection and Immunity,* 69**,** 3350-3358.

FRANCISCO, W. A., ABU-SOUD, H. M., BALDWIN, T. O. & RAUSHEL, F. M. 1993. Interaction of bacterial luciferase with aldehyde substrates and inhibitors. *Journal of Biological Chemistry,* 268**,** 24734-24741.

FRIDHOLM, H. & EVERITT, E. 2005. Rapid and reproducible infectivity end-point titration of virulent phage in a microplate system. *Journal of Virological Methods,* 128**,** 67-71.

FRIEDRICH, T., STEINMÜLLER, K. & WEISS, H. 1995. The proton-pumping respiratory complex I of bacteria and mitochondria and its homologue in chloroplasts. *FEBS Letters,* 367**,** 107-111.

GALLET, R., KANNOLY, S. & WANG, I.-N. 2011. Effects of bacteriophage traits on plaque formation. *BMC Microbiology,* 11**,** 181.

GALLET, R., SHAO, Y. & WANG, I. N. 2009. High adsorption rate is detrimental to bacteriophage fitness in a biofilm-like environment. *BMC Evolutionary Biology,* 9**,** 241.

GANDER, S. & GILBERT, P. 1997. The development of a small-scale biofilm model suitable for studying the effects of antibiotics on biofilms of gram-negative bacteria. *Journal of Antimicrobial Chemotherapy,* 40**,** 329-334.

GIBSON, Q. H. & HASTINGS, J. W. 1962. The oxidation of reduced flavin mononucleotide by molecular oxygen. *Biochemical Journal,* 83**,** 368-377.

GILBERT, P., ALLISON, D. G., EVANS, D. J., HANDLEY, P. S. & BROWN, M. R. 1989. Growth rate control of adherent bacterial populations. *Applied and Environmental Microbiology,* 55**,** 1308-1311.

GILCREASE, E. B., WINN-STAPLEY, D. A., HEWITT, F. C., JOSS, L. & CASJENS, S. R. 2005. Nucleotide Sequence of the Head Assembly Gene Cluster of Bacteriophage L and Decoration Protein Characterization. *Journal of Bacteriology,* 187**,** 2050-2057.

GONZALEZ, R., WEENING, E., FROTHINGHAM, R., SEMPOWSKI, G. & MILLER, V. 2012. Bioluminescence imaging to track bacterial dissemination of *Yersinia pestis* using different routes of infection in mice. *BMC Microbiology,* 12**,** 147.

GOODE, D., ALLEN, V. M. & BARROW, P. A. 2003. Reduction of Experimental *Salmonella* and *Campylobacter* Contamination of Chicken Skin by Application of Lytic Bacteriophages. *Applied and Environmental Microbiology,* 69**,** 5032-5036.

GORDON, D., ABAJIAN, C. & GREEN, P. 1998. Consed: A Graphical Tool for Sequence Finishing. *Genome Research,* 8**,** 195-202.

GRANT, J., ARANTES, A. & STOTHARD, P. 2012. Comparing thousands of circular genomes using the CGView Comparison Tool. *BMC Genomics,* 13**,** 202.

GRAY, J. T., HUNGERFORD, L. L., FEDORKA-CRAY, P. J. & HEADRICK, M. L. 2004. Extended-Spectrum-Cephalosporin Resistance in *Salmonella enterica* Isolates of Animal Origin. *Antimicrobial Agents and Chemotherapy,* 48**,** 3179-3181.

GREENE, B. & KING, J. 1994. Binding of Scaffolding Subunits within the P22 Procapsid Lattice. *Virology,* 205**,** 188-197.

GREENMAN, J., SPENCER, P., MCKENZIE, C., SAAD, S. & DUFFIELD, J. 2005. *In vitro* models for oral malodor. *Oral Diseases,* 11**,** 14-23.

GRIMONT, A. D. & WEILL, F.-X. 2007. Antigenic Formulae of the *Salmonella* Serovars. 9th ed. World Health Organisation Collaborating Centre for Reference and Research on *Salmonella*: Paris, France; Pasteur Institute.

GRUBER, A. R., LORENZ, R., BERNHART, S. H., NEUBÖCK, R. & HOFACKER, I. L. 2008. The Vienna RNA Websuite. *Nucleic Acids Research,* 36**,** W70-W74.

GUENTHER, S., HERZIG, O., FIESELER, L., KLUMPP, J. & LOESSNER, M. J. 2012. Biocontrol of *Salmonella Typhimurium* in RTE foods with the virulent bacteriophage FO1-E2. *International Journal of Food Microbiology,* 154**,** 66-72.

GUERRERO-FERREIRA, R. C. & WRIGHT, E. R. 2013. Cryo-electron tomography of bacterial viruses. *Virology,* 435**,** 179-186.

GUIBOURDENCHE, M., ROGGENTIN, P., MIKOLEIT, M., FIELDS, P. I., BOCKEMÜHL, J., GRIMONT, P. A. D. & WEILL, F.-X. 2010. Supplement 2003–2007 (No. 47) to the White-Kauffmann-Le Minor scheme. *Research in Microbiology,* 161**,** 26-29.

HADAS, H., EINAV, M., FISHOV, I. & ZARITSKY, A. 1997. Bacteriophage T4 Development Depends on the Physiology of its Host Escherichia Coli. *Microbiology,* 143**,** 179-185.

HADDOCK, S. H. D., MOLINE, M. A. & CASE, J. F. 2010. Bioluminescence in the Sea. *Annual Review of Marine Science,* 2**,** 443-493.

HAGENS, S. & LOESSNER, M. J. 2010. Bacteriophage for biocontrol of foodborne pathogens: Calculations and considerations. *Current Pharmaceutical Biotechnology,* 11**,** 58-69.

HAMBLIN, M. R., O'DONNELL, D. A., MURTHY, N., CONTAG, C. H. & HASAN, T. 2002. Rapid control of wound infections by targeted photodynamic therapy monitored by *in vivo* bioluminescence imaging. *Photochemistry and Photobiology,* 75**,** 51-7.

HAMBLIN, M. R., ZAHRA, T., CONTAG, C. H., MCMANUS, A. T. & HASAN, T. 2003. Optical Monitoring and Treatment of Potentially Lethal Wound Infections *In Vivo*. *Journal of Infectious Diseases,* 187**,** 1717-1726.

HANNA, L. F., MATTHEWS, T. D., DINSDALE, E. A., HASTY, D. & EDWARDS, R. A. 2012. Characterization of the ELPhiS Prophage from *Salmonella enterica* Serovar Enteritidis Strain LK5. *Applied and Environmental Microbiology,* 78**,** 1785-1793.

HANNING, R., NUTT, J. & RICKE, S. 2009. Salmonellosis Outbreaks in the United States Due to Fresh Produce: Sources and Potential Intervention Measures. *Foodborne Pathogens and Disease,* 6**,** 635-648.

HARAGA, A., OHLSON, M. B. & MILLER, S. I. 2008. *Salmonella*e interplay with host cells. *Nature Reviews: Microbiology,* 6**,** 53-66.

HARDY, J., CHU, P. & CONTAG, C. H. 2009. Foci of *Listeria monocytogenes* persist in the bone marrow. *Disease Models & Mechanisms,* 2**,** 39-46.

HARDY, J., FRANCIS, K. P., DEBOER, M., CHU, P., GIBBS, K. & CONTAG, C. H. 2004. Extracellular replication of *Listeria monocytogenes* in the murine gall bladder. *Science,* 303**,** 851-3.

HARDY, J., MARGOLIS, J. J. & CONTAG, C. H. 2006. Induced biliary excretion of *Listeria monocytogenes*. *Infection and Immunity,* 74**,** 1819-27.

HARVEY, E. A. 1957. *A history of luminescence from the earliest times until 1900*.

HASTINGS, J. W., BALDWIN, T. O. & NICOLI, M. Z. 1978. Bacterial luciferase: Assay, purification, and properties. *Methods in Enzymology***,** 135-152.

HASTINGS, J. W. & BALNY, C. 1975. The oxygenated bacterial luciferase-flavin intermediate. Reaction products via the light and dark pathways. *Journal of Biological Chemistry,* 250**,** 7288-7293.

HATFULL, G. 2008. Bacteriophage genomics. *Current Opinion in Microbiology,* 11**,** 447-453.

HATFULL, G. F. & HENDRIX, R. W. 2011. Bacteriophages and their genomes. *Current Opinion in Virology,* 1**,** 298-303.

HEITZER, A., MALACHOWSKY, K., THONNARD, J. E., BIENKOWSKI, P. R., WHITE, D. C. & SAYLER, G. S. 1994. Optical biosensor for environmental on-line monitoring of naphthalene and salicylate bioavailability with an immobilized bioluminescent catabolic reporter bacterium. *Applied and Environmental Microbiology,* 60**,** 1487-1494.

HELMS, M., ETHELBERG, S. & MOLBAK, K. 2005. International *Salmonella* Typhimurium DT104 infections, 1992-2001. *Emerging Infectious Diseases,* 11**,** 859-867.

HENDRIX, R. W., SMITH, M. C. M., BURNS, R. N., FORD, M. E. & HATFULL, G. F. 1999. Evolutionary relationships among diverse bacteriophages and prophages: All the world's a phage. *Proceedings of the National Academy of Sciences,* 96**,** 2192-2197.

HENRY, M., BISWAS, B., VINCENT, L., MOKASHI, V., SCHUCH, R., BISHOP-LILLY, K. A. & SOZHAMANNAN, S. 2012. Development of a high throughput assay for indirectly measuring phage growth using the OmniLog^{TM} system. *Bacteriophage,* 2**,** 159-167.

HENSEL, M., SHEA, J. E., WATERMAN, S. R., MUNDY, R., NIKOLAUS, T., BANKS, G., VAZQUEZ-TORRES, A., GLEESON, C., FANG, F. C. & HOLDEN, D. W. 1998. Genes encoding putative effector proteins of the type III secretion system of *Salmonella* pathogenicity island 2 are required for bacterial virulence and proliferation in macrophages. *Molecular Microbiology,* 30**,** 163-174.

HERIKSTAD, H., HAYES, P., MOKHTAR, M., FRACARO, M. L., THRELFALL, E. J. & ANGULO, F. J. 1997. Emerging Quinolone-Resistant *Salmonella* in the United States. *Emerging Infectious Diseases [serial on the Internet].* 3**,** 2.

HEUTS, F., CAROW, B., WIGZELL, H. & ROTTENBERG, M. E. 2009. Use of non-invasive bioluminescent imaging to assess mycobacterial dissemination in mice, treatment with bactericidal drugs and protective immunity. *Microbes and Infection,* 11**,** 1114-1121.

HIGGINS, J., HIGGINS, S., GUENTHER, K., HUFF, W., DONOGHUE, A., DONOGHUE, D. & HARGIS, B. 2005. Use of a specific bacteriophage treatment to reduce *Salmonella* in poultry products. *Poultry Science,* 84**,** 1141-1145.

HO, T. D. & SLAUCH, J. M. 2001. OmpC Is the Receptor for Gifsy-1 and Gifsy-2 Bacteriophages of *Salmonella*. *Journal of Bacteriology,* 183**,** 1495-1498.

HODGSON, A. E., NELSON, S. M., BROWN, M. R. W. & GILBERT, P. 1995. A simple *in vitro* model for growth control of bacterial biofilms. *Journal of Applied Microbiology,* 79**,** 87-93.

HONG, J., KIM, K.-P., HEU, S., LEE, S. J., ADHYA, S. & RYU, S. 2008. Identification of host receptor and receptor-binding module of a newly sequenced T5-like phage EPS7. *FEMS Microbiology Letters,* 289**,** 202-209.

HOOTON, S., TIMMS, A., ROWSELL, J., WILSON, R. & CONNERTON, I. 2011a. *Salmonella* Typhimurium-specific bacteriophage PhiSH19 and the origins of species specificity in the Vi01-like phage family. *Virology Journal,* 8**,** 498.

HOOTON, S. P. T., ATTERBURY, R. J. & CONNERTON, I. F. 2011b. Application of a bacteriophage cocktail to reduce *Salmonella* Typhimurium U288 contamination on pig skin. *International Journal of Food Microbiology,* 151**,** 157-163.

HOSSEINKHANI, S., SZITTNER, R. & MEIGHEN, E. A. 2005. Random mutagenesis of bacterial luciferase: critical role of Glu175 in the control of luminescence decay. *Journal of Biochemistry,* 385**,** 575-80.

HU, J., MIYANAGA, K. & TANJI, Y. 2010. Diffusion properties of bacteriophages through agarose gel membrane. *Biotechnology Progress,* 26**,** 1213-1221.

HU, J., MIYANAGA, K. & TANJI, Y. 2012. Diffusion of bacteriophages through artificial biofilm models. *Biotechnology Progress,* 28**,** 319-326.

HUANG, R. K., KHAYAT, R., LEE, K. K., GERTSMAN, I., DUDA, R. L., HENDRIX, R. W. & JOHNSON, J. E. 2011. The Prohead-I Structure of Bacteriophage HK97: Implications for Scaffold-Mediated Control of Particle Assembly and Maturation. *Journal of Molecular Biology,* 408**,** 541-554.

HYMAN, P. & ABEDON, S. T. 2010. Chapter 7 - Bacteriophage Host Range and Bacterial Resistance. *In:* ALLEN, I. L., SIMA, S. & GEOFFREY, M. G. (eds.) *Advances in Applied Microbiology.* Academic Press.

ICTV 2005. The Double Stranded DNA Viruses. *In:* FAUQUET, C., MAYO, M. A., MANILOFF, J., DESSELBERGER, U. & BALL, L. A. (eds.) *Virus Taxonomy: VIIIth Report of the International Committee on Taxonomy of Viruses.* San Diego: Academic Press.

JASSIM, S. A. A. & GRIFFITHS, M. W. 2007. Evaluation of a rapid microbial detection method via phage lytic amplification assay coupled with Live/Dead fluorochromic stains. *Letters in Applied Microbiology,* 44**,** 673-678.

JAWHARA, S. & MORDON, S. 2004. In vivo imaging of bioluminescent Escherichia coli in a cutaneous wound infection model for evaluation of an antibiotic therapy. *Antimicrobial Agents and Chemotherapy,* 48**,** 3436-41.

JAYASHEELA, M., SINGH, G., SHARMA, N. C. & SAXENA, S. N. 1987. A new scheme for phage typing *Salmonella bareilly* and characterization of typing phages. *Journal of Applied Microbiology,* 62**,** 429-432.

JIANG, W., CHANG, J., JAKANA, J., WEIGELE, P., KING, J. & CHIU, W. 2006. Structure of epsilon15 bacteriophage reveals genome organization and DNA packaging/injection apparatus. *Nature,* 439**,** 612-616.

JIANG, W., LI, Z., ZHANG, Z., BAKER, M. L., PREVELIGE, P. E. & CHIU, W. 2003. Coat protein fold and maturation transition of bacteriophage P22 seen at subnanometer resolutions. *Nature Structural & Molecular Biology,* 10**,** 131-135.

JOHN, Y. 1991. A quantifiable phenotype of viral propagation. *Biochemical and Biophysical Research Communications,* 174**,** 1009-1014.

JOHNSON, J. E. & CHIU, W. 2007. DNA packaging and delivery machines in tailed bacteriophages. *Current Opinion in Structural Biology,* 17**,** 237-243.

JOHNSTON, T. C., RUCKER, E. B., COCHRUM, L., HRUSKA, K. S. & VANDEGRIFT, V. 1990. The nucleotide sequence of the *luxA* and *luxB* genes of *Xenorhabdus luminescens* HM and a comparison of the amino acid sequences of luciferases from four species of bioluminescent bacteria. *Biochemical and Biophysical Research Communications,* 170**,** 407-15.

JOHNSTON, T. C., THOMPSON, R. B. & BALDWIN, T. O. 1986. Nucleotide sequence of the *luxB* gene of *Vibrio harveyi* and the complete amino acid sequence of the beta subunit of bacterial luciferase. *Journal of Biological Chemistry,* 261**,** 4805-4811.

JONES, B. D., GHORI, N. & FALKOW, S. 1994. *Salmonella typhimurium* initiates murine infection by penetrating and destroying the specialized epithelial M cells of the Peyer's patches. *The Journal of Experimental Medicine,* 180**,** 15-23.

JONES, C., ROBSON, G. D., GREENHAULGH, M., EASTWOOD, I. & HANDLEY, P. S. 2002. The Development of a Bioluminescence Assay to Compare the Efficacy of Biocides Incorporated into Plasticised PVC. *Biofouling: The Journal of Bioadhesion and Biofilm Research,* 18**,** 21 - 27.

JOSHI, A., SIDDIQI, J. Z., RAO, G. R. & CHAKRAVORTY, M. 1982. MB78, a virulent bacteriophage of *Salmonella typhimurium*. *Journal of Virology,* 41**,** 1038-1043.

JOUENNE, T., TRESSE, O. & JUNTER, G.-A. 1994. Agar-entrapped bacteria as an *in vitro* model of biofilms and their susceptibility to antibiotics. *FEMS Microbiology Letters,* 119**,** 237-242.

KADURUGAMUWA, J. L. & FRANCIS, K. P. 2008. Bioluminescent imaging of bacterial biofilm infections in vivo. *Methods in Molecular Biology,* 431**,** 225-39.

KADURUGAMUWA, J. L., MODI, K., COQUOZ, O., RICE, B., SMITH, S., CONTAG, P. R. & PURCHIO, T. 2005. Reduction of Astrogliosis by Early Treatment of Pneumococcal Meningitis Measured by Simultaneous Imaging, *In Vivo*, of the Pathogen and Host Response. *Infection and Immunity,* 73**,** 7836-7843.

KADURUGAMUWA, J. L., SIN, L. V., YU, J., FRANCIS, K. P., KIMURA, R., PURCHIO, T. & CONTAG, P. R. 2003. Rapid Direct Method for Monitoring Antibiotics in a Mouse Model of Bacterial Biofilm Infection. *Antimicrobial Agents and Chemotherapy,* 47**,** 3130-3137.

KANG, H.-W., KIM, J.-W., JUNG, T.-S. & WOO, G.-J. 2013. A new biocontrol agent, wksl3, for *Salmonella* Enteritidis and Typhimurium in Foods: Characterization, Application, Sequence Analysis, and Oral Acute Toxicity Study. *Applied and Environmental Microbiology*.

KAPLAN, D. A., NAUMOVSKI, L., ROTHSCHILD, B. & JOHN COLLIER, R. 1981. Appendix: A model of plaque formation. *Gene,* 13**,** 221-225.

KARSI, A., HOWE, K., KIRKPATRICK, T. B., WILLS, R., BAILEY, R. H. & LAWRENCE, M. L. 2008. Development of bioluminescent *Salmonella* strains for use in food safety. *BMC Microbiology,* 8**,** 10.

KATSURA, I. 1990. Mechanism of length determination in bacteriophage lambda tails. *Advances in Biophysics,* 26**,** 1-18.

KATSURA, I. & HENDRIX, R. W. 1984. Length determination in bacteriophage lambda tails. *Cell,* 39**,** 691-698.

KAUFFMANN, F. 1961. The species-definition in the family *Enterobacteriaceae*. *International Bulletin of Bacteriological Nomenclature and Taxonomy,* 11**,** 5-6.

KIM, M., KIM, S. & RYU, S. 2012a. Complete Genome Sequence of Bacteriophage SSU5 Specific for *Salmonella enterica* serovar Typhimurium Rough Strains. *Journal of Virology,* 86**,** 10894.

KIM, M. & RYU, S. 2011. Characterization of a T5-Like Coliphage, SPC35, and Differential Development of Resistance to SPC35 in *Salmonella enterica* Serovar Typhimurium and *Escherichia coli*. *Applied and Environmental Microbiology,* 77**,** 2042-2050.

KIM, S.-H., PARK, J.-H., LEE, B.-K., KWON, H.-J., SHIN, J.-H., KIM, J. & KIM, S. 2012b. Complete Genome Sequence of *Salmonella* Bacteriophage SS3e. *Journal of Virology,* 86**,** 10253-10254.

KIM, S., SCHULER, B., TEREKHOV, A., AUER, J., MAUER, L. J., PERRY, L. & APPLEGATE, B. 2009. A bioluminescence-based assay for enumeration of lytic bacteriophage. *Journal of Microbiological Methods,* 79**,** 18-22.

KING, A. M. Q., LEFKOWITZ, E., ADAMS, M. J. & CARSTENS, E. B. (eds.) 2011. *Ninth Report of the International Committee on Taxonomy of Viruses* Elsevier.

KINGSFORD, C., AYANBULE, K. & SALZBERG, S. 2007. Rapid, accurate, computational discovery of Rho-independent transcription terminators illuminates their relationship to DNA uptake. *Genome Biology,* 8**,** R22.

KNEZEVIC, P. & PETROVIC, O. 2008. A colorimetric microtiter plate method for assessment of phage effect on *Pseudomonas aeruginosa* biofilm. *Journal of Microbiological Methods,* 74**,** 114-118.

KOCH, A. L. 1964. The growth of viral plaques during the enlargement phase. *Journal of Theoretical Biology,* 6**,** 413-431.

KOGA, K., HARADA, T., SHIMIZU, H. & TANAKA, K. 2005. Bacterial luciferase activity and the intracellular redox pool in Escherichia coli. *Molecular Genetics and Genomics,* 274**,** 180-188.

KOKJOHN, T. A. & SAYLER, G. S. 1991. Attachment and replication of Pseudomonas aeruginosa bacteriophages under conditions simulating aquatic environments. *Journal of General Microbiology,* 137**,** 661-666.

KOVACH, M. E., ELZER, P. H., STEVEN HILL, D., ROBERTSON, G. T., FARRIS, M. A., ROOP, R. M. & PETERSON, K. M. 1995. Four new derivatives of the broad-host-range cloning vector pBBR1MCS, carrying different antibiotic-resistance cassettes. *Gene,* 166**,** 175-176.

KROGH, A., LARSSON, B., VON HEIJNE, G. & SONNHAMMER, E. L. L. 2001. Predicting transmembrane protein topology with a hidden markov model: application to complete genomes. *Journal of Molecular Biology,* 305**,** 567-580.

KRONE, S. M. & ABEDON, S. T. 2008. Modelling phage plaque growth. *In:* ABEDON, S. T. (ed.) *Bacteriophage Ecology: Population Growth Evolution and Impact of Bacterial Viruses.* Cambridge University Press.

KROPINSKI, A., LINGOHR, E. & ACKERMANN, H.-W. 2011. The genome sequence of enterobacterial phage 7-11, which possesses an unusually elongated head. *Archives of Virology,* 156**,** 149-151.

KROPINSKI, A. M. 2009. Measurement of the rate of attachment of bacteriophage to cells. *Methods in Molecular Biology,* 501**,** 151-155.

KROPINSKI, A. M., KOVALYOVA, I. V., BILLINGTON, S. J., PATRICK, A. N., BUTTS, B. D., GUICHARD, J. A., PITCHER, T. J., GUTHRIE, C. C., SYDLASKE, A. D., BARNHILL, L. M., HAVENS, K. A., DAY, K. R., FALK, D. R. & MCCONNELL, M. R. 2007a. The genome of ε15, a serotype-converting, Group E1 *Salmonella enterica*-specific bacteriophage. *Virology,* 369**,** 234-244.

KROPINSKI, A. M., PRANGISHVILI, D. & LAVIGNE, R. 2009. Position paper: The creation of a rational scheme for the nomenclature of viruses of Bacteria and Archaea. *Environmental Microbiology,* 11**,** 2775-2777.

KROPINSKI, A. M., SULAKVELIDZE, A., KONCZY, P. & POPPE, C. 2007b. *Salmonella* Phages and Prophages—Genomics and Practical Aspects. *Methods in Molecular Biology,* 394**,** 133-175.

KRUMSIEK, J., ARNOLD, R. & RATTEI, T. 2007. Gepard: a rapid and sensitive tool for creating dotplots on genome scale. *Bioinformatics,* 23**,** 1026-1028.

KUKLIN, N. A., PANCARI, G. D., TOBERY, T. W., COPE, L., JACKSON, J., GILL, C., OVERBYE, K., FRANCIS, K. P., YU, J., MONTGOMERY, D., ANDERSON, A. S., MCCLEMENTS, W. & JANSEN, K. U. 2003. Real-Time Monitoring of Bacterial Infection In Vivo: Development of Bioluminescent Staphylococcal Foreign-Body and Deep-Thigh-Wound Mouse Infection Models. *Antimicrobial Agents and Chemotherapy,* 47**,** 2740-2748.

KUTTER, E. 2009. Phage host range and efficiency of plating. *Methods in Molecular Biology,* 501**,** 141-149.

KUZNETSOV, Y. G., CHANG, S.-C. & MCPHERSON, A. 2011. Investigation of bacteriophage T4 by atomic force microscopy. *Bacteriophage,* 1**,** 165-173.

KWON, H.-J., CHO, S.-H., KIM, T.-E., WON, Y.-J., JEONG, J., PARK, S. C., KIM, J.-H., YOO, H.-S., PARK, Y.-H. & KIM, S.-J. 2008. Characterization of a T7-Like lytic bacteriophage (ϕSG-JL2) of *Salmonella enterica* serovar Gallinarum biovar Gallinarum. *Applied and Environmental Microbiology,* 74**,** 6970-6979.

LABRIE, S. J., SAMSON, J. E. & MOINEAU, S. 2010. Bacteriophage resistance mechanisms. *Nature Reviews: Microbiology,* 8**,** 317-327.

LACROIX-GUEU, P., BRIANDET, R., LÉVÊQUE-FORT, S., BELLON-FONTAINE, M.-N. & FONTAINE-AUPART, M.-P. 2005. In situ measurements of viral particles diffusion inside mucoid biofilms. *Comptes Rendus Biologies,* 328**,** 1065-1072.

LAMBRECHTS, S. A., DEMIDOVA, T. N., AALDERS, M. C., HASAN, T. & HAMBLIN, M. R. 2005. Photodynamic therapy for *Staphylococcus aureus* infected burn wounds in mice. *Photochemical & Photobiological Sciences,* 4**,** 503-9.

LANDER, G. C., EVILEVITCH, A., JEEMBAEVA, M., POTTER, C. S., CARRAGHER, B. & JOHNSON, J. E. 2008. Bacteriophage Lambda Stabilization by Auxiliary Protein gpD: Timing, Location, and Mechanism of Attachment Determined by Cryo-EM. *Structure,* 16**,** 1399-1406.

LARKIN, M. A., BLACKSHIELDS, G., BROWN, N. P., CHENNA, R., MCGETTIGAN, P. A., MCWILLIAM, H., VALENTIN, F., WALLACE, I. M., WILM, A., LOPEZ, R., THOMPSON, J. D., GIBSON, T. J. & HIGGINS, D. G. 2007. Clustal W and Clustal X version 2.0. *Bioinformatics,* 23**,** 2947-2948.

LASLETT, D. & CANBACK, B. 2004. ARAGORN, a program to detect tRNA genes and tmRNA genes in nucleotide sequences. *Nucleic Acids Research,* 32**,** 11-16.

LAUPLAND, K., SCHONHEYDER, H., KENNEDY, K., LYYTIKAINEN, O., VALIQUETTE, L., GALBRAITH, J. & COLLIGNON, P. 2010. *Salmonella enterica* bacteraemia: a multi-national population-based cohort study. *BMC Infectious Diseases,* 10**,** 95.

LAVIGNE, R., DARIUS, P., SUMMER, E., SETO, D., MAHADEVAN, P., NILSSON, A., ACKERMANN, H. & KROPINSKI, A. 2009. Classification of *Myoviridae* bacteriophages using protein sequence similarity. *BMC Microbiology,* 9**,** 224.

LAVIGNE, R., SETO, D., MAHADEVAN, P., ACKERMANN, H.-W. & KROPINSKI, A. M. 2008. Unifying classical and molecular taxonomic classification: analysis of the *Podoviridae* using BLASTP-based tools. *Research in Microbiology,* 159**,** 406-414.

LAWES, J. & KIDD, S. 2011. *Salmonella* in livestock production in Great Britain 2011. Epidemiology, Surveillance and Risk Group, Animal Health and Veterinary Laboratories Agency, UK.

LAWRENCE, J. G., HATFULL, G. F. & HENDRIX, R. W. 2002. Imbroglios of Viral Taxonomy: Genetic Exchange and Failings of Phenetic Approaches. *Journal of Bacteriology,* 184**,** 4891-4905.

LE MINOR L, POPOFF MY, LAURENT B & D., H. 1986. Characterization of a 7th subspecies of *Salmonella*: *S. choleraesuis* subsp. *indica* subsp. *nov*. *Annales de Institut Pasteur Microbiologie,* 137B**,** 211-217.

LEE, J.-H., SHIN, H., KIM, H. & RYU, S. 2011. Complete Genome Sequence of *Salmonella* Bacteriophage SPN3US. *Journal of Virology,* 85**,** 13470-13471.

LEE, J.-H., SHIN, H. & RYU, S. 2012. Complete Genome Sequence of *Salmonella* enterica Serovar Typhimurium Bacteriophage SPN3UB. *Journal of Virology,* 86**,** 3404-3405.

LEE, J. 2008. Bioluminescence: the First 3000 years (Review). *Journal of Siberian Federal University. Biology.,* 3**,** 194.

LEE, Y. & YIN, J. 1996a. Detection of evolving viruses. *Nature Biotechnology,* 14**,** 491-493.

LEE, Y. & YIN, J. 1996b. Imaging the propagation of viruses. *Biotechnology and Bioengineering,* 52**,** 438-442.

LEI, B. & TU, S.-C. 1998. Mechanism of Reduced Flavin Transfer from *Vibrio harveyi* NADPH−FMN Oxidoreductase to Luciferase. *Biochemistry,* 37**,** 14623-14629.

LEPLAE, R., LIMA-MENDEZ, G. & TOUSSAINT, A. 2010. ACLAME: A CLAssification of Mobile genetic Elements, update 2010. *Nucleic Acids Research,* 38**,** D57-D61.

LEVERENTZ, B., CONWAY, W., ALAVIDZE, Z., JANISIEWICZ, W., FUCHS, Y., CAMP, M., CHIGHLADZE, E. & SULAKVELIDZE, A. 2001. Examination of bacteriophage as a biocontrol method for *Salmonella* on fresh-cut fruit: a model study. *Journal of Food Protection,* 64**,** 1116-1121.

LEVINGS, R. S., LIGHTFOOT, D., PARTRIDGE, S. R., HALL, R. M. & DJORDJEVIC, S. P. 2005. The Genomic Island SGI1, Containing the Multiple Antibiotic Resistance Region of *Salmonella enterica* Serovar Typhimurium DT104 or Variants of It, Is Widely Distributed in Other *S. enterica* Serovars. *Journal of Bacteriology,* 187**,** 4401-4409.

LEWIS, R. J., BALDWIN, A., O'NEILL, T., ALLOUSH, H. A., NELSON, S. M., DOWMAN, T. & SALISBURY, V. 2006a. Use of *Salmonella enterica* serovar Typhimurium DT104 expressing lux genes to assess, in real time and in situ, heat inactivation and recovery on a range of contaminated food surfaces. *Journal of Food Engineering,* 76**,** 41-48.

LEWIS, R. J., BALDWIN, A., O'NEILL, T., ALLOUSH, H. A., NELSON, S. M., DOWMAN, T. & SALISBURY, V. 2006b. Use of *Salmonella enterica* serovar Typhimurium DT104 expressing lux genes to assess, in real time and *in situ*, heat inactivation and recovery on a range of contaminated food surfaces. *Journal of Food Engineering,* 76**,** 41-48.

LHUILLIER, S., GALLOPIN, M., GILQUIN, B., BRASILÈS, S., LANCELOT, N., LETELLIER, G., GILLES, M., DETHAN, G., ORLOVA, E. V., COUPRIE, J., TAVARES, P. & ZINN-JUSTIN, S. 2009. Structure of bacteriophage SPP1 head-to-tail connection reveals mechanism for viral DNA gating. *Proceedings of the National Academy of Sciences,* 106**,** 8507-8512.

LI, J., OCHMAN, H., GROISMAN, E. A., BOYD, E. F., SOLOMON, F., NELSON, K. & SELANDER, R. K. 1995. Relationship between evolutionary rate and cellular location among the Inv/Spa invasion proteins of *Salmonella enterica*. *Proceedings of the National Academy of Sciences,* 92**,** 7252-7256.

LI, Z., SZITTNER, R. & MEIGHEN, E. A. 1993. Subunit interactions and the role of the luxA polypeptide in controlling thermal stability and catalytic properties in recombinant luciferase hybrids. *Biochimica et Biophysica Acta,* 1158**,** 137-45.

LIM, T.-H., KIM, M.-S., LEE, D.-H., LEE, Y.-N., PARK, J.-K., YOUN, H.-N., LEE, H.-J., YANG, S.-Y., CHO, Y.-W., LEE, J.-B., PARK, S.-Y., CHOI, I.-S. & SONG, C.-S. 2012. Use of bacteriophage for biological

control of *Salmonella* Enteritidis infection in chicken. *Research in Veterinary Science,* 93**,** 1173-1178.

LIM, T.-H., LEE, D.-H., LEE, Y.-N., PARK, J.-K., YOUN, H.-N., KIM, M.-S., LEE, H.-J., YANG, S.-Y., CHO, Y.-W., LEE, J.-B., PARK, S.-Y., CHOI, I.-S. & SONG, C.-S. 2011. Efficacy of Bacteriophage Therapy on Horizontal Transmission of *Salmonella* Gallinarum on Commercial Layer Chickens. *Avian Diseases,* 55**,** 435-438.

LIMA-MENDEZ, G., TOUSSAINT, A. & LEPLAE, R. 2011. A modular view of the bacteriophage genomic space: identification of host and lifestyle marker modules. *Research in Microbiology,* 162**,** 737-746.

LIMA-MENDEZ, G., VAN HELDEN, J., TOUSSAINT, A. & LEPLAE, R. 2008. Reticulate Representation of Evolutionary and Functional Relationships between Phage Genomes. *Molecular Biology and Evolution,* 25**,** 762-777.

LINDBERG, A. A. & HOLME, T. 1969. Influence of O Side Chains on the Attachment of the Felix O-1 Bacteriophage to *Salmonella* Bacteria. *Journal of Bacteriology,* 99**,** 513-519.

LINGOHR, E., FROST, S. & JOHNSON, R. P. 2009. Determination of bacteriophage genome size by pulsed-field gel electrophoresis. *Methods in Molecular Biology,* 502**,** 19-25.

LIU, J., DEHBI, M., MOECK, G., ARHIN, F., BAUDA, P., BERGERON, D., CALLEJO, M., FERRETTI, V., HA, N., KWAN, T., MCCARTY, J., SRIKUMAR, R., WILLIAMS, D., WU, J. J., GROS, P., PELLETIER, J. & DUBOW, M. 2004. Antimicrobial drug discovery through bacteriophage genomics. *Nature Biotechnology,* 22**,** 185-191.

LIU, J. & MUSHEGIAN, A. 2004. Displacements of Prohead Protease Genes in the Late Operons of Double-Stranded-DNA Bacteriophages. *Journal of Bacteriology,* 186**,** 4369-4375.

LLAGOSTERA, M., BARBÉ, J. & GUERRERO, R. 1986. Characterization of SE1, a New General Transducing Phage of *Salmonella typhimurium*. *Journal of General Microbiology,* 132**,** 1035-1041.

LOESSNER, M. J., INMAN, R. B., LAUER, P. & CALENDAR, R. 2000. Complete nucleotide sequence, molecular analysis and genome structure of bacteriophage A118 of *Listeria monocytogenes* : implications for phage evolution. *Molecular Microbiology,* 35**,** 324-340.

LOESSNER, M. J., REES, C. E., STEWART, G. S. & SCHERER, S. 1996. Construction of luciferase reporter bacteriophage A511::*luxAB* for rapid and sensitive detection of viable *Listeria* cells. *Applied and Environmental Microbiology,* 62**,** 1133-40.

LOESSNER, M. J., RUDOLF, M. & SCHERER, S. 1997. Evaluation of luciferase reporter bacteriophage A511::*luxAB* for detection of *Listeria monocytogenes* in contaminated foods. *Applied and Environmental Microbiology,* 63**,** 2961-5.

LOPEZ, J. & WEBSTER, R. E. 1983. Morphogenesis of filamentous bacteriophage f1: Orientation of extrusion and production of polyphage. *Virology,* 127**,** 177-193.

LORENZ, U., SCHÄFER, T., OHLSEN, K., TIURBE, G. C., BÜHLER, C., GERMER, C. T. & KELLERSMANN, R. 2011. *In Vivo* Detection of *Staphylococcus aureus* in Biofilm on Vascular Prostheses Using Non-invasive Biophotonic Imaging. *European Journal of Vascular and Endovascular Surgery,* 41**,** 68-75.

LORIAN, V. & STRAUSS, L. 1966. Increased bacterial density at the edge of antibiotic zones of inhibition. *Journal of Bacteriology,* 92**,** 1256-1257.

LOS, M., GOLEC, P., LOS, J., WEGLEWSKA-JURKIEWICZ, A., CZYZ, A., WEGRZYN, A., WEGRZYN, G. & NEUBAUER, P. 2007. Effective inhibition of lytic development of bacteriophages lambda, P1 and T4 by starvation of their host, Escherichia coli. *BMC Biotechnology,* 7**,** 13.

MA, Y., PACAN, J. C., WANG, Q., XU, Y., HUANG, X., KORENEVSKY, A. & SABOUR, P. M. 2008. Microencapsulation of bacteriophage Felix O1 into chitosan-alginate microspheres for oral delivery. *Applied and Environmental Microbiology,* 74**,** 4799-4805.

MAHADEVAN, P., KING, J. & SETO, D. 2009. CGUG: in silico proteome and genome parsing tool for the determination of "core" and unique genes in the analysis of genomes up to ca. 1.9 Mb. *BMC Research Notes,* 2**,** 168.

MAHONY, J., MAULIFFE, O., ROSS, R. P. & VAN SINDEREN, D. 2010. Bacteriophages as biocontrol agents of food pathogens. *Current Opinion in Biotechnology,* 22**,** 1-7.

MANN, N. H. 2005. The Third Age of Phage. *PLoS Biology,* 3**,** e182.

MARCHLER-BAUER, A., LU, S., ANDERSON, J. B., CHITSAZ, F., DERBYSHIRE, M. K., DEWEESE-SCOTT, C., FONG, J. H., GEER, L. Y., GEER, R. C., GONZALES, N. R., GWADZ, M., HURWITZ, D. I., JACKSON, J. D., KE, Z., LANCZYCKI, C. J., LU, F., MARCHLER, G. H., MULLOKANDOV, M., OMELCHENKO, M. V., ROBERTSON, C. L., SONG, J. S., THANKI, N., YAMASHITA, R. A., ZHANG, D., ZHANG, N., ZHENG, C. & BRYANT, S. H. 2011. CDD: a Conserved Domain Database for the functional annotation of proteins. *Nucleic Acids Research,* 39**,** D225-D229.

MARINELLI, L. J., HATFULL, G. F. & PIURI, M. 2012. Recombineering: A powerful tool for modification of bacteriophage genomes. *Bacteriophage,* 2**,** 5-14.

MARSHALL, B. M. & LEVY, S. B. 2011. Food Animals and Antimicrobials: Impacts on Human Health. *Clinical Microbiology Reviews,* 24**,** 718-733.

MAZZOCCO, A., WADDELL, T. E., LINGOHR, E. & JOHNSON, R. P. 2009. Enumeration of Bacteriophages Using the Small Drop Plaque Assay System. *Methods in Molecular Biology,* 501**,** 81-85.

MCCLELLAND, M., SANDERSON, K. E., SPIETH, J., CLIFTON, S. W., LATREILLE, P., COURTNEY, L., PORWOLLIK, S., ALI, J., DANTE, M., DU, F., HOU, S., LAYMAN, D., LEONARD, S., NGUYEN, C., SCOTT, K., HOLMES, A., GREWAL, N., MULVANEY, E., RYAN, E., SUN, H., FLOREA, L., MILLER, W., STONEKING, T., NHAN, M., WATERSTON, R. & WILSON, R. K. 2001. Complete genome sequence of *Salmonella enterica* serovar Typhimurium LT2. *Nature,* 413**,** 852-856.

MCLAUGHLIN, M. R. 2007. Simple colorimetric microplate test of phage lysis in *Salmonella enterica*. *Journal of Microbiological Methods,* 69**,** 394-398.

MCNAIR, K., BAILEY, B. A. & EDWARDS, R. A. 2012. PHACTS, a computational approach to classifying the lifestyle of phages. *Bioinformatics,* 28**,** 614-618.

MEIGHEN, E. A. 1991. Molecular biology of bacterial bioluminescence. *Microbiology and Molecular Biology Reviews,* 55**,** 123-142.

MEIGHEN, E. A. & DUNLAP, P. V. 1993. Physiological, Biochemical and Genetic Control of Bacterial Bioluminescence. *In:* ROSE, A. H. (ed.) *Advances in Microbial Physiology.* Academic Press.

MESAK, L. R., YIM, G. & DAVIES, J. 2009. Improved lux reporters for use in *Staphylococcus aureus*. *Plasmid,* 61**,** 182-187.

MIDDELBOE, M. 2000. Bacterial Growth Rate and Marine Virus–Host Dynamics. *Microbial Ecology,* 40**,** 114-124.

MILLER, E. S., KUTTER, E., MOSIG, G., ARISAKA, F., KUNISAWA, T. & RÜGER, W. 2003. Bacteriophage T4 Genome. *Microbiology and Molecular Biology Reviews,* 67**,** 86-156.

MILLER, R. V. & RIPP, S. A. 2002. Pseudolysogeny: a bacteriophage strategy for increasing longevity in situ. *In:* MICHAEL SYVANEN & KADO, C. (eds.) *Horizontal Gene Transfer.* 2 ed.: Academic Press.

MILLER, S. D., HADDOCK, S. H. D., ELVIDGE, C. D. & LEE, T. F. 2005. Detection of a bioluminescent milky sea from space. *Proceedings of the National Academy of Sciences of the United States of America,* 102**,** 14181-14184.

MITCHELL, E., O'MAHONY, M., LYNCH, D., WARD, L. R., ROWE, B., UTTLEY, A., ROGERS, T., CUNNINGHAM, D. G. & WATSON, R. 1989. Large outbreak of food poisoning caused by *Salmonella typhimurium* definitive type 49 in mayonnaise. *BMJ,* 298**,** 99-101.

MITRA, A., KESARWANI, A. K., PAL, D. & NAGARAJA, V. 2010. WebGeSTer DB—a transcription terminator database. *Nucleic Acids Research,* 39**,** D129-D135.

MITTELMAN, M. W., KING, J. M. H., SAYLER, G. S. & WHITE, D. C. 1992. On-line detection of bacterial adhesion in a shear gradient with bioluminescence by a Pseudomonas fluorescens (lux) strain. *Journal of Microbiological Methods,* 15**,** 53-60.

MIYAMOTO, C., BOYLAN, M., GRAHAM, A., MEIGHEN, E., MARLENE, A. D. & WILLIAM, D. M. 1986. Cloning and expression of the genes from the bioluminescent system of marine bacteria. *Methods in Enzymology,* 133**,** 70-83.

MMOLAWA, P. T., SCHMIEGER, H. & HEUZENROEDER, M. W. 2003a. Bacteriophage ST64B, a Genetic Mosaic of Genes from Diverse Sources Isolated from *Salmonella enterica* Serovar Typhimurium DT 64. *Journal of Bacteriology,* 185**,** 6481-6485.

MMOLAWA, P. T., SCHMIEGER, H., TUCKER, C. P. & HEUZENROEDER, M. W. 2003b. Genomic Structure of the *Salmonella enterica* Serovar Typhimurium DT 64 Bacteriophage ST64T: Evidence for Modular Genetic Architecture. *Journal of Bacteriology,* 185**,** 3473-3475.

MODI, R., HIRVI, Y., HILL, A. & GRIFFITHS, M. 2001. Effect of phage on survival of *Salmonella* Enteritidis during manufacture and storage of cheddar cheese made from raw and pasteurized milk. *Journal of Food Protection,* 64**,** 927-933.

MOLINEUX, I. J. 2006. Fifty-three years since Hershey and Chase; much ado about pressure but which pressure is it? *Virology,* 344**,** 221-229.

MORAIS, M. C., CHOI, K. H., KOTI, J. S., CHIPMAN, P. R., ANDERSON, D. L. & ROSSMANN, M. G. 2005. Conservation of the Capsid Structure in Tailed dsDNA Bacteriophages: the Pseudoatomic Structure of ϕ29. *Molecular Cell,* 18**,** 149-159.

MORTIN, L. I., LI, T., VAN PRAAGH, A. D. G., ZHANG, S., ZHANG, X.-X. & ALDER, J. D. 2007. Rapid Bactericidal Activity of Daptomycin against Methicillin-Resistant and Methicillin-Susceptible *Staphylococcus aureus* Peritonitis in Mice as Measured with Bioluminescent Bacteria. *Antimicrobial Agents and Chemotherapy,* 51**,** 1787-1794.

MOSMANN, T. 1983. Rapid colorimetric assay for cellular growth and survival: Application to proliferation and cytotoxicity assays. *Journal of Immunological Methods,* 65**,** 55-63.

MULVEY, M. R., BOYD, D. A., OLSON, A. B., DOUBLET, B. & CLOECKAERT, A. 2006. The genetics of *Salmonella* genomic island 1. *Microbes and Infection,* 8**,** 1915-1922.

NAIDE, Y., NIKAIDO, H., MÄKELÄ, P. H., WILKINSON, R. G. & STOCKER, B. A. D. 1965. SEMIROUGH STRAINS OF *SALMONELLA*. *Proceedings of the National Academy of Sciences,* 53**,** 147-153.

NAVARRO LLORENS, J. M., TORMO, A. & MARTÍNEZ-GARCÍA, E. 2010. Stationary phase in gram-negative bacteria. *FEMS Microbiology Reviews,* 34**,** 476-495.

NELSON, H., LINGOH, E. J., VILLEGAS, A., COLE, L. & KROPINKSI, A. M. 2012. Genomic characterisation of two new *Salmonella* bacteriophages: vB_SosS_Oslo and vB_SemP_Emek. *Annals of Agrarian Science,* 10**,** 18-23.

NEWTON, H. E. 1957. *A history of luminescence from the earliest times until 1900,* Philadelphia, American Philosophical Society.

NILSSON, A. S. & HAGGÅRD-LJUNGQUIST, E. 2001. Detection of Homologous Recombination among Bacteriophage P2 Relatives. *Molecular Phylogenetics and Evolution,* 21**,** 259-269.

NIU, Y. D., JOHNSON, R. P., XU, Y., MCALLISTER, T. A., SHARMA, R., LOUIE, M. & STANFORD, K. 2009. Host range and lytic capability of four bacteriophages against bovine and clinical human isolates of Shiga toxin-producing *Escherichia coli* O157:H7. *Journal of Applied Microbiology,* 107**,** 646-656.

NYSTRÖM, T. 2004. Stationary-phase physiology. *Annual Review of Microbiology,* 58**,** 161-181.

O'CALLAGHAN, D. & CHARBIT, A. 1990. High efficiency transformation of *Salmonella* Typhimurium and *Salmonella* Typhi by electroporation. *Molecular and General Genetics,* 223**,** 156-8.

O'FLYNN, G., COFFEY, A., FITZGERALD, G. F. & ROSS, R. P. 2006. The newly isolated lytic bacteriophages st104a and st104b are highly virulent against *Salmonella enterica*. *Journal of Applied Microbiology,* 101**,** 251-259.

O'FLYNN, G., ROSS, R. P., FITZGERALD, G. F. & COFFEY, A. 2004. Evaluation of a Cocktail of Three Bacteriophages for Biocontrol of *Escherichia coli* O157:H7. *Applied and Environmental Microbiology,* 70**,** 3417-3424.

OLSON, N. H., GINGERY, M., EISERLING, F. A. & BAKER, T. S. 2001. The Structure of Isometric Capsids of Bacteriophage T4. *Virology,* 279**,** 385-391.

ORLOVA, E. V., GOWEN, B., DROGE, A., STIEGE, A., WEISE, F., LURZ, R., VAN HEEL, M. & TAVARES, P. 2003. Structure of a viral DNA gatekeeper at 10 Å resolution by cryo-electron microscopy. *EMBO Journal,* 22**,** 1255-1262.

ORTEGA-CEJAS, V., FORT, J., MÉNDEZ, V. & CAMPOS, D. 2004. Approximate solution to the speed of spreading viruses. *Physical Review E,* 69**,** 031909.

PADDISON, P., ABEDON, S. T., DRESSMAN, H. K., GAILBREATH, K., TRACY, J., MOSSER, E., NEITZEL, J., GUTTMAN, B. & KUTTER, E. 1998. The Roles of the Bacteriophage T4 r Genes in Lysis Inhibition and Fine-Structure Genetics: A New Perspective. *Genetics,* 148**,** 1539-1550.

PAO, S., ROLPH, S. P., WESTBROOK, E. W. & SHEN, H. 2004. Use of bacteriophages to control *Salmonella* in experimentally contaminated sprout seeds. *Journal of Food Science,* 69**,** M127-M130.

PARENT, K. N., GILCREASE, E. B., CASJENS, S. R. & BAKER, T. S. 2012. Structural evolution of the P22-like phages: Comparison of Sf6 and P22 procapsid and virion architectures. *Virology,* 427**,** 177-188.

PARK, M., LEE, J.-H., SHIN, H., KIM, M., CHOI, J., KANG, D.-H., HEU, S. & RYU, S. 2011. Characterization and Comparative Genomic Analysis of a Novel Bacteriophage SFP10 Simultaneously Inhibiting Both *Salmonella* and *Escherichia coli* O157:H7. *Applied and Environmental Microbiology*.

PARK, S. F., STEWART, G. S. A. B. & KROLL, R. G. 1992. The use of bacterial luciferase for monitoring the environmental regulation of expression of genes encoding virulence factors in *Listeria monocytogenes*. *Journal of General Microbiology,* 138**,** 2619-2627.

PARRY, C. M., HIEN, T. T., DOUGAN, G., WHITE, N. J. & FARRAR, J. J. 2002. Typhoid Fever. *New England Journal of Medicine,* 347**,** 1770-1782.

PARVEEN, A., SMITH, G., SALISBURY, V. & NELSON, S. M. 2001. Biofilm culture of *Pseudomonas aeruginosa* expressing *lux* genes as a model to study susceptibility to antimicrobials. *FEMS Microbiology Letters,* 199**,** 115-118.

PAYNE, R. J. H. & JANSEN, V. A. A. 2001. Understanding Bacteriophage Therapy as a Density-dependent Kinetic Process. *Journal of Theoretical Biology,* 208**,** 37-48.

PELL, L. G., KANELIS, V., DONALDSON, L. W., LYNNE HOWELL, P. & DAVIDSON, A. R. 2009a. The phage λ major tail protein structure reveals a common evolution for long-tailed phages and the type VI bacterial secretion system. *Proceedings of the National Academy of Sciences,* 106**,** 4160-4165.

PELL, L. G., LIU, A., EDMONDS, L., DONALDSON, L. W., HOWELL, P. L. & DAVIDSON, A. R. 2009b. The X-Ray Crystal Structure of the Phage λ Tail Terminator Protein Reveals the Biologically Relevant Hexameric Ring Structure and Demonstrates a Conserved Mechanism of Tail Termination among Diverse Long-Tailed Phages. *Journal of Molecular Biology,* 389**,** 938-951.

PELLUDAT, C., MIROLD, S. & HARDT, W.-D. 2003. The SopEΦ Phage Integrates into the ssrA Gene of *Salmonella* enterica Serovar Typhimurium A36 and Is Closely Related to the Fels-2 Prophage. *Journal of Bacteriology,* 185**,** 5182-5191.

PERLER, F. B. 2002. InBase: the Intein Database. *Nucleic Acids Research,* 30**,** 383-384.

PERLER, F. B., DAVIS, E. O., DEAN, G. E., GIMBLE, F. S., JACK, W. E., NEFF, N., NOREN, C. J., THORNER, J. & BELFORT, M. 1994. Protein splicing elements: inteins and exteins — a definition of terms and recommended nomenclature. *Nucleic Acids Research,* 22**,** 1125-1127.

PETERSEN, T. N., BRUNAK, S., VON HEIJNE, G. & NIELSEN, H. 2011. SignalP 4.0: discriminating signal peptides from transmembrane regions. *Nature Methods,* 8**,** 785-786.

PETKAU, A., STUART-EDWARDS, M., STOTHARD, P. & VAN DOMSELAAR, G. 2010. Interactive microbial genome visualization with GView. *Bioinformatics,* 26**,** 3125-3126.

PFEIFER, C. G., MARCUS, S. L., STEELE-MORTIMER, O., KNODLER, L. A. & FINLAY, B. B. 1999. *Salmonella* typhimurium Virulence Genes Are Induced upon Bacterial Invasion into Phagocytic and Nonphagocytic Cells. *Infection and Immunity,* 67**,** 5690-5698.

PICKARD, D., THOMSON, N. R., BAKER, S., WAIN, J., PARDO, M., GOULDING, D., HAMLIN, N., CHOUDHARY, J., THREFALL, J. & DOUGAN, G. 2008. Molecular characterization of the *Salmonella enterica* serovar Typhi Vi-typing bacteriophage E1. *Journal of Bacteriology,* 190**,** 2580-2587.

PICKARD, D., TORIBIO, A. L., PETTY, N. K., VAN TONDER, A., YU, L., GOULDING, D., BARRELL, B., RANCE, R., HARRIS, D., WETTER, M., WAIN, J., CHOUDHARY, J., THOMSON, N. & DOUGAN, G. 2010. A Conserved Acetyl Esterase Domain Targets Diverse Bacteriophages to the Vi Capsular Receptor of *Salmonella enterica* Serovar Typhi. *Journal of Bacteriology,* 192**,** 5746-5754.

PIWNICA-WORMS, D., GAMMON, S. T., FLENTIE, K. N., QI, M., RAZIA, Y., LUI, F., MARPEGAN, L., MANGLIK, A. & MCKINNEY, J. S. 2008. Stably Integrated *luxCDABE* for Assessment of *Salmonella* Invasion Kinetics. *Molecular Imaging,* 7**,** 1536-0121.

PRICE-CARTER, M., ROY-CHOWDHURY, P., POPE, C. E., PAINE, S., DE LISLE, G. W., COLLINS, D. M., NICOL, C. & CARTER, P. E. 2011. The evolution and distribution of phage ST160 within *Salmonella enterica* serotype Typhimurium. *Epidemiology and Infection,* 139**,** 1262-1271.

PUNTA, M., COGGILL, P. C., EBERHARDT, R. Y., MISTRY, J., TATE, J., BOURSNELL, C., PANG, N., FORSLUND, K., CERIC, G., CLEMENTS, J., HEGER, A., HOLM, L., SONNHAMMER, E. L. L., EDDY,

S. R., BATEMAN, A. & FINN, R. D. 2012. The Pfam protein families database. *Nucleic Acids Research,* 40**,** D290-D301.

QAZI, S. N., COUNIL, E., MORRISSEY, J., REES, C. E., COCKAYNE, A., WINZER, K., CHAN, W. C., WILLIAMS, P. & HILL, P. J. 2001a. agr expression precedes escape of internalized Staphylococcus aureus from the host endosome. *Infection & Immunity,* 69**,** 7074-82.

QAZI, S. N., COUNIL, E., MORRISSEY, J., REES, C. E., COCKAYNE, A., WINZER, K., CHAN, W. C., WILLIAMS, P. & HILL, P. J. 2001b. *agr* expression precedes escape of internalized *Staphylococcus aureus* from the host endosome. *Infection and Immunity,* 69**,** 7074-82.

QAZI, S. N. A., HARRISON, S. E., SELF, T., WILLIAMS, P. & HILL, P. J. 2004. Real-Time Monitoring of Intracellular *Staphylococcus aureus* Replication. *Journal of Bacteriology,* 186**,** 1065-1077.

QIN, L., FOKINE, A., O'DONNELL, E., RAO, V. B. & ROSSMANN, M. G. 2010. Structure of the Small Outer Capsid Protein, Soc: A Clamp for Stabilizing Capsids of T4-like Phages. *Journal of Molecular Biology,* 395**,** 728-741.

QUEVILLON, E., SILVENTOINEN, V., PILLAI, S., HARTE, N., MULDER, N., APWEILER, R. & LOPEZ, R. 2005. InterProScan: protein domains identifier. *Nucleic Acids Research,* 33**,** W116-W120.

RABINOVITCH, A., AVIRAM, I. & ZARITSKY, A. 2003. Bacterial debris—an ecological mechanism for coexistence of bacteria and their viruses. *Journal of Theoretical Biology,* 224**,** 377-383.

REEN, F. J., BOYD, E. F., PORWOLLIK, S., MURPHY, B. P., GILROY, D., FANNING, S. & MCCLELLAND, M. 2005. Genomic Comparisons of *Salmonella enterica* Serovar Dublin, Agona, and Typhimurium Strains Recently Isolated from Milk Filters and Bovine Samples from Ireland, Using a *Salmonella* Microarray. *Applied and Environmental Microbiology,* 71**,** 1616-1625.

REES, C. E. & DODD, C. E. 2006a. Phage for rapid detection and control of bacterial pathogens in food. *Advances in Applied Microbiology,* 59**,** 159-186.

REES, C. E. D. & DODD, C. E. R. 2006b. Phage for Rapid Detection and Control of Bacterial Pathogens in Food. *Advances in Applied Microbiology,* 59**,** 159-186.

RIEDEL, C. U., MONK, I. R., CASEY, P. G., MORRISSEY, D., O'SULLIVAN, G. C., TANGNEY, M., HILL, C. & GAHAN, C. G. M. 2007. Improved Luciferase Tagging System for *Listeria monocytogenes* Allows Real-Time Monitoring In Vivo and In Vitro. *Applied and Environmental Microbiology,* 73**,** 3091-3094.

RIEDEL, C. U., MONK, I. R., CASEY, P. G., WAIDMANN, M. S., GAHAN, C. G. M. & HILL, C. 2009. AgrD-dependent quorum sensing affects biofilm formation, invasion, virulence and global gene expression profiles in *Listeria monocytogenes*. *Molecular Microbiology,* 71**,** 1177-1189.

RIPP, S., JEGIER, P., JOHNSON, C., BRIGATI, J. & SAYLER, G. 2008. Bacteriophage-amplified bioluminescent sensing of *Escherichia coli* O157:H7. *Analytical and Bioanalytical Chemistry,* 391**,** 507-514.

RIPP, S. & MILLER, R. V. 1997. The role of pseudolysogeny in bacteriophage-host interactions in a natural freshwater environment. *Microbiology,* 143**,** 2065-2070.

ROBINSON, G. M., TONKS, K. M., THORN, R. M. S. & REYNOLDS, D. M. 2011. Application of Bacterial Bioluminescence To Assess the Efficacy of Fast-Acting Biocides. *Antimicrobial Agents and Chemotherapy,* 55**,** 5214-5219.

ROCCHETTA, H. L., BOYLAN, C. J., FOLEY, J. W., IVERSEN, P. W., LETOURNEAU, D. L., MCMILLIAN, C. L., CONTAG, P. R., JENKINS, D. E. & PARR, T. R., JR. 2001. Validation of a Noninvasive, Real-Time Imaging Technology Using Bioluminescent *Escherichia coli* in the Neutropenic Mouse Thigh Model of Infection. *Antimicrobial Agents and Chemotherapy,* 45**,** 129-137.

ROHWER, F. & EDWARDS, R. 2002. The Phage Proteomic Tree: a Genome-Based Taxonomy for Phage. *Journal of Bacteriology,* 184**,** 4529-4535.

ROSSMANN, M. G., MORAS, D. & OLSEN, K. W. 1974. Chemical and biological evolution of a nucleotide-binding protein. *Nature,* 250**,** 194-199.

ROUCOURT, B. & LAVIGNE, R. 2009. The role of interactions between phage and bacterial proteins within the infected cell: a diverse and puzzling interactome. *Environmental Microbiology,* 11**,** 2789-2805.

ROWE, B., WARD, L. R. & THRELFALL, E. J. 1997. Multidrug-Resistant *Salmonella typhi*: A Worldwide Epidemic. *Clinical Infectious Diseases,* 24**,** S106-S109.

ROWE, B., WARD, L. R., THRELFALL, E. J., WALLACE, M. & YOUSIF, A. 1990. Spread of multiresistant *Salmonella typhi*. *The Lancet,* 336**,** 1065-1066.

RUTHERFORD, K., PARKHILL, J., CROOK, J., HORSNELL, T., RICE, P., RAJANDREAM, M. A. & BARRELL, B. 2000. Artemis: sequence visualization and annotation. *Bioinformatics,* 16**,** 944-5.

SAEZ, A. C., ZHANG, J., ROSTAGNO, M. H. & EBNER, P. D. 2011. Direct Feeding of Microencapsulated Bacteriophages to Reduce *Salmonella* Colonization in Pigs. *Foodborne Pathogens and Disease,* 8**,** 1269-1274.

SALISBURY, V., PFOESTL, A., WIESINGER-MAYR, H., LEWIS, R., BOWKER, K. E. & MACGOWAN, A. P. 1999. Use of a clinical *Escherichia coli* isolate expressing lux genes to study the antimicrobial pharmacodynamics of moxifloxacin. *Journal of Antimicrobial Chemotherapy,* 43**,** 829-832.

SALMON, D. E. 1884. The Discovery of the Germ of Swine-Plague. *Science,* 3**,** 155-158.

SAMBROOK, J. 2001. *Molecular cloning: a laboratory manual,* Cold Spring Harbor, New York, Cold Spring Harbor Laboratory.

SANTOS, A. C., ROBERTS, J. A., COOK, A. J. C., SIMONS, R., SHEEHAN, R., LANE, C., ADAK, G. K., CLIFTON-HADLEY, F. A. & RODRIGUES, L. C. 2011a. *Salmonella* Typhimurium and *Salmonella* Enteritidis in England: costs to patients, their families, and primary and community health services of the NHS. *Epidemiology & Infection,* 139**,** 742-753.

SANTOS, S. B., KROPINSKI, A. M., CEYSSENS, P.-J., ACKERMANN, H.-W., VILLEGAS, A., LAVIGNE, R., KRYLOV, V. N., CARVALHO, C. M., FERREIRA, E. C. & AZEREDO, J. 2011b. Genomic and Proteomic Characterization of the Broad-Host-Range *Salmonella* Phage PVP-SE1: Creation of a New Phage Genus. *Journal of Virology,* 85**,** 11265-11273.

SANZ, P., TEEL, L. D., ALEM, F., CARVALHO, H. M., DARNELL, S. C. & O'BRIEN, A. D. 2008a. Detection of Bacillus anthracis spore germination in vivo by bioluminescence imaging. *Infection and Immunity,* 76**,** 1036-47.

SANZ, P., TEEL, L. D., ALEM, F., CARVALHO, H. M., DARNELL, S. C. & O'BRIEN, A. D. 2008b. Detection of Bacillus anthracis spore germination in vivo by bioluminescence imaging. *Infection and Immunity,* 76**,** 1036-47.

SCHATTNER, P., BROOKS, A. N. & LOWE, T. M. 2005. The tRNAscan-SE, snoscan and snoGPS web servers for the detection of tRNAs and snoRNAs. *Nucleic Acids Research,* 33**,** W686-W689.

SCHMIEGER, H. 1999. Molecular Survey of the *Salmonella* Phage Typing System of Anderson. *Journal of Bacteriology,* 181**,** 1630-1635.

SCHOFIELD, D. A., MOLINEUX, I. J. & WESTWATER, C. 2009. Diagnostic bioluminescent phage for detection of *Yersinia pestis*. *Journal of Clinical Microbiology,* 47**,** 3887-94.

SCHOFIELD, D. A. & WESTWATER, C. 2009. Phage-mediated bioluminescent detection of *Bacillus anthracis*. *Journal of Applied Microbiology,* 107**,** 1468-78.

SELIFONOVA, O., BURLAGE, R. & BARKAY, T. 1993. Bioluminescent sensors for detection of bioavailable Hg(II) in the environment. *Applied and Environmental Microbiology,* 59**,** 3083-3090.

SHAO, Y. & WANG, N. 2008. Bacteriophage adsorption rate and optimal lysis time. *Genetics,* 180**,** 471-482.

SHIN, H., LEE, J.-H., KIM, H., CHOI, Y., HEU, S. & RYU, S. 2012a. Receptor Diversity and Host Interaction of Bacteriophages Infecting *Salmonella enterica* Serovar Typhimurium. *PLoS ONE,* 7**,** e43392.

SHIN, H., LEE, J.-H., LIM, J.-A., KIM, H. & RYU, S. 2012b. Complete Genome Sequence of *Salmonella enterica* Serovar Typhimurium Bacteriophage SPN1S. *Journal of Virology,* 86**,** 1284-1285.

SIGRIST, C. J. A., CERUTTI, L., DE CASTRO, E., LANGENDIJK-GENEVAUX, P. S., BULLIARD, V., BAIROCH, A. & HULO, N. 2010. PROSITE, a protein domain database for functional characterization and annotation. *Nucleic Acids Research,* 38**,** D161-D166.

SIRAGUSA, G. R., NAWOTKA, K., SPILMAN, S. D., CONTAG, P. R. & CONTAG, C. H. 1999. Real-time monitoring of *Escherichia coli* O157:H7 adherence to beef carcass surface tissues with a bioluminescent reporter. *Applied and Environmental Microbiology,* 65**,** 1738-45.

SMITH, M. G. 1985. The generation time, lag time, and minimum temperature of growth of coliform organisms on meat, and the implications for codes of practice in abattoirs. *Epidemiology and Infection,* 94**,** 289-300.

SMITH, T. & REAGH, A. L. 1903. The non-identity of agglutinins acting upon the flagella and upon the body of bacteria. *Journal of Medical Research,* 10**,** 89-100.

SÖDING, J. 2005. Protein homology detection by HMM–HMM comparison. *Bioinformatics,* 21**,** 951-960.

SÖDING, J., BIEGERT, A. & LUPAS, A. N. 2005. The HHpred interactive server for protein homology detection and structure prediction. *Nucleic Acids Research,* 33**,** W244-W248.

STEINBACHER, S., BAXA, U., MILLER, S., WEINTRAUB, A., SECKLER, R. & HUBER, R. 1996. Crystal structure of phage P22 tailspike protein complexed with *Salmonella sp.* O-antigen receptors. *Proceedings of the National Academy of Sciences,* 93**,** 10584-10588.

STEINBACHER, S., MILLER, S., BAXA, U., BUDISA, N., WEINTRAUB, A., SECKLER, R. & HUBER, R. 1997. Phage P22 tailspike protein: crystal structure of the head-binding domain at 2.3 A, fully refined structure of the endorhamnosidase at 1.56 A resolution, and the molecular basis of O-antigen recognition and cleavage. *Journal of Molecular Biology,* 267**,** 865 - 880.

STEINBACHER, S., SECKLER, R., MILLER, S., STEIPE, B., HUBER, R. & REINEMER, P. 1994. Crystal structure of P22 tailspike protein: interdigitated subunits in a thermostable trimer. *Science,* 265**,** 383 - 386.

STEINHUBER, A., LANDMANN, R., GOERKE, C., WOLZ, C. & FLÜCKIGER, U. 2008. Bioluminescence imaging to study the promoter activity of hla of Staphylococcus aureus in vitro and in vivo. *International Journal of Medical Microbiology,* 298**,** 599-605.

STEWART, G. S. A. B. 1990. In vivo bioluminescence: new potentials for microbiology. *Letters in Applied Microbiology,* 10**,** 1-8.

STONE, R. 2002. Food and agriculture: testing grounds for phage therapy. *Science,* 298**,** 730.

STOTHARD, P. & WISHART, D. S. 2005. Circular genome visualization and exploration using CGView. *Bioinformatics,* 21**,** 537-539.

SULAKVELIDZE, A. & BARROW, P. 2004. Phage Therapy in Animals and Agribusiness. *Bacteriophages.* CRC Press.

SUN, W., BROVKO, L. & GRIFFITHS, M. 2001. Use of bioluminescent *Salmonella* for assessing the efficiency of constructed phage-based biosorbent. *Journal of Industrial Microbiology & Biotechnology,* 27**,** 126-128.

SUSSKIND, M. M. & BOTSTEIN, D. 1978. Molecular genetics of bacteriophage P22. *Microbiological Reviews,* 42**,** 385-413.

SZITTNER, R. & MEIGHEN, E. 1990. Nucleotide sequence, expression, and properties of luciferase coded by *lux* genes from a terrestrial bacterium. *Journal of Biological Chemistry,* 265**,** 16581-16587.

TAMURA, K., PETERSON, D., PETERSON, N., STECHER, G., NEI, M. & KUMAR, S. 2011. MEGA5: Molecular Evolutionary Genetics Analysis Using Maximum Likelihood, Evolutionary Distance, and Maximum Parsimony Methods. *Molecular Biology and Evolution,* 28**,** 2731-2739.

TANAKA, K., NISHIMORI, K., MAKINO, S.-I., NISHIMORI, T., KANNO, T., ISHIHARA, R., SAMESHIMA, T., AKIBA, M., NAKAZAWA, M., YOKOMIZO, Y. & UCHIDA, I. 2004. Molecular Characterization of a Prophage of *Salmonella enterica* Serotype Typhimurium DT104. *Journal of Clinical Microbiology,* 42**,** 1807-1812.

TAURIAINEN, S., KARP, M., CHANG, W. & VIRTA, M. 1998. Luminescent bacterial sensor for cadmium and lead. *Biosensors and Bioelectronics,* 13**,** 931-938.

TAVARES, P., ZINN-JUSTIN, S. & ORLOVA, E. V. 2012. Genome Gating in Tailed Bacteriophage Capsids. *Advances in Experimental Medicine and Biology,* 726**,** 585-600.

THINGSTAD, T. F. 2000. Elements of a theory for the mechanisms controlling abundance, diversity, and biogeochemical role of lytic bacterial viruses in aquatic systems. *Limnology and Oceanography***,** 1320-1328.

THOMAS-CHOLLIER, M., DEFRANCE, M., MEDINA-RIVERA, A., SAND, O., HERRMANN, C., THIEFFRY, D. & VAN HELDEN, J. 2011. RSAT 2011: regulatory sequence analysis tools. *Nucleic Acids Research,* 39**,** W86-W91.

THOMSON, N. R., CLAYTON, D. J., WINDHORST, D., VERNIKOS, G., DAVIDSON, S., CHURCHER, C., QUAIL, M. A., STEVENS, M., JONES, M. A., WATSON, M., BARRON, A., LAYTON, A., PICKARD, D., KINGSLEY, R. A., BIGNELL, A., CLARK, L., HARRIS, B., ORMOND, D., ABDELLAH, Z., BROOKS,

K., CHEREVACH, I., CHILLINGWORTH, T., WOODWARD, J., NORBERCZAK, H., LORD, A., ARROWSMITH, C., JAGELS, K., MOULE, S., MUNGALL, K., SANDERS, M., WHITEHEAD, S., CHABALGOITY, J. A., MASKELL, D., HUMPHREY, T., ROBERTS, M., BARROW, P. A., DOUGAN, G. & PARKHILL, J. 2008. Comparative genome analysis of *Salmonella* Enteritidis PT4 and *Salmonella* Gallinarum 287/91 provides insights into evolutionary and host adaptation pathways. *Genome Research,* 18**,** 1624-1637.

THORN, R. M. S. & GREENMAN, J. 2009. A novel *in vitro* flat-bed perfusion biofilm model for determining the potential antimicrobial efficacy of topical wound treatments. *Journal of Applied Microbiology,* 107**,** 2070-2079.

THORN, R. M. S., NELSON, S. M. & GREENMAN, J. 2007. Use of a Bioluminescent *Pseudomonas aeruginosa* Strain within an *In Vitro* Microbiological System, as a Model of Wound Infection, To Assess the Antimicrobial Efficacy of Wound Dressings by Monitoring Light Production. *Antimicrobial Agents and Chemotherapy,* 51**,** 3217-3224.

TIWARI, B. R., KIM, S. & KIM, J. 2012. Complete Genomic Sequence of *Salmonella enterica* Serovar Enteritidis Phage SE2. *Journal of Virology,* 86**,** 7712.

TOBAR, J. A., CARREÑO, L. J., BUENO, S. M., GONZÁLEZ, P. A., MORA, J. E., QUEZADA, S. A. & KALERGIS, A. M. 2006. Virulent *Salmonella enterica* Serovar Typhimurium Evades Adaptive Immunity by Preventing Dendritic Cells from Activating T Cells. *Infection and Immunity,* 74**,** 6438-6448.

TRČEK, J., BERSCHL, K. & TRÜLZSCH, K. 2010. In vivo analysis of *Yersinia enterocolitica* infection using *luxCDABE*. *FEMS Microbiology Letters,* 307**,** 201-206.

TURNER, D., HEZWANI, M., NELSON, S., SALISBURY, V. & REYNOLDS, D. 2012. Characterization of the *Salmonella* bacteriophage vB_SenS-Ent1. *Journal of General Virology,* 93**,** 2046-2056.

TURNER, D., REYNOLDS, D., SETO, D. & MAHADEVAN, P. 2013. CoreGenes3.5: a webserver for the determination of core genes from sets of viral and small bacterial genomes. *BMC Research Notes,* 6**,** 140.

ULITZUR, N. & ULITZUR, S. 2006. New rapid and simple methods for detection of bacteria and determination of their antibiotic susceptibility by using phage mutants. *Applied and Environmental Microbiology,* 72**,** 7455-9.

ULITZUR, S. 1986. Determination of antibiotic activities with the aid of luminous bacteria. *Methods in Enzymology,* 133**,** 275-84.

ULITZUR, S. & BARAK, M. 1988. Detection of genotoxicity of metallic compounds by the bacterial bioluminescence test. *Journal of Bioluminescence and Chemiluminescence,* 2**,** 95-99.

ULITZUR, S. & HASTINGS, J. W. 1979. Evidence for tetradecanal as the natural aldehyde in bacterial bioluminescence. *Proc Natl Acad Sci U S A,* 76**,** 265-7.

ULITZUR, S. & KUHN, J. 1987. Introduction of *lux* genes into bacteria, a new approach for specific determination of bacteria and their antibiotic susceptibility,. *In:* J. SCLOMERICH, R. ANDREESEN, A. KAPP, M. ERNST & WOODS, W. G. (eds.) *Bioluminescence and chemiluminescence: new perspectives.* Bristol, UK: Wiley Interscience.

ULITZUR, S. & WEISER, I. 1981. Acridine dyes and other DNA-intercalating agents induce the luminescence system of luminous bacteria and their dark variants. *Proceedings of the National Academy of Sciences,* 78**,** 3338-3342.

UZZAU, S., BROWN, D. J., WALLIS, T., RUBINO, S., LEORI, G., BERNARD, S., CASADESUS, J., PLATT, D. J. & OLSEN, J. E. 2000. Host adapted serotypes of *Salmonella enterica*. *Epidemiology and Infection,* 125**,** 229-255.

VAHABOGLU, H., FUZI, M., CETIN, S., GUNDES, S., UJHELYI, E., COSKUNKAN, F. & TANSEL, O. 2001. Characterization of Extended-Spectrum β-Lactamase (TEM-52)-Producing Strains of *Salmonella enterica* Serovar Typhimurium with Diverse Resistance Phenotypes. *Journal of Clinical Microbiology,* 39**,** 791-793.

VALKOVA, N., SZITTNER, R. & MEIGHEN, E. A. 1999. Control of luminescence decay and flavin binding by the LuxA carboxyl-terminal regions in chimeric bacterial luciferases. *Biochemistry,* 38**,** 13820-8.

VAN DER LELIE, D., REGNIERS, L., BORREMANS, B., PROVOOST, A. & VERSCHAEVE, L. 1997. The VITOTOX® test, an SOS bioluminescence *Salmonella typhimurium* test to measure

genotoxicity kinetics. *Mutation Research/Genetic Toxicology and Environmental Mutagenesis,* 389**,** 279-290.

VAN DIEPEN, A., VAN DE GEVEL, J. S., KOUDIJS, M. M., OSSENDORP, F., BEEKHUIZEN, H., JANSSEN, R. & VAN DISSEL, J. T. 2005. Gamma Irradiation or CD4+-T-Cell Depletion Causes Reactivation of Latent *Salmonella enterica* Serovar Typhimurium Infection in C3H/HeN Mice. *Infection and Immunity,* 73**,** 2857-2862.

VAN KESSEL, J. C., MARINELLI, L. J. & HATFULL, G. F. 2008. Recombineering mycobacteria and their phages. *Nature Reviews: Microbiology,* 6**,** 851-857.

VAZQUEZ-TORRES, A., JONES-CARSON, J., BAUMLER, A. J., FALKOW, S., VALDIVIA, R., BROWN, W., LE, M., BERGGREN, R., PARKS, W. T. & FANG, F. C. 1999. Extraintestinal dissemination of *Salmonella* by CD18-expressing phagocytes. *Nature,* 401**,** 804-808.

VEESLER, D. & CAMBILLAU, C. 2011. A Common Evolutionary Origin for Tailed-Bacteriophage Functional Modules and Bacterial Machineries. *Microbiology and Molecular Biology Reviews,* 75**,** 423-433.

VELGE, P., CLOECKAERT, A. & BARROW, P. 2005. Emergence of *Salmonella* epidemics: The problems related to *Salmonella enterica* serotype Enteritidis and multiple antibiotic resistance in other major serotypes. *Veterinary Research,* 36**,** 267-288.

VILLAFANE, R., ZAYAS, M., GILCREASE, E., KROPINSKI, A. & CASJENS, S. 2008. Genomic analysis of bacteriophage epsilon34 of *Salmonella enterica* serovar Anatum (15+). *BMC Microbiology,* 8**,** 227.

VOETSCH, A. C., VAN GILDER, T. J., ANGULO, F. J., FARLEY, M. M., SHALLOW, S., MARCUS, R., CIESLAK, P. R., DENEEN, V. C. & TAUXE, R. V. 2004. FoodNet estimate of the burden of illness caused by nontyphoidal *Salmonella* infections in the United States. *Clinical Infectious Diseases,* 38**,** S127-S134.

WADDELL, T. E. & POPPE, C. 2000. Construction of mini-Tn10luxABcam/Ptac-ATS and its use for developing a bacteriophage that transduces bioluminescence to Escherichia coli O157:H7. *FEMS Microbiology Letters,* 182**,** 285-9.

WAIDMANN, M. S., BLEICHRODT, F. S., LASLO, T. & RIEDEL, C. U. 2011. Bacterial luciferase reporters: The Swiss army knife of molecular biology. *Bioengineered,* 2**,** 8-16.

WALKER, A. J., JASSIM, S. A. A., HOLAH, J. T., DENYER, S. P. & STEWART, G. S. A. B. 1992. Bioluminescent *Listeria monocytogenes* provide a rapid assay for measuring biocide efficacy. *FEMS Microbiology Letters,* 91**,** 251-255.

WALL, L. A., BYERS, D. M. & MEIGHEN, E. A. 1984. *In vivo* and *in vitro* acylation of polypeptides in *Vibrio harveyi*: identification of proteins involved in aldehyde production for bioluminescence. *Journal of Bacteriology,* 159**,** 720-4.

WALLIS, T. S. & GALYOV, E. E. 2000. Molecular basis of *Salmonella*-induced enteritis. *Molecular Microbiology,* 36**,** 997-1005.

WALTER, M., FIEDLER, C., GRASSL, R., BIEBL, M., RACHEL, R., HERMO-PARRADO, X. L., LLAMAS-SAIZ, A. L., SECKLER, R., MILLER, S. & VAN RAAIJ, M. J. 2008. Structure of the Receptor-Binding Protein of Bacteriophage Det7: a Podoviral Tail Spike in a Myovirus. *Journal of Virology,* 82**,** 2265-2273.

WANG, N. 2006. Lysis timing and bacteriophage fitness. *Genetics,* 172**,** 17-26.

WARD, L. R., DE SA, J. D. H. & ROWE, B. 1987. A phage-typing scheme for *Salmonella enteritidis*. *Epidemiology and Infection,* 99**,** 291-294.

WARRINER, K., EVELEIGH, K., GOODMAN, J., BETTS, G., GONZALES, M. & WAITES, W. M. 2001. Attachment of Bacteria to Beef from Steam-Pasteurized Carcasses. *Journal of Food Protection,* 64**,** 493-497.

WEBB, V., LEDUC, E. & SPIEGELMAN, G. B. 1982. Burst size of bacteriophage SP82 as a function of growth rate of its host Bacillus subtilis. *Canadian Journal of Microbiology,* 28**,** 1277-1280.

WEIGELE, P. R., SCANLON, E. & KING, J. 2003. Homotrimeric, β-Stranded Viral Adhesins and Tail Proteins. *Journal of Bacteriology,* 185**,** 4022-4030.

WEINBAUER, M. G. & RASSOULZADEGAN, F. 2004. Are viruses driving microbial diversification and diversity? *Environmental Microbiology,* 6**,** 1-11.

WHICHARD, J. M., SRIRANGANATHAN, N. & PIERSON, F. W. 2003. Suppression of *Salmonella* growth by wild-type and large-plaque variants of bacteriophage Felix O1 in liquid culture and on chicken frankfurters. *Journal of Food Protection,* 66**,** 220-225.

WHICHARD, J. M., WEIGT, L. A., BORRIS, D. J., LI, L. L., ZHANG, Q., KAPUR, V., PIERSON, F. W., LINGOHR, E. J., SHE, Y.-M., KROPINSKI, A. M. & SRIRANGANATHAN, N. 2010. Complete genomic sequence of bacteriophage Felix O1. *Viruses,* 2**,** 710-730.

WHITE, P. B. 1926. Further Studies of the *Salmonella* Group. *Great Britain Medical Research Council (Her Majesty's Stationary Office),* 103**,** 3-160.

WIDDER, E. A. 2010. Bioluminescence in the Ocean: Origins of Biological, Chemical, and Ecological Diversity. *Science,* 328**,** 704-708.

WIKOFF, W. R., LILJAS, L., DUDA, R. L., TSURUTA, H., HENDRIX, R. W. & JOHNSON, J. E. 2000. Topologically Linked Protein Rings in the Bacteriophage HK97 Capsid. *Science,* 289**,** 2129-2133.

WILES, S., CLARE, S., HARKER, J., HUETT, A., YOUNG, D., DOUGAN, G. & FRANKEL, G. 2004. Organ specificity, colonization and clearance dynamics in vivo following oral challenges with the murine pathogen Citrobacter rodentium. *Cellular Microbiology,* 6**,** 963-72.

WILSON, T. & HASTINGS, J. W. 1998. BIOLUMINESCENCE. *Annual Review of Cell and Developmental Biology,* 14**,** 197-230.

WOLLIN, R., ERIKSSON, U. & LINDBERG, A. A. 1981. *Salmonella* Bacteriophage Glycanases: Endorhamnosidase Activity of Bacteriophages P27, 9NA, and KB1. *Journal of Virology,* 38**,** 1025-1033.

WOMMACK, K. E., RAVEL, J., HILL, R. T., CHUN, J. & COLWELL, R. R. 1999a. Population Dynamics of Chesapeake Bay Virioplankton: Total-Community Analysis by Pulsed-Field Gel Electrophoresis. *Applied and Environmental Microbiology,* 65**,** 231-240.

WOMMACK, K. E., RAVEL, J., HILL, R. T. & COLWELL, R. R. 1999b. Hybridization Analysis of Chesapeake Bay Virioplankton. *Applied and Environmental Microbiology,* 65**,** 241-250.

XI, L., CHO, K. W. & TU, S. C. 1991. Cloning and nucleotide sequences of lux genes and characterization of luciferase of Xenorhabdus luminescens from a human wound. *Journal of Bacteriology,* 173**,** 1399-405.

XIONG, Y. Q., WILLARD, J., KADURUGAMUWA, J. L., YU, J., FRANCIS, K. P. & BAYER, A. S. 2005. Real-Time In Vivo Bioluminescent Imaging for Evaluating the Efficacy of Antibiotics in a Rat Staphylococcus aureus Endocarditis Model. *Antimicrobial Agents and Chemotherapy,* 49**,** 380-387.

XU, J., HENDRIX, R. W. & DUDA, R. L. 2004. Conserved Translational Frameshift in dsDNA Bacteriophage Tail Assembly Genes. *Molecular Cell,* 16**,** 11-21.

YAMAMOTO, N. 1978. A Generalized Transducing *Salmonella* Phage ES18 Can Recombine with a Serologically Unrelated Phage Fels 1. *Journal of General Virology,* 38**,** 263-272.

YAMAMOTO, N. & MCDONALD, R. J. 1986. Genomic structure of phage F22, a hybrid between serologically and morphologically unrelated *Salmonella typhimurium* bacteriophages P22 and Fels 2. *Genetics Research,* 48**,** 139-143.

YIN, J. 1993. Evolution of bacteriophage T7 in a growing plaque. *Journal of Bacteriology,* 175**,** 1272-1277.

YIN, J. 1994. Spatially Resolved Evolution of Virusesa. *Annals of the New York Academy of Sciences,* 745**,** 399-408.

YIN, J. & MCCASKILL, J. S. 1992. Replication of viruses in a growing plaque: a reaction-diffusion model. *Biophysical Journal,* 61**,** 1540-1549.

YOU, L., SUTHERS, P. F. & YIN, J. 2002. Effects of Escherichia coli Physiology on Growth of Phage T7 In Vivo and In Silico. *Journal of Bacteriology,* 184**,** 1888-1894.

YOU, L. & YIN, J. 1999. Amplification and Spread of Viruses in a Growing Plaque. *Journal of Theoretical Biology,* 200**,** 365-373.

YOUNG, R. 2002. Bacteriophage holins: deadly diversity. *Journal of Molecular Microbiology and Biotechnology,* 4**,** 21-36.

YOUNG, R. & BLÄSI, U. 1995. Holins: form and function in bacteriophage lysis. *FEMS Microbiology Reviews,* 17**,** 195-205.

ZHAO, H., DOYLE, T. C., COQUOZ, O., KALISH, F., RICE, B. W. & CONTAG, C. H. 2005. Emission spectra of bioluminescent reporters and interaction with mammalian tissue determine the sensitivity of detection *in vivo*. *Journal of Biomedical Optics,* 10**,** 041210-041210.

ZHAO, L., KANAMARU, S., CHAIDIREK, C. C. & ARISAKA, F. 2003. P15 and P3, the Tail Completion Proteins of Bacteriophage T4, Both Form Hexameric Rings. *Journal of Bacteriology,* 185**,** 1693-1700.

ZHAO, X. & DRLICA, K. 2001. Restricting the Selection of Antibiotic-Resistant Mutants: A General Strategy Derived from Fluoroquinolone Studies. *Clinical Infectious Diseases,* 33**,** S147-S156.

Appendix II: Supplementary Material

8.1 Supplemental Tables

Supplemental Table 1. Functional annotation of predicted coding sequences of the vB_SenS-Ent1 genome.

ORF	Strand	Co-ordinates	pI [a]	MW [a]	Predicted Function [b]	Best Homologue [c]	E-value	Accession
gp01	+	88..594	5.99	18823.37	Putative phage terminase small subunit	*Salmonella* phage SE2	2.13E-97	AEX56169.1
gp02	+	584..1855	5.92	47669.65	Putative phage terminase large subunit	*Salmonella* SETP7	0	ABN70691.1
gp03	+	1868..3337	4.78	53767.14	Putative portal protein	*Salmonella* phage SETP3	0	YP_001110831.1
gp04	-	3367..4017	5.87	25012.55	Unknown	*Salmonella* phage SETP3	6.25E-155	YP_001110832.1
gp05	+	4183..5226	5.83	38627.79	Putative head morphogenesis protein	*Salmonella* phage SETP3	0	YP_001110833.1
gp06	+	5229..5687	4.53	16415.54	Putative head decoration protein	*Salmonella* phage SETP3	4.16E-86	YP_001110834.1
gp07	+	6005..6391	9.04	14320.98	Unknown	*Salmonella* phage SETP3	5.03E-81	YP_001110835.1
gp08[d]	+	6327..6500	4.56	6566.68	Unknown	*Salmonella* phage MB78	1.92E-26	CAA60564.1
gp09	+	6585..7286	5.97	25782.05	Putative scaffold protein	*Salmonella* phage SS3e	6.31E-128	YP_005097801.1
gp10	+	7290..8339	4.62	37812.29	Putative major coat protein	*Salmonella* phage SS3e	0	YP_005097800.1
gp11	+	8400..8687	9.52	9435.76	Putative head fibre	*Salmonella* phage SE2	5.43E-42	AEX56179.1
gp12	+	8699..9049	4.38	12198.54	Putative Wac protein	*Salmonella* phage SE2	2.66E-77	AEX56180.1
gp13	+	9086..9274	4.92	7139.91	Unknown	*Salmonella* phage SETP3	3.03E-36	YP_001110840.1
gp14	+	9278..9787	4.8	17716.82	Unknown	*Salmonella* phage SE2	2.43E-119	AEX56182.1
gp15	+	9790..10395	7.99	20595.52	Putative phage neck protein	*Salmonella* phage SE2	5.27E-139	AEX56183.1
gp16	+	10395..10754	8.86	13168.25	Putative phage neck protein	*Salmonella* phage SETP3	2.92E-71	YP_001110843.1
gp17	+	10751..11146	9.69	14444.35	Putative structural protein	*Salmonella* phage SETP3	8.55E-75	YP_001110844.1
gp18	+	11146..11565	4.56	15058.02	Unknown	*Salmonella* phage SETP3	1.88E-98	YP_001110845.1
gp19	+	11565..12734	4.65	41332.24	Putative major tail protein	*Salmonella* phage SE2	0	AEX56187.1
gp20	-	12763..13434	7.82	25635.46	Putative DNA-binding protein	*Salmonella* phage SETP3	5.24E-161	YP_001110847.1
gp21	-	13546..13776	6.05	8690.86	Unknown	*Salmonella* phage SETP3	5.61E-50	YP_001110848.1
gp22	-	13786..14286	9.85	19266.94	Putative HNH endonuclease	*Enterobacteria* phage T1	2.03E-65	YP_003930.1
gp23	-	14302..15456	8.58	43684	Putative recombination endonuclease subunit	*Salmonella* phage SETP3	0	YP_001110849.1
gp24	-	15519..15698	9.7	6603.13	Putative superinfection immunity membrane protein	*Salmonella* phage SETP3	1.44E-33	YP_001110850.1
gp25	+	15868..16284	5.03	15892.02	Unknown	*Salmonella* phage SE2	1.81E-97	AEX56193.1

gp26	+	16290..16649	4.69	13625.27	Unknown	*Salmonella* phage SE2	1.69E-83	AEX56194.1
gp27	+	16642..18975	4.8	83037.7	Putative tape measure protein	*Salmonella* phage SS3e	0	YP_005097846.1
gp28	+	18977..19477	4.87	18638.88	Unknown	*Salmonella* phage SS3e	2.80E-119	YP_005097845
gp29	+	19474..19989	4.53	19266.9	Unknown	*Salmonella* phage MB78	1.21E-123	CAB36891.1
gp30	+	19986..20351	6.27	13865.56	Unknown	*Salmonella* phage SE2	9.51E-84	AEX56198.1
gp31	+	20342..22900	5.36	93938.1	Putative tail fibre protein	*Salmonella* phage SE2	0	AEX56199.1
gp32	+	22913..24967	5.07	72938.68	Putative tailspike protein	*Salmonella* phage SETP13	0	ABN70698.1
gp33	-	25086..25256	4.85	6529.48	Unknown	*Salmonella* phage SETP3	2.79E-29	YP_001110805.1
gp34	-	25253..27718	8.82	92422.04	Putative intein containing helicase precursor	*Salmonella* phage SETP3	0	YP_001110806.1
gp35	-	27715..27906	9.45	7027.22	Unknown	*Escherichia* phage K1-dep(4)	1.92E-36	ADA82278.1
gp36	-	27938..28225	9.6	10917.63	Putative restriction endonuclease	*Salmonella* phage SS3e	1.75E-61	YP_005097835.1
gp37	-	28312..31410	8.05	115917.58	Putative intein containing DNA polymerase precursor	*Salmonella* phage SETP3	0	YP_001110810.1
gp38	-	31468..32094	5.02	23498.22	Unknown	*Salmonella* phage SETP3	2.42E-137	YP_001110811.1
gp39	-	32176..32352	10.28	6991.52	Unknown	No significant database matches		
gp40	-	32352..33776	7.56	52935.79	Unknown	*Salmonella* phage SETP3	0	YP_001110812.1
gp41	-	33819..34349	4.54	20029.55	Unknown	*Salmonella* phage SETP3	6.55E-92	YP_001110813.1
gp42	+	34483..34701	8.8	7920.14	Putative DNA-binding protein	*Salmonella* phage SETP3	1.04E-46	YP_001110814.1
gp43	-	34716..36902	4.98	80366.01	Putative phage replicative helicase primase	*Salmonella* phage SETP3	0	YP_001110815.1
gp44	-	36959..37192	9.56	8569.84	Putative uvsX-like protein	*Salmonella* phage SS3e	1.34E-43	YP_005097824.1
gp45	-	37189..37359	9.38	6637.7	Putative DNA-binding protein	*Salmonella* phage SS3e	2.66E-33	YP_005097823.1
gp46	+	38359..38640	4.99	10254.71	Unknown	No significant database matches		
gp47	+	38637..38840	7.82	7461.58	Unknown	*Salmonella* phage SETP3	4.16E-29	YP_001110819.1
gp48	+	38843..39214	10.43	14160.68	Unknown	*Salmonella* phage SE2	1.73E-69	AEX56158.1
gp49	+	39220..39654	4.63	15380.4	Unknown	*Salmonella* phage SS3e	1.34E-102	YP_005097818.1
gp50	+	39734..40015	7.69	10295	Unknown	*Salmonella* phage SETP3	3.12E-60	YP_001110821.1
gp51	+	40017..40304	9.95	10574.75	Putative holin, class II	*Salmonella* phage SE2	1.44E-42	AEX56160.1
gp52	+	40285..40773	9.91	17329.74	Putative lysozyme	*Salmonella* phage SE2	1.70E-87	AEX56161.1
gp53	+	40958..41143	5.59	6880.89	Unknown	*Salmonella* phage SS3e	7.54E-38	YP_005097815.1
gp54	+	41140..41298	4.44	6092.7	Unknown	*Salmonella* phage SETP3	9.36E-08	YP_001110825.1

gp55	+	41295..41450	10.29	5733.65	Unknown	*Salmonella* phage SE2	2.97E-29	AEX56163.1
gp56	+	41447..41803	7.02	13663.51	Putative NinH-like protein	*Salmonella* phage SS3e	1.95E-47	YP_005097811.1
gp57	+	41800..42099	9.89	11667.84	Unknown	*Salmonella* phage SS3e	2.39E-52	YP_005097810.1
gp58	+	42115..42345	5.81	8163.12	Unknown	*Salmonella* phage SETP3	1.36E-47	YP_001110828.1

[a]Calculated from translated nucleotide sequences using Compute pI/Mw (www.web.expasy.org).

[b]Inferred from BLASTP homolog function and presence of PFAM domains.

[c]Highest scoring blastp homolog.

[d]Multiple possible translational starts (see text).

Supplemental Table 2. Functional annotation of predicted coding sequences of the vB_SenS-Ent2 genome.

ORF	Strand	Co-ordinates	pI [a]	MW [a]	Predicted Function [b]	Best Homologue [c]	E-value	Accession
gp01	+	66..572	6.00	18854.42	putative phage terminase, small subunit	SETP3	3.07E-95	YP_001110829
gp02	+	562..1833	5.92	47654.76	putative phage terminase, large subunit	vB _SenS-Ent1	0	CCG55184
gp03	+	1846..3315	4.78	53811.27	putative portal protein	vB _SenS-Ent1	0	CCG55185
gp04	-	3345..3995	5.87	24999.60	hypothetical protein	vB _SenS-Ent1	2.76E-159	CCG55186
gp05	+	4161..5204	5.83	38642.90	putative head morphogenesis protein, SPP1 gp7 family	vB _SenS-Ent1	0	CCG55187
gp06	+	5207..5665	4.53	16416.57	putative head decoration protein	vB _SenS-Ent1	1.19E-85	CCG55188
gp07	+	5983..6369	9.04	14352.04	hypothetical protein	vB _SenS-Ent1	1.96E-88	CCG55189
gp08	+	6332..6478	4.76	5581.51	hypothetical protein	vB _SenS-Ent1	1.86E-128	CCG55191
gp09	+	6563..7264	5.97	25783.10	putative scaffold protein	vB _SenS-Ent1	1.86E-128	CCG55191
gp10	+	7268..8317	4.62	37813.37	putative major coat protein	vB _SenS-Ent1	0	CCG55192
gp11	+	8377..8748	6.09	12109.65	putative head fibre protein	phiEB49	1.22E-11	AEI91253
gp12	+	8760..9110	4.47	12127.51	putative Hoc protein	vB _SenS-Ent1	1.56E-74	CCG55194
gp13	+	9147..9335	4.91	7140.93	hypothetical protein	vB _SenS-Ent1	5.32E-36	CCG55195
gp14	+	9339..9848	4.70	17817.99	hypothetical protein	SE2	4.10E-118	YP_005098139
gp15	+	9851..10456	9.05	20649.67	putative neck protein	SE2	4.34E-138	YP_005098140
gp16	+	10456..10815	8.86	13169.30	putative neck protein	vB _SenS-Ent1	2.16E-79	CCG55198
gp17	+	10812..11207	9.69	14445.38	putative structural protein	vB _SenS-Ent1	3.37E-73	YP_001110844
gp18	+	11207..11626	4.61	15059.06	hypothetical protein	vB _SenS-Ent1	9.88E-97	YP_001110845
gp19	+	11626..12795	4.62	41163.15	putative major tail protein	vB _SenS-Ent1	0	CCG55201
gp20	-	12824..13495	7.87	25485.38	putative DNA-binding protein	vB _SenS-Ent1	2.44E-137	CCG55202
gp21	-	13607..13837	6.05	8691.90	hypothetical protein	vB _SenS-Ent1	1.63E-48	YP_001110848
gp22	-	13847..14347	9.85	19268.01	putative HNH endonuclease	vB _SenS-Ent1	3.39E-118	CCG55204
gp23	-	14363..15517	8.58	43661.18	putative recombination endonuclease subunit protein	SE2	0	YP_001110849
gp24	-	15580..15759	9.70	6604.16	putative imm immunity to superinfection protein	vB _SenS-Ent1	2.99E-32	YP_001110850
gp25	+	15929..16345	5.03	15879.04	hypothetical protein	vB _SenS-Ent1	1.60E-96	CCG55207
gp26	+	16351..16710	4.69	13626.32	hypothetical protein	vB _SenS-Ent1	1.41E-82	CCG55208
gp27	+	16703..19036	4.78	83020.85	putative tape measure protein	vB _SenS-Ent1	0	CCG55209

gp28	+	19095..19538	4.57	16502.49	hypothetical protein	vB _SenS-Ent1	1.29E-105	CCG55210
gp29	+	19535..20050	4.53	19267.96	hypothetical protein	vB _SenS-Ent1	2.90E-122	CCG55211
gp30	+	20047..20412	6.28	13866.60	hypothetical protein	vB _SenS-Ent1	1.21E-85	CCG55212
gp31	+	20403..22961	5.36	93981.35	putative tail fibre protein	vB _SenS-Ent1	0	CCG55213
gp32	+	22974..25028	5.02	73014.90	putative tailspike protein	SETP13	0	ABN70698
gp33	-	25147..25368	4.86	8652.82	hypothetical protein	SS3e	1.51E-29	YP_005097839
gp34	-	25365..27830	8.82	92294.14	putative intein containing helicase precursor	vB _SenS-Ent1	0	CCG55216
gp35	-	27827..28018	9.45	7056.29	hypothetical protein	vB _SenS-Ent1	6.54E-36	CCG55217
gp36	-	28050..28337	9.60	10877.59	putative restriction endonuclease	vB _SenS-Ent1	3.04E-61	CCG55218
gp37	-	28424..31522	7.91	115947.92	putative intein containing DNA polymerase precursor	vB _SenS-Ent1	0	CCG55219
gp38	-	31580..32206	5.04	23499.27	hypothetical protein	vB _SenS-Ent1	4.15E-136	CCG55220
gp39	-	32288..32464	10.28	6992.57	hypothetical protein	vB _SenS-Ent1	3.09E-33	CCG55221
gp40	-	32464..33888	7.56	52966.94	hypothetical protein	vB _SenS-Ent1	0	CCG55222
gp41	-	33931..34461	4.54	20030.59	hypothetical protein	vB _SenS-Ent1	1.85E-94	CCG55223
gp42	+	34595..34813	8.80	7921.18	putative DNA-binding protein	SETP3	2.85E-45	YP_001110814
gp43	-	34828..37014	4.98	80394.28	putative phage replicative helicase primase	vB _SenS-Ent1	0	CCG55225
gp44	-	37071..37304	9.47	8674.01	putative uvsX-like protein	vB _SenS-Ent1	9.12E-43	CCG55226
gp45	-	37301..37471	9.38	6638.74	putative DNA-binding protein	SS3e	2.86E-33	YP_005097823
gp46	+	38478..38681	6.71	7457.59	hypothetical protein	vB _SenS-Ent1	3.11E-40	CCG55229
gp47	+	38684..39049	10.52	13846.43	hypothetical protein	SS3e	1.65E-63	YP_005097819
gp48	+	39055..39489	4.72	15323.43	hypothetical protein	vB _SenS-Ent1	1.04E-99	YP_005097818
gp49	+	39569..39850	7.69	10296.04	hypothetical protein	vB _SenS-Ent1	3.28E-60	CCG55232
gp50	+	39852..40139	9.95	10538.76	putative holin, class II	SE2	2.05E-60	YP_005098117
gp51	+	40120..40608	9.64	17424.76	putative lysozyme	SS3e	5.23E-89	YP_005097816
gp52	+	40795..40980	7.89	6880.98	hypothetical protein	vB _SenS-Ent1	4.82E-37	CCG55235
gp53	+	40977..41132	10.29	5768.69	hypothetical protein	vB _SenS-Ent1	4.73E-28	CCG55237
gp54	+	41129..41485	7.02	13692.63	hypothetical protein	vB _SenS-Ent1	9.03E-82	CCG55238
gp55	+	41482..41781	9.89	11668.89	hypothetical protein	vB _SenS-Ent1	5.00E-65	CCG55239
gp56	+	41795..42025	5.81	8164.14	hypothetical protein	vB _SenS-Ent1	7.36E-47	CCG55240

[a]Calculated from translated nucleotide sequences using Compute pI/Mw (www.web.expasy.org).

[b]Inferred from BLASTP homolog function and presence of PFAM domains.

[c]Highest scoring blastp homolog.

[d]Multiple possible translational starts (see text).

Supplemental Table 3. Functional annotation of predicted coding sequences of the vB_SenS-Ent3 genome.

ORF	Strand	Co-ordinates	pI [a]	MW [a]	Predicted Function [b]	Best Homologue [c]	E-value	Accession
gp01	+	66..572	6.00	18854.42	putative phage terminase, small subunit	SETP3	3.27E-95	YP_001110829
gp02	+	562..1833	5.92	47670.76	putative phage terminase, large subunit	vB_SenS-Ent1	0	CCG55184
gp03	+	1846..3318	4.75	53763.26	putative portal protein	vB_SenS-Ent1	0	CCG55185
gp04	-	3349..3999	5.87	25013.63	hypothetical protein	vB_SenS-Ent1	1.08E-159	CCG55186
gp05	+	4165..5208	5.83	38628.87	putative head morphogenesis protein, SPP1 gp7 family	vB_SenS-Ent1	0	CCG55187
gp06	+	5211..5669	4.53	16416.57	putative head decoration protein	vB_SenS-Ent1	1.27E-85	CCG55188
gp07	+	5987..6373	9.04	14322.01	hypothetical protein	vB_SenS-Ent1	4.47E-89	CCG55189
gp08	+	6339..6482	4.76	5450.31	hypothetical protein	vB_SenS-Ent1	1.02E-25	CCG55190
gp09	+	6567..7268	5.97	25783.10	putative scaffold protein	vB_SenS-Ent1	1.98E-128	CCG55191
gp10	+	7272..8321	4.62	37813.37	putative major coat protein	vB_SenS-Ent1	0	CCG55192
gp11	+	8381..8752	6.09	12109.65	putative head fibre protein	phiEB49	1.30E-11	AEI91253
gp12	+	8764..9114	4.47	12127.51	putative Hoc protein	vB_SenS-Ent1	1.66E-74	CCG55194
gp13	+	9151..9339	4.91	7140.93	hypothetical protein	vB_SenS-Ent1	5.67E-36	CCG55195
gp14	+	9343..9852	4.70	17817.99	hypothetical protein	SE2	4.37E-118	YP_005098139
gp15	+	9855..10460	9.05	20649.67	putative neck protein	SE2	4.62E-138	YP_005098140
gp16	+	10460..10819	8.86	13169.30	putative neck protein	vB_SenS-Ent1	2.30E-79	CCG55198
gp17	+	10816..11211	9.69	14445.38	putative structural protein	SETP3	3.59E-73	YP_001110844
gp18	+	11211..11630	4.61	15059.06	hypothetical protein	SETP3	1.05E-96	YP_001110845
gp19	+	11630..12799	4.62	41163.15	putative major tail protein	vB_SenS-Ent1	0	CCG55201
gp20	-	12828..13499	7.87	25485.38	putative DNA-binding protein	wksl3	2.28E-159	AFO12386
gp21	-	13611..13841	6.05	8691.90	hypothetical protein	SETP3	1.74E-48	YP_001110848
gp22	-	13851..14351	9.85	19268.01	putative HNH endonuclease	vB_SenS-Ent1	3.61E-118	CCG55204
gp23	-	14367..15521	8.58	43685.16	putative recombinase endonuclease subunit protein	SETP3	0	YP_001110849
gp24	-	15584..15763	9.70	6604.16	putative imm immunity to superinfection membrane protein	SETP3	3.18E-32	YP_001110850
gp25	+	15933..16349	5.03	15879.04	hypothetical protein	vB_SenS-Ent1	1.71E-96	CCG55207
gp26	+	16355..16714	4.69	13626.32	hypothetical protein	vB_SenS-Ent1	4.61E-83	CCG55208
gp27	+	16707..19040	4.78	83020.85	putative tape measure protein	vB_SenS-Ent1	0	CCG55209

gp28	+	19099..19542	4.57	16502.49	hypothetical protein	vB_SenS-Ent1	1.38E-105	CCG55210
gp29	+	19539..20054	4.53	19267.96	hypothetical protein	vB_SenS-Ent1	3.09E-122	CCG55211
gp30	+	20051..20416	6.28	13866.60	hypothetical protein	vB_SenS-Ent1	1.28E-85	CCG55212
gp31	+	20407..22965	5.36	93939.27	putative tail fibre protein	vB_SenS-Ent1	0	CCG55213
gp32	+	22978..25032	5.07	72939.83	putative tailspike protein	vB_SenS-Ent1	0	CCG55214
gp33	-	25151..25321	4.86	6530.49	hypothetical protein	vB_SenS-Ent1	3.13E-29	CCG55215
gp34	-	25318..27699	8.39	88954.06	putative intein containing helicase precursor	vB_SenS-Ent1	0	CCG55216
gp35	-	27780..27971	9.45	7028.24	hypothetical protein	vB_SenS-Ent1	1.09E-36	CCG55217
gp36	-	28003..28290	9.60	10918.65	putative restriction endonuclease	vB_SenS-Ent1	3.21E-62	CCG55218
gp37	-	28377..31475	8.05	115918.95	putative intein-containing DNA polymerase precursor	vB_SenS-Ent1	0	CCG55219
gp38	-	31533..32159	5.04	23499.27	hypothetical protein	vB_SenS-Ent1	4.42E-136	CCG55220
gp39	-	32241..32417	10.28	6992.57	hypothetical protein	vB_SenS-Ent1	3.30E-33	CCG55221
gp40	-	32417..33841	7.56	52936.92	hypothetical protein	vB_SenS-Ent1	0	CCG55222
gp41	-	33884..34414	4.54	20030.59	hypothetical protein	vB_SenS-Ent1	4.67E-100	CCG55223
gp42	+	34548..34766	8.80	7921.18	putative DNA-binding protein	SETP3	3.04E-45	YP_001110814
gp43	-	34781..36967	4.98	80367.28	putative phage replicative helicase primase	vB_SenS-Ent1	0	CCG55225
gp44	-	37024..37257	9.56	8570.86	putative uvsX-like protein	vB_SenS-Ent1	5.83E-48	CCG55226
gp45	-	37254..37424	9.38	6638.74	putative DNA-binding protein	SS3e	3.04E-33	YP_005097823
gp46	+	38424..38705	5.00	10255.78	hypothetical protein	vB_SenS-Ent1	1.36E-61	CCG55228
gp47	+	38702..38905	7.81	7435.54	hypothetical protein	SE2	1.16E-30	YP_005098114
gp48	+	38908..39279	10.43	14161.72	hypothetical protein	vB_SenS-Ent1	1.13E-69	CCG55230
gp49	+	39285..39719	4.62	15381.46	hypothetical protein	SS3e	7.81E-101	YP_005097818
gp50	+	39799..40080	8.49	10223.98	hypothetical protein	vB_SenS-Ent1	9.12E-60	CCG55232
gp51	+	40082..40369	9.95	10512.70	putative holin, class II	vB_SenS-Ent1	2.72E-57	CCG55233
gp52	+	40350..40838	9.61	17395.76	putative lysozyme	vB_SenS-Ent1	6.85E-89	CCG55234
gp53	+	41023..41208	7.89	6880.98	hypothetical protein	ST4	1.50E-37	AFO70791
gp54	+	41205..41363	4.28	6101.76	hypothetical protein	ST4	6.90E-18	AFO70792
gp55	+	41360..41515	10.29	5768.69	hypothetical protein	vB_SenS-Ent1	5.03E-28	CCG55237
gp56	+	41512..41745	7.68	9114.36	putative NinH-like protein	wksl3	3.35E-38	AFO12346

gp57	+	41742..41891	5.34	6095.12	hypothetical protein	SE2	3.89E-20	YP_005098122
gp58	+	41888..42115	9.34	8600.97	putative Nin-H-like protein	vB_SenS-Ent1	1.18E-45	CCG55238
gp59	+	42133..42411	10.00	11361.44	hypothetical protein	vB_SenS-Ent1	8.75E-41	CCG55239
gp60	+	42427..42609	8.19	6776.21	hypothetical protein	SE2	1.34E-29	YP_005098124

[a]Calculated from translated nucleotide sequences using Compute pI/Mw (www.web.expasy.org).

[b]Inferred from BLASTP homolog function and presence of PFAM domains.

[c]Highest scoring blastp homolog.

[d]Multiple possible translational starts (see text).

Supplemental Table 4. Translated sequences of vB_SenS-Ent1 ORFs with matches to domains and motifs in the Pfam and InterProSite databases.

CDS	IPR Accession	Description	Type	Bit score	Evalue
gp02	IPR004921	Terminase, large subunit			
	PF03237.10	Terminase-like family (Terminase_6)	Family	100.5	7.20E-29
gp03	PF13264.1	Domain of unknown function (DUF4055)	Family	146.8	3.60E-43
gp05	IPR006528	Phage head morphogenesis domain			
	IPR017029	Bacteriophage K1H, Orf3			
	PF04233.9	Phage Mu protein F like protein (Phage_Mu_F)	Family	39.6	5.40E-10
gp06	IPR007110	Immunoglobulin-like			
gp12	IPR003599	Immunoglobulin subtype			
	IPR007110	Immunoglobulin-like			
	IPR013783	Immunoglobulin-like fold			
	PF13895.1	Immunoglobulin domain (Ig_2)	Domain	29.3	6.20E-07
gp18	PF13554.1	Domain of unknown function (DUF4128)	Family	87.2	6.00E-25
gp20	IPR005039	Bacteriophage P1, Ant1, C-terminal			
	IPR014054	Bacteriophage regulatory protein, Rha family			
	PF09669.5	Phage regulatory protein Rha (Phage_pRha)	Family	80.5	7.60E-23
	PF03374.9	Phage antirepressor protein KilAC domain (ANT)	Family	48.3	7.80E-13
gp22	PF13392.1	HNH endonuclease (HNH_3)	Domain	48.1	4.80E-13
gp24	IPR016410	Bacteriophage T4, Imm, phage-associated immunity			
	PF14373.1	Superinfection immunity protein (Imm_superinfect)	Family	65.3	2.40E-18
gp25	IPR014859	Protein of unknown function DUF1789			
	PF08748.6	Domain of unknown function (DUF1789)	Domain	32	1.00E-07
gp29	IPR014974	Bacteriophage D3, Orf22			
	PF08875.6	Domain of unknown function (DUF1833)	Family	158.4	5.90E-47
gp32	IPR011050	Pectin lyase fold/virulence factor			
	IPR012332	P22 tailspike C-terminal domain-like			
	IPR015331	P22 tailspike C-terminal domain			
	PF09251.5	*Salmonella* phage P22 tail-spike (PhageP22-tail)	Domain	1121.1	0
gp34	IPR000330	SNF2-related			
	IPR004042	Intein DOD homing endonuclease			
	IPR006141	Intein splice site			
	IPR007868	Hom-end-associated Hint			
	IPR014001	DEAD-like helicase			
	PF05203.11	Hom_end-associated Hint (Hom_end_hint)	Domain	99.5	2.00E-28
	PF00176.18	SNF2 family N-terminal domain (SNF2_N)	Family	36.8	1.70E-09
	PF05203.11	Hom_end-associated Hint (Hom_end_hint)	Domain	36.6	3.50E-09
gp36	IPR014883	VRR-NUC domain			
	PF08774.6	VRR-NUC domain (VRR_NUC)	Domain	47.4	1.30E-12
gp37	IPR001098	DNA-directed DNA polymerase, family A, palm domain			

	IPR006141	Intein splice site			
	IPR012337	Ribonuclease H-like domain			
	PF00476.15	DNA polymerase family A (DNA_pol_A)	Family	32.4	3.30E-08
gp38	IPR022595	Bacteriophage APSE-1, protein 50			
	PF10991.3	Domain of unknown function (DUF2815)	Family	182.3	5.50E-54
gp40	IPR021229	Protein of unknown function DUF2800			
	PF10926.3	Domain of unknown function (DUF2800)	Family	336	2.60E-100
gp42	IPR001387	Helix-turn-helix type 3			
	IPR010982	Lambda repressor-like, DNA-binding			
	PF12844.2	Helix-turn-helix domain (HTH_19)	Domain	38.2	9.70E-10
gp43	PF13481.1	AAA domain (AAA_25)	Domain	95.5	2.30E-27
gp45	PF12728.2	Helix-turn-helix domain (HTH_17)	Domain	37.4	2.00E-09
gp52	IPR002196	Glycoside hydrolase, family 24			
	IPR023346	Lysozyme-like domain			
	PF00959.14	Glycoside hydrolase family 24 (Phage_lysozyme)	Domain	54	1.50E-14
gp55	IPR020295	Protein of unknown function DUF2737			
	PF10930.3	Domain of unknown function (DUF2737)	Family	84.7	2.10E-24

Supplemental Table 5. Translated sequences of vB_SenS-Ent2 ORFs with matches to domains and motifs in the Pfam and InterProSite databases.

CDS	Accession	Description	Type	Bit score	E-value
gp02	IPR004921	Terminase, large subunit			
	PF03237.10	Terminase-like family (Terminase_6)	Family	99.3	1.70E-28
gp03	IPR025129	Domain of unknown function DUF4055			
	PF13264.1	Domain of unknown function (DUF4055)	Family	146.7	4.00E-43
gp05	IPR006528	Phage head morphogenesis domain			
	IPR017029	Putative phage head morphogenesis protein			
	PF04233.9	Phage Mu protein F like protein (Phage_Mu_F)	Family	39.8	4.60E-10
gp06	IPR007110	Immunoglobulin-like			
gp12	IPR003599	Immunoglobulin subtype			
	IPR007110	Immunoglobulin-like			
	IPR013783	Immunoglobulin-like fold			
	PF13895.1	Immunoglobulin domain (Ig_2)	Domain	29.3	6.30E-07
gp18	IPR025395	Protein of unknown function DUF4128			
	PF13554.1	Domain of unknown function (DUF4128	Family	87.2	6.00E-25
gp20	IPR005039	Bacteriophage P1, Ant1, C-terminal			
	IPR014054	Bacteriophage regulatory protein, Rha family			
	PF09669.5	Phage regulatory protein Rha (Phage_pRha)	Family	73.2	1.50E-20
	PF03374.9	Phage antirepressor protein KilAC domain (ANT)	Family	50.6	1.50E-13
gp22	PF13392.1	HNH endonuclease (HNH_3)	Domain	48.1	4.80E-13
gp24	IPR016410	Bacteriophage-associated immunity protein			
	PF14373.1	Superinfection immunity protein (Imm_superinfect)	Family	65.3	2.40E-18
gp25	IPR014859	Protein of unknown function DUF1789			
	PF08748.6	Domain of unknown function (DUF1789)	Domain	32.2	8.20E-08
gp29	IPR014974	Bacteriophage D3, Orf22			
	PF08875.6	Domain of unknown function (DUF1833)	Family	158.4	5.90E-47
gp32	IPR011050	Pectin lyase fold/virulence factor			
	IPR012332	P22 tailspike C-terminal domain-like			
	IPR015331	P22 tailspike C-terminal domain			
	PF09251.5	*Salmonella* phage P22 tailspike (PhageP22-tail)	Domain	1115.2	0
gp34	IPR000330	SNF2-related			
	IPR004042	Intein DOD homing endonuclease			
	IPR006141	Intein splice site			
	IPR007868	Hom-end-associated Hint			
	IPR014001	Helicase, superfamily 1/2, ATP-binding domain			
	PF05203.11	Hom end-associated Hint (Hom_end_hint)	Domain	99.5	1.90E-28
	PF05203.11	Hom end-associated Hint (Hom_end_hint)	Domain	35.9	5.30E-09
	PF00176.18	SNF2 family N-terminal domain (SNF2_N)	Family	37.8	8.80E-10
gp36	IPR014883	VRR-NUC domain			
	PF08774.6	VRR-NUC domain (VRR_NUC)	Domain	47.2	1.60E-12
gp37	IPR001098	DNA-directed DNA polymerase, family A, palm domain			

	IPR006141	Intein splice site			
	IPR012337	Ribonuclease H-like domain			
	PF00476.15	DNA polymerase Family A (DNA_pol_A)	Family	32.4	3.30E-08
gp38	IPR022595	Bacteriophage APSE-1, protein 50			
	PF10991.3	Domain of unknown function (DUF2815	Family	182.3	5.50E-54
gp40	IPR021229	Protein of unknown function DUF2800			
	PF10926.3	Domain of unknown function (DUF2800	Family	335.6	3.30E-100
gp42	IPR001387	Helix-turn-helix type 3			
	IPR010982	Lambda repressor-like, DNA-binding domain			
	PF12844.2	Helix-turn-helix domain (HTH_19)	Domain	38.2	9.70E-10
gp43	PF13481.1	AAA domain (AAA_25)	Domain	95.3	2.60E-27
gp45	IPR009061	DNA binding domain, putative			
	IPR011991	Winged helix-turn-helix transcription repressor DNA-binding			
gp45	PF12728.2	Helix-turn-helix domain (HTH_17)	Domain	37.4	2.00E-09
gp51	IPR002196	Glycoside hydrolase, family 24			
	IPR023346	Lysozyme-like domain			
	IPR023347	Lysozyme domain			
	PF00959.14	Glycoside hydrolase family 24 (Phage_lysozyme)	Domain	57.6	1.20E-15
gp53	IPR020295	Protein of unknown function DUF2737			
	PF10930.3	Domain of unknown function (DUF2737)	Family	86.3	6.80E-25

Supplemental Table 6. Translated sequences of vB_SenS-Ent3 ORFs with matches to domains and motifs in the Pfam and InterProSite databases.

ORF ID	IPR ID	Description	Type	Bit score	E-value
gp02	IPR004921	Terminase, large subunit			
	PF03237.10	Terminase-like family (Terminase_6)	Family	100.5	7.20E-29
gp03	IPR025129	Domain of unknown function DUF4055			
	PF13264.1	Domain of unknown function (DUF4055)	Family	146.7	4.00E-43
gp05	IPR006528	Phage head morphogenesis domain			
	IPR017029	Bacteriophage K1H, Orf3			
	PF04233.9	Phage Mu protein F like protein (Phage_Mu_F)	Family	39.6	5.40E-10
gp06	IPR007110	Immunoglobulin-like			
gp12	IPR003599	Immunoglobulin subtype			
	IPR007110	Immunoglobulin-like			
	IPR013783	Immunoglobulin-like fold			
	PF13895.1	Ig_2	Domain	29.3	6.30E-07
gp18	IPR025395	Protein of unknown function DUF4128			
	PF13554.1	DUF4128	Family	87.2	6.00E-25
gp20	IPR005039	Bacteriophage P1, Ant1, C-terminal			
	IPR014054	Bacteriophage regulatory protein, Rha family			
	PF09669.5	Phage regulatory protein Rha (Phage_pRha)	Family	73.2	1.50E-20
	PF03374.9	Phage antirepressor KilAC domain (ANT)	Family	50.6	1.50E-13
gp22	PF13392.1	HNH endonuclease (HNH_3)	Domain	48.1	4.80E-13
gp24	IPR016410	Bacteriophage-associated immunity protein			
	PF14373.1	Superinfection immunity protein (Imm_superinfect)	Family	65.3	2.40E-18
gp25	IPR014859	Protein of unknown function DUF1789			
	PF08748.6	Domain of unknown function (DUF1789)	Domain	32.2	8.20E-08
gp29	IPR014974	Bacteriophage D3, Orf22			
	PF08875.6	Domain of unknown function (DUF1833	Family	158.4	5.90E-47
gp32	IPR011050	Pectin lyase fold/virulence factor			
	IPR012332	P22 tailspike C-terminal domain-like			
	IPR015331	P22 tailspike C-terminal domain			
	PF09251.5	*Salmonella* phage P22 tailspike (PhageP22-tail)	Domain	1121.1	0
gp34	IPR000330	SNF2-related			
	IPR004042	Intein DOD homing endonuclease			
	IPR006141	Intein splice site			
	IPR007868	Hom-end-associated Hint			
	IPR014001	Helicase, superfamily 1/2, ATP-binding domain			
	PF05203.11	Hom end-associated Hint (Hom_end_hint)	Domain	99.5	1.90E-28
	PF05203.11	Hom end-associated Hint (Hom_end_hint)	Domain	36.7	3.20E-09
	PF00176.18	SNF2 family N-terminal domain (SNF2_N)	Family	36.9	1.60E-09
gp36	IPR014883	VRR-NUC domain			
	PF08774.6	VRR-Nuc domain (VRR_NUC)	Domain	47.4	1.30E-12
gp37	IPR001098	DNA-directed DNA polymerase, family A, palm domain			
	IPR006141	Intein splice site			

	IPR012337	Ribonuclease H-like domain			
	PF00476.15	DNA polymerase family A (DNA_pol_A)	Family	32.4	3.30E-08
gp38	IPR022595	Bacteriophage APSE-1, protein 50			
	PF10991.3	Domain of unknown function (DUF2815)	Family	182.3	5.50E-54
gp40	IPR021229	Protein of unknown function DUF2800			
	PF10926.3	Domain of unknown function (DUF2800)	Family	336	2.60E-100
gp42	IPR001387	Helix-turn-helix type 3			
	IPR010982	Lambda repressor-like, DNA-binding domain			
	PF12844.2	Helix-turn-helix domain (HTH_19)	Domain	38.2	9.70E-10
gp43	PF13481.1	AAA domain (AAA_25)	Domain	95.5	2.30E-27
gp45	IPR009061	DNA binding domain, putative			
	IPR011991	Winged helix-turn-helix transcription repressor DNA-binding			
	PF12728.2	Helix-turn-helix domain (HTH_17)	Domain	37.4	2.00E-09
gp52	IPR002196	Glycoside hydrolase, family 24			
	IPR023346	Lysozyme-like domain			
	IPR023347	Lysozyme domain			
	PF00959.14	Glycoside hydrolase, family 24 (Phage_lysozyme)	Domain	54.3	1.20E-14
gp55	IPR020295	Protein of unknown function DUF2737			
	PF10930.3	Domain of unknown function (DUF2737)	Family	86.3	6.80E-25

Supplemental Table 7. Open reading frames shared between proposed members of the *Setp3likevirus*.

Putative function	Ent1	Ent2	Ent3	Wksl3	SS3e	SE2	SETP3	K1H	K1G	K1ind1	K1ind2	K1ind3
Terminase, small subunit	gp01	gp01	gp01	gp04	gp17	gp30	gp29	ORF47	ORF49	ORF48	ORF45	ORF46
Terminase, large subunit	gp02	gp02	gp02	gp03	gp16	gp31	gp30	ORF1	ORF1	ORF1	ORF1	ORF1
Portal protein	gp03	gp03	gp03	gp02	gp15	gp32	gp31	ORF2	ORF2	ORF2	ORF2	ORF2
DNA-binding KilA-N	gp04	gp04	gp04	gp01	gp14	gp33	gp32	-	-	-	-	-
SPP1 gp7	gp05	gp05	gp05	gp64	gp13	gp34	gp33	ORF3	ORF3	ORF3	ORF3	ORF3
Unique hypothetical protein	-	-	-	-	-	-	-	-	-	-	-	ORF4
Putative head decoration protein	gp06	gp06	gp06	gp63	gp12	gp35	gp34	ORF4	ORF4	ORF4	ORF4	ORF5
Hypothetical protein	gp07	gp07	gp07	gp62	gp11	gp36	gp35	ORF5	ORF5	ORF5	ORF5	ORF6
Hypothetical protein	gp08	gp08	gp08	-	-	gp37	-	ORF6	ORF6	ORF6	ORF6	ORF7
Putative scaffold protein	gp09	gp09	gp09	gp61	gp10	gp38	gp36	ORF7	ORF7	ORF7	ORF7	ORF8
Major capsid protein	gp10	gp10	gp10	gp60	gp09	gp39	gp37	ORF8	ORF8	ORF8	ORF8	ORF9
Putative head fibre protein	gp11	gp11	gp11	gp59	gp08	gp40	gp38	ORF9	ORF9	ORF9	ORF9	ORF10
Putative Hoc protein	gp12	gp12	gp12	gp58	gp07	gp41	gp39	-	ORF10	ORF10	ORF10	ORF11
Hypothetical protein	gp13	gp13	gp13	gp57	gp06	gp42	gp40	-	ORF11	ORF11	ORF11	ORF12
HNH endonuclease (unique)	-	-	-	-	-	-	-	-	ORF12	-	-	-
Hypothetical protein	gp14	gp14	gp14	gp56	gp05	gp43	gp41	ORF10	ORF13	ORF12	ORF12	ORF13
Putative neck protein	gp15	gp15	gp15	gp55	gp04	gp44	gp42	ORF11	ORF15	ORF13	ORF13	ORF14
Hypothetical (frameshift?)	gp16	gp16	gp16	gp54	gp03	gp45	gp43	ORF12	ORF14	ORF14	ORF14	ORF15
Hypothetical (frameshift?)	-	-	-	-	-	-	-	ORF13	-	-	-	-
Hypothetical (frameshift?)	gp17	gp17	gp17	gp53	gp02	gp46	gp44	ORF13	ORF14	ORF14	ORF14	ORF15
Hypothetical protein	gp18	gp18	gp18	gp52	gp01	gp47	gp45	ORF14A	ORF16	ORF15	ORF15	ORF15
Major tail protein	gp19	gp19	gp19	gp51	-	gp48	gp46	ORF14B	ORF17	ORF16	ORF16	ORF17
Putative ATPase	-	-	-	-	-	-	-	ORF15	ORF18	ORF17	ORF17	ORF18
Putative polynucleotide kinase	-	-	-	-	-	-	-	ORF16	ORF19	ORF18	ORF18	ORF19
DNA binding protein	gp20	gp20	gp20	gp50	-	gp49	gp47	-	-	-	-	-
Unique hypothetical protein	-	-	-	-	-	gp50	-	-	-	-	-	-

DNA-methylase	-	-	-	-	-	gp51	-	-	-	-	-	-
Hypothetical protein	gp21	gp21	gp21	gp49	-	-	gp48	-	-	-	-	-
HNH endonuclease	gp22	gp22	gp22	gp48	-	-	-	-	-	-	-	-
Recombination endonuclease	gp23	gp23	gp23	gp47	-	gp52	gp49	ORF17	ORF20	ORF19	ORF19	ORF20
Unique hypothetical protein	-	-	-	-	-	-	-	ORF18	-	-	-	-
Immunity protein	gp24	gp24	gp24	gp46	gp58	gp53	gp50	-	ORF21	ORF20	ORF20	ORF21
Hypothetical protein	gp25	gp25	gp25	gp45	gp57	gp54	gp51	ORF19	ORF22	ORF21	ORF21	ORF22
Hypothetical protein	gp26	gp26	gp26	gp44	gp56	gp55	gp52	ORF19	ORF22	ORF21	ORF21	ORF22
Tape measure protein	gp27	gp27	gp27	gp43	gp55	gp56	gp53	ORF20	ORF23	ORF22	ORF22	ORF23
Hypothetical protein	gp28	gp28	gp28	gp42	gp54	gp57	gp54	ORF21	ORF24	ORF23	ORF23	ORF24
Hypothetical protein	gp29	gp29	gp29	gp41	gp53	gp58	gp01	ORF22	ORF25	ORF24	ORF24	ORF25
Hypothetical protein	gp30	gp30	gp30	gp40	gp52	gp59	-	?	?	?	?	?
Tail fiber or baseplate	gp31	gp31	gp31	gp39	gp50	gp60	gp02	ORF23	ORF26	ORF25	ORF25	ORF26
	-	-	-	-	gp51	-	gp03	-	-	-	-	-
Tailspike: P22-like	gp32	gp32	gp32	gp38	gp52	gp61	gp04	-	-	-	-	-
Tailspike - K1F and HK620-like	-	-	-	-	-	-	-	ORF24	ORF27	ORF26	ORF26	ORF27
Hypothetical protein	Gp33	Gp33	Gp33	Gp37	gp48	-	gp05	ORF25	-	-	-	-
Hypothetical protein	-	-	-	-	-	-	-	ORF26	ORF28	-	-	-
Helicase	Gp34	Gp34	Gp34	Gp36	Gp47	Gp01	Gp06	ORF27	ORF29	ORF27	ORF27	ORF28
MTE-like protein	-	-	-	-	-	-	-	ORF28	ORF30	ORF28	ORF28	ORF29
C-specific methylase	-	-	-	-	-	-	-	ORF29	ORF31	ORF29	ORF29	ORF30
HNH Homing endonuclease (pdb:1u3e)	-	-	-	-	Gp46	Gp02	Gp09	-	-	-	-	-
Hypothetical protein	Gp35	Gp35	Gp35	Gp35	Gp45	Gp03	Gp07	ORF30	ORF32	-	-	-
Holliday-junction resolvase (pdb:1hh1)	Gp36	Gp36	Gp36	Gp34	Gp44	Gp04	Gp08	ORF31	ORF33	-	-	-
Hypothetical protein	-	-	-	Gp33	-	-	-	-	-	-	-	-
DNA polymerase	Gp37	Gp37	Gp37	Gp32	Gp41	Gp05	Gp10	ORF32	ORF34	ORF30	ORF30	ORF31
					Gp43	Gp06						
Gp2.5-like protein (pdb:1je5)	Gp38	Gp38	Gp38	Gp31	Gp40	Gp07	Gp11	ORF33	ORF35	-	ORF31	ORF32
					Gp39							

Hypothetical protein	Gp39	Gp39	Gp39	-	-	-	-	-	-	-	-	-
Helicase subunit (pbd:3u4q)	Gp40	Gp40	Gp40	Gp30	Gp38	Gp08	Gp12	ORF34	ORF36	ORF31	ORF32	ORF33
Hypothetical protein	-	-	-	-	Gp37	-	-	-	-	ORF32	-	-
Hypothetical protein	-	-	-	Gp29	-	Gp09	-	ORF35	ORF37	ORF33		
Hypothetical protein	-	-	-	Gp28	-	Gp10	-	-	-	-	-	-
Hypothetical protein	Gp41	Gp41	Gp41	Gp27	Gp36	Gp11	Gp13	ORF36	ORF38	ORF34	ORF33	ORF34
Transcriptional regulator (pdb:3bs3)	Gp42	Gp42	Gp42	Gp26	Gp35	Gp12	Gp14	-	-	-	-	-
Hypothetical protein	-	-	-	-	-	-	-	-	ORF39	-	-	-
Helicase-primase	Gp43	Gp43	Gp43	Gp25	Gp34	Gp13	Gp15	ORF38	ORF40	ORF35	ORF34	ORF35
Uvsx-like (not evidence from hhpred)	Gp44	Gp44	Gp44	Gp24	Gp33	Gp14	-	ORF37	-	ORF36	-	-
DNA-binding (pdb:1z4h)	Gp45	gp45	gp45	Gp23	Gp32	Gp15	GP16	-	-	ORF37	-	-
Hypothetical protein	-	-	-	-	-	-	-	ORF39	ORF41	-	ORF35	ORF36
Hypothetical protein	gp46	-	Gp46	-	-	-	-	ORF40	ORF42	ORF38	ORF36	ORF37
Hypothetical protein	gp47	gp46	gp47	gp19	gp29	gp18	gp19	-	-	-	-	-
Hypothetical protein	gp48	gp47	gp48	gp18	gp28	gp19	gp20	ORF41	ORF43	ORF39	ORF37	ORF38
Hypothetical protein	gp49	gp48	gp49	gp17	gp27	gp20	-	-	-	-	-	-
Hypothetical protein	gp50	gp49	gp50	gp16	-	-	gp21	ORF42	ORF44	ORF40	ORF38	ORF39
Holin class II	gp51	gp50	gp51	gp15	gp26	gp21	gp22	ORF43	ORF45	ORF41	ORF39	ORF40
Lysozyme	gp52	gp51	gp52	gp14	gp25	gp22	gp23	ORF44	ORF46	ORF42	ORF40	ORF41
Holin class I						gp27		ORF45	ORF47	ORF44	ORF42	ORF43
Hypothetical protein	-	-	-	-	-	-	-	-	-	ORF45	ORF43	ORF44
Unique hypothetical protein	-	-	-	-	-	-	-	-	-	ORF46	-	-
Hypothetical protein	gp53	gp52	gp53	gp13	gp24	gp23	gp24	-	-	-	-	-
Hypothetical protein	gp54		gp54	gp12	-	-	gp25	-	-	-	-	-
Hypothetical protein	gp55	gp53	gp55	gp11	gp23	gp24	-	-	-	-	-	-
Hypothetical protein	gp56	gp54	gp58	gp08	gp20 gp22	gp25	gp26	ORF46	ORF48	ORF47 gp43?	ORF44	ORF45 gp42?
Hypothetical protein	-	gp57	-	gp09	-	gp26	gp27	-	-	-	-	-
Hypothetical protein	gp57	gp55	gp59	gp07	gp19	-	-	-	-	-	-	-

Hypothetical protein	gp58	gp56	-	-	-	-	gp28	-	-	-	-	-
Hypothetical protein	-	-	gp60	gp06	gp18	gp28	-	-	-	-	-	-
Hypothetical protein	-	-	-	gp05	-	gp29	-	-	-	-	-	-